



Glycinergic neurons and inhibitory transmission in the cerebellar nuclei

Zoe Husson

► **To cite this version:**

Zoe Husson. Glycinergic neurons and inhibitory transmission in the cerebellar nuclei. Neurons and Cognition [q-bio.NC]. Université Pierre et Marie Curie - Paris VI, 2014. English. <NNT : 2014PA066279>. <tel-01205721>

HAL Id: tel-01205721

<https://tel.archives-ouvertes.fr/tel-01205721>

Submitted on 27 Sep 2015

HAL is a multi-disciplinary open access archive for the deposit and dissemination of scientific research documents, whether they are published or not. The documents may come from teaching and research institutions in France or abroad, or from public or private research centers.

L'archive ouverte pluridisciplinaire **HAL**, est destinée au dépôt et à la diffusion de documents scientifiques de niveau recherche, publiés ou non, émanant des établissements d'enseignement et de recherche français ou étrangers, des laboratoires publics ou privés.



THÈSE

Présentée à
L'UNIVERSITÉ PIERRE ET MARIE CURIE
École doctorale : Cerveau Cognition Comportement
Par : Zoé HUSSON

Pour obtenir le grade de :
DOCTEUR
Spécialité : BIOLOGIE – Mention NEUROSCIENCES

Glycinergic neurons and inhibitory transmission in the cerebellar nuclei

Directeur de recherche : Stéphane DIEUDONNÉ

Soutenue le : 26 Septembre 2014
Devant la commission d'examen formée de :

M. Marco BEATO	DR	University College London	Rapporteur
M. Philippe ISOPE	CR	INCI, Université de Strasbourg	Rapporteur
M. Chris DE ZEEUW	DR	Netherlands Institute for Neuroscience	Examineur
M. Régis LAMBERT	PU	Université Paris VI	Examineur
M. Stéphane DIEUDONNE	DR	IBENS, Ecole Normale Supérieure	Directeur de thèse

RÉSUMÉ

Neurones glycinergiques et transmission inhibitrice dans les noyaux cérébelleux

Le système olivo-cérébelleux est le circuit responsable de l'apprentissage et du contrôle fin de la posture et des mouvements. Le cervelet à proprement parler est composé d'un cortex et de noyaux cérébelleux. Les noyaux cérébelleux ont longtemps été considérés comme une simple station de relais vers les centres moteurs, opérant sous le contrôle inhibiteur massif des cellules de Purkinje du cortex cérébelleux. Les données les plus récentes intègrent dorénavant les noyaux profonds dans l'organisation modulaire du cervelet, en tenant compte de leur rôle central dans la boucle olivo-cérébelleuse via les neurones nucléo-olivaires, ainsi que des interactions plastiques avec le système des fibres moussues. En plus des cellules principales, glutamatergiques, et des neurones nucléo-olivaires, GABAergiques, les noyaux profonds sembleraient contenir une population de neurones inhibiteurs glycinergiques dont les propriétés sont peu connues.

L'objectif de cette thèse est d'établir les caractères distinctifs de ce troisième type cellulaire et d'en détailler la connectivité ainsi que les fonctions dans le circuit cérébelleux. À cette fin, nous avons combiné une approche génétique, basée en particulier sur l'utilisation de souris transgéniques sous le contrôle du transporteur neuronal de glycine GlyT2, avec des traçages anatomiques, des marquages immuno-histochimiques et des expériences d'électrophysiologie et d'optogénétique. Nous montrons que les neurones inhibiteurs glycinergiques des noyaux profonds constituent une population de neurones distincts des autres types cellulaires, clairement identifiables par leur phénotype inhibiteur mixte GABAergique/glycinergique. Ces neurones inhibiteurs se distinguent également par leur plexus axonal qui comporte une arborisation locale dans les noyaux cérébelleux et une projection vers le cortex cérébelleux, essentiellement confinée à la couche granulaire.

Le plexus axonal intranucléaire des neurones inhibiteurs forme des synapses fonctionnelles sur les cellules principales des noyaux cérébelleux. Leurs varicosités axonales sont en apposition avec des agrégats de récepteurs inhibiteurs, enrichis en récepteurs de la glycine et pratiquement dépourvus des principales sous-unités $\gamma 2$ et $\alpha 1$ des récepteurs du GABA. Des stimulations optogénétiques spécifiques de ces interneurons évoquent des courants inhibiteurs rapides dans les cellules principales, inhibés en partie par un antagoniste des récepteurs de la glycine (Strychnine) et totalement par application additionnelle d'un inhibiteur des récepteurs du GABA (SR95531 alias Gabazine). Ces données électrophysiologiques confirment la nature inhibitrice mixte GABA/glycine des neurones inhibiteurs des noyaux cérébelleux.

Les axones nucléo-corticaux des neurones inhibiteurs forment un plexus peu dense dans la couche granulaire du cortex cérébelleux. Nos données préliminaires indiquent que ces varicosités, de contenu mixte GABA/glycine, contactent spécifiquement les cellules de Golgi du cortex cérébelleux, dont la connectivité divergente vers les cellules granulaires offre un potentiel important d'amplification.

Enfin des données combinées d'optogénétique, d'électrophysiologie et d'immunohistochimie indiquent que les neurones inhibiteurs des noyaux cérébelleux reçoivent des afférences inhibitrices des cellules de Purkinje et pourraient également être contactés par les fibres moussues ou les fibres grimpantes.

L'ensemble de nos données établissent les neurones inhibiteurs mixtes des noyaux cérébelleux comme la troisième composante cellulaire des noyaux profonds. Leur importance dans l'organisation modulaire du cervelet, ainsi que leur impact sur l'intégration sensori-motrice, devront être confirmés par des études optogénétiques *in vivo*.

SUMMARY

Glycinergic neurons and inhibitory transmission in the cerebellar nuclei

The olivo-cerebellar circuit is responsible for the learned fine control of posture and movements. The cerebellum *per se* is composed of a three-layered cortex and of nuclei. Those nuclei have been considered for a long time as a simple relay to downstream motor centers, operating under the massive inhibitory control of Purkinje cells, the principal neurons of the cerebellar cortex. More recent studies have integrated the cerebellar nuclei in the modular organization of the cerebellum, taking into account their central role in the olivo-cerebellar loop via the nucleo-olivary neurons, as well as the plastic synaptic inputs from the mossy fiber system. In addition to the glutamatergic principal cells and the GABAergic nucleo-olivary neurons, the cerebellar nuclei seem to include a population of inhibitory glycinergic neurons whose properties are poorly understood.

The aim of this thesis is to establish the distinctive characteristics of this third cell type and to detail their connectivity and their role in the cerebellar circuitry. To this end, we took a genetic approach, based in particular on the use of transgenic mouse lines under the control of the promoter of the neuronal glycine transporter GlyT2. We combined these genetics tools with anatomical tracings, immunohistochemical stainings, electrophysiological recordings and optogenetic stimulations. We showed that the glycinergic inhibitory neurons of the cerebellar nuclei constitute a neuronal population distinct from the other cell types, as numerous as principal neurons, and characterized by their mixed inhibitory GABAergic/glycinergic phenotype. Those inhibitory neurons are also distinguished by their axonal plexus which includes a local arborization with the cerebellar nuclei and a projection to the granular layer of the cerebellar cortex.

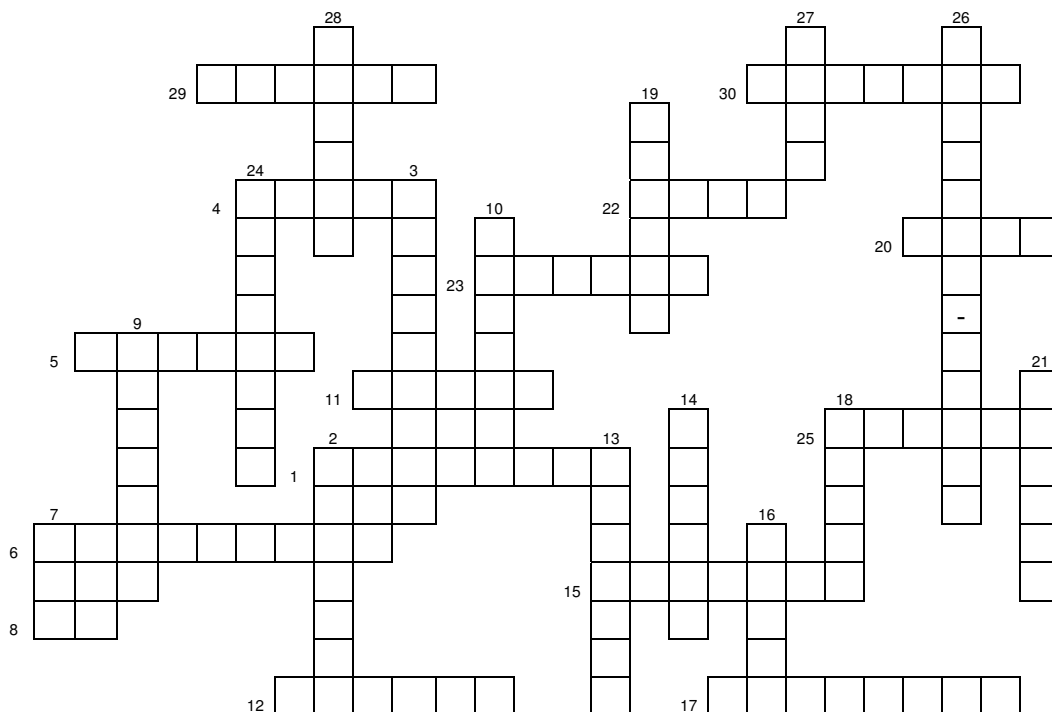
The intra-nuclear plexus of the inhibitory neurons forms functional synapses on the principal neurons of the cerebellar nuclei. The axonal varicosities are in apposition to inhibitory receptor clusters, enriched in glycine receptors and virtually devoid of the main $\gamma 2$ and $\alpha 1$ subunits of GABA_A receptors. Specific optogenetic stimulations of the inhibitory neuron population evoked fast inhibitory currents in principal neurons, which were inhibited partially by the glycine receptors antagonist strychnine. The remaining component was fully blocked by application of the GABA_A receptors antagonist gabazine (SR95531). These electrophysiological data confirmed the mixed GABA/ glycine phenotype of the inhibitory neurons of the cerebellar nuclei.

Branches of the inhibitory neurons axons leave the cerebellar nuclei through the white matter forming a widespread nucleo-cortical projection, which forms a low-density plexus in the granular layer of the cerebellar cortex. Our preliminary data indicate that these axonal varicosities, which also display a mixed GABA/glycine phenotype, contact specifically the Golgi cells of the cerebellar cortex. The divergence of the Golgi cell to granule cell connectivity offers a high potential for amplification of the nuclear neurons output.

Finally, combined optogenetic, electrophysiological and immunohistochemical evidence indicate that the inhibitory neurons of the cerebellar nuclei receive inhibitory afferents from Purkinje cells and may be contacted by mossy fibers or climbing fibers.

Overall, our data establish the glycine-containing inhibitory neurons as the third cellular component of the cerebellar nuclei. Their importance in the modular organization of the cerebellum and their impact on sensory-motor integration need to be confirmed by optogenetic experiments *in vivo*.

Remerciements *(English version and solutions at the end.)*



- 1- Le numéro 1
- 2- D'Agen ou de Paris, des petits ou des grands, ceux qui comptent toujours
- 3- Ils font la paire, mais leurs différences font la force de leur équipe
- 4- Amateur de pommes et de grammaire anglaise
- 5- Marseillais aux pantalons colorés
- 6- Souvent masqué, parfois inquiet, tout le temps taquet
- 7- Bibliographe averti
- 8- Qui parle peu
- 9- En mange deux quand j'en mange un
- 10- Culturiste qui me transporte
- 11- Mange du fenouil cru
- 12- Ligérien adepte des liens YouTube et de camping sauvage
- 13- Orateur reconnu
- 14- Le soudeur fou
- 15- Jeune papa
- 16- Compagne de route (et de déroutes)
- 17- Futur médecin bien équilibré
- 18- Italien à lunettes

- 19- Accompagnateur des débuts
- 20- Certains arrachent sa chemise, d'autres se contentent de ses qualités de grimpeur ou de sa bonne humeur.
- 21- Propriétaire des frigos remplis d'anticorps intéressants du 3ème étage
- 22- Celle qui lance le café pour les travailleurs du matin
- 23- Maman de Pénélope qui m'a légué son premier bébé
- 24- Responsable plateforme plutôt en forme
- 25- Formatrice retraitée de l'injection olivaire chez les "pups"
- 26- Gestionnaires, techniciens, animaliers et autres trop souvent délaissés des remerciements
- 27- Ceux qui ont accepté la lecture et la critique
- 28- Notre "N- maître -DA" à tous
- 29- Jeune maman aux savoirs immunohistochimiques précieux
- 30- Tous ceux dont le nom ne figure pas dans les petites cases de mots croisés mais resteront dans celles de ma mémoire.

TABLE OF CONTENTS

INTRODUCTION	7
CHAPTER 1: THE MAIN LOOP THROUGH THE CEREBELLAR NUCLEI: PRINCIPAL NEURONS AND MOTOR CONTROL	8
1.1. SEGMENTATION AND TOPOGRAPHY OF THE CEREBELLUM.....	8
1.1.1. Cerebellar cortex	8
1.1.2. Cerebellar nuclei	9
1.2. SENSORI-MOTOR CIRCUITRY IN THE CEREBELLUM: MOSSY FIBERS SYSTEM AS EXTRACEREBELLAR INPUTS – CEREBELLAR NUCLEI AS FINAL CEREBELLAR OUTPUT	11
1.2.1. Mossy fibers system: sensori-motor inputs.....	11
1.2.1.1. Topography and somatotopy in the cerebellar cortex	11
1.2.1.2. Mossy fibers innervation of the cerebellar nuclei	12
1.2.2. The cerebellar nuclei: the cerebellar output to control motor function	14
1.3. CN PRINCIPAL NEURONS: A KEY SYNAPTIC INTEGRATOR FOR THE MOTOR FUNCTION	14
1.3.1. Synaptic inputs in principal neurons: Excitation versus Inhibition	15
1.3.1.1. Excitatory inputs	15
1.3.1.2. Purkinje cell inhibitory inputs.....	16
1.3.1.3. Sequential integration of excitatory and inhibitory inputs	16
1.3.2. Principal neurons excitability and their electrophysiological properties.....	17
1.3.2.1. Spontaneous firing	17
1.3.2.2. Characteristics of the rebound discharge.....	18
1.3.2.3. Does the rebound discharge exist in vivo?	19
1.3.3. Principal neuron output activity: Rate coding versus temporal coding.....	21
CHAPTER 2: THE OLIVO-CORTICO-NUCLEAR LOOP	23
2.1. INFERIOR OLIVE PROJECTION TO THE CEREBELLAR CORTEX	23
2.1.1. Olivo-cortical innervation	23
2.1.1.1. One-to-one innervation of the Purkinje cells	23
2.1.1.2. Climbing fiber input elicit complex spike	23
2.1.2. Parasagittal segmentation of the climbing fibers inputs.....	24
2.2. THE CEREBELLO-OLIVARY FEEDBACK LOOP.....	25
2.2.1. The nucleo-olivary cells	25
2.2.2. Cerebellar control of the inferior olive activity.....	26
2.2.2.1. Structural organization of the inferior olive: electrotonic coupling and subthreshold oscillations.....	26
2.2.2.2. Inhibitory action of the nucleo-olivary neurons on the inferior olive physiology	26
2.3. MODULAR ORGANIZATION OF THE OLIVO-CORTICO-NUCLEAR SYSTEM.....	28
2.3.1. Olivary-nuclear innervation	28
2.3.2. The olivo-cerebellar module	29
2.3.2.1. The olivo-cerebellar module: a functional unit to control movement?	29
2.3.2.2. Mossy fibers inputs with respect to the cerebellar modules.....	30
2.3.3. Functional impact of the modular organization of the olivo-cerebellar system.....	32
2.3.3.1. Nuclear neurons activity within the modules	32
2.3.3.2. Homeostasis of the olivary, cortical and nuclear activities in the cerebellar feedback loops.....	33
2.4. CLIMBING FIBERS GIVE INSTRUCTIONS: SUPERVISED LEARNING IN THE CEREBELLUM	33
2.4.1. Synaptic plasticity and error signaling in the cerebellar cortex by climbing fiber inputs	33
2.4.2. Synaptic plasticity in the cerebellar nuclei: another degree of freedom for olivo-cerebellar mediated motor learning?	34
CHAPTER 3: INHIBITORY NEURONS OF THE CEREBELLAR NUCLEI, A THIRD NUCLEAR CIRCUIT	37
3.1. INHIBITORY NEURONS OF THE CEREBELLAR NUCLEI: A HETEROGENEOUS POPULATION	37
3.1.1. Evidence for the presence of a third nuclear cell type and the question of their neurotransmitter contents	37
3.1.2. Electrophysiological properties of the glycinergic neurons	38
3.2. EVIDENCE FOR NON-PURKINJE CELLS INHIBITORY TRANSMISSION IN THE PRINCIPAL NEURONS	39
3.2.1. GABA _A and glycine receptors: common features and specific characteristics	39
3.2.2. Interaction between GABAergic and glycinergic transmission: the case of mixed transmission	40
3.2.3. Searching for a glycinergic component of synaptic transmission in the cerebellar nuclei	41

3.3. CEREBELLAR NUCLEO-CORTICAL PATHWAY: ANOTHER FEEDBACK FOR FINE MODULATION OF PRINCIPAL NEURON ACTIVITY	42
3.3.1. <i>The nucleo-cortical pathway: a forgotten feedback loop</i>	42
3.3.2. <i>Cell type identity of the nucleo-cortical neurons: a role for the inhibitory neurons</i>	43

MATERIALS AND METHODS..... 45

RESULTS..... 54

CHAPTER 4: DIFFERENTIAL GABAERGIC AND GLYCINERGIC INPUTS OF INHIBITORY INTERNEURONS AND PURKINJE CELLS TO PRINCIPAL NEURONS OF THE CEREBELLAR NUCLEI..... 55

4.1. ARTICLE.....	55
4.2. SUPPLEMENTARY DATA	70
4.2.1. <i>Transient expression of GlyT2 in nucleo-olivary neurons</i>	70
4.2.2. <i>Extracellular recordings of the GlyT2-expressing interneurons</i>	71
4.3. CONCLUDING REMARKS.....	71

CHAPTER 5: BEYOND PRINCIPAL CELLS: THE EXTENDED CONNECTIVITY OF THE INHIBITORY GLYCINERGIC NEURONS OF THE CEREBELLAR NUCLEI..... 73

5.1. INTRA-CEREBELLAR OUTPUT OF THE CEREBELLAR NUCLEI: THE INHIBITORY NUCLEO-CORTICAL PATHWAY	73
5.2. INPUTS TO INHIBITORY NEURONS OF THE CEREBELLAR NUCLEI.....	76
5.2.1. <i>Purkinje cells inputs onto inhibitory neurons</i>	77
5.2.2. <i>Excitatory inputs onto glycinergic neurons</i>	77
5.2.3. <i>Excitatory inputs onto the principal neurons: mossy fiber versus climbing fiber inputs</i>	79
5.3. CONCLUDING REMARKS.....	81

DISCUSSION..... 84

BIBLIOGRAPHY..... 93

LIST OF ABBREVIATIONS..... 112

LIST OF FIGURES..... 113

INTRODUCTION

CHAPTER 1: The main loop through the cerebellar nuclei: principal neurons and motor control

The cerebellum is a phylogenetically old structure, since it is found in the most primitive vertebrates such as lampreys. The cerebellum is composed of a three-layered cortex and of nuclei, called deep cerebellar nuclei as they are enclosed in the cortical sheet within the fiber bundles of the white matter. These cerebellar nuclei constitute the only projection site (except for the vestibulo-cerebellar system) for the principal cells of the cortex, the Purkinje cells. The cerebellar system is generally associated to the motor systems, as the cerebellum is involved in the fine control of postural balance and movements, both reflex and voluntary. The high degree of organization of the neuronal networks among the cerebellar system is central for the control of motor function (Apps and Garwicz, 2005).

1.1. Segmentation and topography of the cerebellum

1.1.1. Cerebellar cortex

In the rat, as described by Larsell (Larsell, 1952), the cerebellum is divided along the transversal axis in three parts: a central region called the vermis, and two lateral hemispheres, flanked more ventrally by the paraflocculus and the flocculus. Studies of the cerebellar afferents and efferents have classically led to a subdivision of the cerebellum into three main parts (Jansen and Brodal, 1940; Kandel et al., 2000). The *vestibulo-cerebellum*, phylogenetically old, consists of the flocculo-nodular lobe and receives direct inputs from the vestibular nerve. The *spino-cerebellum*, formed by the vermis and paravermal region receives spinal projections. The vermis receives in addition visual and auditory inputs, as well as vestibular and somato-sensory inputs from the head and proximal limbs, while the paravermal regions receive inputs from areas related to distal limbs. The *cerebro-cerebellum* is in relation with cortical areas from the cerebrum, mostly the motor and sensory cortices, through the pontine nucleus. The organization of cerebellar inputs is now known to include further levels of complexity which will be highlighted in the next paragraphs.

In birds and mammals, the cerebellum is foliated and those folds define further subdivisions of the cerebellar surface along the coronal plane. Two main folds are distinguishable: the primary fissure which separates the anterior lobe from the posterior lobe, and the secondary fissure which grossly separates the posterior lobe into two parts (lobule VI to VIII and lobule IX and X in the rat, *Figure 1.1.*). Within these coarse territories, folding defines the lobules (*Figure 1.1.*). Their nomenclature differs depending on whether they belong to the vermis, where they are numbered from I to X, or to the hemispheres, where their names vary among the species. Using the nomenclature established by Larsell (Larsell, 1952) in rodents and adopted by Voogd and Glickstein (Voogd and

Glickstein, 1998), we find in the posterior lobe arranged along the antero-posterior axis: the lobule simplex, the lobules Crus I and II, the paramedian lobule, the dorsal and ventral paraflocculus and finally the flocculus.

Although there are no obvious histological differences among different areas of the cerebellar cortex, the differential expression of various molecular biomarkers by sub-populations of Purkinje cells defines alternating longitudinal zones. The idea of a strong heterogeneity in protein expression within the cerebellum first emerged with the discovery of a peculiar expression of the enzyme 5'-nucleotidase in the anterior and posterior portions of the mouse cerebellum (Scott, 1963). Later, using appropriate staining methods and specific monoclonal antibodies, various others makers expressed by the Purkinje cells were found to be distributed in stripes (Hess and Voogd, 1986; Hawkes and Leclerc, 1987; Leclerc et al., 1990). For example, the “Zebrin II” epitope in rat allows distinguishing seven longitudinal bands Zebrin II + or Zebrin II – distributed along the medio-lateral axis (see *figure 1.1.*) (Brochu et al., 1990). Great similarities in this zonal pattern exist among species (birds (Feirabend and Voogd, 1986), fish (Brochu et al., 1990) and mammals (Leclerc et al., 1990)).

1.1.2. Cerebellar nuclei

In the cerebellar nuclei, early studies (Weidenreich, 1899; Brunner, 1919) distinguished at least three different nuclei, named by their position along the medio-lateral axis: the *nucleus medialis* or *fastigii*, the *nucleus interpositus* (or *nucleus intermedius*) and the *nucleus lateralis* or *dentatus*. Further divisions of the interposed nucleus into nucleus interpositus anterior in a rostral position and more caudal nucleus interpositus posterior were made according to cyto- and myeloarchitectonic studies (Snider, 1940; Flood and Jansen, 1961). As the cerebellar nuclei form a more or less continuous cell mass, any sharp delimitation between the separate nuclei is difficult, and the limits of each subnucleus differ between authors and species (*Figure 1.1.*).

Further delimitations of the cerebellar nuclei are defined by the topography of their inputs and notably the cortico-nuclear projections from the Purkinje cells of the cortex, which send their axons to the cerebellar and vestibular nuclei. The cortico-nuclear projections are highly topographically organized in parallel longitudinal zones. Three mains zones were first described: the lateral (hemispherical), intermediate (paravermal) and vermal compartments of the cerebellar cortex, projecting preferentially to the lateral, the interpositus (anterior and posterior subdivisions) and the medial nuclei, respectively (Jansen and Brodal, 1940). This tripartite organization was strongly supported by Chambers and Sprague's functional studies (Chambers and Sprague, 1955), where selective ablations and stimulations of one or another of those cortico-nuclear zones highlighted differential physiological roles for each regions. However, thirty years later, additional mappings of the cortical projections indicated that the projections of a given cortical area covers more than one cerebellar nucleus (Eager, 1963; Brodal and Courville, 1973; Courville et al., 1973) and that the organization of cortical afferents may be more complex than previously thought. Nowadays, the different zones of cortico-nuclear projections are extensively described¹ (for review, see Apps and Hawkes, 2009).

Projections from the zebrin II – positive or - negative Purkinje cell bands distinguish between different subnuclei (Sugihara and Shinoda, 2007) (*Figure 1.1.*) and illustrate the crossed organization

¹ The cortico-nuclear projections defined zones which have specific orderly extracerebellar afferents and that are called “modules”. This concept will be described in the Chapter 2.

of the cerebellar cortex and the nuclei. In addition to the gross regionalization of the cerebellar nuclei by zebrin - positive or - negative terminals, expression of various molecular markers by the different neuronal subpopulations (calcium-binding proteins (Fortin et al., 1998) (Rogers, 1989), transcription factors, enzymes and transporters of neurotransmitters (Chung et al., 2009)) identify a dozen of smaller expression domains.

Overall, a basic diagram emerges from those anatomical and functional studies. The three cerebellar nuclei are processing cerebellar cortical information through the cortico-nuclear afferents and extracerebellar inputs from diverse brain area. In turn, the cerebellar nuclei constitute the final output of the cerebellum and link it with a variety of premotor areas.

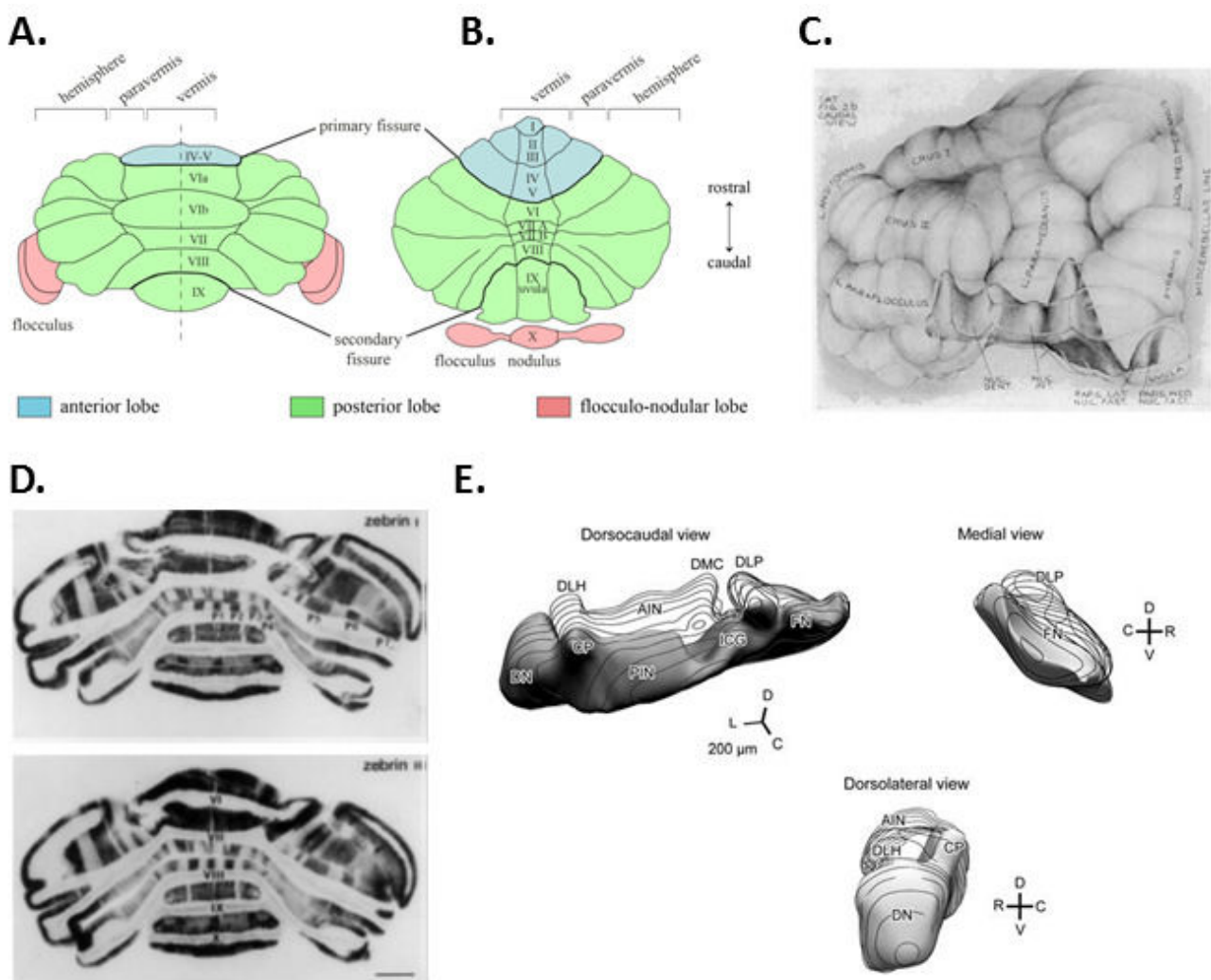


Figure 1.1: Anatomical and molecular segmentation of the cerebellar cortex and nuclei. A- Schematic drawing from a dorso-caudal view of the cerebellum. B- Schematic drawing of the "unfolded" cerebellar cortex. C- Drawing of the left half of cat cerebellum, with the cerebellar nuclei enclosed in the cortical sheet (From Snider, 1940). D- Longitudinal bands in the cerebellar cortex revealed by Zebrin I and Zebrin II epitopes expression (From Brochu et al., 1990). E- Three-dimensional reconstruction of the molecular pattern of Zebrin II - Aldolase C expression in the cerebellar nuclei. (From Sugihara and Shinoda, 2007).

1.2. *Sensori-motor circuitry in the cerebellum: Mossy fibers system as extracerebellar inputs – Cerebellar nuclei as final cerebellar output*

1.2.1. *Mossy fibers system: sensori-motor inputs*

To achieve online modulation of the motor command, the cerebellum receives sensori-motor information from various brain areas. Various brainstem nuclei, called *precerebellar nuclei*, such as the spinal cord, the lateral reticular nucleus, the paramedian reticular nuclei, the nucleus reticularis tegmenti pontis, or the basal pontine nuclei give rise to mossy fiber projections to the cerebellum that convey sensorimotor information. The multiplicity of precerebellar nuclei is one of the arguments against the broad functional topology of the three cerebellar subparts presented earlier: the distribution of their inputs may not overlap with the three main subdivisions and the situation may be more complicated than described in the previous section.

1.2.1.1. *Topography and somatotopy in the cerebellar cortex*

Mossy fibers enter the cerebellum rostrally through the superior (spinocerebellar fibers), middle (pontocerebellar fibers), or inferior (spinocerebellar, cuneocerebellar, vestibulocerebellar and reticulocerebellar fibers) cerebellar peduncles. Many of the mossy fibers cross the midline in the cerebellar commissure and distribute bilaterally. A single mossy fiber axon spreads widely in the mediolateral direction and makes collaterals in multiple lobules (Shinoda, 1999; Wu et al., 1999). The mossy fiber terminals end in the input layer of the cerebellar cortex, called the *granular layer*. Within the granular layer, the mossy fibers contact the dendrites of small and compact cells, the granule cells, within a tight synaptic structure: the *glomerulus*. Granule cell axons leave the granule cell layer to “ascend” to the output cortical layer: the *molecular layer* where they bifurcate to become the *parallel fibers*. Beams of parallel fibers are oriented along the coronal plane, and cross the dendritic arborization of the Purkinje cells perpendicularly, making contacts on their way (*Figure 1.2.*).

Therefore, mossy fiber inputs are relayed to the Purkinje cells via a di-synaptic pathway involving the granule cells and the parallel fibers, modulating the spontaneous firing frequency of simple spikes of the Purkinje cells. Mossy fiber activity can range from high-frequency bursts (Chadderton et al., 2004; Rancz et al., 2007) to slow and continuous firing modulation (Arenz et al., 2008; Arenz et al., 2009) both of which can be transmitted to granule cells (Rancz et al., 2007; Schwartz et al., 2012). Thus, as the activity in the granule cell layer is sparse, the firing patterns occurring in parallel fibers can be extremely diverse. This phenomenon is amplified by the gigantic number of parallel fibers synapses onto Purkinje cell spines (about 170 000 contacts by Purkinje cell (De Saint Jan et al., 2001)). Individual parallel fiber inputs elicit small responses (Isope and Barbour, 2002) and simultaneous activation of 50 granule cells is needed to excite a Purkinje cell (Barbour, 1993).

Mossy fibers convey multiple types of information: cutaneous (Eccles et al., 1971), proprioceptive (Balakrishnan and Trussell, 2008), somatosensory (Chadderton et al., 2004), vestibular (Lisberger and Fuchs, 1978) or visual (Noda, 1981) depending on the nature of the precerebellar nucleus from which they are originating. The diversity of mossy fiber inputs is somehow reflected in their organization. Mossy fiber projections from a given precerebellar nucleus terminate in specific lobules. This projection can be predominantly ipsilateral (for example the cuneocerebellar mossy

fibers) or contralateral (for example the spinocerebellar mossy fibers) and can innervate one or several lobules ((Wu et al., 1999; Cicirata et al., 2005), for review, see Shinoda and Sugihara, 2013).

Mossy fiber afferents to the cerebellar cortex are also finely organized topographically along the medio-lateral axis. Cartography of mossy fiber terminals reveals patterns of multiple longitudinal strip-like zones arranged successively along the mediolateral axis (Epema et al., 1985; Yaginuma and Matsushita, 1987). The mossy fiber input bands correlate with the zebrin band patterns found in the cerebellar cortex (Gravel and Hawkes, 1990; Sillitoe et al., 2010; Gebre et al., 2012), thus defining another level of molecular patterning of the cerebellar cortex.

Superimposed with this anatomical arrangement of mossy fiber terminals, with respect to their precerebellar origin and thus the type of information they are relaying (Gebre et al., 2012), a somatotopical organization of mossy fibers was described by Shambes *et al.* (Shambes et al., 1978) in anesthetized rats. Mossy fibers with identical tactile receptive fields project in multiples small areas in the cerebellar cortex, sometimes called “patches” and which can vary considerably in size and shape (Apps and Hawkes, 2009). These patches represent smaller functional areas within the larger longitudinal bands defined by anatomy and molecular expression. Shambes and colleagues described here an important concept of fractured somatotopical map, in which the cortex comprises a patchy mosaic of receptive fields arising from different body parts. The details of this “fractured somatotopy” are illustrated in *Figure 1.2*. A single mossy fibers can give several collaterals ending in several patches, (Woolston et al., 1981) and such redundancy might play an important role to link different somatosensory information provided by different areas of the body within a restricted cerebellar zone.

1.2.1.2. Mossy fibers innervation of the cerebellar nuclei

The cerebellar nuclei receive mossy fiber inputs from the same precerebellar nuclei: the nucleus reticularis tegmenti pontis (Van der Want et al., 1987), the spinal cord (Matsushita and Ikeda, 1970), the lateral reticular nucleus (Matsushita and Ikeda, 1976), the red nucleus (Courville and Brodal, 1966) or the vestibular system (Carpenter et al., 1959). However, the importance of mossy fiber projections from each particular precerebellar nucleus to one or the three nuclei vary and the existence of some mossy fiber pathways are still discussed (Brodal et al., 1986; Qvist, 1989; Pham et al., 2011). Mossy fiber inputs to the nuclei are collaterals from the fibers ending in the cerebellar cortex (Qvist, 1989; Wu et al., 1999).

As in the cerebellar cortex, mossy fiber inputs to the nuclei are nucleus-specific and depend on their precerebellar source, projecting to one or all cerebellar nuclei, either unilaterally or bilaterally with preferences for contralateral or ipsilateral innervation (Matsushita and Ikeda, 1970; Gerrits and Voogd, 1987; Cicirata et al., 2005). Although the topography of mossy fiber inputs to the cerebellum was investigated less thoroughly in the nuclei than in the cortex, a certain degree of somatotopy was described in the literature by tracing experiments (Courville and Brodal, 1966; Eccles et al., 1974d) or by electrophysiological mapping of cerebral inputs to cerebellar nuclei in monkeys (Allen et al., 1977; Allen et al., 1978)².

² It should be noticed that this somatotopic pattern may be weakly defined by the direct nuclear inputs from mossy fibers themselves, but rather shaped by the strong indirect inputs from the cortical Purkinje cells which are excited by the same groups of mossy fibers. Convergence of direct and indirect inputs onto nuclear neurons will be discussed latter.

Ultra-structural identification of mossy fiber terminals in the cerebellar nuclei was based on their supposed similarity with the characteristic morphology of the mossy terminals in the cerebellar cortex. Although well-defined glomerular structures were never described within the nuclei, some resemblance was noted (Van der Want et al., 1987). The shape of the terminals is irregular and they vary in diameter between 0.5 and 5 μm (Matsushita and Iwahori, 1971c; Van der Want et al., 1987). Mossy fiber terminals were generally found associated with distal dendritic compartments rather than axo-somatic or proximal dendritic areas (Courville and Brodal, 1966; Chan-Palay, 1973b; Van der Want et al., 1987).

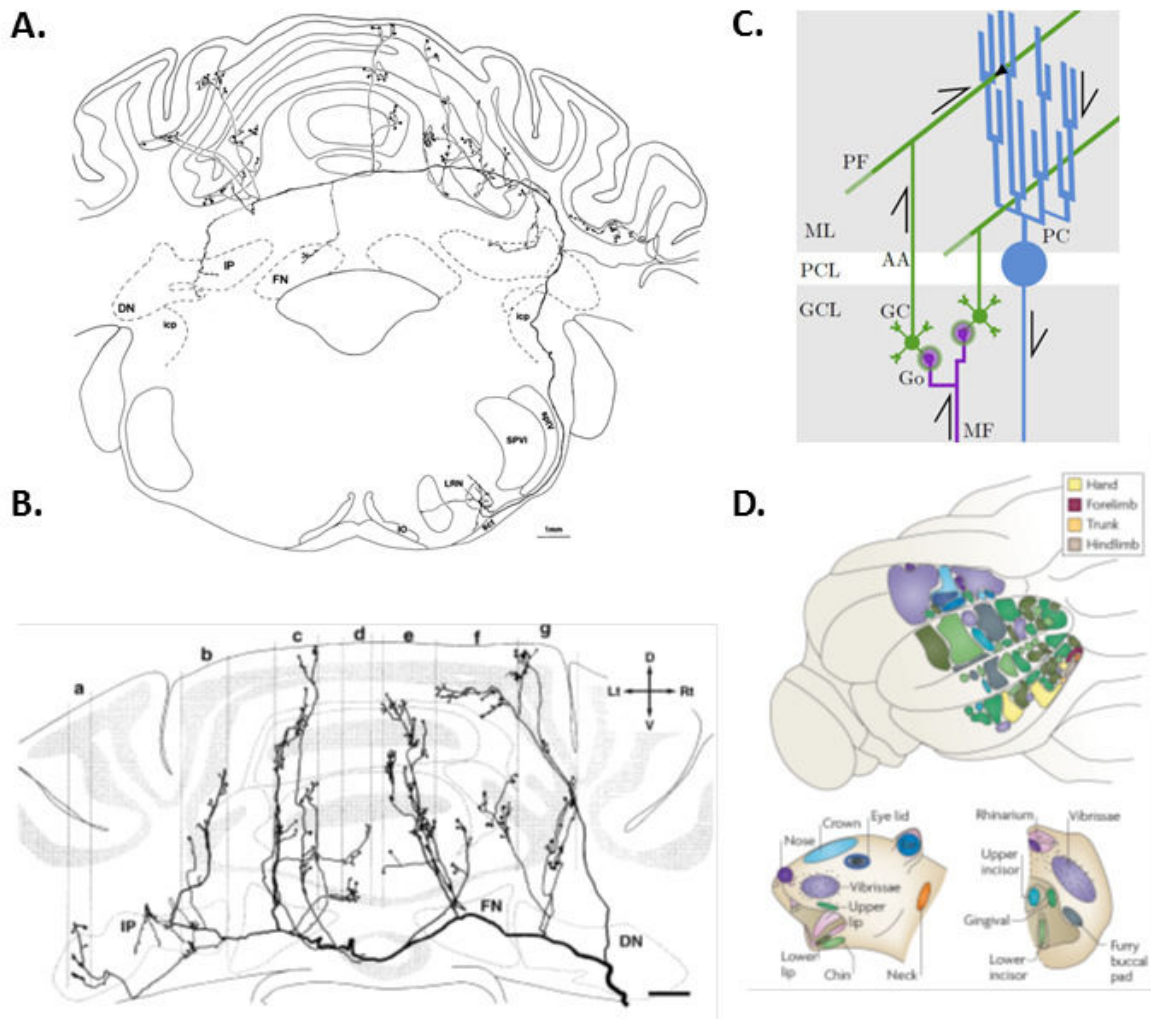


Figure 1.2: Mossy fibers inputs to the cerebellar cortex. A- Pathway of a single mossy fibers axon arising from the lateral reticular nucleus (LRN) (from Shinoda, 1999). B- Collateralizations of a single mossy fiber define longitudinal bands arranged along the medio-lateral axis (from Wu et al., 1999). C- Schematic drawing of the main circuit of the cerebellar cortex: mossy fiber (MF) enter the granular layer (GCL) where it contacts granule cells (GC) dendrites within the glomeruli (Go). The ascending axons (AA) of the granule cells reach the molecular layer (ML) and bifurcate to become parallel fibers (PF) which contact the Purkinje cells (PC) dendrites. D- “Fractured somatotopy” and patchy organization of the mossy fibers receptive fields in the granular layer of the cerebellar cortex (from Apps and Hawkes, 2009). Abbreviations: DN, IP, FN, and LRN, dentate, posterior interpositus, fastigial, and lateral reticular nucleus; icp, inferior cerebellar peduncle; IO, inferior olive; sct, sptV, and SPVI, spinocerebellar tract, spinal trigeminal tract and

nucleus interpositus PCL : Purkinje cells layer.

Therefore, mossy fibers provide a large diversity of sensori-motor information to the cerebellum, arising from the whole body. This important and diversified extracerebellar input is computed both at cortical and nuclear levels, before the final cerebellar output is sent to the rest of the brain.

1.2.2. The cerebellar nuclei: the cerebellar output to control motor function

The cerebellar nuclei constitute the final cerebellar output and project back to the various regions of the brain. Direct projections from one or multiple cerebellar nuclei were described to the thalamus (Angaut et al., 1985), the reticular pontine nucleus (Tsukahara and Bando, 1970), the red nucleus (Tsukahara et al., 1983), the vestibular system (Carpenter et al., 1959; Compoin et al., 1997), the nucleus reticularis tegmenti pontis (Verveer et al., 1997), several brainstem nuclei (Teune et al., 2000) or the spinal cord (Asanuma et al., 1980). The cerebellar nuclear outputs are topographically distributed (Rispoli-padel et al., 1982; Angaut et al., 1985; Cicirata et al., 1992) and define somatotopic maps in several premotor areas such as the thalamus (Asanuma et al., 1983).

The principal neurons³ of the cerebellar nuclei, which project to those regions, are large glutamatergic neurons (Schwarz and Schmitz, 1997), although it should be pointed out that a subpopulation of large glycinergic neurons in the medial nucleus are found to project to brainstem nuclei (Bagnall et al., 2009). They send most of their axons through the superior cerebellar peduncle (Jansen and Jansen, 1955). The principal neurons of the cerebellar nuclei consist of a heterogeneous population of neurons with different size, shape and dendritic pattern depending on their location within the nuclei (Sotelo and Angaut, 1973; Beitz and Chan-Palay, 1979a, b)⁴. Most of the neurons have a size between 25 and 50 μm and have a large dendritic field (300 to 500 μm in length), spreading within the limits of the nucleus (Matsushita and Iwahori, 1971a, b; Sotelo and Angaut, 1973).

Distinction of the different principal neuron subpopulations based on their morphology (*Figure 1.3.*) (Beitz and Chan-Palay, 1979a; Ristanovic et al., 2010) suggests a certain degree of organization within each cerebellar nucleus (Chan-Palay, 1973d; Beitz and Chan-Palay, 1979a). Whether this spatial and anatomical organization of the principal nuclear neurons is linked to the organization of the cortical or extracerebellar inputs is not clear.

1.3. CN principal neurons: a key synaptic integrator for the motor function

The principal neurons constitute the only cerebellar output and integrate different inputs, either inhibitory or excitatory. It is crucial to understand how this diversity of synaptic information will be processed by the principal neurons, and how it will influence the output motor command.

The cell surface of the principal neurons is mostly covered by axon terminals: up to 50% of the membrane is in direct apposition to synaptic boutons (Angaut and Sotelo, 1973). Purkinje cells axons and two other types of fibers, presumably from extracerebellar sources, are found converging onto nuclear cells (Matsushita and Iwahori, 1971c).

³ Another type of output cerebellar nuclear neurons exists, the GABAergic nucleo-olivary neurons, projecting only to the inferior olive, which will be described in the next sections in further details.

⁴ However, in those studies, principal neurons were not clearly distinguished from the other cell types found in the cerebellar nuclei. It is therefore possible that part of this heterogeneity within the principal neurons actually reflects the heterogeneity found among the different neuronal populations of the cerebellar nuclei.

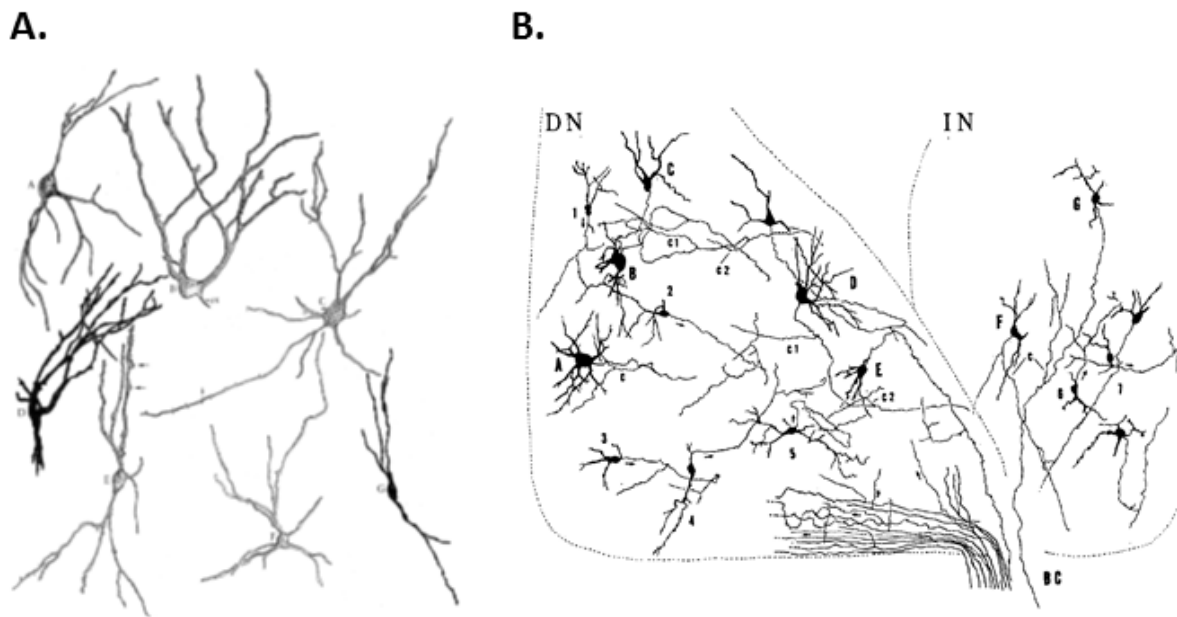


Figure 1.3: Principal neurons of the cerebellar nuclei convey the output information. A- Distinction between different populations of nuclear neurons was made possible with respect to their morphological characteristics. In the medial nucleus, seven classes of neurons were defined (from Beitz and Chan-Palay, 1979). B- Principal neurons send their axons through the cerebellar peduncles to premotor areas (from Matsushita & Iwahori, 1971b).

1.3.1. Synaptic inputs in principal neurons: Excitation versus Inhibition

1.3.1.1. Excitatory inputs

While the inhibitory inputs from Purkinje cells were extensively studied, little is known about excitatory inputs driving the nuclear neurons.

The principal neurons of the cerebellar nuclei express both non-NMDA (non-N-methyl-D-aspartate) and NMDA receptors (Gardette and Crepel, 1986; Audinat et al., 1990; Anchisi et al., 2001). AMPA (alpha-amino-3-hydroxy-5-methyl-4-isoxazole propionate) receptors seem to be only moderately expressed in the adult cerebellar nuclei (Beneyto and Meador-Woodruff, 2004) and may mainly be involved in developmental processes and networks maturation (Garcialadona et al., 1990), although no electrophysiological data exist to support the decrease of AMPA component of EPSCs in adult rodents. The properties of NMDA receptors combined weak agonist sensitivity and fast kinetics, suggesting they are hetero-trimeric assemblies from NR1, NR2A/2B and NR2C/2D (Akazawa et al., 1994; Cull-Candy et al., 1998; Anchisi et al., 2001).

The major source of excitatory inputs to the cerebellar nuclei is arising from extra-cerebellar sources in the form of mossy fiber collaterals. However, nuclear principal neurons occasionally give rise to recurrent collateral which could be involved in the local excitatory inputs to neighboring neurons (Matsushita and Iwahori, 1971a; Chan-Palay, 1973b; Mccrea et al., 1978). As those branched collaterals are generated from the axons on their way out of the nucleus, it is hard to preserve them in acute slices experiments, making their study complicated. This may explain why, to our knowledge, spontaneous excitatory activity has not been reported in the principal neurons in slices.

1.3.1.2. Purkinje cell inhibitory inputs

The Purkinje cells axons are thick and myelinated and contact the principal neurons in the downstream cerebellar nuclei, mostly via axo-dendritic and axo-somatic *en passant* giant boutons (Matsushita and Iwahori, 1971c). One Purkinje cell axon can innervate more than one nucleus (De Zeeuw et al., 1994) with the size and shape of the terminal arbors depending on the targeted nucleus (Sugihara et al., 2009). Within the nuclei, a Purkinje cell axon contacts primarily 3 to 6 principal neurons on their somata while providing weak input to many more (Palkovits et al., 1977). Furthermore, different Purkinje cells converge onto the same nuclear cell. Palkovits and colleagues (Palkovits et al., 1977) initially evoked a convergence of 860 Purkinje cells upon a single nuclear cell by counting the number of terminals ending onto it. However, this number was reevaluated in recent studies (Person and Raman, 2012a), bringing back this ratio to 30-50 Purkinje cells per nuclear cell (for discussion, see Person and Raman, 2012a). One of the most probable biases which could explain this difference comes from the presence of about ten active zones per Purkinje cell boutons (Pedroarena and Schwarz, 2003; Telgkamp et al., 2004).

The Purkinje cell terminals in the cerebellar nuclei release γ -aminobutyric acid (GABA) (Chan-Palay et al., 1979) and exert an inhibitory action onto the nuclear cells (Ito et al., 1970). The Purkinje cells inhibitory postsynaptic potentials (IPSPs) onto nuclear cells are mediated mainly by ionotropic GABA_A receptors (Mouginot and Gahwiler, 1995), although the principal neurons express also metabotropic GABA_B receptors (Morishita and Sastry, 1995). The IPSPs decay was first considered as being very slow (tens of milliseconds; Mouginot and Gahwiler, 1995; Anchisi et al., 2001; Pedroarena and Schwarz, 2003; Telgkamp et al., 2004; Pugh and Raman, 2005). Recordings at near-physiological temperature rather than room temperature invalidate this idea, revealing the brief decay time of the Purkinje cells IPSCs (around 2,5 milliseconds, Person and Raman, 2012b) which qualify amongst the fastest known GABA_A receptor mediated currents (Bartos et al., 2001).

The Purkinje cells are known to fire spontaneously around 30 Hz in the absence of synaptic inputs and up to 250 Hz (Thach, 1968; Armstrong and Rawson, 1979a; Hausser and Clark, 1997; Raman and Bean, 1997). It is known that at many synapses, high frequency activity leads to short-term depression of the inhibitory postsynaptic currents (IPSCs). This is indeed the case at Purkinje cells to principal neurons synapses (Mouginot and Gahwiler, 1995; Telgkamp and Raman, 2002; Pedroarena and Schwarz, 2003). However, mechanisms exist to limit synaptic depression: one Purkinje cell bouton contains about ten active zones (Pedroarena and Schwarz, 2003; Telgkamp et al., 2004) which each have a low release probability (Telgkamp et al., 2004) and promote spillover mediated transmission⁵ via this multi-sited release (Pedroarena and Schwarz, 2003; Telgkamp et al., 2004) or properties of desensitization and occupancies times of the receptors within the postsynaptic densities (Pugh and Raman, 2005).

1.3.1.3. Sequential integration of excitatory and inhibitory inputs

Consistent with the circuitry of the mossy fiber inputs previously described, recordings of the principal neurons show responses to a direct and indirect pathways following stimulation of the precerebellar nuclei. Electric or sensory-motor stimulation of mossy fibers evoked in the nuclear

⁵ However, spillover-mediated transmission was investigated at room temperature and need to be confirmed at more physiological temperatures.

neurons a direct excitation via the extracerebellar inputs, followed by an inhibition period due to the activation of the Purkinje cells in the cerebellar cortex by the same extracerebellar fibers (Ito et al., 1970; Eccles et al., 1974a; Armstrong and Rawson, 1979b; Llinas and Muhlethaler, 1988). Interactions between the direct excitatory inputs and the indirect inhibitory inputs depend on the strength of each of the converging inputs and above all on their respective timing (Eccles et al., 1974b; Amatuni et al., 1981). Excitation from mossy fiber activation is seen in the principal neurons 1 to 3 milliseconds and in the Purkinje cells 3 to 4 milliseconds after the stimulation of upstream precerebellar areas (Ito et al., 1970). Since it takes about one more millisecond for the activated Purkinje cells to inhibit the nuclear neurons, initiation of the inhibition following the direct excitation is expected 4 to 6 milliseconds after stimulation of the afferents. This characteristic sequence of “excitation-inhibition” in the nuclear neurons following sensory-motor stimulation is thought to be involved in mechanisms of plasticity and motor learning⁶.

In addition, a period of increased excitability sometimes follows the inhibitory effect provided by Purkinje cells. This late excitation could be explained by the disinhibition from Purkinje cells silenced by excitatory inputs and intra-cortical inhibitory interneurons and by the intrinsic electric properties of the principal neurons, as we will see in the next paragraph.

1.3.2. Principal neurons excitability and their electrophysiological properties

The intrinsic electrophysiological properties of the nuclear principal neurons have been studied in a variety of different preparations (for review, (Sastry et al., 1997)), including isolated brain stem-cerebellum slices (Llinas and Muhlethaler, 1988), cerebellar slices (Jahnsen, 1986b, a), organotypic cultures (Mouginot and Gahwiler, 1995) or dissociated neurons (Raman et al., 2000).

1.3.2.1. Spontaneous firing

The nuclear principal neurons, like the Purkinje cells, discharge spontaneous action potentials at rates close to 30 Hz (Thach, 1968; Jahnsen, 1986a; Llinas and Muhlethaler, 1988; Mouginot and Gahwiler, 1995; Aizenman and Linden, 1999; Raman et al., 2000). The firing rate can reach 300 Hz when a depolarizing current is injected to the neurons (Jahnsen, 1986a). Spontaneous firing is generated and maintained by the intrinsic properties of the nuclear neurons, as suggested by studies on dissociated neurons (Raman et al., 2000) and after blockade of all synaptic inputs (Mouginot and Gahwiler, 1995; Aizenman and Linden, 1999). Expression of a variety of different ionic channels allow the generation of pace-maker like currents to maintain the cycle of firing (Jahnsen, 1986a, b; Llinas and Muhlethaler, 1988; Sastry et al., 1997; Raman et al., 2000; Alvina and Khodakhah, 2008; Ovsepian et al., 2013).

The firing rate of the nuclear neurons is modulated by both their excitatory and inhibitory synaptic inputs (Mouginot and Gahwiler, 1995; Zhang et al., 2004). Consistently, the principal neuron discharge rates are modulated during motor behaviors (Thach, 1968; Armstrong and Edgley, 1984). *In vivo*, the influence of the inhibitory inputs may be more complex than a simple decrease in the nuclear neuron firing rate. When McDevitt and colleagues (Mcdevitt et al., 1987) recorded simultaneously from Purkinje cells and their related nuclear neuron, their firing rates did not always vary inversely suggesting that the Purkinje cells and the principal neurons do not have necessarily a

⁶ Plasticity in the cerebellar nuclei will be discussed in Chapter 2.

reciprocal relationship. This result indicates that a single Purkinje cell does not dominate the discharge activity of the principal neurons it contacts, and implies more heterogeneous and complex interactions with other afferents to the cerebellar nuclei. Intrinsic electrophysiological properties of nuclear neurons, such as their ability to generate rebound firing, may also explain this non-reciprocity.

1.3.2.2. *Characteristics of the rebound discharge*

In addition to their spontaneous firing, a characteristic of principal nuclear neurons is their ability to show pronounced rebound depolarization, often accompanied by a high-frequency burst of spikes or just by a more prolonged period of increased firing, immediately after an hyperpolarization period (Jahnsen, 1986a, b; Llinas and Muhlethaler, 1988; Aizenman and Linden, 1999; Pedroarena, 2010). The rebound depolarization is dependent on the membrane potential of the cell and on the duration and amplitude of the hyperpolarizing pulse: it is more prominent following longer and deeper hyperpolarization steps, or when the holding membrane potential is between -60 and -70 mV (Aizenman and Linden, 1999; Pedroarena, 2010). The rebound is readily induced by hyperpolarizing current injection at the soma, and can also be evoked by more physiological manipulations like the local uncaging of GABA or the electrical stimulation of hyperpolarizing IPSPs originating from Purkinje cell inputs (Llinas and Muhlethaler, 1988; Aizenman et al., 1998; Aizenman and Linden, 1999; Alvina et al., 2009). Interestingly, high-frequency trains of IPSPs were more effective at inducing a rebound discharge than a single IPSP or hyperpolarizing current pulses of similar amplitude and duration. This could be explained by the wide distribution of the Purkinje cell inputs on the dendritic arbor of the principal neurons. Distal inhibitory inputs will produce effective dendritic hyperpolarization which is most likely not achieved by hyperpolarization delivered from the soma. Diverse dynamic parameters of these synapses (as discussed in the section 1.3.1.1.) may also be involved in the efficiency of synaptic hyperpolarization to trigger rebounds.

During the rebound, the increased excitability and associated spike burst induce large intracellular calcium transients in the principal neurons (Aizenman et al., 1998; Zhang et al., 2004; Schneider et al., 2013). By this way, inhibitory Purkinje cell inputs can drive postsynaptic excitation and calcium entry in the nuclear neurons, which mechanism may be the basis for plasticity at the Purkinje cell to principal neurons synapse (Aizenman et al., 1998)⁷.

Several attempts have been made to link the different firing and bursting phenotypes of nuclear cells to their morphological characteristics, with no clear success (Aizenman et al., 2003). Bursting phenotypes seem to be specific of principal neurons (Czubayko et al., 2001), however other cell types in the cerebellar nuclei also exhibit spontaneous firing (Uusisaari and Knopfel, 2011)⁸.

The principal nuclear neurons express voltage-gated calcium channels, and notably the T-type channels (Muri and Knopfel, 1994; Gauck et al., 2001; McKay et al., 2006; Molineux et al., 2006; Molineux et al., 2008; Tadayonnejad et al., 2010), which are known to support burst firing (Cain and Snutch, 2010). The different isoforms of T-type channels, Cav3.1 ($\alpha 1G$), Cav3.2 ($\alpha 1H$), Cav3.3 ($\alpha 1I$), exhibit non-uniform distribution on the membrane of the principal neurons: Cav3.1 channels are expressed mainly in somatic compartments while Cav3.3 are found also in distal dendrites (Gauck et al., 2001; McKay et al., 2006). They are also associated with different bursting phenotypes: high

⁷ Mechanisms and properties of plasticity in the cerebellar nuclei will be discussed in further details in the next sections.

⁸ Other cell types present in the cerebellar nuclei and their physiological properties will be described in the next sections

bursting neurons are associated with the rapidly gating Cav3.1 isoform, whereas neurons with weak bursts preferentially express the slower gating Cav3.3 (Figure 1.4.) (Molineux et al., 2006; Molineux et al., 2008), suggesting a differential role of each of those isoforms in agreement with their distinct kinetic properties (for review, see Cain and Snutch, 2010). Moreover, their rebound discharges are blocked by T-type channel antagonists (Molineux et al., 2008; Alvina et al., 2009; Boehme et al., 2011; Schneider et al., 2013) indicating the central role of T-type channels in the mechanisms underlying the rebound.

Taken together, the high dependency of the rebound discharge to a hyperpolarizing step and its following bursting phenotype and calcium entry suggest that the rebound depolarization is mediated, at least in large part, by the opening of low-threshold voltage-dependent T-type calcium channels.

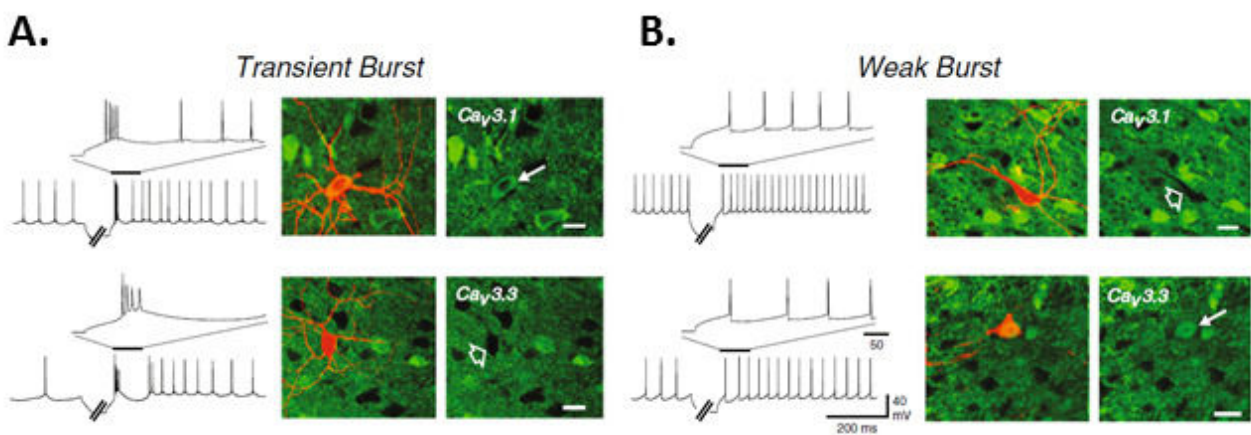


Figure 1.4. Rebound discharge phenotypes in the principal neurons of the cerebellar nuclei. A- Transient bursts are defined by high frequency bursts after a hyperpolarization period, and are correlated with the expression of the T-type voltage-gated calcium channels isoform Cav3.1. B- On the contrary, weak burst phenotypes are associated with the expression of Cav3.3 channels (from Tadayonnejad et al., 2010).

1.3.2.3. Does the rebound discharge exist in vivo?

Despite the biophysical robustness of rebound firing in the principal neurons, its prevalence in response to physiological stimuli is still debated. After sensory stimulation, the responses of nuclear neurons *in vivo* do not present the expected rebound discharge after inhibition periods, but rather consist in a sequence of early excitation – intermediate inhibition – late increase in firing rate (Armstrong et al., 1975; Rowland and Jaeger, 2005). The late excitation, which could perhaps be the consequence of a rebound depolarization after the intermediate inhibition from the Purkinje cell inputs, was however the least reliable component of the response (Rowland and Jaeger, 2005). As previously discussed in section 1.3.1.3., this late excitation may be due in part to the nuclear disinhibition resulting from pauses in the Purkinje cell firing (Ito et al., 1970; Armstrong et al., 1975; Witter et al., 2013). Moreover, direct and strong activation of the Purkinje cell inputs upon a nuclear neuron *in vivo* does not result in rebound firing in the majority of the recorded cells (Alvina et al., 2008; Chaumont et al., 2013). Occurrence of the rebound firing also differs between the experimental paradigm used (for reviews of protocols, Alvina et al., 2008; De Zeeuw et al., 2011).

As the rebound discharge phenomenon is entirely based on the occurrence of an inhibition period and on its efficiency to activate several conductances like the T-Type channels, the main open

question is the extent to which *in vivo* synaptic inhibition can efficiently recruit T-type currents and lead to observable rebound firing. Several discrepancies have been pointed out. First, *in vivo* activation of GABA_A receptors cannot hyperpolarize cells further than the membrane reversal potential for chloride ions (E_{Cl}). This later has been repeatedly measured to be near -75 mV in the principal neurons (Jahnsen, 1986b; Aizenman and Linden, 1999; Alvina et al., 2008; Zheng and Raman, 2009). The known voltage-dependence of T-type channels makes it unlikely that they recover substantially even at E_{Cl} under those conditions (Cain and Snutch, 2010). Therefore, only the neurons which are hyperpolarized (by current injections for example) beyond E_{Cl} will generate a rebound burst. Modeling studies suggest that the E_{Cl} value for nuclear neurons was in a critical region where small changes on the order of 5–10 mV only would have a strong influence on rebound strength (Steuber et al., 2011). Secondly, Zheng *et al.* (Zheng and Raman, 2009) reported that high-frequency IPSPs evoke little post-inhibitory current through T-type channels, without evidence of T-type mediated large and brief calcium transients even in dendrites during imaging studies. Additionally, the late elevation in the firing rate observed after strong inhibition is very slow and persists for several hundred milliseconds (Armstrong et al., 1975; Rowland and Jaeger, 2005; Alvina et al., 2009; Zheng and Raman, 2009), far outlasting the duration of T-type current (Cain and Snutch, 2010).

An interesting alternative hypothesis is that the T-type channel currents mediating the rebound firing are highly modulated *in vivo* and act synergically with other conductances. In the cerebellum, complex interactions between T-type channels and other conductances influence the net effect of T-type channels on neuronal excitability (Engbers et al., 2013). Window current, which relies on the few channels that are stochastically opened at approximately -60 mV thus creating a steady-state conductance (Cain and Snutch, 2010), may also play an additional role in the generation of rebound firing by modulating the basal intracellular calcium level and therefore act on intracellular machinery to modulate the neuronal excitability (Engbers et al., 2012; Engbers et al., 2013).

The post-inhibitory propensity to burst has been shown to increase with the strength of stimulation of Purkinje afferents (Aizenman and Linden, 1999; Tadayonnejad et al., 2009), but as the depth of hyperpolarization won't change significantly with increased synaptic inhibition, this raises the possibility that stronger stimulations facilitate the rebound discharge by engaging additional mechanisms. First inhibition may activate other ionic conductances. Indeed, several channels expressed by the nuclear neurons have been shown to play a role in the rebound discharge (high-voltage-activated calcium current (HVA) (Muri and Knopfel, 1994; Gauck et al., 2001), potassium channels (Molineux et al., 2008), hyperpolarization-activated cyclic-nucleotide (HCN) (Engbers et al., 2011)). Moreover, interactions between diverse background synaptic conductances in the nuclear neurons have been found to exert a great influence on the appearance of the rebound phenotype and its strength (Steuber et al., 2011). Second, neuromodulatory systems may also have a strong influence on the rebound bursting phenotypes *in vivo* (Gould et al., 1997; Saitow et al., 2009; Murano et al., 2011; Schneider et al., 2013), but have been poorly studied. Modulations in the E_{Cl} itself, which may become more negative under certain conditions such as modulations in the expression of the chloride co-transporters NKCC1 and KCC2 known to control the E_{Cl} in neurons (Rivera et al., 1999; Banke and McBain, 2006), could also explain the variable occurrence of rebound discharge *in vivo*.

Importantly, rebound patterns are also significantly shaped and influenced by the inputs received by the nuclear neurons (Steuber et al., 2011) and by the intrinsic excitability of the nuclear neurons. Relative timing and strength of the inhibitory inputs will have a major impact on the oc-

currence of the rebound discharge, as synchronous recruitment of several Purkinje cells⁹ has been shown to more likely to have an effect on principal neurons output activity (Gauck and Jaeger, 2000; Person and Raman, 2012a, b). In addition, as demonstrated in my thesis work, synaptic inhibition upon nuclear neurons is not restricted to the Purkinje cells inputs but can also be provided by local interneurons of the cerebellar nuclei, which inhibitory properties could be different from cortical inputs¹⁰.

In conclusion, the debate about the existence of a rebound discharge phenomenon during physiological processes is mainly due to our poor understanding of the integration by the nuclear cells of a wide range of excitatory, inhibitory and neuromodulatory inputs with respect to the own excitability state and intrinsic properties of the nuclear neuron. Therefore, further dissection of the cerebellar nuclei circuitry is crucial to improve our knowledge of the nuclear neuron physiology *in vivo*.

1.3.3. Principal neuron output activity: Rate coding versus temporal coding

To predict the nuclear neuron output spiking activity, one needs to understand their mechanisms of synaptic integration and their interactions with the intrinsic membrane properties of these principal neurons. Understanding which information is transmitted to the nuclear neurons and how they encode it into output activity is fundamental (Person and Raman, 2012b). Neuronal coding can be broadly categorized as “rate coding” or “temporal coding”. The number or rate of spikes in a particular time window carries information in the rate coding mode, whereas for temporal coding, the information is represented by the timing of individual spikes or bursts of spikes. Both rate coding and temporal coding seem to occur in the cerebellar nuclei (Steuber and Jaeger, 2013).

Rate coding in the nuclear neurons would imply that the relative firing rates coming from excitatory and inhibitory inputs determine the output spike frequency of the cerebellar nuclear cells. Indeed, dynamic clamp studies have suggested that the rate of Purkinje cell inputs results in a rate code in the nuclear cells (Gauck and Jaeger, 2000, 2003) and that increases in excitatory mossy fiber input rates or decreases in inhibitory Purkinje cell input rates are translated into smooth increases of the nuclear spike rates (Steuber et al., 2011). Modulation of Purkinje cell spike rates has been proposed to encode information in the cerebellar nuclei by linear summation more efficiently than pauses (Walter and Khodakhah, 2009).

The ability of nuclear neurons to exhibit rebound firing make them good candidates for temporal coding, as the rebound discharge may create well-timed spike burst following certain patterns of Purkinje cell inputs. Rebound firing has been incorporated into recent theories of cerebellar function (Kistler and De Zeeuw, 2003; Wetmore et al., 2008) and several functional roles have been assigned to it, such as timing and encoding information in association with plasticity mechanisms both at cortical and nuclear levels (Aizenman et al., 1998; Kistler and De Zeeuw, 2003; Pugh and Raman, 2006; Wetmore et al., 2008).

One of those models involving rebound discharge was described by Wetmore and colleagues (Wetmore et al., 2008) who defined a model of cerebellar motor memory and learning, called the

⁹ Mechanisms responsible for synchronization of the Purkinje cells will be detailed in further details in Chapter 2.

¹⁰ Evidence for the involvement of local inhibition in the cerebellar nuclei will be discussed in the Chapter 3.

“lock and key” hypothesis. In this model, the mechanisms of plasticity in the cerebellar cortex were necessary but not sufficient to generate a desired cerebellar output. The cortical output activity arising from those operations has to result in the appropriate temporal patterns to elicit rebound in the downstream nuclear cells, *i.e.* an increase (to hyperpolarize the neurons) followed by a decrease in the Purkinje cell spike rate (releasing the inhibition and allowing the neurons to fire). According to Wetmore *et al.*, the cortical temporal spike patterns represent a “key”, while the temporal filtering properties of the nuclear neurons that determine whether or not a rebound response occurs is a “lock”. Therefore, successful learning shapes neural activity to match a temporal filter that prevents expression of stored but inappropriate motor responses.

According to another model (Kistler and De Zeeuw, 2003), under some specific assumptions about cerebellar anatomy and physiology¹¹, rebound discharge of the nuclear neurons translate inhibitory Purkinje cell inputs into a delayed excitatory nuclear output independent of the strength or temporal synchronization of the simulated inputs. For example, the authors have shown that random and independent activation of Purkinje cell inputs upon the same nuclear neuron result in a somatic membrane potential that is fluctuating around the resting potential without triggering any action potentials. On the other hand, if the Purkinje cell inputs are synchronized, several action potentials are evoked in the principal neurons, with a delay of about 100 millisecond independent of the size or the temporal dispersion of the inhibitory volley.

Indeed, synchronization of activity among a group of several Purkinje cells has an important impact on principal neuron output activity and nuclear neurons preferentially relay information emerging from the activity of synchronized Purkinje cells to downstream premotor areas, notably by their time-locked spiking (Gauck and Jaeger, 2000; Person and Raman, 2012a, b; Witter *et al.*, 2013). This constitutes one great example of temporal coding within the olivo-cerebellar system.

Evidence for the presence of both rate coding and temporal coding in nuclear neurons suggest that they are indeed able to use both encoding depending on the conditions. It has already been proposed that the Purkinje cells are able to alternate between a rate and a

temporal coding strategies (Hausser and Clark, 1997; De Schutter and Steuber, 2009) and that this switch between regular firing and pauses in spiking of the Purkinje cells interact to control the cerebellar nuclei output activity (De Schutter and Steuber, 2009; discussed in section 1.3.3.1.).

One could also imagine a form of rate coding within the rebound discharge, where information could also be carried by the rate of spikes in the rebound burst, in addition to the more common forms of rate coding described.

¹¹ Authors notably based their model on the organization and the characteristics of the olivo-cerebellar system, to which we will refer in the Chapter 2.

CHAPTER 2: The olivo-cortico-nuclear loop

The inferior olive complex is an ensemble of nuclei located bilaterally in the ventral part of the brainstem. The inferior olive gives rise to the second system of excitatory inputs to the cerebellum: the climbing fibers system. This olivary afferent system is a strong organizer, both spatially and functionally, and the close relationship between cerebellum and inferior olive lead to the definition of an olivo-cerebellar system.

2.1. Inferior olive projection to the cerebellar cortex

2.1.1. Olivo-cortical innervation

2.1.1.1. One-to-one innervation of the Purkinje cells

Contrarily to the mossy fiber system and its large variety of precerebellar nuclei of origin, all the climbing fibers arise from the inferior olive (Desclin, 1974).

The olivo-cerebellar axons originate from one of the three main nuclei of the inferior olive (the principal olive and the medial and dorsal accessory olive) and enter the cerebellum through the contralateral inferior cerebellar peduncle (Sugihara et al., 1999; Sugihara et al., 2001). Within the cerebellum, a single olivo-cerebellar axon bifurcates in several thick branches (up to seven), each one of them innervating one Purkinje cell (Sugihara et al., 1999; Sugihara et al., 2001). Each olivary fiber “climbs” on the main shafts of a Purkinje cells dendritic tree in the molecular layer of the cortex (see *figure 2.1.*), giving its name to this olivo-cerebellar fiber. During the development, the Purkinje cell is initially contacted by about five different climbing fibers (Crepel et al., 1976; Sugihara, 2006; Watanabe and Kano, 2011). Only one of them is selected and strengthened¹² allowing the maturation of the climbing fiber synapses, while the others degenerate (Bosman and Konnerth, 2009; Hashimoto et al., 2009; Watanabe and Kano, 2011) leading in the adult to a one-to-one relationship between the climbing fibers and the Purkinje cells.

2.1.1.2. Climbing fiber input elicit complex spike

In the Purkinje cells, climbing fiber activation produces a strong all-or-nothing excitatory response of large amplitude and a large depolarization called the complex spike (Eccles et al., 1966; Konnerth et al., 1990). The shape of the complex spike is characteristic: a first large and sharp spike followed by several oscillations of decreasing amplitudes (see *figure 2.1.*) (Eccles et al., 1966;

¹² This synaptic selection seems to require both genetic determinants and early synaptic activity (Bosman and Konnerth, 2009).

Armstrong and Rawson, 1979a; Mathy et al., 2009).

One of the most striking properties of the complex spikes on the Purkinje cell activity is that the generation of the complex spike usually prevents the Purkinje cell to fire simple spikes for tens of milliseconds (Armstrong and Rawson, 1979a; Sato et al., 1992; De Zeeuw et al., 2011). The complex spike occurs at very low frequency around 1 Hz in vivo (Armstrong and Rawson, 1979a; Lang et al., 1999; Loewenstein et al., 2005; Mathy et al., 2009) and is essential for plasticity and motor learning¹³.

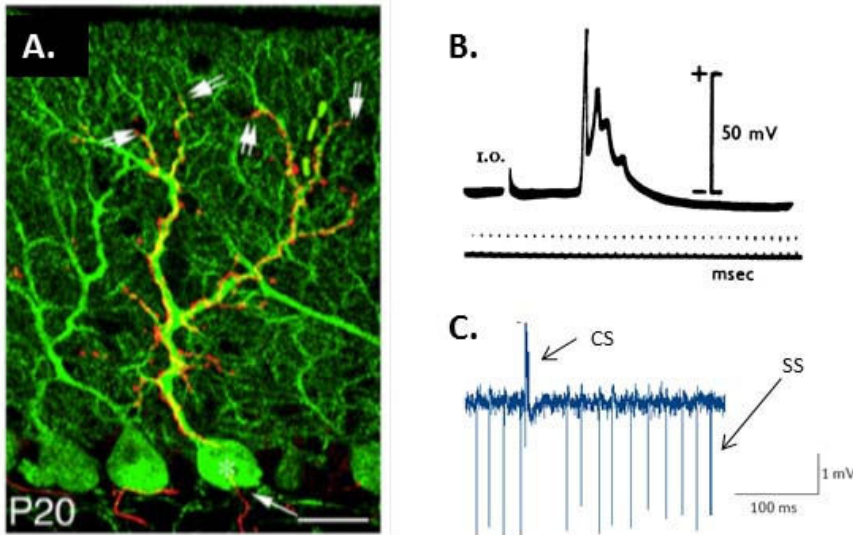


Figure 2.1. Climbing fiber innervation in the cerebellar cortex. A- The climbing fiber, in red, labelled by biotinylated dextran amine injection in the inferior olive, innervates extensively the main shaft of the Purkinje cell, in green, revealed by immunostaining against Calbindin. Scale bar: 20 μ m (from Hashimoto et al., 2009). B- The activation of climbing fibers through inferior olive stimulation induces a complex spike in the Purkinje cells (from Eccles et al., 1966). C- Generation of a complex spike (CS) in Purkinje cells results in a pause in the simple spike (SS) firing (from De Zeeuw et al., 2011).

2.1.2. Parasagittal segmentation of the climbing fibers inputs

While mossy fibers from a given source display extensive transverse branching and diverge to terminate in multiple longitudinal zones (*see section 1.1.1.*), climbing fibers arising from a given nucleus of the olive are mainly directed to one or two longitudinal zones of the cerebellar cortex (Voogd and Glickstein, 1998; Apps and Hawkes, 2009).

The multiple climbing fibers originating from the same olivo-cerebellar axon innervate Purkinje cells arranged in the same parasagittal planes (Sugihara et al., 2001) and thereby, stimulation of one of the branches in one place of the cortex can elicit responses in other Purkinje cells contacted by the same olivo-cerebellar axon and located in the same longitudinal bands by retro-propagation (Armstrong et al., 1973a). The climbing fiber projections to the cerebellar cortex are arranged topographically in those specific narrow sagittal bands (Brodal et al., 1975; Courville, 1975; Brodal, 1976; Chan-Palay et al., 1977; Wiklund et al., 1984) and follow the zebrin expression pattern in the cerebellar cortex (Sugihara and Shinoda, 2004). The investigation had been prompted by previous physiological data (Oscarsson, 1968; Armstrong et al., 1973b).

This parasagittal organization of the climbing fiber cortical inputs has important consequences on the Purkinje cell activity within and across the longitudinal bands thereby defined. A circumscribed subdivision of the inferior olive innervates many Purkinje cells within a longitudinal zone, and the activation of this beam of climbing fibers thus induces synchronized complex spikes

¹³ This will be described in further details in the next paragraphs.

within this parasagittal band of Purkinje cells, with millisecond precision (Welsh et al., 1995; Hanson et al., 2000; Ozden et al., 2009; Schultz et al., 2009; Wise et al., 2010). This synchronization of complex spike activity results in a pause in the Purkinje cell simple spike firing, and therefore synchronized activity of several Purkinje cells within a longitudinal band leads to a common sensitivity to sensori-motor stimuli (Wise et al., 2010; De Zeeuw et al., 2011).

2.2. The cerebello-olivary feedback loop

The olivo-cerebellar system is a closed loop, where the cerebellum gives rise to a reciprocal feedback projection onto the inferior olive. This cerebello-olivary pathway originates from the cerebellar nuclei and is arising from small neurons, called the nucleo-olivary neurons.

2.2.1. The nucleo-olivary cells

The first discovery of the cerebello-olivary pathway was made in the seventies, notably by Graybiel and colleagues (Graybiel et al., 1973) in the cat and confirmed later in other species (rat (Brown et al., 1977), opossum (Martin et al., 1976), monkeys (Kalil, 1979)). This nucleo-olivary projection leaves the cerebellum in a separate bundle through the superior cerebellar peduncle and mainly innervates the contralateral inferior olive (Graybiel et al., 1973; Tolbert et al., 1976b) in a topographical manner (Graybiel et al., 1973; Beitz, 1976; Tolbert et al., 1976b; Kalil, 1979; Ruigrok and Voogd, 1990). Although strong projections were found from the interposed and lateral nuclei, olivary inputs from the medial nucleus appeared more diffuse (Graybiel et al., 1973; Martin et al., 1976; Legendre and Courville, 1987; Ruigrok and Voogd, 1990) or could not be demonstrated (Tolbert et al., 1976b; Kalil, 1979). Importantly, this orderly projection is reciprocal: the circumscribed area of inferior olive projecting to a given cerebellar sub-nucleus receives inputs from this later (Beitz, 1976; Dietrichs and Walberg, 1986; De Zeeuw et al., 1997).

The origin of the nucleo-olivary fibers is a population of small neurons predominantly located in the ventral part of the nucleus (Martin et al., 1976; Tolbert et al., 1976b; Buisseret-Delmas and Batini, 1978) and already described in early studies (Flood and Jansen, 1961; Matsushita and Iwahori, 1971d). Their somata size (10 to 20 μm) and their ovoid shape usually distinguish them from the large principal neurons¹⁴ even though size distributions are somehow overlapping (Martin et al., 1976; Legendre and Courville, 1987).

One of the particular features of these nucleo-olivary cells is their GABAergic phenotype (Angaut and Sotelo, 1987; De Zeeuw et al., 1988; Fredette and Mugnaini, 1991) and their inhibitory effect on the inferior olive (Andersson and Hesslow, 1987; Andersson et al., 1988; Garifoli et al., 2001; Svensson et al., 2006). In the neuropil of the inferior olive the dendritic spines of the olivary neurons, which exhibit a remarkably long neck, are enclosed in glomeruli together with axonal terminals of both excitatory and inhibitory inputs (King, 1976; De Zeeuw et al., 1990a; De Zeeuw et al., 1990b; De Gruijl et al., 2013). Interestingly, terminals of nucleo-olivary axons are found to end on

¹⁴ However, the use of a size threshold and morphological parameters to distinguish the nucleo-olivary neurons, notably from the nuclear medium-size interneurons should be taken cautiously, as the values differs between studies (15 - 20 μm (Legendre and Courville, 1987), 10 - 15 μm (Tolbert et al., 1976), 11 - 16.5 μm (Martin et al., 1976), less than 10 μm (Fredette and Mugnaini 1991)) and that the distribution of somata diameter are overlapping. In the next sections, we will come back on the distinction between these two populations of nuclear neurons.

dendrites near gap junctions which are electrically coupling the olivary neurons (Angaut and Sotelo, 1987, 1989; De Zeeuw et al., 1989; Fredette and Mugnaini, 1991) and thus are thought to have an important effect on the synchronization of inferior olive neurons.

2.2.2. Cerebellar control of the inferior olive activity

2.2.2.1. Structural organization of the inferior olive: electrotonic coupling and subthreshold oscillations

The inferior olive is mainly composed of two types of morphologically distinct projection neurons which both give rise to climbing fibers (De Zeeuw et al., 1998; De Gruijl et al., 2013). One of the major characteristic of the olivary neurons is their rhythmic activity. Olivary neurons generate prominent endogenous subthreshold oscillation of two types: 3 – 10 Hz sinusoidal subthreshold oscillations and 1 – 3 Hz low-threshold calcium oscillations (see *figure 2.2.*) (Llinas and Yarom, 1986; Khosrovani et al., 2007; Mathy and Clark, 2013). The intrinsic membrane properties of the olivary neurons, together with the electrotonic coupling which exists between the olivary cells through gap junctions connections within the glomeruli (Llinas and Volkind, 1973; King, 1976; De Zeeuw et al., 1990a) determined frequency and pattern of oscillations (De Zeeuw et al., 2003; Placantonakis et al., 2006). Those oscillations can have an impact on the pattern of spontaneous discharge of the olivary neurons.

The olivary neurons fire rhythmically both *in vitro* (Llinas and Yarom, 1986) and *in vivo* (Khosrovani et al., 2007), although their spiking rate is surprisingly low (not exceeding 5-8 Hz) compared to the generally very active olivo-cerebellar circuit elements. The olivary neuron spike has a complex shape (see *figure 2.2.*) consisting of an initial fast and sharp sodium spike followed by a broad after-depolarization on which one to seven spikelets are superimposed, occurring at high-frequency (200–500 Hz) (Mathy and Clark, 2013). These somatic spikelets propagate to the axon and initiate a burst of spiking, which number of spikes is determined by the phase of the subthreshold oscillations during which they were emitted. This burst is efficiently transmitted to the post-synaptic Purkinje cells and shape their complex spike itself (Eccles et al., 1966; Maruta et al., 2007; Mathy et al., 2009; De Gruijl et al., 2013; Mathy and Clark, 2013), thus providing a temporal information relative to the olivary oscillatory state up to the cerebellum.

As dendritic spines of olivary neurons are electrotonically coupled, spikes and oscillations can spread and synchronize among the neighboring neuronal population (Devor and Yarom, 2002b, a; Leznik et al., 2002). The synchronization of small groups of olivary neurons which project to defined circumscribed groups of Purkinje cells within a parasagittal band is one of the key element for the synchronization of the downstream Purkinje cells activity (Lang et al., 1996; Lang, 2002; Marshall et al., 2007). Synaptic inputs to the inferior olive influence the formation of ensembles of synchronously active neurons by modulating the strength of electrotonic coupling (Lang et al., 1996; Placantonakis et al., 2000; Placantonakis and Welsh, 2001; Lang, 2002; Hoge et al., 2011; Lefler et al., 2014; Mathy et al., 2014) and thereby are able to influence the impact of olivary activity on cerebellar physiology.

2.2.2.2. Inhibitory action of the nucleo-olivary neurons on the inferior olive physiology

The nucleo-olivary electrophysiological properties were poorly studied. It was suggested

however that those neurons could fire spontaneously between 6 and 10 Hz (Uusisaari and Knopfel, 2013) although clear characterization is lacking.

Nucleo-olivary neurons release GABA asynchronously onto olivary neurons (Best and Regehr, 2009), rendering the transmission extremely frequency-dependent, low frequency inputs being poorly transmitted. Together with the slow activation kinetics of the somatic olivary neurons GABA_A receptors (extra-synaptic clusters containing the $\alpha 3\beta 2/3\gamma 2$ subunits, (Devor et al., 2001)), the characteristics of the nucleo-olivary pathway are therefore a good way to translate the firing rate of the nuclear neurons into delayed sustained inhibition of the inferior olive.

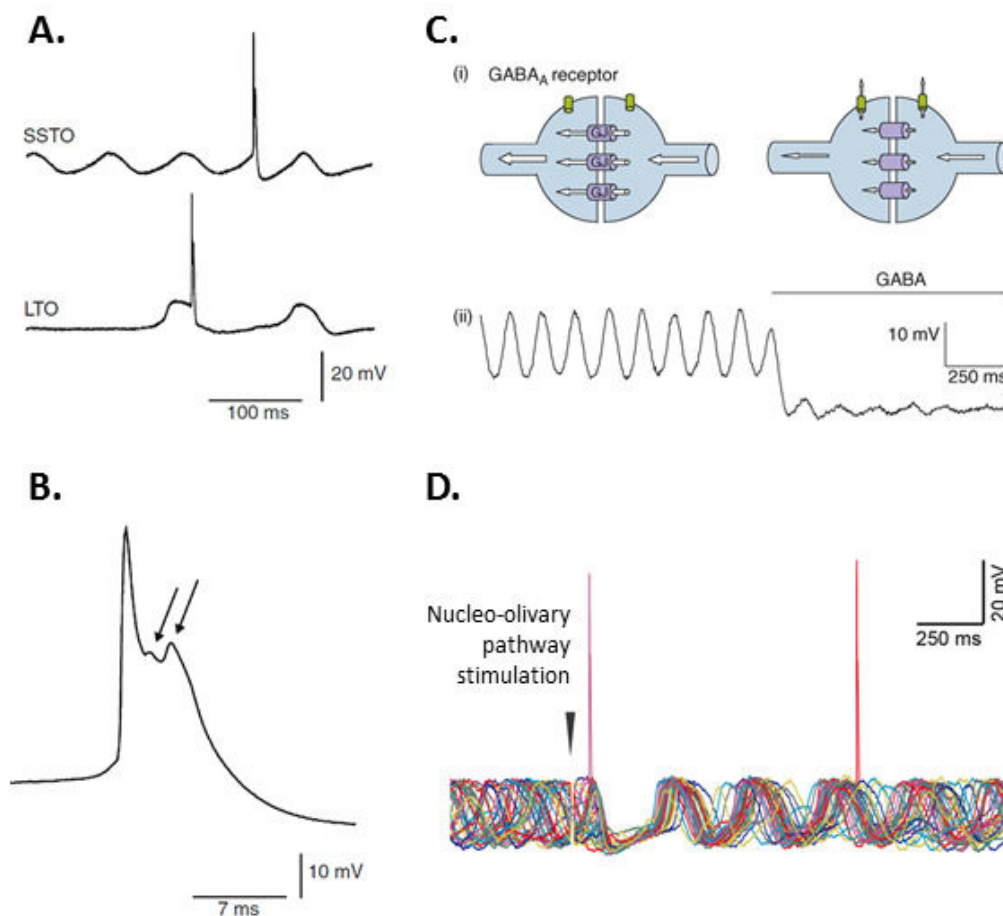


Figure 2.3: Oscillatory phenotypes in the inferior olive and its control by the nucleo-olivary pathway. A- Recordings from olivary neurons *in vivo*. The top panel shows a neuron with spontaneous sinusoidal subthreshold oscillation (SSTO) whereas the bottom trace shows an olivary neuron that expresses spontaneous low-threshold calcium depolarizations (LTO). B- The inferior olive neurons exhibit a characteristic action potential. Arrows indicate wavelets on top of the after depolarization (from De Gruijl et al., 2013). C- (i) Shunting effect of GABA conductance on electrotonic coupling through gap junctions (GJ) which connect two olivary neuron dendrites. As denoted by the size and direction of the arrows, opening of GABA_A receptors invoke chloride current flow into the dendrites, thereby reducing the current flow between the coupled neurons. (ii) Indeed, bath application of GABA suppresses olivary oscillations, during whole cell recording (from Jacobson et al., 2008). D- In addition to the abolition of the olivary oscillations, the nucleo-olivary pathway reset the phase and timing of the oscillation, as shown here by the overlay of 36 recordings from the same unit in the inferior olive after electrical stimulation of the cerebellar nuclei (from Bazzigaluppi et al., 2012).

The peculiar synaptic organization of GABAergic nucleo-olivary inputs located near the gap

junctions within the glomeruli led to the suggestion that the role of the inhibitory inputs might be to uncouple the olivary neurons by shunting the intercellular currents (Llinas et al., 1974) (*Figure 2.2.*), thereby reducing the size of oscillating neuronal assemblies and dampening the amplitude of the oscillations themselves (Jacobson et al., 2008). Indeed, local application of GABA in the inferior olive abolishes the subthreshold oscillations (Devor and Yarom, 2000) while antagonism of GABA_A receptors enhance synchronization within the inferior olive (Lang et al., 1996; Leznik et al., 2002). Therefore, GABAergic nucleo-olivary afferents are thought to rearrange the inferior olive pattern activity by creating discrete clusters of coupled neurons. If the results of those early studies did not indicate whether physiological nucleo-olivary inputs are sufficient to induced olivary oscillations abolition, recent studies demonstrated this shunting effect *in vivo* and *in vitro*. Specific activation of the nucleo-olivary inhibitory inputs using optogenetical tools *in vitro* suppressed subthreshold oscillations and reduced the strength of electrical coupling between two olivary neurons (Lefler et al., 2014). In the same manner, Bazzigaluppi and colleagues (Bazzigaluppi et al., 2012) electrically stimulated the nucleo-olivary projections *in vivo* and observed inhibitory currents in the olivary neurons which abolished their rhythmic activity. In addition to the temporary block of the synaptic transmission through the inferior olive due to the inhibitory shunt provided by nucleo-olivary afferents, a resetting of the oscillation phases was observed (see *figure 2.2.*).

Overall, those data indicate a role of the inferior olive in the generation of olivo-cerebellar temporal patterns (De Zeeuw et al., 2011). Clusterization of ensembles of coupled olivary neurons by topographic nucleo-olivary inputs will have a major impact on the inferior olive output and notably on the discharge of a selected beam of climbing fibers in the cerebellar cortex, thereby drawing a clear segmented organization of the olivo-cerebellar system.

2.3. Modular organization of the olivo-cortico-nuclear system

2.3.1. Olivary-nuclear innervation

The olivo-cerebellar axons form many thin collaterals which terminate in the cerebellar nuclei (Sugihara et al., 1996, 1999). All the collaterals found in the nuclei derive from olivo-cerebellar axons which also reach the cerebellar cortex as climbing fibers, and there are no direct projections from the inferior olive to the cerebellar nuclei. Some subnuclei of the inferior olive, mainly involved in vestibular function, do not make collaterals to the cerebellar nuclei (Ruigrok and Voogd, 2000).

A single olivo-cerebellar axon gives rise to several collaterals (up to six) which innervate only one given cerebellar nucleus (Sugihara et al., 1996, 1999) although territories covered by each nuclear collaterals are only partially overlapping (Sugihara et al., 1996). Therefore, innervation from climbing fibers appears to be more circumscribed than mossy fiber inputs. Olivo-cerebellar nuclear collaterals are very thin, with a diameter ranging from 0.2 to 0.5 μm , and bear *en passant* swellings and terminal swellings comparable with swellings morphology found at the climbing fiber to Purkinje cell synapse (Van der Want and Voogd, 1987; Van der Want et al., 1989; Sugihara et al., 1996, 1999), much smaller than mossy fiber endings (see *section 1.1.1.1.*, for review, see Shinoda and Sugihara, 2013).

Oливо-cerebellar collaterals contact large principal neurons (see *figure 2.3.*) (Sugihara et al., 1996, 1999), mainly on their dendritic compartment (Van der Want and Voogd, 1987), as well as the nucleo-olivary neurons (*Figure 2.3.*) (Chan-Palay, 1973c; De Zeeuw et al., 1997; Sugihara et al.,

1999). Indeed, stimulations of the inferior olive elicit excitatory responses in the cerebellar nuclear neurons (Ito et al., 1970; Eccles et al., 1974c; Kitai et al., 1977; Shinoda et al., 1987; Llinas and Muhlethaler, 1988; Audinat et al., 1992), with no characteristic complex spike shape, in contrast to the Purkinje cells. No one-to-one relationship between climbing fibers and nuclear neurons was found as in the cerebellar cortex (Audinat et al., 1992). Instead, several different climbing fibers appear to converge onto the same nuclear neurons, even though clear anatomical evidence of multiple innervations of the principal neurons by olivo-cerebellar fibers is still lacking.

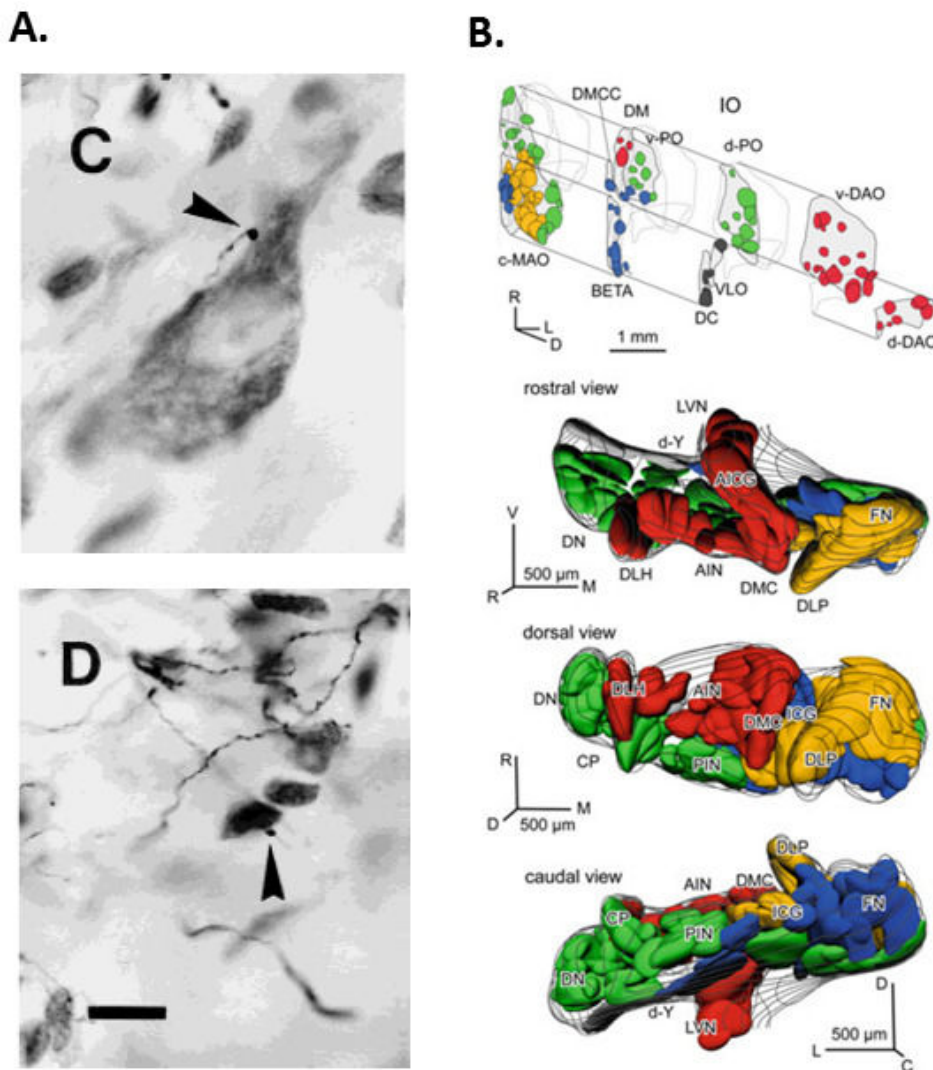


Figure 2.3: Climbing fiber innervation in the cerebellar nuclei. A- Olivo-cerebellar collateral swellings contact both large neurons, putatively principal neurons (C) and small neurons (D), presumably nucleo-olivary neurons. Scale bar: 10 μm. (from Sugihara et al., 1999). B- Topographic projections from inferior olive to the cerebellar nuclei (from Shinoda et al., 2013). Abbreviations: PO, MAO and DAO principal, medial and dorsal accessory olive (v- ventral, d-dorsal), BETA group beta, DM dorsomedial group, DMCC dorsomedial cell column, DC dorsal cap of Kooy, VLO ventrolateral outgrowth, ICG the interstitial cell group, DMC the dorsomedial crest, CP the caudal pole; DLH the dorso-lateral hump, DLP dorsolateral protuberance, FN and DN fastigial and dentate nuclei, PIN and AIN posterior and anterior interposed nuclei, LVN lateral vestibular nucleus, d-Y dorsal group Y nucleus.

2.3.2. The olivo-cerebellar module

2.3.2.1. The olivo-cerebellar module: a functional unit to control movement?

Similarly to what happens in the cerebellar cortex, the climbing fiber inputs are topographically organized in the cerebellar nuclei (Figure 2.3.) (Beitz, 1976; Van der Want et al., 1989; Ruigrok and Voogd, 2000). Nucleo-olivary neurons, and in a lesser extent the principal neurons, receive

topographic inputs both from Purkinje cells (De Zeeuw and Berrebi, 1995a; Teune et al., 1998) and climbing fiber collaterals (De Zeeuw et al., 1997).

This spatial configuration of inputs within a circumscribed region of the cerebellar nuclei suggest a global organization of the cerebellum in small unit where a confined area of the inferior olive project to a segregated strip of Purkinje cells in the cerebellar cortex and to a given part of the cerebellar nuclei which receive from this specific band of cortex. In turn, this area of the cerebellar nucleus is innervating the inferior olive sub-nucleus from which it is receiving. This organization in reciprocal loops implements a modular organization of the cerebellum.

The first anatomical evidence of a modular organization was provided by Groenewegen and Voogd (Groenewegen and Voogd, 1977). The large longitudinal bands of cerebellar cortex together with their olivary afferents and their cortico-nuclear projections define “modules”, which are arranged perpendicularly to the long axis of the cerebellar lobules. Reviewing early anatomical and functional data, Oscarsson (Oscarsson, 1979) proposed the hypothesis that cerebellar modules form the basic operational units of the cerebellum and are involved in the cerebellar function in a manner defined by the topography of their specific afferences and efferences from given sensory-motor areas. This idea is now admitted by a lot of authors (Garwick et al., 1998; Voogd and Glickstein, 1998; Apps and Garwicz, 2005; Apps and Hawkes, 2009; Ruigrok, 2011). Nevertheless, the specific role of each module in the control of motor function is still unclear and may be overlapping for some particular aspects of motor control (Pijpers et al., 2008; Ruigrok et al., 2008; Cerminara and Apps, 2011; Ruigrok, 2011).

Nowadays, extensive mapping of the olivo-cortico-nuclear connectivity in several species was performed (*Figure 2.4.*) (for review (Buisseret-Delmas and Angaut, 1993; Voogd and Glickstein, 1998; Apps and Hawkes, 2009). The olivo-cerebellar modules can extend across one or more lobules some span the entire rostro-caudal length of the cerebellum. The width of the zones varies greatly among mammals. In some species, such as the rat, additional zones are present (Buisseret-Delmas, 1988).). Moreover, modular organization of inputs and outputs is correlated with the zebrin expression pattern of the longitudinal cortical bands and the nuclear subdivisions (Sugihara and Shinoda, 2004; Pijpers et al., 2005; Sugihara and Shinoda, 2007).

Therefore, climbing fiber inputs impose a very precise order on cerebellar cortical organization in relation to previously described molecular and inputs/outputs projections segmentation of the cerebellum.

2.3.2.2. Mossy fibers inputs with respect to the cerebellar modules

Mossy fiber inputs have also been described to arrange in longitudinal bands (*see section 1.1.1.1.*, (Chan-Palay et al., 1977; Jasmin and Courville, 1987; Heckroth and Eisenman, 1988; Ji and Hawkes, 1994; Gebre et al., 2012)). The question was raised about the influence of the mossy fiber inputs with respect to the olivo-cerebellar modules. In fact, both anatomical and physiological studies indicate that the mossy fiber projections are closely related to the climbing fiber innervation patterns and that the concept of modular organization can be extended to the mossy fiber afferents (*Figure 2.4.*) (Eccles et al., 1972; Ekerot and Larson, 1973, 1980; Brown and Bower, 2001; Ruigrok, 2003; Voogd et al., 2003; Apps and Garwicz, 2005; Pijpers et al., 2006; Pijpers and Ruigrok, 2006; Ruigrok, 2011; Cerminara et al., 2013).

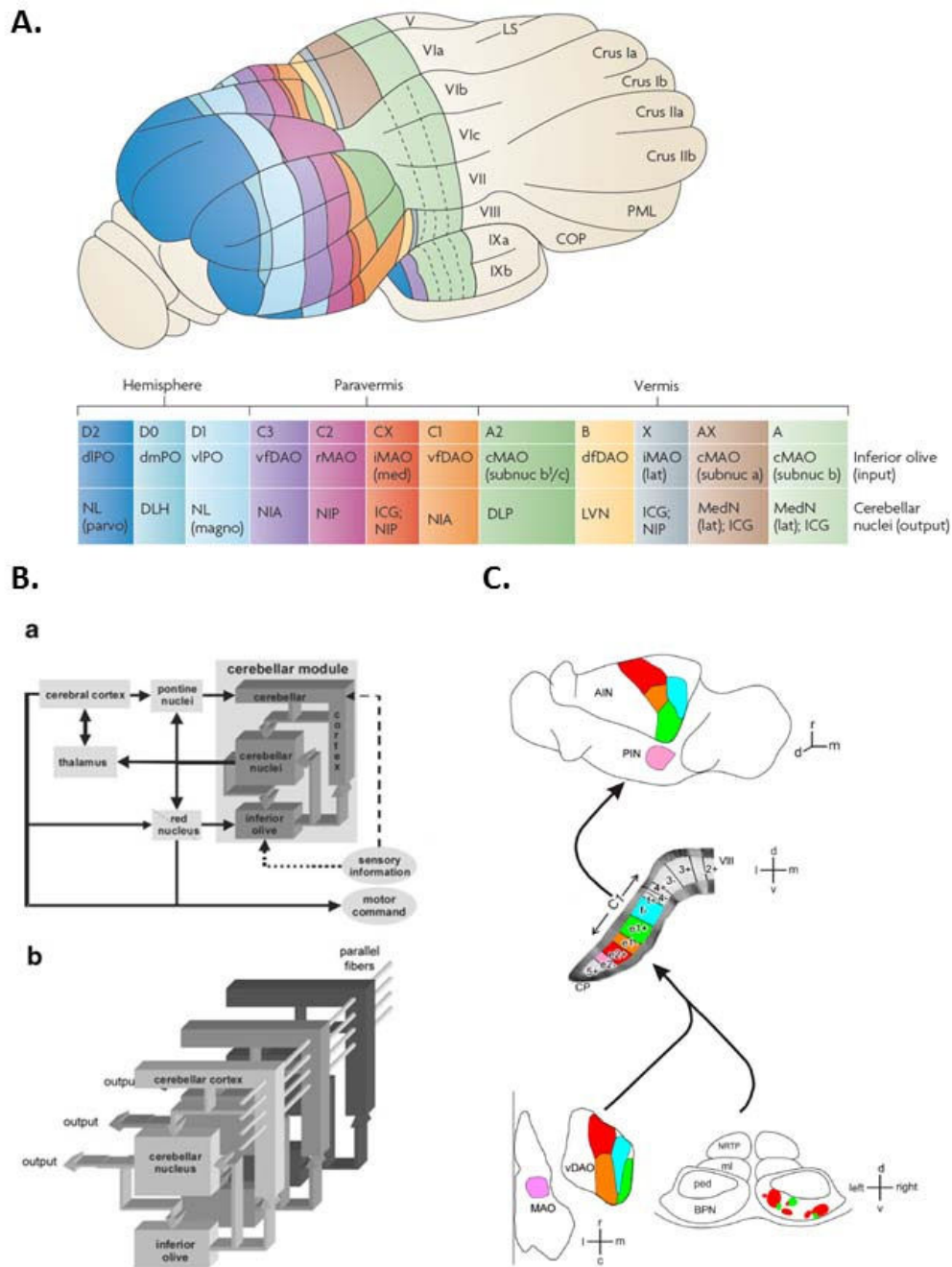


Figure 2.5: Modular organization of the olivo-cortico-nuclear system. A- Olivo-cerebellar projections are arranged in longitudinal bands in the cerebellar cortex, which are receiving from a circumscribed sub-nucleus of the inferior olive and projecting to a confined area in the cerebellar nuclei (from Apps and Hawkes, 2009). B- Schematic diagram of the cerebellar modules (a). Parallel fiber beams are an obvious way to connect different cerebellar modules (b) (from Ruigrok, 2011). C- Cerebellar modules also include mossy fiber inputs (as described here for the pontine nuclei projections) and follow the molecular identity of the cortical segmentation (here with the zebrin bands) (from Cerninara et al., 2013). Abbreviations : c, caudal; d, dorsal; l, lateral; m, medial; MAO, medial accessory olive; ml, medial lemniscus; ped, cerebral peduncle; NRT, nucleus reticularis tegmenti pontis; PIN, posterior interpositus nucleus; r, rostral; v, ventral; VIII, lobule 8.

However, if mossy fiber activity is correlated to the climbing fiber activity within a defined module, the activity of parallel fibers arising from the granule cells contacted by those mossy fibers is not restricted to the olivo-cerebellar modules. On the contrary, the parallel fiber receptive field is in fact anti-correlated with the complex spike and mossy fibers receptive fields (Ekerot and Jorntell, 2001). The parallel fibers which run perpendicularly activate the Purkinje cells in the neighboring modules (Cohen and Yarom, 1998; Apps and Garwicz, 2005) and thus may be involved in distributing information across several cerebellar cortical modules.

Overall, the congruence in the spatial organization of the two cerebellar afferent systems, in addition to the interconnections between the cerebellar modules through the orthogonal parallel fiber pathway, tend to optimize the formation of associations between information supported by one set of climbing fibers and many combinatorial subsets of mossy fibers.

2.3.3. Functional impact of the modular organization of the olivo-cerebellar system

2.3.3.1. Nuclear neurons activity within the modules

Stimulations of the inferior olive elicit a sequential response of “excitation-inhibition” in the nuclear neurons (Ito et al., 1970; Llinas and Muhlethaler, 1988; Audinat et al., 1992; Rowland and Jaeger, 2008; Blenkinsop and Lang, 2011) confirming the anatomical definition of the olivo-cerebellar modules. The initial EPSP is due to direct monosynaptic climbing fiber inputs onto the nuclear neurons while the late inhibition is provided by the Purkinje cells activated by the same climbing fibers in the cerebellar cortex. The initial climbing fiber excitatory response was not always observed (Ito et al., 1970; Llinas and Muhlethaler, 1988; Rowland and Jaeger, 2008; Bengtsson et al., 2011; Blenkinsop and Lang, 2011), suggesting that the patch of cerebellar nuclei innervated by the climbing fiber collateral may be more restricted than the nuclear area covered by the Purkinje cells controlled by the same set of climbing fibers. However, the inhibitory component is highly reproducible and presents approximately the same properties, whether it is preceded by an EPSP or not (Llinas and Muhlethaler, 1988). This may suggest that the preferential effect of the inferior olive onto the cerebellar nuclei activity is an indirect inhibitory effect via the cortical Purkinje cell rather than a direct excitation via the olivo-cerebellar collaterals.

This control of the nuclear neurons activity by the Purkinje cell inputs have been shown to be critical for motor control (Witter et al., 2013), notably by the fact that the principal neurons can elicit rebound firing after a profound hyperpolarization followed by a release of the inhibition (*see section 1.3.2.*). One good candidate mechanism for such input pattern is given by the climbing fiber activity and its ensuing synchronization of the Purkinje cell complex spikes. Indeed, the multiple spikelets in each complex spike propagate as two or three high-frequency action potentials in the Purkinje cell axons (Debanne, 2004; Khaliq and Raman, 2005; Monsivais et al., 2005), likely to elicit a brief burst of postsynaptic IPSCs in the nuclear neurons. Thereafter, the Purkinje cell spiking pause after the complex spike cause a disinhibition of the cerebellar nuclei, which may favor the rebound discharge. If concomitantly synchronized Purkinje cells within the same sagittal band converge their axons upon the same nuclear neurons, this phenomenon would be largely amplified and thus sufficient to provide inhibition onto principal neurons to deactivate the T-type channels (*see section 1.3.2.*) and to trigger the rebound firing. Rebound discharge of the nuclear neurons indeed appears after inferior olive activation (Rowland and Jaeger, 2008; Hoebeek et al., 2010; Bengtsson et

al., 2011).

2.3.3.2. Homeostasis of the olivary, cortical and nuclear activities in the cerebellar feedback loops

Anatomical description of the feedback loops and the complex interconnectivity within a cerebellar module has found an additional support in functional studies describing the interactions between neuronal activity of the inferior olive, the cerebellar cortex and nuclei, mostly using gain or loss of function for one of the element of the tripartite olivo-cerebello-nuclear modules.

Destruction of the inferior olive induces an expected decrease or stop of the complex spike activity in the Purkinje cells, while the simple spike firing is increased (Colin et al., 1980; Benedetti et al., 1984). Consequently, an increase in metabolic activity of the Purkinje cell terminals is observed in the cerebellar nuclei (Bardin et al., 1983b; Bardin et al., 1983a; Batini et al., 1984; Oltmans et al., 1985), resulting in the suppression of the nuclear neurons activity (Benedetti et al., 1983; Rowland and Jaeger, 2008).

Specific stimulation of the Purkinje cells induced inhibition of the nucleo-olivary neurons which themselves disinhibit the inferior olive (Chaumont et al., 2013). An increase in the complex spike activity of the Purkinje cells belonging to the area that was stimulated ensues, indicating that the Purkinje cells are able to retro-control their own complex spike activity. On the contrary, if the Purkinje cell to nuclear neurons transmission is decreased rather than facilitated the consecutive disinhibition of the cerebellar nuclei activity cause the loss of complex spikes activity in the Purkinje cells by increasing the nucleo-olivary action onto olivary neurons (Chen et al., 2010). Blockade of the nucleo-olivary pathways intensified in the same manner the complex spikes occurrence in the cerebellar cortex (Bengtsson et al., 2004).

In addition, it has been shown that elevation of the inferior olive activity provoked an augmentation of the metabolic activity in the red nucleus (Bardin et al., 1983b). The larger number of complex spikes generated in the Purkinje cell led to the disinhibition of the principal neurons of the cerebellar nuclei which project to the red nucleus. Strikingly, this series of retro-control loops within the cerebellar module seems to finely adjust the level of output activity of the cerebellar nuclei.

2.4. Climbing fibers give instructions: supervised learning in the cerebellum

Besides being a strong topographic organizer of the cerebellum, the climbing fiber system is involved in the induction of supervised plasticity which it thought to underlie the motor learning.

2.4.1. Synaptic plasticity and error signaling in the cerebellar cortex by climbing fiber inputs

Extensive knowledge about the cerebellum anatomy was the basis of the formulation of diverse theories about its function, notably on motor learning (Marr, 1969; Albus, 1971). A decade later, Ito and Kano (Ito and Kano, 1982) provided the first experimental demonstration of their principal hypothesis: the synaptic plasticity at the parallel fibers to Purkinje cells synapse. Indeed, it has been proposed that the Purkinje cells learn to respond to particular patterns of parallel fibers activity (induced by different inputs from mossy fibers) by modifying the strength (or weight) of parallel fibers to Purkinje cell synapses and that this synaptic plasticity is under supervision of the

climbing fiber (Marr, 1969; Albus, 1971).

Schematically, during a movement, appropriate sensory-motor patterns (provided by a given mossy fibers activity pattern and resulting in the correct Purkinje cell output motor command) will be strengthened by long-term potentiation of the parallel fiber to Purkinje cell synapses (Salin et al., 1996; Hansel et al., 2001), while inappropriate gestures will cause the conjunctive activation of an “error signal” from climbing fibers, thus leading to a long-term depression of the active parallel fibers to Purkinje cell synapses (Ito and Kano, 1982; Ekerot and Kano, 1985; Hansel et al., 2001; Bidoret et al., 2009). This paradigm, whereby synaptic connections between granule cells and Purkinje cells are modified in order to minimize the errors carried through the climbing fiber inputs, is called “supervised learning”. This concept has received support from behavioral studies in monkeys (Gilbert and Thach, 1977; Ojakangas and Ebner, 1992, 1994; Medina and Lisberger, 2008). In one of these studies, for example, it was demonstrated that a complex spike occurring during learning of ocular pursuit provokes a decrease in the number of simple spikes emitted during the following trial, thus correcting the eye movement (Medina and Lisberger, 2008).

Besides the extensive study of the parallel fiber to Purkinje cell synapse plasticity, other sites of plasticity are found in the cerebellar cortex (*Figure 2.5.*) such as the climbing fiber to Purkinje cell synapses (which is depressed if climbing fibers are repeatedly activated without pairing to the parallel fiber inputs), the molecular layer interneurons to Purkinje cell synapses (which are potentiated by repetitive activation of the climbing fibers) or the mossy fibers to granule cell synapses (strongly potentiated by high-frequency stimulation of the mossy fibers while the synapse is depressed when the frequency of stimulation is lower) (for review, see Hansel et al., 2001).

Complex spikes, in addition to being involved in long-term plasticity during motor learning, exert online control, or online correction of the movement, by synchronizing the neuronal firing of the different cerebellar elements during the movement (Welsh et al., 1995; Welsh and Llinas, 1997; Kitazawa et al., 1998).

2.4.2. Synaptic plasticity in the cerebellar nuclei: another degree of freedom for olivo-cerebellar mediated motor learning?

Cerebellar nuclei are also considered as another site of motor learning in the cerebellum, involved in memory retention (McCormick and Thompson, 1984). Learning processes first occurred in the cerebellar cortex, and next are consolidated in the cerebellar nuclei (Garcia and Mauk, 1998; Ohyama and Mauk, 2001; Ohyama et al., 2006).

During acquisition of motor learning, the Purkinje cells activity is proposed to control plasticity in the cerebellar nuclei, by generating instructive signals that regulate the strength of mossy fiber synapses onto nuclear cells ultimately, changing cerebellar output to produce adaptive responses (Medina and Mauk, 1999), while the climbing fiber input itself acts on the parallel fiber to Purkinje cell synapse plasticity upstream rather than directly on nuclear neurons (Aksenov et al., 2005).

Crucial involvement of the inhibition upon nuclear neurons was confirmed by studies investigating long-term plasticity at the mossy fiber to nuclear neuron synapses. This synapse is potentiated when presynaptic high-frequency bursts of EPSPs precede a post-inhibitory rebound by 400 milliseconds (Pugh and Raman, 2006, 2008). If the EPSPs burst is not followed by a hyperpolarization period or instead precede a depolarization of the soma (Zhang and Linden, 2006), or if the in-

hibition appears after 400 milliseconds or before the excitation (Pugh and Raman, 2006, 2008), the synapse is depressed. Moreover, inhibitory inputs from the Purkinje cells can be potentiated (Ouardouz and Sastry, 2000) or depressed (Morishita and Sastry, 1996) depending on the amount of postsynaptic calcium transients induced by synaptic activity (Aizenman et al., 1998), large postsynaptic activation resulting in long-term potentiation while smaller postsynaptic calcium rises induce long-term depression of the IPSPs. Additionally to the long-term changes in synaptic strength, storage of the information during motor learning may also involve activity-dependent changes in the intrinsic excitability of the nuclear neurons, as bursts of either EPSPs or IPSPs induce an increase in nuclear cells excitability (Zhang et al., 2004; D’Hulst et al., 2009).

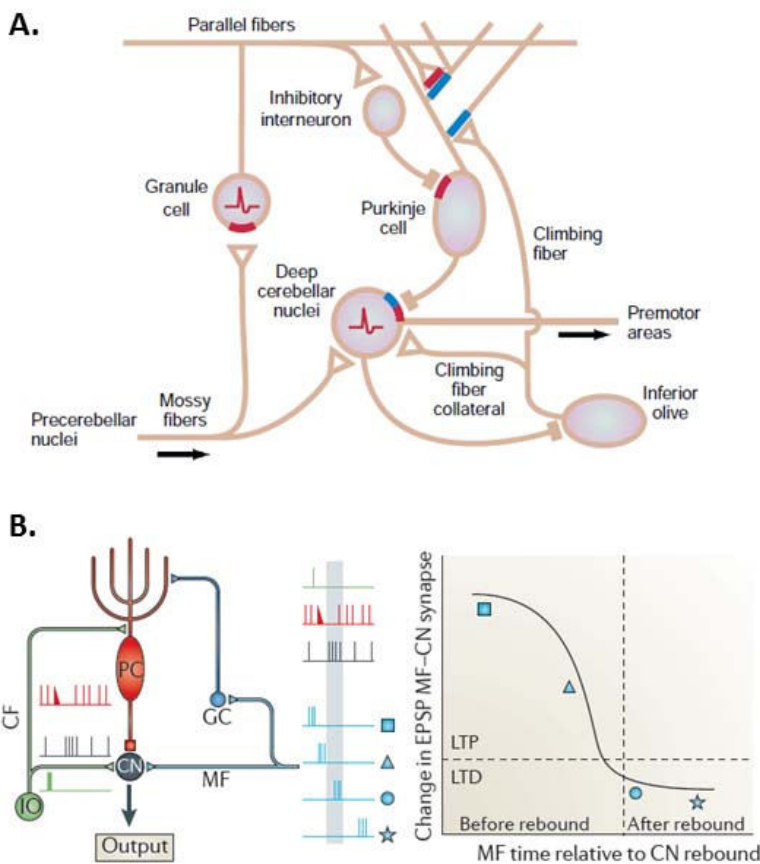


Figure 2.5: Synaptic plasticity in the cerebellum. A- Summary of the sites of plasticity in the cerebellum. Occurrence of synaptic plasticity is indicated by bars of colors (blue for depression and red for potentiation) while red action potentials drawn in neuronal somata persistent increases in intrinsic excitability (from Hansel et al., 2001). B- Synaptic plasticity in the cerebellar nuclei at mossy fiber to principal neuron synapses is dependent on the rebound firing induced by the inhibition period from the Purkinje cells (from De Zeeuw et al., 2011). Abbreviations: MF mossy fiber, GC granule cells, CF climbing fiber, PC Purkinje cell, CN principal neuron of the cerebellar nucleus.

These results confirmed the “Medina-Mauk model” where the sequential activation of direct excitatory inputs followed by the Purkinje cells inhibition is a key component for motor learning in the cerebellar nuclei (Pugh and Raman, 2009; Zheng and Raman, 2010). Timing of the mossy fiber collateral inputs onto nuclear neurons with respect to the occurrence of a rebound induced by the Purkinje cells inhibition is crucial for the directionality of the synaptic plasticity (*Figure 2.5*). This may suggest that whenever the Purkinje cells inputs is occurring at the right interval with the direct collaterals inputs onto the nuclear neurons, these excitatory inputs are selected and strengthened to improve the spiking output of the cerebellar nuclei (De Zeeuw et al., 2011).

All the plasticity protocols in the cerebellar nuclei were executed at the synapse onto the principal projecting neurons, under the assumption that these neurons have the most striking im-

pact on the control of the motor command. However, we know that cortical inputs to the nuclei are arranged in such a manner that a single Purkinje cell terminates on both nucleo-olivary and principal neurons (Teune et al., 1998). It would be interesting to investigate the effect of long-term plasticity at other synapses in the cerebellar nuclei, and notably the impact on the nucleo-olivary pathway. It has already been suggested that the nucleo-olivary pathway play a key role in gating responses to excitatory input during learning processing (Kim et al., 1998). Strengthening or weakening of this pathway could lead to modulation of the electrotonic coupling of olivary neurons (Tokuda et al., 2013). Therefore, each cerebellar circuitry element is involved in complex plasticity mechanisms which lead to modulation of the whole olivo-cerebellar loop activity during motor learning.

CHAPTER 3: Inhibitory neurons of the cerebellar nuclei, a third nuclear circuit

3.1. Inhibitory neurons of the cerebellar nuclei: a heterogeneous population

3.1.1. Evidence for the presence of a third nuclear cell type and the question of their neurotransmitter contents

The existence, in the cerebellar nuclei, of a population of small inhibitory neurons with local axons has been reported by early morphological studies (Matsushita and Iwahori, 1971d; Chan-Palay, 1973a; Mccrea et al., 1978). Those interneurons were proposed to contact the principal neurons of the cerebellar nuclei (Chan-Palay, 1973a). Incidental findings in some electrophysiological experiments similarly suggested the presence of local inhibition onto the principal neurons. Stimulation of peripheral nerves to limbs produced a small number of inhibitory responses in the interposed nucleus neurons of cats, which persisted even after cooling of the cerebellar cortex to inhibit Purkinje cells firing (Rosen and Scheid, 1972). In some cases, when the mossy fiber inputs were stimulated, some IPSPs were recorded in the principal neurons a few milliseconds before the expected indirect action of Purkinje cells, suggesting that in addition to the cortical pathway, a more direct inhibitory pathway is involved (Ito et al., 1970).

Inhibitory neurons of the cerebellar nuclei appeared to constitute a large population with heterogeneous neurotransmitter contents. Most of the small neurons colocalize GABA and glycine at their somata (Chen and Hillman, 1993; Baurle and GrusserCornehl, 1997; Baurle et al., 1997; Sultan et al., 2002; Tanaka and Ezure, 2004), while the remaining population is stained for either GABA or glycine. Glycine immunoreactivity is found in many small somata in the CN (Rampon et al., 1996; Baurle and GrusserCornehl, 1997; Zeilhofer et al., 2005), and the abundance of glycinergic synapses in the cerebellar nuclei (Chen and Hillman, 1993; De Zeeuw and Berrebi, 1995b) established glycine as a key neurotransmitter in the intra-nuclear inhibition. However, as cortico-nuclear projections massively inhibit the nuclei, local inhibition onto principal neurons was not easily observed and therefore less commonly investigated. Characterization of this local inhibitory circuit is still incomplete four decades after those first observations and constitutes the main topic of this thesis.

Taking advantage of Purkinje cell – degeneration (PCD) mutant mice, Wassef and colleagues (Wassef et al., 1986) provided the first unquestionable evidence for a source of nuclear inhibition different from Purkinje cells, which shall account for a small percentage (< 15%) of all the inhibitory inputs. In other mutants of Purkinje cells degeneration, an up-regulation of the inhibitory

interneuronal population, defined by the authors by their labelling by parvalbumin¹⁵, was found (Baurle et al., 1997; Baurle et al., 1998), together with an increase in the size and number of inhibitory terminals (Sultan et al., 2002). In those pathological model mice with Purkinje cell innervation loss, there are no changes in the number of GABA-containing cell bodies when the phenotype is completed and stable after the initial reduction in GABA content, (Rofflertarlov et al., 1979; Wassef et al., 1986; Baurle and GrusserCornehl, 1997) while the density of glycinergic neurons and terminals increase (Baurle and GrusserCornehl, 1997; Baurle et al., 1997; Sultan et al., 2002). Those differential compensatory mechanisms depending on the neurotransmitter contents of the nuclear neurons presume of the existence of a heterogeneous interneuronal population within the cerebellar nuclei.

3.1.2. Electrophysiological properties of the glycinergic neurons

Recently, the advent of genetically targeted fluorescent labelling in transgenic mouse line has made possible the electrophysiological examination of the different neuronal populations in the cerebellar nuclei.

As GABAergic local neurons cannot be distinguished from the nucleo-olivary neuron population in GAD67-eGFP transgenic mouse in which the expression of GFP is induced under the control of the GAD67 promoter¹⁶ (Esclapez et al., 1994; Tamamaki et al., 2003), a good way to characterize glycinergic neurons would be to use the GlyT2-eGFP transgenic mouse, in which GlyT2-expressing¹⁷ neurons are genetically encoding and expressing the enhanced GFP (Zeilhofer et al., 2005). Uusisaari & Knöpfel (Uusisaari and Knöpfel, 2010) described two distinct populations of GlyT2-positive neurons in the cerebellar nuclei by using the GlyT2-eGFP mouse. The first population is composed of GFP-expressing neurons, inactive in acute slices, which were found projecting to the cerebellar cortex¹⁸. Those nucleo-cortical neurons generate axonal collaterals within the cerebellar nuclei and may also be involved in local inhibition. The second population of GFP-positive neurons is spontaneously active, firing around 10 Hz, and is thought to constitute the population of local inhibitory neurons as their axonal arborization extent less within the nuclei.

Those GFP-positive neurons share some of their electrophysiological characteristics with the GAD67-eGFP positive neurons, the authors proposed that they constituted a population of mixed GABA/glycine interneurons of the cerebellar nuclei (Uusisaari and Knöpfel, 2011; Uusisaari and Knöpfel, 2013). Indeed, using the GAD67-eGFP mouse line, Uusisaari and co-workers described a population of GAD67-positive neurons which exhibit different electrophysiological properties compared to GAD67-negative neurons (putatively glutamatergic principal neurons) (Uusisaari et al., 2007; Uusisaari and Knöpfel, 2008). Their action potentials are usually wide and exhibit a slow after-hyperpolarization period (Uusisaari et al., 2007). They receive inhibitory inputs from the Purkinje cells, mediated mostly by $\gamma 2$ and $\alpha 3$ subunits-containing GABA_A receptors (Uusisaari and Knöpfel,

¹⁵ The parvalbumin is a calcium binding protein found mainly in the GABAergic interneurons, notably in the cerebellar and cerebral cortex.

¹⁶ Glutamic Acid Decarboxylase (GAD) is the enzyme responsible for the synthesis of GABA in the terminals. Two isoforms exist: GAD67 and GAD65 with differential expression within the GABAergic neurons (Esclapez et al., 1994).

¹⁷ GlyT2 is the glycine transporter 2 expressed in neuronal presynaptic terminals and involved in up-taking glycine from the extracellular medium (Zafra et al., 1997).

¹⁸ This nucleo-cortical projection will be described in the next paragraphs.

2008). However, this cortico-nuclear projection is less important on small cells than on the principal neurons (Angaut and Sotelo, 1973; Chan-Palay, 1973a; De Zeeuw and Berrebi, 1995a; Sultan et al., 2002; Uusisaari and Knopfel, 2008). When inhibitory inputs are blocked, EPSPs are recorded in GAD67-positive neurons, while no such glutamatergic inputs were seen in the GAD67-negative cells. Altogether such electrophysiological characteristics could also be attributed to GABAergic nucleo-olivary neurons, as they were also found to receive inhibition from Purkinje cells and excitation from olivary collaterals and that dense innervation of GAD67-GFP-positive fibers were found in the inferior olive (Tamamaki et al., 2003). Therefore, it is possible that some, if not all, of the GAD67-eGFP neurons recorded belong to the nucleo-olivary neurons.

It appeared difficult to extrapolate data obtained from two different transgenic mouse lines and some questions remain unsolved: if glycinergic and mixed interneurons constitute the same neuronal population is not clear at the moment and the electrophysiological characteristics of this later class of neurons were never described in details. Moreover, functional intra-nuclear inhibition provided by glycinergic and/or mixed GABA/glycine neurons was poorly studied.

3.2. Evidence for Non-Purkinje cells inhibitory transmission in the principal neurons

Even if the presence of mixed neurons have been reported (Chen and Hillman, 1993; Baurle et al., 1997; Sultan et al., 2002; Tanaka and Ezure, 2004) and while mixed inhibitory transmission has been thoroughly described in the cerebellar cortex (Dumoulin et al., 2001; Rousseau et al., 2012), it had never been investigated in the cerebellar nuclei.

3.2.1. GABA_A and glycine receptors: common features and specific characteristics

Glycine receptors are classically responsible for inhibitory transmission in the spinal cord, the brainstem, and some upper brain regions (Dieudonné, 1995; Trombley et al., 1999; Legendre, 2001; Danglot et al., 2004; Lynch, 2004). The glycine receptor is a pentameric Cys-loop chloride channel, composed of α (α_1 to α_4) and β subunits. Distinct, but overlapping (Legendre, 2001; Lynch, 2004), ligand binding sites for agonists and antagonists, are located at the subunits interfaces (Lynch, 2004; Betz and Laube, 2006). Glycine receptors can form homomeric channels solely composed of α subunits¹⁹ which are mainly expressed during development stages or at extra-synaptic sites during adulthood. Heteromeric glycine receptors with both α and β subunits mediate most of the fast synaptic neurotransmission (Legendre, 2001; Lynch, 2004, 2009), and the β subunit interact with gephyrin, a post-synaptic scaffolding protein necessary for the synaptic localization of the receptor (Kirsch et al., 1993; Meyer et al., 1995; Sola et al., 2004). If most glycine receptors are found post-synaptically, some presynaptic clusters act directly on neurotransmitter release (Turecek and Trussell, 2001).

As glycine receptors, GABA_A receptors belong to the pentameric Cys-loop ion channel family and form a chloride-permeant pore at the membrane. A large diversity of GABA_A receptor agonists and antagonists act on different binding sites (Macdonald and Olsen, 1994; D'Hulst et al., 2009). Nineteen different GABA_A receptor subunits have been identified so far in mammals: α (α_1 to α_6), β

¹⁹ β subunits do not form functional receptors in the absence of α subunits

(β_1 to β_3), γ (γ_1 to γ_3), δ , ϵ , ρ (ρ_1 to ρ_3), θ and π (Olsen and Sieghart, 2008). The majority of native receptors are an association of α - β - γ subunits (Macdonald and Olsen, 1994; McKernan and Whiting, 1996; D'Hulst et al., 2009). The different combinations exhibit different sensitivity to agonists and antagonists, with specific conductances and kinetics (Porter et al., 1992; Olsen and Sieghart, 2008; D'Hulst et al., 2009). The γ_2 subunit is essential for postsynaptic accumulation of GABA_A receptors (Essrich et al., 1998; Sassoe-Pognetto and Fritschy, 2000).

Despite these molecular differences, glycinergic and GABAergic synapses display functional similarities. While on the postsynaptic side GABA_A and glycine receptors bind to the same anchoring protein to co-cluster at postsynaptic sites and share the same ionic selectivity, on the presynaptic side glycine and GABA share the same presynaptic vesicular transporter (the vesicular inhibitory amino acid transporter, VIAAT) (Sagne et al., 1997; Dumoulin et al., 1999) thus allowing co-accumulation of the two neurotransmitters in the synaptic vesicles and their co-release in the synaptic cleft (Jonas et al., 1998).

3.2.2. Interaction between GABAergic and glycinergic transmission: the case of mixed transmission

Functional co-transmission of GABA and glycine was demonstrated in several brain regions such as the spinal lumbar motoneurons (Jonas et al., 1998), in the brainstem hypoglossal motoneurons (O'Brien and Berger, 1999), the spinal neurons (Chery and De Koninck, 1999; Gao et al., 2001), the abducens motoneurons (Russier et al., 2002) or the cerebellar Golgi cells (Dumoulin et al., 2001). In several brain areas, mixed inhibitory synapses are generally observed at earlier stages of development and a switch to either GABAergic or glycinergic transmission occurs during neuronal maturation (Kotak et al., 1998; Gao et al., 2001; Keller et al., 2001). Complex time-dependent interactions between GABA and glycine receptors during the development of mixed synapses have been described (Dumoulin et al., 2000; Muller et al., 2004).

If most of the mixed transmission might be lost after the neuronal networks maturation, during adulthood co-release of GABA and glycine exhibit a large variety of post-synaptic structural configurations and functional properties (for review of the different synaptic articulations found in mixed transmission, see Dieudonné and Diana, 2009).

Interestingly, if post-synaptic clustering of GABA_A and glycine receptors can arrange very differently among the known mixed synapses (Dieudonné and Diana, 2009), the decay kinetics of the GABAergic and glycinergic components of IPSCs were always found to be significantly different (Grudt and Henderson, 1998; Jonas et al., 1998; Chery and De Koninck, 1999; O'Brien and Berger, 1999; Gao et al., 2001; Russier et al., 2002; Kuo et al., 2009; Dufour et al., 2010). Glycine receptor-mediated currents decay faster than GABA_A receptor-mediated currents in most structures, except in the cerebellum (Dumoulin et al., 2001) and the dorsal cochlear nucleus (Balakrishnan and Trussell, 2008) where GABAergic inhibition is faster. Therefore the co-activation of glycine and GABA_A receptors can significantly change the kinetics of the inhibitory events compared to GABAergic- or glycinergic-only synapses, and can modulate the strength and the timing of inhibition to precisely tune the firing rate of post-synaptic cells (Russier et al., 2002). Moreover, interactions between GABAergic and glycinergic transmission at mixed synapses increase the possibilities of inhibitory events kinetics modulation. In the auditory system, the time windows for effective inhibition can be narrowed by the direct action of the co-released GABA on the post-synaptic glycine re-

ceptors (Lu et al., 2008) which decay kinetics is speeded up by this low efficacy agonist²⁰ (De Saint Jan et al., 2001; Legendre, 2001). On the other hand, activation of glycine receptors inhibited GABA-induced currents by decreasing their amplitude and accelerating their desensitization rate (Li et al., 2003).

Additionally, the two neurotransmitters could activate receptors with different subcellular localization, such as presynaptic GABA_B or glycine receptors to provide negative feedback control for neurotransmitter release (Grudt and Henderson, 1998; Jonas et al., 1998; Chery and De Koninck, 1999; Lim et al., 2000; Turecek and Trussell, 2001), or extra-synaptic receptors with distinct binding and kinetics properties (Chery and De Koninck, 1999).

Mixed GABA/glycine transmission appears to be a powerful mechanism to increase the possibility of modulation of the inhibition and notably has an important functional relevance in differentially shaping the inhibitory currents.

3.2.3. Searching for a glycinergic component of synaptic transmission in the cerebellar nuclei

In the cerebellar nuclei, although the co-existence of GABA and glycine in putative local neurons, functional mixed transmission has never been described so far. The non-Purkinje cell GABAergic inputs onto principals neurons were poorly studied and the few studies on inhibitory inputs coming from putative interneurons were focusing on glycinergic transmission, as it can be easily distinguished from GABAergic Purkinje cell inputs. As there is no known extra-nuclear source of glycinergic inputs to the cerebellar nuclei, if glycinergic transmission could be demonstrated, it would come from local interneurons releasing either glycine alone, or GABA and glycine simultaneously.

Both α and β subunits of glycine receptors are expressed in the cerebellar nuclei (Malosio et al., 1991; Sato et al., 1991; Weltzien et al., 2012), supporting the hypothesis that they can form functional channels and underlie glycinergic currents. Application of glycine to the nuclear neurons of young rats evoked large inhibitory currents blocked by strychnine, a potent glycine receptor antagonist (Legendre, 2001; Lynch, 2004). Evidence for functional glycinergic transmission in the nuclear neurons was first provided by Kawa (Kawa, 2003) and confirmed few years later by Pedroarena and Kamphausen (Pedroarena and Kamphausen, 2008). In these two studies, spontaneous glycinergic IPSCs were very rarely recorded in the principal neurons and electrical stimulations within the nuclei or pharmacological stimulations of neurotransmitter release (by application of saline solution with high concentration of potassium or application of potassium channels blockers) were necessary to induced strychnine-sensitive IPSCs.

Glycinergic transmission appears to mature during the first postnatal weeks. In neonatal rats (aged <P14), glycinergic IPSCs with relatively slow kinetics properties could be recorded. Those currents are mainly mediated by $\alpha 2$ -containing glycine receptors (Kawa, 2003; Pedroarena and Kamphausen, 2008), which are preferentially blocked by picrotoxin antagonist compared to $\alpha 1$ - β glycine receptors (Pribilla et al., 1992; Ye, 2000). This is consistent with the known developmental switch from $\alpha 2$ to $\alpha 1$ subunit and in favor of heteromeric assemblies of glycine receptors which happens during the two first week of life and is fully completed by the third postnatal weeks (Becker et

²⁰ On the contrary, GABA_A receptors cannot be activated by glycine.

al., 1988; Watanabe and Akagi, 1995; Friauf et al., 1997; Lynch, 2004) leading to the situation in mature networks (Becker et al., 1988; Lynch, 2004). $\alpha 2$ -containing glycine receptors have longer open times and slower decay times than $\alpha 1$ - β receptors, therefore the developmental change in subunits leads to an acceleration of the IPSC kinetics in the mature neurons (Takahashi et al., 1992; Lynch, 2004), as observed in the cerebellar nuclei (Pedroarena and Kamphausen, 2008). Additionally, Pedroarena and Kamphausen (Pedroarena and Kamphausen, 2008) were able to record glycinergic currents in older animals (aged P18 to P23), but no currents could be evoked in P13 to P17 animals, despite the presence of glycine receptor immunoreactivity on the somata of the principal neurons. The latter results confirmed that effective glycinergic transmission may be highly dependent on developmental stages and maturation of the cerebellar networks.

Glycinergic transmission, alone or through co-release with GABA, was still poorly studied in the cerebellar nuclei when I undertook my work, but a small body of evidence suggested that it could have a substantial role in the intra-nuclear inhibition of the principal neurons, contrasting with the GABAergic Purkinje cell inhibition.

3.3. Cerebellar nucleo-cortical pathway: another feedback for fine modulation of principal neuron activity

3.3.1. The nucleo-cortical pathway: a forgotten feedback loop

The existence of a projection between the cerebellar nuclei and the cerebellar cortex was demonstrated in 1976 by two independent studies in the cat (Gould and Graybiel, 1976; Tolbert et al., 1976a), following some early studies raising the possibility that some cells in the nuclei were sending their axons to the cerebellar cortex (for review : (Haines and Manto, 2009)). This nucleo-cortical pathway was later confirmed in several species (Clarke, 1977; Tolbert et al., 1977; Haines and Pearson, 1979; Haines, 1988; Batini et al., 1989; Buisseret-Delmas and Angaut, 1989).

The nucleo-cortical axons end in the granular layer of the cerebellar cortex (Tolbert et al., 1976a; Dietrichs and Walberg, 1979; Hamori et al., 1981; Legendre and Courville, 1986) within the glomeruli in a rosette-like shape (Tolbert et al., 1980; Hamori et al., 1981). The nucleo-cortical fiber terminals are similar to the extracerebellar mossy fiber terminals, although 'smoother' with fewer irregularities than most normal rosettes (Tolbert et al., 1980; Hamori et al., 1981). The terminals have a central location within the glomeruli where they contact the granule cells dendrites. In addition, some of the fibers terminals are also found in the non-glomeruli neuropil between granule cells bodies where they putatively contacted large dendrites of Golgi cells²¹ } (Tolbert et al., 1980).

The nucleo-cortical pathway is not a dense projection compared to the others sources of mossy fibers inputs. Legendre and Courville (Legendre and Courville, 1986) counted 4 to 15 nucleo-cortical terminals per mm² while cuneocerebellar mossy fiber projections represent more than 45 terminals per mm² of granular layer. In the same way, about 5% of the mossy fibers found in the granular layer could be attributed to the nucleo-cortical tract, which is preserved when the cerebellar peduncles were damaged (Hamori et al., 1981).

²¹ Golgi cells are large inhibitory interneurons of the granular layer of the cerebellar cortex which constitute the only source of inhibition for billions of granule cells. They inhibit the mossy fiber to granule cell relay within the glomeruli and receive various synaptic inputs from mossy fibers, granule cells. Thus, they are involved in feedforward and feedback inhibitory loops onto granule cells (for review, see Pietrajtis and Dieudonné, 2012).

The nucleo-cortical projection is topographically organized in zones and is mainly reciprocal with the cortico-nuclear Purkinje cell pathway (Tolbert et al., 1978a; Dietrichs and Walberg, 1979; Gould, 1979; Haines and Pearson, 1979; Tolbert and Bantli, 1979; Dietrichs, 1981; Buisseret-Delmas, 1988; Buisseret-Delmas and Angaut, 1989; Angaut et al., 1996; Provini et al., 1998; Trott et al., 1998a; Houck and Person, 2014). However, some of the projections are non-reciprocal, where the nucleo-cortical neurons are not directly controlled by the cortical zones to which they project (Dietrichs and Walberg, 1979; Haines and Pearson, 1979; Tolbert and Bantli, 1979; Buisseret-Delmas, 1988; Buisseret-Delmas and Angaut, 1989). This may result from the wide collateralization of nucleo-cortical axons within the cerebellar cortex (Tolbert et al., 1978b; Buisseret-Delmas, 1988; Haines, 1988; Houck and Person, 2014).

Reciprocal and non-reciprocal projections therefore participate to closed- and open-loop, respectively. Reciprocal loops may be particularly involved to control the nuclear neurons activity: the nucleo-cortical neurons excited by nuclear afferents would induce a rapid feedback from the Purkinje cells to finally modulate the cerebellar nuclei output. Nucleo-cortical branching in non-reciprocal projections allows binding functionally related but spatially different areas of the cerebellar cortex (Provini et al., 1998). Moreover, the nucleo-cortical projections are related to the olivo-cerebellar somatotopic maps (Provini et al., 1998) suggesting a putative role of the nucleo-cortical neurons within the cerebellar modules (Apps and Garwicz, 2005). Together, those results strongly suggest an important role of both reciprocal and non-reciprocal loops in linking the internal circuits between the different cortical compartments (Trott et al., 1998a; Apps and Garwicz, 2005; Houck and Person, 2014).

Differential computations may appear along the mediolateral axis of the cerebellum, as it was shown that lateral zones are generating more reciprocal connections than the medial areas (Tolbert et al., 1978b; Tolbert and Bantli, 1979). Moreover, some cortico-nuclear zones are devoid of nucleo-cortical innervations while others exhibit stronger inputs than neighboring areas (Buisseret-Delmas, 1988; Haines, 1988; Buisseret-Delmas and Angaut, 1989; Provini et al., 1998; Trott et al., 1998a)(for review, (Houck and Person, 2014)). This quantitative non-uniformity in the distribution of the nucleo-cortical projections suggests that some cortical zones would be more retro-activated by nuclear cells than others. Consequently, nucleo-cortical pathway would play a more predominant role in some modules rather than in others, although the physiological importance of those intra-cerebellar feedback loops remains to be clarified.

3.3.2. Cell type identity of the nucleo-cortical neurons: a role for the inhibitory neurons

A fraction of the nucleo-cortical fibers appear to arise from collaterals of the glutamatergic projection neurons (Tolbert et al., 1976a, 1977, 1978a; Hamori et al., 1981; Payne, 1983). About half of the nuclear neurons retrogradely labeled from the cerebellar cortex are stained for glutamate (Batini et al., 1992). The principal neurons of the cerebellar nuclei are part of the circuitry involved in motor control and therefore those findings are consistent with the hypothesis that they would send copies of the sensori-motor information they processed in the cerebellar cortex via mossy-fiber like feedback loops.

The remaining half of the nucleo-cortical neurons seems to arise from inhibitory neurons. GABA-immunoreactive neurons are found to project to the cerebellar cortex (Batini et al., 1989; Angaut et al., 1996) and GABAergic nucleo-cortical mossy fibers were found in the glomeruli of the

granular layer (Chan-Palay et al., 1979; Hamori and Takacs, 1989). About one third of the nucleo-cortical projections seem to be GABAergic (Batini et al., 1992; Houck and Person, 2014). However, GABAergic nucleo-cortical projections may not be found in all the cortical regions (Batini et al., 1989; Kolston et al., 1995) and may only be involved in the retro-control of specific areas, such as the vestibulo-cerebellum (Gould, 1979)²².

Some authors proposed that the GABAergic nucleo-cortical fibers may arise from nucleo-olivary neurons (Tolbert et al., 1978b; Haines, 1988), notably based on the fact that the neurons have relatively small somata diameter (Haines, 1988). However, despite many authors attempts, it was not possible to separate the nuclear neurons into three distinct populations of small, medium and large sized neurons on the sole basis of their cell body diameters and therefore to classify small neurons as nucleo-olivary neurons only (Tolbert et al., 1978b; Houck and Person, 2014). Moreover, the somata size of the GABAergic nucleo-cortical neurons vary among the studies and some authors indicated that they are rather middle-sized neurons (Batini et al., 1989) and may constitute a separated population of projecting neurons in the cerebellar nuclei, in comparison to the nucleo-olivary neurons. Whether those GABAergic nucleo-cortical neurons are distinct from the population of GABAergic interneurons is unclear.

More recently a population of glycinergic neurons in the lateral nucleus has been shown to project to the cerebellar cortex (Uusisaari and Knopfel, 2010). Patch-clamp recordings of those neurons in the GlyT2-eGFP transgenic mouse indicated that they are not spontaneously active in acute slices, compared to the other population of GFP-expressing neurons, putatively interneurons (see *section 3.1.2.*). The presence of such glycinergic nucleo-cortical neurons was not confirmed in other cerebellar nuclei, such as the interposed nucleus.

The presence of both glycinergic and GABAergic nucleo-cortical neurons raises the possibility that some of the nucleo-cortical neurons would be actually mixed and co-release both GABA and glycine, as proposed for the interneurons of the cerebellar nuclei (see *section 3.1.2.*). However, the synaptic properties of the nucleo-cortical terminals were never investigated in details in the cerebellar cortex and remains to be further understood.

To conclude, the nucleo-cortical projections were described in the seventies-eighties with respect to their topographic organization and their reciprocity, or non-reciprocity, with the cortico-nuclear pathways. However, no further studies later reported on the functional implication of such intra-cerebellar feedback loops which may have critical influence on the timing and modulation of the cerebellar output activity. The identity and the physiology of the nucleo-cortical neurons are still poorly understood and need to be clarified.

²² A population of glycinergic projecting neurons similar to the glutamatergic principal neurons was described in the medial nucleus, using the GlyT2-eGFP transgenic mouse (Bagnall et al., 2009). It is possible that those neurons are also co-releasing GABA and providing nucleo-cortical collaterals, and would constitute the population of GABAergic neurons found by Gould (1979) in the vestibulo-cerebellum.

MATERIALS and METHODS

MATERIALS AND METHODS

Animals

Adult (3-5 months old) GlyT2-eGFP transgenic mice (Zeilhofer et al., 2005) were used to perform immunostainings and stereotaxic injections of constitutive Adeno-Associated Virus (AAVs). Heterozygous GlyT2-Cre mice (kind gift of HU Zeilhofer, from University of Zurich) were used for stereotaxic injections of floxed AAVs (aged P30), for immunostainings (10-11 months old) and for breeding with either homozygous Rosa26-Floxed-mTmG (Muzumdar et al., 2007) or Rosa 26-Floxed-mTmT female mice. Cre-positive offspring (2-3 months old) were used for immunostainings. Adult Thy1-ChR2-YFP mouse (15 months old, line 18, (Wang et al., 2007)) was used for immunostainings. Adult L7-CHR2-YFP mice (males or females, 3-4 months old, (Chaumont et al., 2013)) were used for immunostainings and for breeding with GlyT2-eGFP mouse (males or females). Heterozygous Thy1-CFP animals (aged P30-P60, line 23, (Feng et al., 2000)) were used to patch principal cells in electrophysiological experiments. Wild type OF1 pups were used for inferior olive injection. Either males or females were used in all experiments. All animal manipulations were made in accordance with guidelines of the Centre National de la Recherche Scientifique.

Genotyping

Digestion of the tails: Pieces of tails were digested at 55°C in a solution of 250 µg proteinase K (Euromedex) in 250 µL of Buffer Direct Tail PCR (Viagen) per tails during 5 hours, followed by inactivation of the proteinase K at 95°C during 20 min. Samples were centrifuged 10 min at 4°C before being included in the PCR mix. Occasionally, the tails were digested using Fast Tissue-to-PCR Kit (ThermoFisher), during 10 min at 55°C and 3 min at 95°C in 100 µL of Tissue Lysis Solution and 10 µL of Proteinase K per tails. 100 µL of Neutralization mix per tails were then added to the mix to stop the proteinase K reaction.

PCR mix for GlyT2-Cre mouse line: The PCR mix for one tail (30 µL) of GlyT2-Cre mouse was composed of 1X Green GoTaq® Flexi Buffer (GoTaq® Flexi DNA Polymeras Kit, Promega), 50 nM of both primers (primer F and primer R), 1.5 mM MgCl₂, 0.5 mM dNTP and 1.25 units GoTaq® DNA polymerase (GoTaq® Flexi DNA Polymeras Kit, Promega), completed with water and 2 µL of sample. The PCR protocol follows this sequence of temperatures : 5 min at 95°C, 35 times (30 sec at 95°C, 30 sec at 60°C, 40sec at 72°C), 2 min at 72°C.

PCR mix for L7-ChR2-YFP mouse line: The PCR mix for one tail (20 µL) of L7-ChR2-YFP mouse was composed of 1X Tissue Green Solution PCR Master Mix (ThermoScientific, Fast Tissue-to-PCR Kit), 0.5 mM of both primers (primer 1 and primer 2). The mix was completed with water and 4 µL of sample. The PCR protocol follows this sequence of temperatures : 3 min at 95°C, 40 times (30 sec at 95°C, 30 sec at 61°C, 30 sec at 72°C), 3 min at 72°C.

Primers: Primer F of GlyT2-Cre mouse: 5'-GAAATCAGTGC GTTCGAACGCTAGA-3'. Primer R of GlyT2-Cre mouse: 5'-TGATGGACATGTTTCAGGGATC-3'. Primer 1 of L7-ChR2-YFP mouse: 5'-AAAAATGTGTTTCGCGCCATA-3'; Primer 2 of L7-ChR2-YFP mouse: 5'-GCTTCTTCAACCTGCTGACC -3'.

Electrophoresis gel and migration: 0.1% agarose (InVitrogen) electrophoresis gels with 5% of bromidure d'ethidium (Sigma-Aldrich) were prepared in 1X TBE buffer. 5 to 10 µL of PCR samples were loaded in each wells and 200 mV current was applied through the gel during 15 to 30 minutes,

before the gel was revealed under ultraviolet lights.

GlyT2-eGFP phenotyping: GlyT2-eGFP males were bred with C57BL6 females. Litters were phenotyped at birth using GFP glasses to detect fluorescence in the brainstem and spinal cord. Only positive animals were kept for experiments.

Thy1-CFP phenotyping: Thy1-CFP colony was kept homozygous. For experiments, Thy1-CFP males were bred with C57BL6 females and all the heterozygous animals of the litter were used.

Stereotaxic injections

Animals and tracers: GlyT2-Cre mice (1 month old for electrophysiological experiments, 10-11 months old for immunostainings experiments) were injected in the cerebellar nuclei with 500 nanoliters of virus AAV2.1.EF1 α .DIO.hChR2(H134R).eYFP (plasmid from Deisseroth K., Stanford University, virus from Laboratoire de Thérapie Génique – UMR 649, Nantes). Adult GlyT2-eGFP animals (3-5 months) were injected in the inferior olive with 10 to 50 nanoliters of Retrograde Beads (Red Retrobeads, Lumafuor) from a dorsal entry point, or in the cerebellar nuclei with 200 nanoliters of constitutive virus AAV1.CB7.CI.mCherry.WPRE.r (University of Pennsylvania, Penn Vector Core). Wild type OF1 pups were injected in the inferior olive with about 50 nanoliters of virus AAV1.hSyn.ChR2(H134R).eYFP.WPRE.hGH (University of Pennsylvania, Penn Vector Core).

Capillaries and loading of the pipettes: Quartz capillaries with filament (1.0 x 0.50 mm x 7.5 cm, Sutter Instruments) were pulled using a vertical laser puller (Sutter). The tips of the pipettes were cut to reach 35-40 μ m of tip diameter. The pipette were loaded and stored in the fridge before the surgery.

Stereotaxic injection protocol – Dorsal approach in adult animals: All the procedure was the same between the different experiments (inferior olive or cerebellar nuclei injections). The animals were deeply anesthetized by intra-peritoneal injection of ketamine-xylazine (106mg/kg and 7.5mg/kg, respectively). The depth of anesthesia was assessed before manipulating the animals by pinching the paw without any responses. Local analgesic (Lidocaine Prilocaine 5 % cream, Biogaran) was applied in the ears and on the top of the head at the place of incision. Animals were placed in a stereotaxic frame and the good maintenance of the head position was carefully assessed before starting the surgery. The eyes were covered with ophthalmologic cream (Humigel, Virbac) to avoid eye dryness. Incision was made with a scalpel blade (number 11, Swann-Norton) on the top of the head and the surface of the skull was cleaned with cotton buds and physiological serum. Sometimes, the neck muscles are gently detached from the occipital bone to allow better access to the cerebellum during injections. The skull was aligned with respect to the position of bregma and lambda references. Holes were made in the skull with the milling machine (Foredom) at the right location. A capillary previously loaded was gently lowered in the brain at the proper coordinates. After waiting few seconds to allow the tissue to relax from the constraints applied during the going down, the injection was performed using Picospritzer II (General Valve Corporation) which allows to slowly pressure-injecting at each site at the rate of one 30 msec pulse every 5 seconds, with a pressure of 30 psi. The pipette stayed in position during 5 to 15 minutes, before removing the capillary, to avoid spreading of the injected product, notably in the pipette tract. The wound was cleaned with physiological serum and cotton buds. Local antiseptic (10% iodine povidone gel, Mylan) was applied on the stitches (made with silk suture 4-0 Mersilk Ethicon) and the mouse was rehydrated by subcutaneous injection of physiological solution, sometimes complemented with D-glucose (50 mg / mL Sigma). The mouse was allowed to recover in the cage under infrared light and analgesia was provided by intra-peritoneal injection of buprenorphine (0.05mg/kg). Animals were closely monitored for three days

until recovery from surgery and then housed during the incubation period (three to four weeks for AAVs, seven to ten days for retrobeads).

Stereotaxic injection protocol – Ventral approach in pups: Injections were made on pups 12 to 24 hours after birth. The mother was tranquilized by an intra-peritoneal injection of ketamine (100mg/kg), in order to reduce the stress induced by the manipulation of her babies and reduce the post-surgery cannibalism. Pups were anesthetized on ice during 5 to 6 minutes, and then placed on a metal plate itself refrigerated to avoid the waking up of the pup during the surgery. A thin and superficial cut was made with a scalpel blade (number 11, Swann-Norton) along the throat to open the skin. Muscles and fats were gently pushed on the side to allow access to the *foramen magnum* by a ventral approach. The *foramen magnum* is the large opening in the occipital bone of the cranium, through which medulla oblongata enters and exits the skull. The inferior olive is located on the ventral part of the medulla oblongata, just below the crossing of the basal artery and the vertebral arteries. Tissues and bones were maintained by little home-made retractors during the injection procedure. In pups, meninges covering the medulla oblongata are thin and can be easily pierced with the tip of the quartz pipette compared to adult mice. About 50 nanoliters of virus were pressure-injected with a Picospritzer II (General Valve Corporation). Once the injection completed, tissues were put back in place, the wound was carefully cleaned with physiological serum and cotton buds. No stitches or surgical adhesive were applied to avoid acts of cannibalism by the mother, the wound was dried and closed in a way to avoid post-surgery infections. The whole procedure happened in less than 10 minutes. Pups were allowed to recover under infrared light. One to two hours after the surgery, pups are placed back in the cage with the mother and closely monitored during the next days.

Immunohistochemistry

Paraformaldehyde preparation: 4% w/v Paraformaldehyde powder (PAF; VWR) was dissolved under agitation in 1X phosphate buffer saline (PBS; Sigma) in a water-bath at 60°C. 0.01M NaOH (Merck) was added to the solution. Once the powder was dissolved, the solution was removed from the water-bath and 0.01M KCl (VWR) was added to adjust pH to 7.4. Fresh PAF solution was filtered and allowed to cool down before being used during the day. For some experiments, 1% w/v glutaraldehyde (Sigma-Aldrich) was added to the solution before filtering.

Perfusion and fixation of the animals: Animals were deeply anesthetized with intra-peritoneal injection of sodium pentobarbital (50 mg/kg) and perfused through the aorta with ice-cold solution of 1X PBS followed by 50-75 ml of 4% PAF solution. For GABA immunostaining, tracheotomy was performed before opening the rib cage and assisted-ventilation with medical oxygen was maintained during the intra-aortic perfusion, first with oxygenated (95 % O₂ – 5 % CO₂) ice-cold solution of 1X PBS followed by 4 % PAF - 1 % glutaraldehyde. In both cases, the entire brain was dissected and kept overnight in 4 % PAF solution at 4°C.

Paraffin embedding and slices preparations: Samples were rinsed with 1X PBS. The cerebellum was dissected out and dehydrated by 1 hour-baths of increasing concentration of ethanol (70%, 80%, 95% twice, and 100% (Merck)), butanol (Merck) and xylene (two 1 hour- bath, histological quality, QP Pancreac)). Bleaching of the tissue was used as an indicator of the dehydration process. The cerebellum was then transferred to small dishes with melted paraffin (“X-tra”, Leica) between 58-64°C in a vacuum incubator (-25 mmHg, BioBlock Scientific) to remove air bubbles in the tissue. Three baths of 45 minutes were necessary to efficiently embed the pieces of tissues in the paraffin. The cerebellum was then positioned in a last flat-bottom dish which was allowed to cool down overnight

and can be stored at room temperature until slicing. Blocks of paraffin were put on a microtome (Leica) with the proper orientation. Ribbons of 7 μm thickness slices were cut and dropped few seconds into warm water (45°C) to avoid wrinkles before being mounted on SuperFrost Ultra Plus slides (Thermo Scientific). The slides were dried overnight in an oven at 40°C and stored at room temperature until use.

Antigen-retrieval protocol on paraffin-embedded slices: Paraffin-embedded slices were treated for antigen retrieval as previously described (Rousseau et al., 2012). Slices were put on a hot plate (60°C) before use to improve adhesion of the samples. All the following steps were done under agitation at room temperature, unless specified. Slices are rehydrated (10 min xylene 4 times, 10 min 100% ethanol 3 times, 5 min 95% ethanol 3 times, 5 min 85% ethanol, 5 min 75% ethanol, 5 min 50% ethanol) and rinsed with PBS (10 min 4 times). Fixatives are known to restrict the access to some epitopes due to steric hindrance by cross-linking with neighboring partners. To recover an effective binding of antibodies, trypsin-digestion can be used but is not relevant for all types of epitopes (Werner et al., 1996). Here, we chose to perform a heat-induced unmasking (Shi et al., 1991). For this purpose, slice immersed in a commercial antigen decloaking solution (Biocare medical) were transferred in a decloaking chamber (Biocare Medical) heated up to 115°C during 20 minutes. When the slices reached back the room temperature after at least 30 min of cooling, they are rinsed and incubated for one hour in a solution of 0.1% sodium borohydride (Sigma Aldrich), followed by 45 minutes in a solution of 15% methanol (Sigma Aldrich) and 0.3% H₂O₂ (Sigma Aldrich) in PBS. Once the antigen-retrieval procedure was achieved, the tissue sections were rinsed and permeabilize using solutions of 0.1% cold fish skin gelatin (Sigma) in PBS (called PBSg, during 20 min) and 0.1% v/v Triton (Sigma) in PBSg (called PBSgt, two times 20 min). The sections were incubated overnight at 4°C with primary antibodies diluted in PBSgt in a dark and wet chamber. The next days, the slices are rinsed (3 times 10 min in PBS, 3 times 20 min in PBSgt) before being incubated with secondary antibodies diluted in PBSgt during 2 hours at room temperature in the same chamber. Slices were then rinsed (3 times 10 min in PBS, 3 times 20 min in PBSgt, once 20 min in PBSg, once 20 min in PBS) and mounted in Prolong Gold Antifade Reagent (Sigma). The mounted sections dried overnight and were sealed with Entellan (Merck) the next days. The slices were stored for few days at 4°C during the acquisition period, and were transferred at -20°C or -80°C for longer periods.

Cryo-microtome sections and free-floating slices preparation: Samples were rinsed with 1X PBS and cryo-protected by equilibration in 30 % sucrose (Euromedex) w/v PBS solution for at least 48h at 4°C, complemented with sodium azide (Sigma) to avoid contamination. The cerebellum was then cut on a cryo-microtome (Leica) at -20 °C (30 to 60 μm thicknesses) and the slices were transferred to wells containing PBS.

Free-floating immunostaining protocol: Free-floating sections were washed twice 10 minutes in PBS and permeabilized 2h at room temperature in 0.4 % v/v Triton - PBS. Non-specific sites were saturated by incubation in 0.4 % Triton - 1.5 % cold fish skin gelatin - PBS at room temperature for 3h. Primary antibodies were applied overnight at 4°C in a PBS solution containing 0.1 % Triton - 1.5 % fish gelatin. After 3 washes of 30 minutes in 0.1 % Triton - PBS solution, slices were incubated overnight at 4°C with secondary antibodies diluted in PBS - 0.1% Triton-1.5% cold fish skin gelatin. Slices were finally rinsed with PBS 3 times 30 minutes and mounted in either Fluoromount (Sigma) either Mowiol solution (made from powder, Fluka-Sigma).

Primary and secondary antibodies: The list of primary and secondary antibodies used is summarized in the following tables.

PRIMARY ANTIBODIES			
Species	Targeted protein	Company	Final dilution
chicken	GFP	Avès	1/1000
mouse	Pan-GlyR (mAB4a)	Synaptic Systems	1/1000
mouse	VGluT2	Millipore	1/1500
mouse	GABA (mAB 3A12)	Swant	1/10000
mouse	GAD65-67 (mAB 9A6)	Enzo Life Sciences	1/500
mouse	VGLUT2	Millipore	1./1500
rabbit	α 1-GlyR	kind gift of Andrea Dumoulin, (Machado et al., 2011)	1/500
rabbit	Neurogranin	Abcam	1/500
rabbit	γ 2-GABAR	Synaptic Systems	1/1500
rabbit	α 1-GABAR	Synaptic Systems	1/500
guinea pig	GlyT2	Chemicon Millipore	1/1500
guinea pig	VIAAT	Synaptic Systems	1/1500
guinea pig	Calbindin D-28K	Synaptic Systems	1/200
guinea pig	VGLUT1	Millipore	1./1500

SECONDARY ANTIBODIES				
Species	Targeted species	Fluorophores	Company	Final dilution
donkey	chicken	DyLight 488	Jackson ImmunoResearch	1/500
donkey	mouse	DyLight 549	Jackson ImmunoResearch	1/500
donkey	mouse	DyLight 649	Jackson ImmunoResearch	1/500
donkey	mouse	Alexa Fluor 555	In vitrogen	1/500
donkey	rabbit	DyLight 549	Jackson ImmunoResearch	1/500
donkey	rabbit	DyLight 649	Jackson ImmunoResearch	1/500
donkey	guinea pig	DyLight 649	Jackson ImmunoResearch	1/500

Image acquisition and Analysis

Acquisition: Images stacks were acquired with an inverted confocal microscope (Leica, SP5) at 60 x 60 x 170 nm voxel size, using a 63X oil immersion objective (NA 1.4). Tile scan stacks used for somata counting (see Results, *section 1.1.*) were acquired with a direct confocal microscope (Leica, SP5) at 750 nm x 750 nm x 8 μ m with a 10X air objective (NA 0.4, opened pinhole to 3 airy arbitrary units). In Results, Chapter 2, *section 2.2.*, images stacks were acquired with an inverted confocal microscope (Leica, SP8) using a 63X oil immersion objective (NA 1.3).

Deconvolution: Whatever the optical system used for acquisition (the “convolution”), it introduces deformation of the real signal. Indeed a fluorescent point will appear as a blurry “blob” in images. Therefore, “deconvolution” aims to restore the original signal. Deconvolution process necessitates knowing the model of deformation performed by the optical system, the point-spread function, which is specific of the microscope and the wavelength which were used for acquisition. Here, we chose to use experimental point-spread functions (PSFs) to be used in the deconvolution routine.

Sub-resolution (175 nm) fluorescent beads (PS-Speck, Invitrogen) for each wavelength (green, orange and deep-red beads) were embedded in 7.5% w/v porcine gelatin in 1X PBS at the final dilution of 1/50. 7 μ m thickness slices of gelatin with fluorescent beads were cut using a cryostat (Leica) and mounted on SuperFrost Ultra Plus slides (Thermo Scientific) in Prolong Gold Antifade Reagent (Sigma), to mimic the mounting condition of the tissue samples²³. Stacks of the fluorescent beads were acquired with an inverted confocal microscope (Leica, SP5) at 30 x 30 x 170 nm voxel size, using a 63X oil immersion objective (NA 1.4). Bead images were extracted from image stacks and averaged to obtain an experimental PSF. Each stack was separated into four quadrants, computed in parallel with the routine and reassembled at the end of the deconvolution process, in order to reduce the time necessary for the deconvolution (see details in Results, *section 1.1.*).

Cluster detection and quantification: Stacks with tens of z-slices in both channels for GABA_A receptors and glycine receptors stainings were used to detect synaptic clusters. To decrease the signal to noise ratio and in order to estimate the subcellular localization of the different clusters, we chose to average sequentially five to ten optical slices (800 to 1700 nm Z projection, about the size of a PSF) along the stack, rather than projecting the whole stack. Clusters of receptors were detected on the resulting images of summed (GABA_A + Glycine receptors channels) stacks as regions of interest (ROIs) using a threshold based method. ROI statistics were then retrieved for each ROI on individual color channels and computed with GNU R (“R: A Language and Environment for Statistical-Computing”, R Core Team, R Foundation for Statistical Computing, Vienna, Austria, 2013, <http://www.R-project.org>).

Colocalization analysis: Authors tried for many years to develop satisfying colocalization analysis (Bolte and Cordelieres, 2006). It appears that the choice of an efficient strategy among those already described dependent on the experimental paradigm and the question you want to solve. Here, we decided to design our own custom routine using Fiji (Schindelin et al., 2012) to assess colocalization in the whole stack with a certain degree of 3D (see Results, *section 1.1.*). Stacks were sequentially averaged and projected over five to ten optical slices as previously described. Principles of the routine are exposed in details in Results, *section 1.1.*

Apposition analysis: As for the colocalization, quantification of the apposition between to defined markers turns out to be not as simple as we thought. Notably the distance, in 3D, between the two element was very important, and using our averaged projection of the whole stack increased the number of false results (false positives because some elements were close in the projection while they were actually in the two edges of the projected optical slices, or false negatives because some apposed elements were separated by the splicing into different projected slices). Therefore, we chose to use a “real” 3D approach using Imaris 7.2 software (Bitplane). Clusters and varicosities could be easily detected in 3D within the whole stack by thresholding. Distances between the cluster centers and the closest varicosity surface were automatically retrieved in stacks using a Matlab plugin included in the Imaris version.

Electrophysiology

Acute slices preparation/ Electrophysiological recordings / Electrical and optical stimulations / Drugs: Experimental procedures are detailed in Results, *section 1.1.*

²³Therefore, cold fish skin gelatin should have been used to embed the fluorescent beads, as it was used in all the immunohistochemistry protocols. However, the cold fish skin gelatin was not able to solidify enough to allow its cut on the cryostat.

Capillaries: Borosilicate glass electrodes (For whole-cell patch clamping : 1.5 mm outer diameter x 1 mm inner diameter from Hilgenberg or 1.5 mm outer diameter x 1.16 mm inner diameter from Harvard Apparatus; for extracellular recordings: 1.5 mm outer diameter x 0.86 mm inner diameter from Harvard Apparatus) were pulled on a vertical puller in two steps. Tips were embedded with wax.

Extracellular recordings: The activity of the GlyT2-positive neurons in the GlyT2-Cre mouse infected with flexed AAVs expressing the ChR2 was monitored during optical stimulations. Borosilicate pipettes filled with 3M NaCl were approached from the cell body of the neurons, previously located by epifluorescence, and electrophysiological behavior of the neurons was recorded during 470 nm LED illumination (for details, see Electrical and optical stimulations in Results, *section 1.1.*).

Electrophysiological recordings of the GlyT2-eGFP positive neurons: In the L7-ChR2-YFP x GlyT2-eGFP breeding, GlyT2-eGFP positive neurons were identified with epifluorescence and recorded. During whole-cell configuration, neurons were held at -60 mV (for details, see Electrophysiological recordings in Results, *section 1.1.*)

Electrophysiological recordings in principal neurons of animals injected with AAVs-ChR2 in the inferior olive with ventral approach: Animals were injected as previously described at Po-P1. For acute slices experiments, animals were aged between P21 and P44. Patch clamp recordings in whole-cell configuration of principal neurons in the cerebellar nuclei were performed, while pulses of light were shined on the slices (for details, see Electrical and optical stimulations in Results, *section 1.1.*). Using a high-chloride internal solution, principal neurons were held at -70 mV (see Results, *section 2.1.2.*). Using a physiological internal solution (composed of (in mM) 115 Cesium-MethylSulfonate, 10 TEA-Cl, 10 HEPES, 10 QX314, 10 BAPTA, 3 CaCl₂, 1 MgCl₂, 4 ATP-Mg, 0.4 GTP-Na., adjusted at pH 7.4 with CsOH, osmolarity 295 mOsm), neurons were held at -20 or -10 mV (see Results, *section 2.1.2.*).

Electrophysiological recordings of Golgi cells: Slices were moved to the recording chamber mounted on an upright Olympus BX51WI modular microscope equipped with a $\times 40$ water-immersion objective (LUMPlanFL/IR, 0.8NA) and continuously perfused with bubbled BBS (perfusion was regulated by a peristaltic pump with a flow rate ~ 3.5 ml/min; 32 - 33°C). Neurons were visualized for patch-clamp recordings using a combination of gradient contrast and online video contrast enhancement (CoolSNAP cf, Photometrics and MetaVue, Roper Scientific). Patch pipettes (3 - 4 M Ω for Golgi cells) were pulled from borosilicate glass capillaries (0.15mm diameter, Hilgenberg) with a vertical puller (David Kopf Instruments) and coated with dental wax. Recordings were obtained using MultiClamp 700B amplifier and converted by a Digidata 1440A interface (Molecular Devices) at sampling rate of 50 kHz. A Bessel filter at 6 kHz was used. Golgi cells could be unambiguously differentiated from other cells in the granular layer by the size of their soma (10 - 25 μ m) and their bi-exponential capacitive current (Dieudonné, 1995). For whole-cell recordings of Golgi cells pipettes were filled with a physiological Cl⁻ intracellular solution containing (in mM): 140 K-Gluconate, 4 NaCl, 10 HEPES, 5 EGTA, 4 NaCl, 0.5 CaCl₂ and 3 ATP-Mg with pH adjusted to 7.35 by 1M KOH. During whole-cell recordings the holding potential of voltage - clamped GoC -50mV. Few cells were filled through the whole-cell patch pipette with the neurobiotin (5 μ M). All experiments were performed in the presence of 50 μ M D-2-amino-5-phosphonopentanoate (D-APV, Abcam) and 2 μ M 6-nitro-7-sulfamoylbenzo(f)-quinoxaline-2,3-dione (NBQX, Abcam) to block NMDA and AMPA receptors. Strychnine (Abcam) and SR 95531 (gabazine, Abcam) were added during the recordings.

Optical stimulations of L7-ChR2-YFP terminals in the cerebellar nuclei: Optogenetic stimulations of

GlyT2-Cre neurons (see Results, *section 1.1.*) and Purkinje cells terminals in the cerebellar nuclei of L7-ChR2-YFP x GlyT2-eGFP mouse (see Results, *section 2.2.2.*) were achieved with 470 nm LED illumination (Thorlabs) of one millisecond duration with a power density of 0.3 to 4 mW/mm² (measured under the objective lens).

Arbitrary units	Illumination power ($\mu\text{W}/\text{mm}^2$)
Zero	2,6
1	258,7
2	692,7
3	1047,8
4	2160,5
5	3606,4
Maximum	4138.9

Optical stimulations of GlyT2-Crex AAV-ChR2-YFP terminals in the granular layer of the cortex:

Optogenetic stimulations of the inhibitory nucleo-cortical fibers in the granule cell layer were achieved with an optical system combining low-numerical aperture (NA) Gaussian beam illumination and fast acousto – optic pointing. A 473 nm continuous wave diode-pumped solid-state laser (LRS 0473-00100-03, Laserglow Technologies) was used as a 1P light source for ChR2 expressing fibers. The spot size used for the experiments was set to be 10 μm in diameter (details of the system: Hernandez et al. in preparation). Laser beam stimulated one (10 μm in diameter) location for 50 μs and was redirected to another location with minimal OFF time (less than 1 μs). Stimulated FOV was 1.35 μm x 1.08 μm (5 x 4 a.u. points) which resulted in 1 ms duration of stimulation and stimulation was repeated 5 times (giving in total 5ms stimulation) every 20 seconds. Energy used for simulation was: 84.01 \pm 40 nJ. 30-50 sweeps were averaged for each condition. Averages of pharmacologically modulated traces were done only after ~6 minutes from the beginning of the perfusion of the drug into the recording chamber to provide the time for the steady state effect.

Statistical analysis

Statistical analysis was performed using GNU R, Igor Pro (Wavemetrics) and Clampfit 10.4 (Molecular devices). Results are represented as mean \pm SD unless otherwise specified. Statistical tests were performed using non-parametric Wilcoxon rank-sum and signed-rank tests and significance was assumed if $p \leq 0.05$.

RESULTS

CHAPTER 4: Differential GABAergic and glycinergic inputs of inhibitory interneurons and Purkinje cells to principal neurons of the cerebellar nuclei

As exposed in the introduction, the principal neurons of the cerebellar nuclei integrate several types of inputs both excitatory from climbing and mossy fibers, and inhibitory, mostly from the Purkinje cells of the cerebellar cortex. A population of local inhibitory neurons, which could be GABAergic, glycinergic or mixed GABA/ glycine, was described in the cerebellar nuclei and they were proposed to make synapses onto the principal neurons. However, the existence of functional interneuronal inputs onto the projection neurons was not established for now and its impact of intracerebellar inhibition, as compared to the massive GABAergic inhibition received from the Purkinje cells, was unknown.

In this chapter, we will show how we established the functional characteristics of the interneuronal connection to the principal neurons.

4.1. Article

Differential GABAergic and Glycinergic Inputs of Inhibitory Interneurons and Purkinje Cells to Principal Cells of the Cerebellar Nuclei

Zoé Husson,¹ Charly V. Rousseau,¹ Ilja Broll,² Hanns Ulrich Zeilhofer,³ and Stéphane Dieudonné¹

¹Ecole Normale Supérieure, Institut de Biologie de l'ENS (IBENS), Inserm U1024, and CNRS UMR 8197, F-75005 Paris, France, ²Institute of Pharmacology and Toxicology, University of Zurich, CH-8057 Zurich, Switzerland, and ³Institute of Pharmaceutical Sciences, Swiss Federal Institute of Technology (ETH Zurich), CH-8090 Zurich, Switzerland

The principal neurons of the cerebellar nuclei (CN), the sole output of the olivo-cerebellar system, receive a massive inhibitory input from Purkinje cells (PCs) of the cerebellar cortex. Morphological evidence suggests that CN principal cells are also contacted by inhibitory interneurons, but the properties of this connection are unknown. Using transgenic, tracing, and immunohistochemical approaches in mice, we show that CN interneurons form a large heterogeneous population with GABA/glycinergic phenotypes, distinct from GABAergic olive-projecting neurons. CN interneurons are found to contact principal output neurons, via glycine receptor (GlyR)-enriched synapses, virtually devoid of the main GABA receptor (GABAR) subunits $\alpha 1$ and $\gamma 2$. Those clusters account for 5% of the total number of inhibitory receptor clusters on principal neurons. Brief optogenetic stimulations of CN interneurons, through selective expression of channelrhodopsin 2 after viral-mediated transfection of the flexed gene in GlyT2-Cre transgenic mice, evoked fast IPSCs in principal cells. GlyR activation accounted for 15% of interneuron IPSC amplitude, while the remaining current was mediated by activation of GABAR. Surprisingly, small GlyR clusters were also found at PC synapses onto principal CN neurons in addition to $\alpha 1$ and $\gamma 2$ GABAR subunits. However, GlyR activation was found to account for <3% of the PC inhibitory synaptic currents evoked by electrical stimulation. This work establishes CN glycinergic neurons as a significant source of inhibition to CN principal cells, forming contacts molecularly distinct from, but functionally similar to, Purkinje cell synapses. Their impact on CN output, motor learning, and motor execution deserves further investigation.

Key words: cerebellar nuclei; glycinergic; immunohistochemistry; interneurons; mixed inhibition; optogenetics

Introduction

The cerebellar nuclei (CN) form the sole output of the cerebellar system integrating direct pathways and indirect pathways via the cerebellar cortex. Important components of cerebellar plasticity

(Zheng and Raman, 2010) and sensorimotor learning (Miles and Lisberger, 1981; Medina et al., 2000) are implemented in the CN rather than in the cerebellar cortex, although the latter was more extensively studied. Hence, understanding information processing in the CN, including how local connectivity controls the activity of CN principal cells (Uusisaari and Knöpfel, 2012) is a central endeavor for cerebellar studies.

The CN contain different types of projection neurons: output neurons such as glutamatergic principal cells projecting to premotor structures or glycine-containing large neurons of the medial nucleus projecting to brainstem nuclei (Wassef et al., 1986; Bagnall et al., 2009), small GABAergic neurons mediating the nucleo-olivary feedback loop (Fredette and Mugnaini, 1991; De Zeeuw et al., 1997), and nucleo-cortical neurons (Houck and Person, 2014). Purkinje cells (PCs) of the cerebellar cortex provide a massive GABAergic projection to all these neuronal types (De Zeeuw and Berrebi, 1995; Teune et al., 1998; Uusisaari and Knöpfel, 2008), thereby controlling the output of the CN (Ito et al., 1970; Chen et al., 2010; Hoebeek et al., 2010; Person and Raman, 2012a; Chaumont et al., 2013).

The persistence of GABAergic synapses in the CN of PC-degeneration (PCD) mutant mice (Wassef et al., 1986) provided the first evidence for a source of CN inhibition different from

Received Jan. 29, 2014; revised May 16, 2014; accepted June 7, 2014.

Author contributions: Z.H. and S.D. designed research; Z.H. and C.V.R. performed research; I.B. and H.U.Z. contributed unpublished reagents/analytic tools; Z.H. and C.V.R. analyzed data; Z.H. and S.D. wrote the paper.

Research was supported by CNRS, INSERM, and ENS (École Normale Supérieure), and by Agence Nationale de la Recherche (ANR) Grants INNET (BL2011) and Cecomod (MNP2009) to S.D. and by the Advanced Investigator ERC (European Research Council) Grant (DHIISP, 250128) to H.U.Z. This work has received support under the program "Investissements d'Avenir" launched by the French Government and implemented by the ANR (ANR-10-LABX-54 MEMO LIFE; ANR-11-IDEX-0001-02 PSL* Research University). Z.H. is a recipient of a fellowship from Université Pierre et Marie Curie—ED3C. C.V.R. received a fellowship from Fondation pour la Recherche Médicale (FRM). We thank Dr. P. Isopé for making available the L7-ChR2-YFP transgenic mice; Dr. A. Dumoulin for $\alpha 1$ -GlyR antibodies and useful advice on glycine immunostaining; Dr. M. Diana for his help with stereotaxic injections and viruses; Dr. M. Spolidoro for her help with retrobead injections; Dr. R. Provaille for help and advice on GNU R and analysis; B. Mathieu for his help at the IBENS imaging platform financed by FRM, Région Ile de France, FRC, and France Bio-Imaging; and Dr. B. Barbour and Dr. C. Léna for careful reading of the manuscript and helpful discussions.

The authors declare no competing financial interests.

Correspondence should be addressed to Stéphane Dieudonné, IBENS, S4.9, 46 rue d'Ulm, F-75005 Paris, France. E-mail: dieudon@biologie.ens.fr.

C. V. Rousseau's present address: Division of Neurophysiology, MRC National Institute for Medical Research, The Ridgeway, Mill Hill, London NW7 1AA, UK.

DOI:10.1523/JNEUROSCI.0401-14.2014

Copyright © 2014 the authors 0270-6474/14/349418-14\$15.00/0

PCs. Early morphological studies had identified a population of small CN neurons with local axonal arborization (Matsushita and Iwahori, 1971; McCreary et al., 1978). The glycine immunoreactivity of many small somata in the CN (Rampon et al., 1996; Bäurle and Grüsser-Cornehls, 1997; Zeilhofer et al., 2005) and the abundance of glycinergic synapses in the CN of wild-type animals (Chen and Hillman, 1993; De Zeeuw and Berrebi, 1995) and PCD mutants (Bäurle and Grüsser-Cornehls, 1997) established the inhibitory nature of these local neurons. These glycinergic interneurons differ from glycine/aspartate projection neurons by size and electrophysiological properties (Bäurle and Grüsser-Cornehls, 1997; Uusisaari et al., 2007; Uusisaari and Knöpfel, 2010). Glycinergic interneurons thus constitute a separate neuronal class of the CN, but their functional impact in a structure massively innervated by GABAergic inputs from PCs remains to be clarified.

Glycine receptors (GlyRs) are expressed in the CN (Malosio et al., 1991; Pedroarena and Kamphausen, 2008) and inhibitory chloride currents have been evoked by glycine application in principal cells of young rats (Kawa, 2003; Pedroarena and Kamphausen, 2008). Small isolated strychnine-sensitive synaptic currents have been also evoked in principal cells by pharmacological or ionic manipulations of the CN (Kawa, 2003; Pedroarena and Kamphausen, 2008). However, further evidence for functional glycinergic inhibition provided by CN interneurons is still lacking.

Using immunohistochemical and optogenetic approaches, we show here that interneurons provide a significant inhibitory input to CN principal neurons through mixed GABAergic/glycinergic synapses displaying distinctive molecular components. These data argue for a role of glycinergic interneurons, together with PCs, in controlling the output of the CN.

Materials and Methods

Animals

Adult (3- to 5-month-old) *GlyT2-eGFP* transgenic mice (Zeilhofer et al., 2005) were used to perform immunostaining. Heterozygous *GlyT2-Cre* (kind gift from H. U. Zeilhofer, University of Zurich, Zurich, Switzerland) male mice were bred with either homozygous *Rosa26-Floxed-mTmG* or *Rosa26-Floxed-mTmT* female mice, and Cre-positive offspring (2–3 months old) were used for immunostaining. *GlyT2-Cre* heterozygous transgenic adult mice were also used for stereotaxic injections of adeno-associated viruses (AAVs). For optogenetic experiments, injections were performed at P30 and recordings were performed at P50–P55. For GlyT2 immunostaining, adult *GlyT2-Cre* mice (10–11 months old) were injected with the virus and processed 1 month later. Adult *Thy1-ChR2-YFP* mice (15 months old, line 18; Wang et al., 2007) and *L7-CHR2-YFP* mice (3–4 months old; Chaumont et al., 2013) were used for immunostaining. Heterozygous *Thy1-CFP* animals (aged P30–P60; Feng et al., 2000) were used to patch principal cells in electrophysiological experiments. Either males or females were used in all experiments. All animal manipulations were made in accordance with guidelines of the Centre National de la Recherche Scientifique.

Stereotaxic injections

GlyT2-Cre mice (1 month old for electrophysiological experiments, 10–11 months old for immunostaining experiments) were deeply anesthetized with ketamine-xylazine (106 mg/kg and 7.5 mg/kg, respectively) and placed in a stereotaxic frame. Two holes were made in the skull above the right and left CN. A pulled quartz capillary (35–40 μ m tip diameter) was lowered into the brain at the proper coordinates, and 500 μ l of viral constructs AAV2.1.EF1 α .DIO.hChR2(H134R).eYFP (plasmid from K. Deisseroth, Stanford University, Stanford, CA; Kravitz et al., 2010; virus from Laboratoire de Thérapie Génique—UMR 649, Nantes, France) was slowly pressure-injected at each site at the rate of one 30 ms pulse every 5 s, with a pressure of 30 psi (Picospritzer II, General Valve Corporation).

Animals were closely monitored for 3 d until recovery from surgery and then housed for 3–4 weeks. Animals were then killed for acute slice experiments as described below.

Adult *GlyT2-eGFP* animals (3–5 months old) were injected in the inferior olive, with 10–50 nl of Retrograde Beads (Red RetroBeads, Lumafloor) from a dorsal entry point.

Immunohistochemistry

Tissue fixation, preparation, and labeling for GABA receptor-GlyR immunostaining. Animals were deeply anesthetized with an intraperitoneal injection of sodium pentobarbital (50 mg/kg) and perfused through the aorta with an ice-cold solution of 1 \times PBS (Sigma) followed by 50–75 ml of 4% w/v paraformaldehyde (PAF; VWR International) dissolved in 1 \times PBS, pH 7.4. The entire brain was then dissected and kept in 4% PAF at 4°C overnight. Samples were then rinsed and embedded in paraffin (Leica). Slices of 7 μ m thickness were cut with a microtome, mounted on SuperFrost Ultra Plus slides (Thermo Fisher Scientific), and treated for antigen retrieval as previously described (Rousseau et al., 2012). For immunohistochemistry, mounted sections were incubated overnight at 4°C with the following primary antibodies: chicken GFP antibody at 1:1000 final dilution (Avès), mouse pan-GlyR (mAB4a) antibody at 1:1000 final dilution (Synaptic Systems), rabbit α 1-GlyR (kind gift from Andrea Dumoulin; Machado et al., 2011), rabbit γ 2-GABAR (GABA receptor) antibody at 1:1500 final dilution (Synaptic Systems), rabbit α 1-GABAR antibody at 1:500 final dilution (Synaptic Systems), guinea pig GlyT2 antibody at 1:1500 final dilution (Millipore Bioscience Research Reagents), guinea pig VIAAT (vesicular inhibitory amino acid transporter) antibody at 1:1500 final dilution (Synaptic Systems), mouse VGluT2 antibody at 1:1500 final dilution (Millipore). Tissue sections were rinsed with PBS and then incubated with secondary antibodies coupled to 488, 549, or 649 DyLight fluorophores (Jackson ImmunoResearch) or Alexa Fluor 555 IgG (Invitrogen) at room temperature during 2 h at 1:500 final dilution. Slices were mounted in Prolong Gold Antifade Reagent (Sigma).

Tissue fixation and preparation for GABA immunostaining. Animals were deeply anesthetized by intraperitoneal injection of sodium pentobarbital (50 mg/kg). Tracheotomy was performed before opening the rib cage, and assisted-ventilation with medical oxygen was maintained during intra-aortic perfusion with an oxygenated (95% O₂–5% CO₂) ice-cold solution of 1 \times PBS followed by 4% PAF dissolved in 1 \times PBS, pH 7.4. The brain was dissected and kept overnight in 4% PAF solution at 4°C.

Free-floating immunostaining for GABA and GAD65–67 labeling. After perfusions of the animals and postfixations overnight of the brains in 4% PAF dissolved in 1 \times PBS, pH 7.4, brains were cryoprotected by equilibration in 30% sucrose w/v–PBS at 4°C and then cut on a cryomicrotome (–20°C, 30–60 μ m thickness). Free-floating sections were washed twice for 10 min in PBS and permeabilized for 2 h at room temperature in PBS–0.4% v/v Triton X-100. Nonspecific sites were saturated by incubation in PBS–0.4% Triton X-100–1.5% cold fish skin gelatin at room temperature for 3 h. Primary antibodies were applied overnight at 4°C in a PBS solution containing 0.1% Triton X-100–1.5% fish gelatin (mouse GABA antibody mAB 3A12, Swant, final dilution 1:10,000; mouse GAD65–67 antibody mAB 9A6, Enzo Life Sciences, final dilution 1:500). After three washes of 30 min in PBS–0.1% Triton X-100, slices were incubated overnight at 4°C with secondary antibodies diluted in PBS–0.1% Triton X-100–1.5% cold fish skin gelatin. Slices were finally rinsed with PBS 3 times for 30 min each and mounted in either Fluoromount (Sigma) or Mowiol solution (made from powder, Fluka-Sigma).

Image acquisition and analysis

Acquisition and deconvolution. Image stacks were acquired using an inverted confocal microscope (Leica SP5) at 60 \times 60 \times 170 nm voxel size, using a 63 \times oil-immersion objective. For image deconvolution, point-spread functions (PSFs) were measured for each wavelength on subresolution (175 nm) fluorescent beads (PS-Speck, Invitrogen) embedded in 7.5% w/v porcine gelatin in 1 \times PBS, and mounted in Prolong Gold Antifade Reagent (Sigma). Bead images were extracted from image stacks using a custom routine in ImageJ (W. S. Rasband, ImageJ), U.S. National

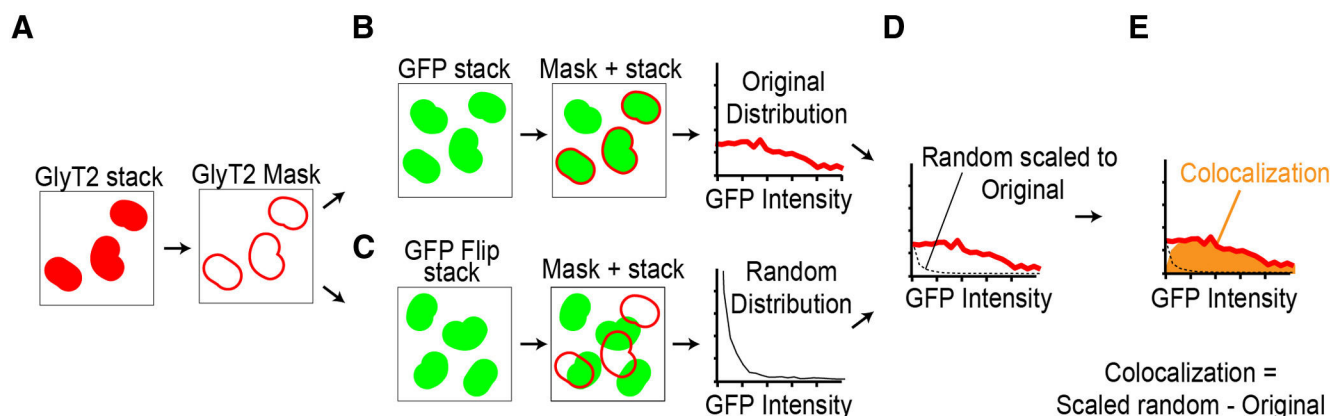


Figure 1. Method for colocalization quantification in confocal Z-stacks. **A**, To quantify the colocalization rate between two markers, for example GlyT2 (red fluorescence signal) over GFP varicosities (green fluorescence signal), GlyT2 + varicosities are detected in stacks and converted as a binary mask. **B, C**, This mask is used to retrieve mean GFP intensities below each immunoreactive aggregate in the original GFP stack (**B**, original distribution in solid red line) and in a flipped GFP stack (**C**, random distribution in black solid line). **D**, This latter distribution is scaled to the original distribution (black dashed line). **E**, The difference between the original distribution and the scaled randomized distribution provides an underestimate of true colocalization (orange).

Institutes of Health, Bethesda, MD, <http://imagej.nih.gov/ij/>, 1997–2012) and averaged to obtain an experimental PSF. Selected image stacks were then deconvolved using a custom routine based on preexisting ImageJ plugins Iterative Deconvolve 3D (Dougherty, 2005, <http://www.optinav.com/imagej.html>) and Objet Counter 3D (Bolte and Cordelières, 2006; <http://rsbweb.nih.gov/ij/plugins/track/objects.html>). Results were then further processed using GNU R (“R: A Language and Environment for Statistical Computing,” R Core Team, R Foundation for Statistical Computing, Vienna, Austria, 2013, <http://www.R-project.org>) and custom routines.

Cluster detection and quantification. Five to 10 optical slices were sequentially averaged (800–1700 nm Z projection) along the whole stack and clusters of receptors were detected on the resulting pictures as ROIs using a threshold-based method. ROI statistics (number of pixels, mean intensity, and total intensity) were then retrieved for each ROI on individual color channels (GlyR and GABAR). Using GNU R, we computed the fraction of labeling intensity attributable to one of the channels for each ROI.

Colocalization analysis. To assess colocalization between two markers, we designed a custom routine using Fiji (Schindelin et al., 2012) and GNU R (Fig. 1). Mean intensities of marker 1 beneath each ROI detected for marker 2 (as previously described; Fig. 1A) were collected in the original stack of marker 1 and plotted (Fig. 1B, red solid lines). To estimate the noise and nonspecific colocalization, mean intensities of marker 1 were also collected in a randomized marker 1 stack (horizontally and vertically flipped; Fig. 1C, black solid line). In the random distribution, the first bins in the initial peak represent ROI with barely undetectable mean intensities and could be considered as noncolocalized elements, whereas the tail of the distribution is considered to be “by-chance” colocalized ROI. Noncolocalized elements would be found in the first low-intensity bins of the original distribution, but it is impossible to draw a clear line between colocalized elements on a low-intensity view of marker 1 and noncolocalized elements. Our *parti-pris* was to systematically underestimate colocalization by assuming that noncolocalized elements in the original distribution had the same bimodal distribution as the random distribution. We obtained the underestimated colocalization (Fig. 1E, in orange) by scaling the randomized distribution to the original distribution (Fig. 1D, black dashed lines), using the average amplitude of the first bins ($n = 3$ in each case) of the histograms and subtracting this scaled random distribution from the original distribution. This custom routine was used to assess rate of colocalization between GlyT2 and GFP markers in different transgenic mice, and between Thy1-YFP and GlyR- and GABAR-enriched clusters. In the case of YFP staining in Thy1-ChR2-YFP mice, YFP intensities of Z-projected sections of the stacks were first scaled according to the slope of the fit to the logarithmic distribution of their pixel intensity. The “subtract background” ImageJ plugin was then applied.

Apposition analysis. Apposition analysis was performed in 3D using Imaris 7.2 software (Bitplane). Clusters and varicosities (either VIAAT-positive or GlyT2-positive) were detected, and distances between the cluster centers and the closest varicosity surface were retrieved in original and randomized stacks (one channel horizontally and vertically flipped).

Statistical analysis. Statistical analysis was performed using GNU R and Igor Pro (Wavemetrics). Results are represented as mean \pm SD unless otherwise specified. Statistical tests were performed using nonparametric Wilcoxon rank-sum and signed-rank tests and significance was assumed if $p \leq 0.05$.

Electrophysiology

Slice preparation. Animals were sedated with isoflurane (4% in medical oxygen) and deeply anesthetized with ketamine-xylazine (106 mg/kg, 7.5 mg/kg) before being perfused with two consecutive iced protective, oxygenated (95% O₂-5% CO₂) solutions [in distilled water; Solution 1 (in mM): 115 NaCl, 26 NaHCO₃, 3 KCl, 0.8 CaCl₂, 8 MgCl₂, 1.25 NaH₂PO₄, 25 glucose, 1 lidocaine, 1 ketamine; Solution 2: 230 sucrose, 26 NaHCO₃, 3 KCl, 0.8 CaCl₂, 8 MgCl₂, 1.25 NaH₂PO₄, 25 glucose, 1 lidocaine, 1 ketamine; Isope and Barbour, 2002]. Animals were then decapitated and the cerebellum was rapidly removed from the skull. The cerebellum was glued (Cyanolit) in the slicing chamber on its anterior face and submerged in ice-cold cutting solution [in Volvic Water, containing the following (in mM): 130 K-gluconate, 14.6 KCl, 2 EGTA, 20 HEPES, 25 glucose, 50 10-3 D-APV, 50 10-6 minocycline] during slicing. Slices (290 μ m thickness) were cut using a ceramic blade (Z deflection < 0.5 μ m) with an oscillating blade microtome (Campden Instruments) and kept in warm (33°C) oxygenated recovery solution [in Volvic Water (containing, in mM): 225 D-mannitol, 2.3 KCl, 1.25 NaH₂PO₄, 25 NaHCO₃, 25 glucose, 0.51 CaCl₂, 7.7 MgCl₂, 50 10-3 D-APV, 50 10-6 minocycline] during several minutes before being transferred to a chamber recirculated with warm (33°C) oxygenated BBS solution [in Volvic Water (containing, in mM): 125.7 NaCl, 3.3 KCl, 1.25 NaH₂PO₄, 24.8 NaHCO₃, 25 glucose, 1.3 CaCl₂, 1.17 MgCl₂, 50 10-6 minocycline].

Electrophysiological recordings. At least 30 min after being cut, slices were transferred to a recording chamber mounted on an Olympus BX51WI microscope equipped with an epifluorescence illumination pathway and a CoolSnap camera (Roper Scientific, Photometrics). Slices were perfused with warm gassed BBS solution (3.5 ml/min, at 33°C). Borosilicate glass patch electrodes (resistance 3–4.5 M Ω) were filled with a high-Cl⁻ intracellular solution containing the following (in mM): 105 CsCl, 20 TEA-Cl, 10 HEPES, 10 QX314, 10 EGTA, 1 CaCl₂, 5 MgCl₂, 4 ATP-Na, 0.4 GTP-Na, pH adjusted to 7.4 with CsOH (290–295 mOsm). Recordings were made in the interposed and lateral nuclei to avoid larger glycinergic projection neurons in the medial nucleus (Bagnall et al., 2009). Whole-cell patch-clamp recordings were performed using a HEKA EPC10 amplifier and PatchMaster acquisition software (HEKA).

Cells were held at -70 mV in the whole-cell configuration and electrophysiological signals were digitized at a sampling rate of 20 kHz. A Bessel filter at 5 kHz was used.

Electrical and optical stimulations. Electrical stimulations of PC axons were performed a few hundred micrometers from the recorded cell in the white matter surrounding the CN, using a Master-9 stimulator (Isoflex Stimulus Isolation Unit, A.M.P.I.). Using regular patch pipettes (3–5 M Ω), bipolar stimulation intensities in the 20–90 V range (200 μ s) were necessary to evoke a stable response in the recorded cells. Optogenetic stimulations of GlyT2-positive CN neurons were achieved with 470 nm LED illumination (Thorlabs) of 1 ms duration with a power density of 0.3–4 mW/mm² (measured under the objective lens). Drugs were bath-applied, and a delay of 5–6 min after addition of the drug was always respected to allow for complete diffusion into the slice.

Drugs. All electrophysiological experiments were performed in the presence of 50 μ M D-APV (Abcam) and 10 μ M NBQX (Abcam) to block NMDA and AMPA receptors. In some experiments, strychnine (Abcam) and SR 95531 (gabazine, Abcam) were added to the bath.

Data analysis. Electrophysiological data were analyzed with Igor Pro 6.1 (Wavemetrics). Statistical analysis was performed using R GNU. Between 250 and 400 sweeps were averaged for each condition. All data are presented as mean \pm SD. For statistical significance, Wilcoxon rank-sum and signed-rank tests were used, as applicable.

Analysis of pharmacological data

To estimate the maximum possible contribution of GlyR to the synaptic currents, gabazine and strychnine were considered to exert independent, nonsynergistic, antagonist effects on GABAR and GlyR. Gabazine fractional block (G) of the GABAR response at a concentration of 300 nM was obtained by applying gabazine in the presence of 1 μ M strychnine. In our calculations, strychnine was considered to block 100% of the GlyR current (Jonas et al., 1998). Let us call Y the fraction of the IPSC amplitude mediated by GlyR and U the unspecific fractional block of GABAR by strychnine (corrections can be performed either for 300 nM or 1 μ M strychnine). Then the fractional block of the IPSC by strychnine alone is $Y + U * (1 - Y)$ and the fractional block of the control response by strychnine after 300 nM gabazine is $[Y + U * G * (1 - Y)]$. Solving these two equations yields Y and U .

Results

Identification of glycinergic interneurons in the CN

We sought to identify the inhibitory interneurons of the CN by their glycinergic phenotype using two transgenic mouse models based on the promoter of the neuronal plasma membrane glycine transporter GlyT2, a specific marker of glycinergic neurons (Zafra et al., 1995). In the first model the eGFP was placed directly under the control of the GlyT2 promoter (*GlyT2-eGFP* mice, Fig. 2A; Zeilhofer et al., 2005), whereas in the second (*GlyT2-Cre* mice) the Cre recombinase was placed under the control of the GlyT2 promoter. To reveal Cre expression, *GlyT2-Cre* mice were bred with *R26-loxed-mTmG* reporter mice in which lox-directed switchable Tomato and GFP are placed under the control of the ubiquitous neuronal promoter *Rosa 26* (Muzumdar et al., 2007; Fig. 2B).

A large number of small GFP+ neurons, putative interneurons, were seen in all subdivisions of the CN in both models and a few large GFP+ projection neurons were seen in the medial nucleus (Fig. 2A,B). In addition to GFP+ cell bodies, all the CN were densely populated by GFP+ neurites, which in many instances could be traced back to small GFP+ cell bodies (Fig. 2C). Coimmunostaining against VIAAT (VGAT), a ubiquitous marker of inhibitory axonal varicosities, identified the majority of these neurites as axons and confirmed the interneuronal nature of small GlyT2-eGFP-positive cells in the CN (Fig. 2Ca). Axons presented clear VIAAT-immunoreactive varicosities (Fig. 2Cb, solid arrows) separated by thin profiles of uniform diame-

ter. Dendrites may also be thin and contorted, but they present more irregular VIAAT-immunonegative profiles (Fig. 2Cb, dashed arrows).

Number of glycinergic neurons in the CN

To estimate the number and density of glycinergic neurons in the CN, fluorescent cell bodies were counted in complete serial sections of *GlyT2-Cre* \times *R26-loxed-mTmT* mouse CN ($n = 3$ animals) and *GlyT2-eGFP* mice ($n = 3$ animals). The number of positive neurons was estimated to 2007 ± 367 and 627 ± 37 in the interposed nuclei of the *GlyT2-Cre* \times *R26-loxed-mTmT* and *GlyT2-eGFP* mice, respectively, and to 2132 ± 567 and 643 ± 68 in the lateral nucleus (cells were not counted in the medial nucleus because large projecting glycinergic neurons were also found in this area). In these two nuclei the density of positive neurons was 5560 ± 1708 neurons/mm³ in *GlyT2-Cre* \times *R26-loxed-mTmT* mice and 1561 ± 32 neurons/mm³ in *GlyT2-eGFP* mice. The large difference of neuron count between the two models suggests either that a fraction of glycinergic neurons do not express GFP in the *GlyT2-eGFP* mouse line or that the expression is not restricted to glycinergic neurons in *GlyT2-Cre* mice, due to developmental leakage of Cre recombinase expression.

To compare the specificity of our two genetic models, we performed immunostaining against the membrane transporter GlyT2 (Fig. 2D,E). GlyT2+ varicosities and axonal profiles were abundant in all nuclei. GlyT2+ varicosities were detected using a threshold-based method, and the rate of GlyT2-GFP colocalization was assessed using a procedure detailed in Figure 1 (see Materials and Methods), which will be used repeatedly in this article (Fig. 2F,G). In the *GlyT2-eGFP* mouse, the rate of colocalization of GlyT2 over GFP was only 40% (Fig. 2D,F), confirming the mosaic expression in this transgenic line. In contrast, >89% of the GlyT2+ varicosities displayed GFP staining in *GlyT2-Cre* \times *R26-loxed-mTmG* offspring (Fig. 2E,G). Hence, most if not all glycinergic interneurons of the CN express the Cre recombinase at one stage of their development in *GlyT2-Cre* mice and are stained by GFP in adult *GlyT2-Cre* \times *R26-loxed-mTmG* offspring. Applying a correction factor of 2.5 for the mosaic expression in the *GlyT2-eGFP* models yields an estimate of the total number of glycinergic neurons of 1567 in the interposed nuclei and 1607 in the lateral nuclei, for an estimated density of 3900 neurons/mm³. This was still much lower than in the *GlyT2-Cre* \times *R26-loxed-mTmT* mice, suggesting the occurrence of non-specific expression in this genetic background.

Closer examination of the *GlyT2-Cre* \times *R26-loxed-mTmT* mice revealed fluorescence expression in some PCs mainly located in the vermis and projecting to the medial nucleus. Furthermore, expression was found in a large number of small cell bodies located in the ventral part of the CN and resembling the morphology of inhibitory neurons projecting to the inferior olive (nucleo-olivary cells; Fig. 2Ha). A specific expression in nucleo-olivary neurons was further confirmed by the observation of numerous fluorescent axons invading the dorsal olive (Fig. 2Hb). Both small neurons concentrated in the ventral part of the CN (Fig. 2Ia), and axons in the olive (Fig. 2Ib) were absent from the *GlyT2-eGFP* animals. When Flexed AAVs were injected into the CN of 1-month-old *GlyT2-Cre* animals, the pattern of expression was similar to the pattern found in *GlyT2-GFP* mice both for the cell density in the CN (the absence of small cells in the ventral CN) and for the absence of fibers in the olive. We conclude that the nonspecific pattern of expression observed in the *GlyT2-Cre* \times *R26-loxed-mTmT* crossings is due to the temporary developmental expression of the Cre recombinase in all glycinergic CN

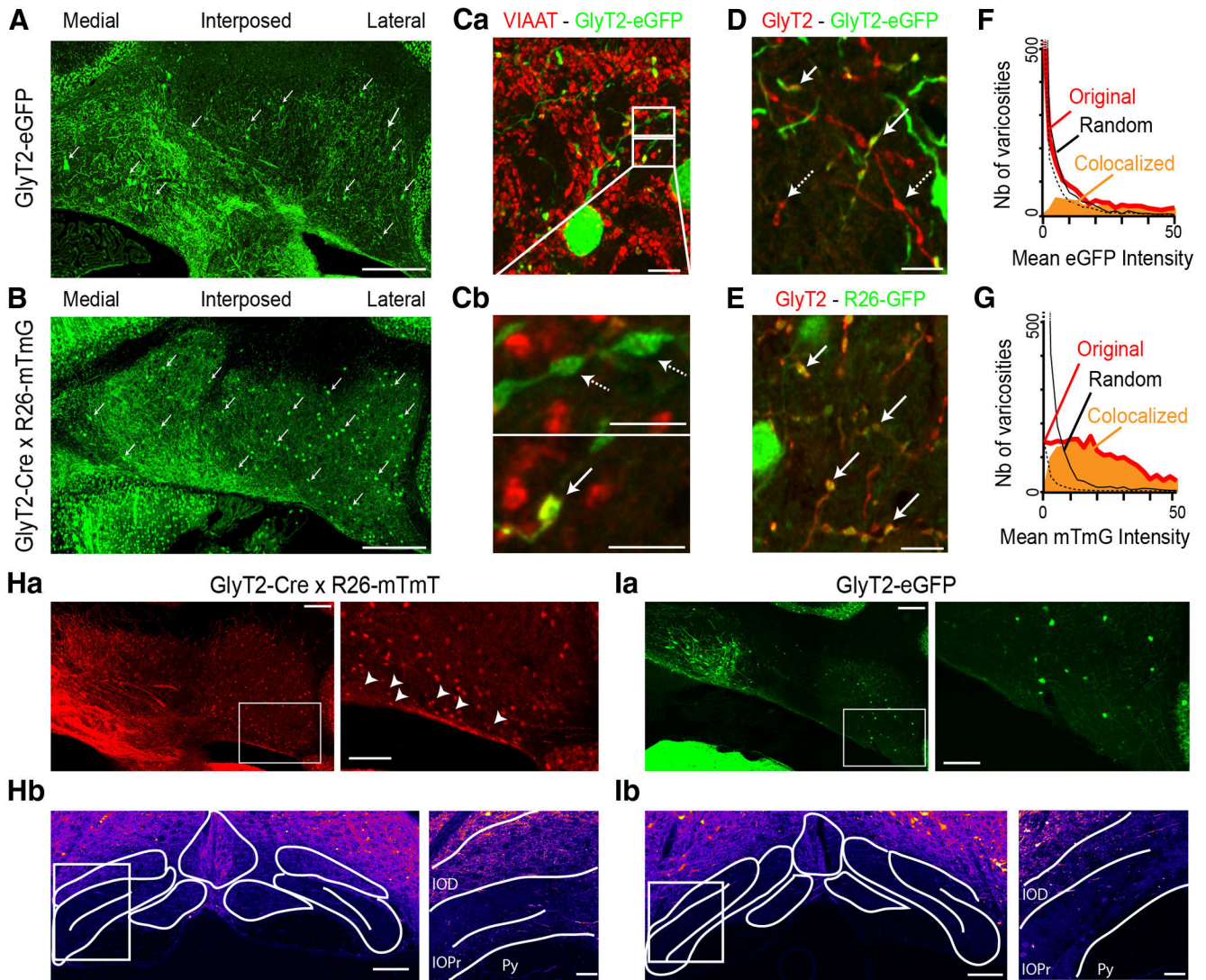


Figure 2. Transgenic mice as tools to study glycinergic interneurons in cerebellar nuclei. **A**, Coronal slice of the CN in the *GlyT2-eGFP* mouse. Arrows indicate *GlyT2-eGFP*⁺ cells within the three cerebellar nuclei (medial, interposed, and lateral nuclei). **B**, Coronal slice of cerebellar nuclei (medial, interposed, and lateral) in a *GlyT2-Cre* × *Rosa26-loxed-mTmG* mouse. Note the abundance of GFP⁺ cells (solid arrows) compared with the *GlyT2-eGFP* mouse. **Ca, Cb**, Costaining of *GlyT2-eGFP* + neurons with VIAAT (red) allows distinguishing between local axonal varicosities (solid arrows) and VIAAT-immunonegative dendrites (dashed arrows). Z-thickness of projection: **Ca**, 8.8 μm; **Cb**, 2 μm. **D**, *GlyT2* costaining of the *GlyT2-eGFP* mouse reveals that only a fraction of *GlyT2*⁺ profiles colocalize with GFP (solid arrows), whereas a majority do not colocalize (dashed arrows). Z-thickness of projection, 1.7 μm. **E**, Near-complete colocalization is found in the *GlyT2-Cre* × *Rosa26-loxed-mTmG* mouse. Z-thickness of projection, 1.7 μm. **F**, In the *GlyT2-eGFP* mouse, distribution histograms of GFP intensities under *GlyT2*⁺ profiles (red) and spatially randomized profile distribution (black; see Materials and Methods and Fig. 1) yield an estimate of colocalization of *GlyT2*⁺ profiles with GFP-positive profiles of 40% (orange area). **G**, In the *Rosa26-loxed-mTmG* × *GlyT2-Cre* mouse, at least 89% of *GlyT2*⁺ varicosities were colocalized with GFP⁺ profiles. **H**, Inferior olive coronal sections in the *GlyT2-Cre* × *Rosa26-loxed-mTmG* mouse. **Ha**, In the cerebellar nuclei of the *GlyT2-Cre* × *Rosa26-loxed-mTmG* mouse, small nucleo-olivary cells are stained and are particularly visible in the ventral part of the nuclei (solid arrowheads). **Hb**, Faint labeling of the axons of nucleo-olivary cells is visible in the inferior olive of the *GlyT2-Cre* × *Rosa26-loxed-mTmG* mouse, particularly in the dorsal subnucleus (Z-thickness of projection, 32 μm). **I**, In the *GlyT2-eGFP* mouse, the nucleo-olivary neuron somata were not visible in the cerebellar nuclei (**Ia**), while virtually no axonal projections were seen in the inferior olive (**Ib**). Z-thickness of projection, 32 μm. Scale bars: **A, B, Ha, Hb, Ia, Ib**, 200 μm; **Ca, D, E**, 10 μm; **Cb**, 5 μm; **Ia, Ib** inset, 100 μm; **Ha, Hb** inset, 50 μm. IOD, Dorsal nucleus of inferior olive; IOPr, principal nucleus of inferior olive, Py, pyramidal tract.

neurons but also in some Purkinje cells and nucleo-olivary neurons. Because of this lack of specificity, the *GlyT2-eGFP* mouse was exclusively used for further morphological studies, keeping in mind that only ~40% of the glycinergic interneurons are eGFP⁺ in this genetic background.

Glycinergic neurons in the CN are distinct from nucleo-olivary cells

To confirm that the GFP⁺ neurons found in the *GlyT2-eGFP* mice and the small nucleo-olivary neurons constitute separate populations of cells, injections of retrograde fluorescent beads were performed in the inferior olive of *GlyT2-eGFP* mice ($n = 3$

animals; Fig. 3A). Retro-labeled cells found in the CN were never eGFP positive (0 of 488 cells; Fig. 3B). However, closer examination revealed a level of fluorescence of their cell bodies slightly above background, indicative of the fact that GFP may have been expressed at earlier developmental stages. Immunostaining for GABA also differentiated glycinergic interneurons from olivary projecting cells. Retrogradely labeled cells did not stain for GABA at their somata (Fig. 3B), although it is well established that GABA neurotransmission occurs at their terminals in the inferior olive through unusual asynchronous release (Best and Regehr, 2009). In contrast, $38.6 \pm 21.5\%$ of the eGFP-positive neurons in the *GlyT2-eGFP* animals ($n = 3$ animals, $n = 570$ eGFP-positive

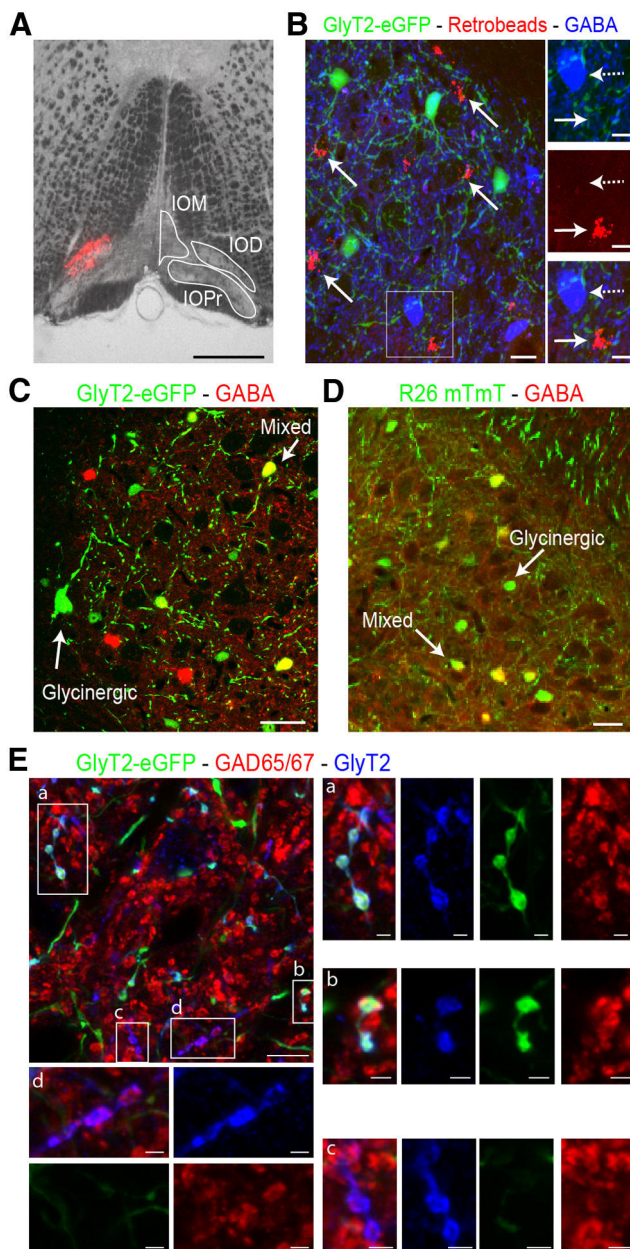


Figure 3. CN interneurons constitute a population distinct from inferior olive-projecting neurons and present mixed GABAergic-glycinergic phenotypes. **A**, Bright-field image of a coronal slice of the inferior olive in a *GlyT2-eGFP* mouse injected with red fluorescent retrograde beads. **B**, In the CN, retrolabeled cells (red; solid arrows) were not GlyT2-eGFP-positive (green) and do not exhibit GABA staining (blue) at their soma (see inset). Z-thickness of projection, 26 μm . **C**, In the *GlyT2-eGFP* mouse, some GFP-positive neurons (green) are found costained for GABA (red). **D**, In a *Rosa26-loxed-mTmT* \times *GlyT2-Cre* mouse, all neurons stained for GABA (red) at their somata are mTmT-positive (green), whereas some mTmT-positive neurons do not show GABA staining. **Ea–Ed**, In the *GlyT2-eGFP* mouse, the mixed GABAergic/glycinergic phenotype of most glycinergic neurons, whether eGFP positive (green) or not, is confirmed by costaining of GlyT2 axonal varicosities (blue) with GAD65–67 (red). Z-thickness, 1.7 μm . IOM, Medial nucleus of inferior olive; IOD, dorsal nucleus of inferior olive; IOPr, principal nucleus of inferior olive. Scale bars: **A**, 50 μm ; **B–D**, 20 μm ; **E**, 10 μm ; **B** inset, 10 μm ; **E** close-ups **a–d** (right), 2 μm .

neurons) displayed GABA immunostaining (Fig. 3C). Conversely, we found that only $42.5 \pm 23.4\%$ of GABA-positive somata were stained for GFP in the *GlyT2-eGFP* mice ($n = 98$ GABA-positive neurons; Fig. 3C), in agreement with the fraction of interneurons stained in this model, whereas $89.1 \pm 15.1\%$ of GABA-positive somata also stained for mTmT in the *Rosa26-*

loxed-mTmT \times *GlyT2-Cre* offspring ($n = 3$ animals, $n = 105$ GABA-positive neurons; Fig. 3D).

As exemplified by the case of the nucleo-olivary cells, somatic staining for GABA is not a reliable marker of the GABAergic phenotype of the transmission at axonal varicosities. To evaluate the extent of GABA and glycine corelease by the CN interneurons, costaining for GlyT2 and GAD65–67 was performed in *GlyT2-eGFP* animals (Fig. 3E). GFP+ axonal varicosities were differentiated from dendrites by their GlyT2 staining, as previously described (Fig. 2D). Those varicosities, as well as GFP-negative GlyT2-positive profiles, were always colabeled for GAD65–67 (Fig. 3E, inset). These data argue for the accumulation and corelease of GABA and glycine at the great majority of interneuron synapses. Thus, inhibitory interneurons of the CN constitute a specific cell type, distinct from the nucleo-olivary cells, and characterized by their mixed glycinergic/GABAergic inhibitory phenotype.

Different types of inhibitory receptor clusters in the CN

To identify the postsynaptic targets of CN mixed inhibitory interneurons and assess the localization and abundance of their synapses relative to the dominant GABAergic innervation coming from PCs, we performed coimmunostaining against glycine receptor subunits (pan-GlyR mAb4a antibody) and the $\gamma 2$ subunit of GABA_A receptors (GABAR- $\gamma 2$), which is strongly expressed in the CN (Araki et al., 1992; Fig. 4A). Numerous GABAR- $\gamma 2$ clusters were found throughout the neuropil and covering the somata and large initial dendrites of presumptive large projection neurons (Fig. 4A). Surprisingly, these clusters appeared colocalized with small glycine receptor clusters. In addition, a population of somewhat larger glycine receptor clusters, which did not appear to costain for GABAR- $\gamma 2$, was present in the neuropil and on the initial dendrites of principal neurons (Fig. 4A).

To quantify these observations, we first performed threshold-based cluster detection (Fig. 1; see Materials and Methods) on the summed GABAR- $\gamma 2$ and pan-GlyR signals. Then GlyR and GABAR immunoreactivities were integrated separately under each cluster area, and the ratio GlyR/(GlyR + GABAR- $\gamma 2$) staining was computed. The distribution of this ratio was bimodal, identifying GlyR-enriched and GABAR-enriched clusters (Fig. 4B). In some cases, low GlyR expression led to the appearance of a probably spurious peak of GABAR-only clusters ($1.1 \pm 0.7\%$ of all clusters; the number of clusters in each stack varies between 1 and 47 clusters, $n = 158$ detected clusters, $n = 7$ stacks, data not shown), which were only slightly more intense than the other GABAR-enriched clusters ($137.3 \pm 39.80\%$, Wilcoxon test $p = 5.4e^{-6}$). We thus considered that GABAR-only clusters represent an extreme form of GABA-enriched clusters but cannot exclude that they constitute a rare synaptic class.

GABAR- $\gamma 2$ labeling was barely detectable in GlyR-enriched clusters ($6.7 \pm 3.5\%$ of the staining of GABAR-enriched clusters, $n = 7$ stacks, $n = 1185$ detected clusters; Fig. 4C). Furthermore, glycine receptor staining intensity in GlyR-enriched clusters was $181.3 \pm 57.0\%$ of that of GABAR-enriched clusters (minimum, 132%; maximum, 280%; Wilcoxon test, $p < 2.2e^{-16}$, $n = 7$ stacks; 2112 ± 547 clusters per stack). Overall, GlyR-enriched clusters represented $8.2 \pm 2.5\%$ of the total number of immunoreactive profiles ($n = 7$ stacks, $n = 14,790$ detected clusters). Similar results were reproduced with an antibody against the $\alpha 1$ subunit of the GABA receptor (Fig. 4D). In this case, the GlyR-enriched population amounted to $8.7 \pm 3.3\%$ of the total number of clusters ($n = 10$ stacks, $n = 23,009$ clusters detected; Fig. 3E,F). Finally, immunostaining against the $\alpha 1$ subunit of the

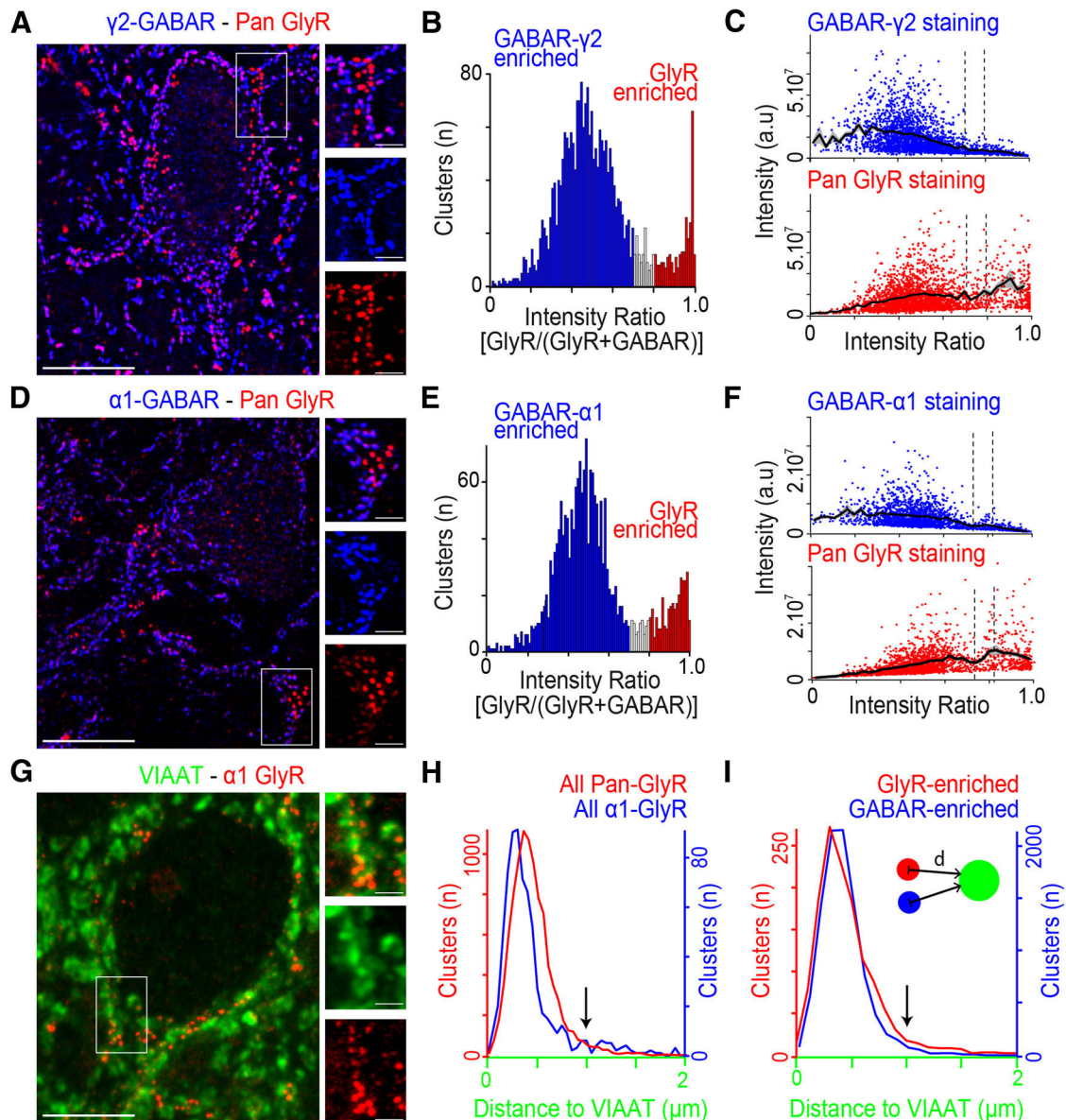


Figure 4. Different types of postsynaptic inhibitory receptor clusters in the CN. **A**, Costaining for the $\gamma 2$ subunit of GABA (blue) and pan-GlyR subunits (red) reveals two main populations of clusters. Z-thickness of projection, $8 \mu\text{m}$. **B**, Example of intensity ratio histogram between the GlyR signal and the sum of the GlyR and GABA signals in all clusters of one stack. The histogram exhibits a bimodal distribution that allow us to distinguish between GABA- $\gamma 2$ -enriched clusters (blue bins) and GlyR-enriched clusters (red bins). **C**, Plot of GABA- $\gamma 2$ and pan-GlyR intensities (in arbitrary units, a.u.), as a function of the intensity ratio. The smoothed average over the 2495 clusters detected is represented (black lines, mean \pm SD), showing the decreasing and increasing intensity trends for GABA- $\gamma 2$ and GlyR clusters, respectively. **D–F**, Similar observations are obtained with costaining for GABA- $\alpha 1$ subunit (blue) and pan-GlyR (red; $n = 2088$ detected clusters). **G**, GlyR $\alpha 1$ subunit immunoreactivity (red) is found on somata of presumptive principal CN cells and clusters are seen apposed to VIAAT-positive varicosities (green). Z-thickness of projection, $8 \mu\text{m}$. **H**, The distribution of distances reveals that the majority of both pan-GlyR (red line) and $\alpha 1$ -GlyR (blue line) clusters are found within $1 \mu\text{m}$ from VIAAT-positive varicosities. **I**, Similarly, both GlyR-enriched (red line) and GABA-enriched (blue line) clusters are located within a distance of $1 \mu\text{m}$ from the VIAAT-positive element. Scale bars: **A, D, G**, $10 \mu\text{m}$; **A, D, G** close-ups (right), $2 \mu\text{m}$.

glycine receptor revealed a very similar size and distribution of glycine receptor clusters, confirming the specificity of pan-GlyR immunostaining (Fig. 4G). These data demonstrate the existence of two types of postsynaptic differentiation in the CN, expressing different ratios of $\gamma 2/\alpha 1$ -containing GABA receptors and $\alpha 1$ -containing glycine receptors, which we shall subsequently call GABA-enriched and GlyR-enriched clusters.

GABA-enriched and GlyR-enriched clusters are in apposition to PC terminals and glycinergic interneurons, respectively

We investigated the localization of GlyR-enriched and GABA-enriched postsynaptic clusters relative to the inhibitory presyn-

aptic terminals identified by immunostaining against VIAAT. The vast majority of glycine receptor clusters were found within $1 \mu\text{m}$ of VIAAT immunostaining (Fig. 4H), whether GlyRs were stained for $\alpha 1$ ($85.0 \pm 8.3\%$, $n = 8$ stacks, $n = 2299$ detected clusters) or for pan-GlyR ($96.7 \pm 0.5\%$, $n = 5$ stacks, $n = 9638$ detected clusters). This was a shorter distance than predicted in the random distribution obtained when flipping VIAAT stacks ($\alpha 1$ -GlyR: original distribution, $0.7 \pm 0.5 \mu\text{m}$ vs random distribution, $1.3 \pm 1.1 \mu\text{m}$, Wilcoxon test $p < 2.2e^{-16}$; pan-GlyR: original distribution, $0.5 \pm 0.2 \mu\text{m}$ vs random distribution, $0.9 \pm 0.5 \mu\text{m}$, Wilcoxon test $p < 2.2e^{-16}$). GABA-enriched clusters and GlyR-enriched clusters were found at similar distances from VIAAT profiles (Fig. 4G; GlyR-enriched

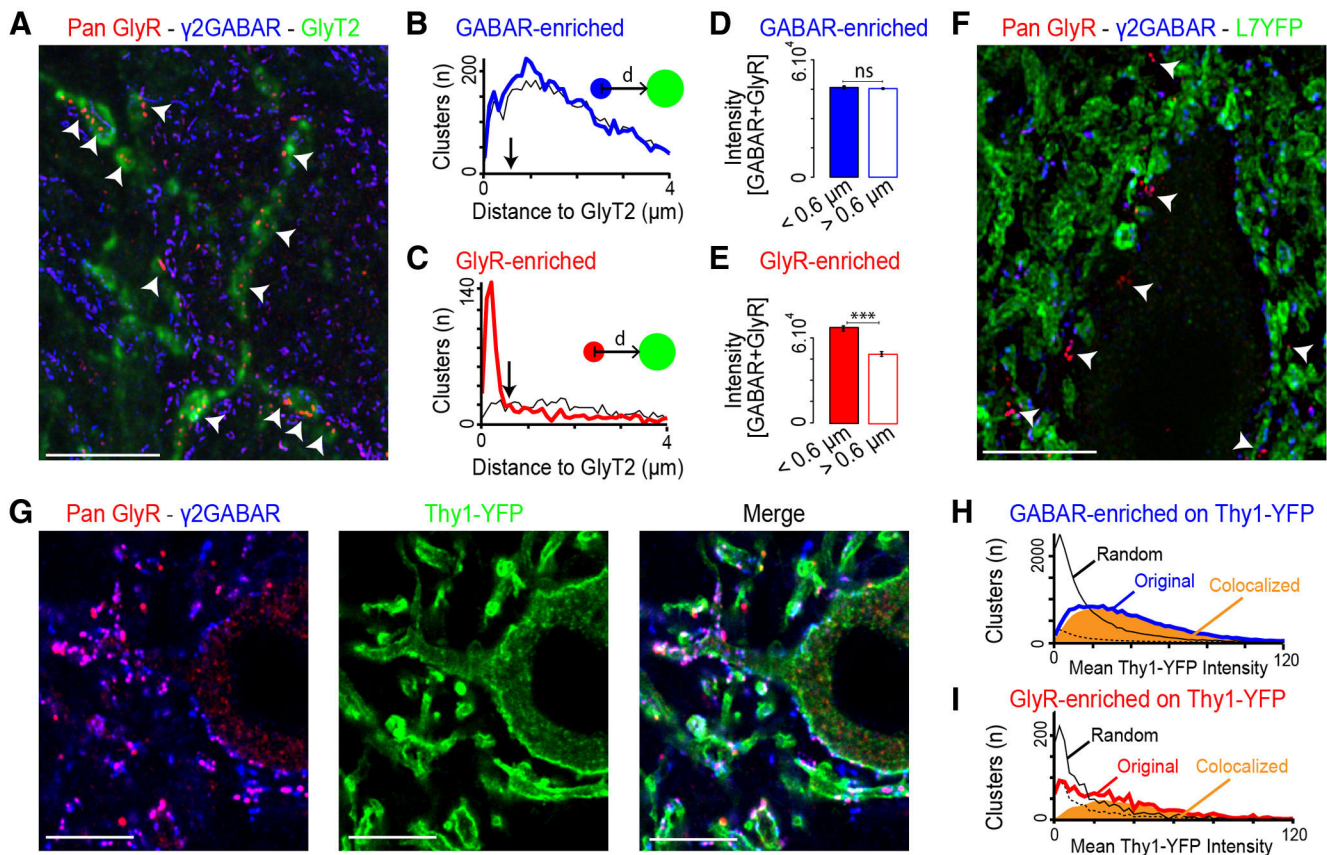


Figure 5. GABA-enriched clusters and GlyR-enriched clusters are located on principal neurons and face Purkinje cell varicosities and GlyT2+ profiles, respectively. **A**, GlyR-enriched clusters are found in front of GlyT2+ varicosities (white arrowheads) as shown in costaining for pan-GlyR (red), GABA- γ 2 (blue), and GlyT2 (green). Z-thickness of projection, 8.3 μ m. **B**, **C**, Analysis of distance distributions to the closest GlyT2-positive varicosities (red lines) reveals that $59.3 \pm 8.5\%$ of GlyR-enriched clusters are found at $<0.6 \mu$ m from a varicosity, whereas distribution of distances for GABA-enriched clusters (blue line) was not different from randomized data (black lines). **D**, **E**, Nonapposed GlyR-enriched clusters have lower intensities (summed GlyR + GABA) than apposed clusters (Wilcoxon test, $p \ll 0.01$). **F**, Costaining for pan-GlyR (red) and GABA- γ 2 (blue) in a *L7-ChR2-YFP* (green) mouse reveals appositions between L7-positive Purkinje cell terminals and GABA-enriched, but not GlyR-enriched, clusters (white arrowheads). Z-thickness of projection, 1.2 μ m. **G**, Costaining for pan-GlyR (red) and GABA- γ 2 (blue) in a *Thy1-ChR2-YFP* (green) mouse, in which CN principal cells exhibit YFP staining at the membrane. Z-thickness of projection, 0.51 μ m. **H**, **I**, Colocalization analysis as previously described (Fig. 2E) reveals that $>88\%$ of GABA- γ 2-enriched clusters and $>59\%$ for GlyR-enriched clusters are colocalized with YFP, indicating that they are located on principal cells. Scale bars: **A**, **B**, **G**, 10 μ m.

clusters, $0.46 \pm 0.21 \mu$ m; GABA-enriched clusters, $0.49 \pm 0.26 \mu$ m), indicating that both types of receptor aggregates are postsynaptic to inhibitory varicosities.

We sought for the identity of presynaptic elements facing the two types of receptor clusters. We used triple staining against pan-GlyR, GABA- γ 2, and GlyT2 (Fig. 5A) to study the spatial relationship between glycinergic terminals from local interneurons and GlyR-enriched clusters. Receptor clusters were detected and GlyT2+ profiles were segmented in 3D (Imaris software; see Materials and Methods). The distance between each cluster center and the closest surface of a GlyT2+ profile was calculated using original and flipped GlyT2 stacks, to control for nonspecific appositions (Fig. 4B,C). The distribution of the distances between GABA-enriched clusters and GlyT2+ varicosities did not show a peak for small values and was similar to the randomized distribution (Fig. 5B). In contrast, the distance distribution of GlyR-enriched clusters showed a marked peak for short distance, and $59.3 \pm 8.5\%$ of GlyR-enriched clusters were found within 0.6 μ m of a GlyT2+ varicosity (Fig. 5C), significantly more than expected at random ($12.8 \pm 4.7\%$; Wilcoxon test, $p < 2.2e^{-16}$). Those appositions were also found in the *GlyT2-eGFP* mouse (data not shown), but only $27.9 \pm 20.9\%$ of GlyR-enriched clusters were found within 0.6 μ m of a GlyT2-eGFP+ varicosity, in agreement with the observed mosaic expression in this transgenic

line. Hence, the most likely explanation for the presence of a substantial fraction of GlyR-enriched clusters at a distance from GlyT2+ profiles is that some of them may be extrasynaptic or intracellular clusters (Hanus et al., 2004), as suggested by the fact that the staining of GlyR-enriched clusters located at $>0.6 \mu$ m from a GlyT2+ varicosity was significantly lower than that of apposed clusters (Fig. 4D,E). However, the presence of GlyR-enriched clusters at synapses that do not face glycinergic interneurons cannot be excluded. Overall, these data indicate that GlyR-enriched clusters are preferentially involved in inhibitory transmission at the synapses of CN interneurons, whereas GABA-enriched clusters are located at PC synapses.

The abundance of GABA-enriched clusters, particularly on the somata of principal neurons, fits well with the known distribution of PC synapses (De Zeeuw and Berrebi, 1995). To confirm this hypothesis, we performed pan-GlyR/GABA- γ 2 costaining in *L7-ChR2-YFP* transgenic mice (Chaumont et al., 2013) in which expression of ChR2 and YFP was under the control of the Purkinje-specific L7 promoter (Fig. 5F). GABA-enriched clusters faced L7-ChR2-YFP+ terminals on the somata and in the neuropil, but the density of L7-YFP staining prevented proper segmentation of the L7-ChR2-YFP+ terminals and distance quantification. In contrast, GlyR-enriched clusters were generally found between L7-ChR2-YFP+ profiles decorating the somata

and proximal dendrites, confirming that they are in apposition to another presynaptic element.

GABAR-enriched clusters and the majority of GlyR-enriched clusters are located on the membranes of principal CN neurons

The CN contain three main cell types: principal projection neurons, nucleo-olivary neurons, and inhibitory interneurons. Whereas PCs target all three cell types (De Zeeuw and Berrebi, 1995; Teune et al., 1998), the targets of local interneurons are not well characterized (Chen and Hillman, 1993; De Zeeuw and Berrebi, 1995). We thus investigated the postsynaptic localization of GlyR-containing postsynaptic clusters. In line 18 *Thy1-ChR2-YFP* mice (Wang et al., 2007), YFP is a specific marker of principal cells as opposed to local interneurons or nucleo-olivary neurons. All large CN projection neurons, characterized by their somatic VGluT2 immunoreactivity (data not shown), but none of the small cells, exhibited YFP staining at their plasma membrane. We performed costaining for pan-GlyR and GABAR- $\gamma 2$ in *Thy1-ChR2-YFP* mouse (Fig. 5G) and classified all clusters as described previously. The total YFP signal located under each cluster in original and flipped YFP stacks was integrated to evaluate colocalization (Figs. 1, 4H,I; see Materials and Methods). Virtually all GABAR-enriched clusters (at least 88%; Fig. 5H) were found colocalized with YFP, indicating that they are located on principal neurons. A majority of GlyR-enriched clusters (59%) were also colocalized with YFP staining and thus located on principal cells (Fig. 5I). The remaining 41% of GlyR-enriched clusters may be located on other cell types or intracellularly in principal cells. We conclude that interneuronal synapses onto CN principal cells should differ from PC synapses by the presence of a large glycinergic component.

Evidence for a small glycinergic component at PC–CN neuron synapses

PC IPSCs recorded in CN principal neurons are generally considered to be purely GABAergic (Obata, 1969; Curtis et al., 1970; De Zeeuw and Berrebi, 1995). We looked for electrophysiological evidence of glycinergic transmission at PC-to-principal CN neuron synapses. CN principal neurons were recorded in whole-cell voltage-clamp configuration in *Thy1-CFP* mice (aged P30–P60) and axons of PCs were electrically stimulated in the white matter surrounding the CN, which is devoid of interneuron axons. Large synaptic currents were evoked (mean, 1108.4 ± 782.1 pA/ 15.8 ± 11.2 nS, $n = 20$ cells) with a fast decay time course (2.7 ± 0.7 ms, $n = 16$ cells; Telgkamp et al., 2004; Pugh and Raman, 2005; Fig. 6A). Application of strychnine at the selective concentration of 300 nM blocked $12.3 \pm 7.8\%$ of the peak current (control, 1347.7 ± 965.5 pA/ 19.3 ± 13.8 nS; strychnine 300 nM, 1198.7 ± 876.2 pA/ 17.1 ± 12.5 nS, $n = 10$ cells). Subsequent application of 1 μ M strychnine produced a further block of the peak current, attaining a total of $39.1 \pm 12.0\%$ (888.9 ± 718.0 pA/ 12.7 ± 10.3 nS, $n = 8$ cells; Wilcoxon test paired, $n = 8$ paired cells, $p = 0.0078$) of the initial peak value (Fig. 6B). Finally, addition of 300 nM gabazine blocked $84.5 \pm 6.5\%$ of the isolated GABAergic component remaining in 1 μ M strychnine ($n = 7$ cells; Fig. 6B). The large additional block by 1 μ M strychnine over 300 nM strychnine is most likely due in part to the well known antagonistic effect of strychnine on GABA receptors (Yakushiji et al., 1987; Jonas et al., 1998), casting doubts on the true size of the glycinergic component at PC synapses.

To provide better quantitative evidence, we applied a two-step strategy. We first blocked $81.4 \pm 8.6\%$ (control, 869.1 ± 481.6

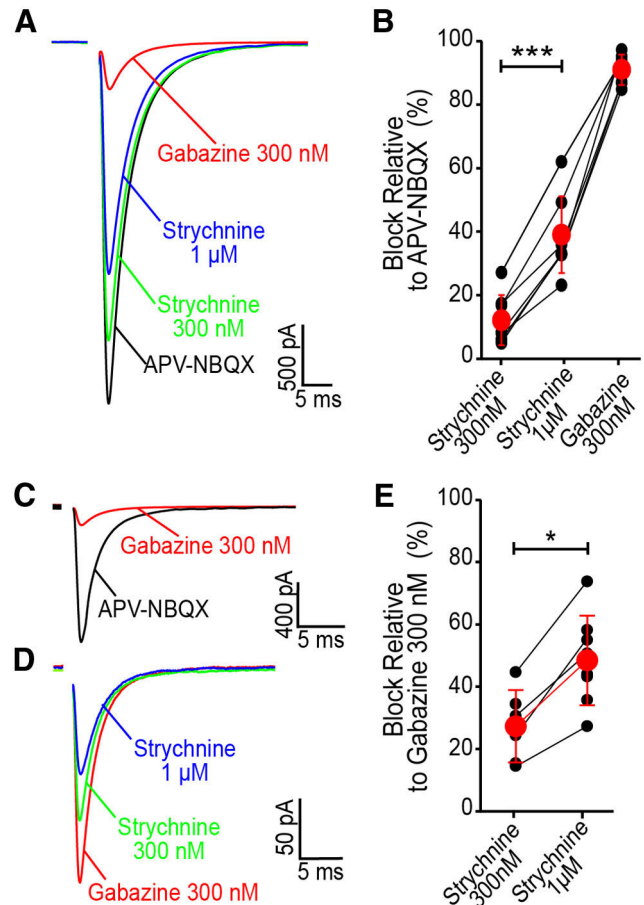


Figure 6. Isolation of a small glycinergic component at Purkinje cell synapses onto principal cells. **A**, Example of averaged synaptic responses elicited by electrical stimulation of Purkinje cell axons in the white matter surrounding the CN and recorded in CN principal neurons in the presence of blockers of glutamate receptors ($50 \mu\text{M}$ D-APV and $10 \mu\text{M}$ NBQX). Strychnine (300 nM, $1 \mu\text{M}$) and gabazine (300 nM) were successively applied in the bath, resulting in reduction of the peak amplitude. **B**, Percentage of block by strychnine 300 nM and $1 \mu\text{M}$ and by gabazine 300 nM relative to the initial response amplitude ($n = 10, 8,$ and 7 cells, respectively). **C**, Application of gabazine 300 nM reduced the peak amplitude by $81.4 \pm 8.6\%$ ($n = 10$ cells) and was used to enrich the responses in glycinergic component by increasing the glycinergic fraction in the remaining component. **D, E**, Block of the remaining current by subsequent application of 300 nM and $1 \mu\text{M}$ strychnine ($n = 6$ and 8 cells, respectively).

pA/ 12.4 ± 6.9 nS; gabazine 300 nM, 151.8 ± 88.5 pA/ 2.2 ± 1.3 nS, $n = 10$ cells) of the synaptic current with a selective concentration of gabazine (SR-95531, 300 nM), an antagonist of GABA_AR (Hamann et al., 1988; Fig. 6C). We then assessed whether strychnine had an enhanced action on the remaining component of synaptic current, putatively enriched in glycinergic conductance. We found the block of the gabazine-resistant current to be $27.2 \pm 11.6\%$ (111.4 ± 73.1 pA/ 1.6 ± 1.0 nS, $n = 6$ cells) and $48.4 \pm 14.3\%$ (83.4 ± 57.1 pA/ 1.2 ± 0.8 nS, $n = 8$ cells) for 300 nM and 1 μ M strychnine, respectively (Wilcoxon test, $p = 0.019$; Fig. 6D,E). This is 14.9% (Wilcoxon test $p = 0.02$) and 9.3% (Wilcoxon test $p = 0.16$) more than before gabazine application. The synaptic component blocked by 300 nM strychnine after application of gabazine corresponded to $3.77 \pm 1.21\%$ ($n = 6$ cells) of the total control current. This value could be corrected for non-specific block of GABA receptors to a high estimate of 2.2%, assuming independence of strychnine and gabazine effects on the GABA receptors (see Materials and Methods).

Optogenetic activation of CN interneurons elicits mixed inhibitory synaptic responses in principal neurons

We then investigated the contribution of glycinergic transmission at interneuron-to-principal cell synapses. The properties of this connection are completely unknown because interneurons cannot be excited specifically by extracellular electrodes. We thus used an optogenetic approach. *GlyT2-Cre* mice (1 month old) were injected into the CN with an adeno-associated virus encoding a flexed channelrhodopsin 2 (ChR2) and YFP reporter construct. Three weeks after injection, YFP was expressed specifically in GlyT2-expressing cells of the infected area (Fig. 7A,B). CN principal neurons from the infected area were recorded in the whole-cell voltage-clamp configuration, whereas interneurons were stimulated by 1 ms illumination of the whole field of view with blue light from a LED at 470 nm (intensities between 0.3 and 4 mW/mm²). Optogenetic stimulations elicited synaptic currents in principal neurons (Fig. 7B,C,E) with variable efficacy. Maximal intensity illumination failed to evoke any IPSCs in 48.3% of the cells recorded (28 of 58). In the remaining cells, the average peak amplitude of the IPSCs varied between 26 and 785 pA (mean, 145.02 ± 152.24 pA/2.1 ± 2.1 nS, *n* = 43 cells; Fig. 7B). As in the *GlyT2-eGFP* mouse, only 40% of GlyT2-positive elements at best are colabeled for YFP in the *GlyT2-Cre* mouse injected with ChR2-YFP viruses at a postnatal stage (data not shown). This partial infection of the glycinergic interneuronal population, as well as variable preservation of connections in the slices, may explain the heterogeneity of the evoked synaptic responses. A paired-pulse ratio (PPR) of 1.00 ± 0.16 (*n* = 14 cells) was measured for a 100 ms interval between optical stimulations, slightly lower than the PPR at PC synapses (1.09 ± 0.13, *n* = 14; Wilcoxon test *p* = 0.021), suggesting similar release probability at the two synapses. The decay times of the synaptic events at these two synapses were not significantly different (Purkinje cell synapse, 2.67 ± 0.66 ms, *n* = 16 cells; interneuronal synapse, 3.07 ± 0.99 ms, *n* = 15 cells; Wilcoxon test *p* = 0.2316).

Strychnine and gabazine were applied to quantify the contribution of glycinergic transmission at the interneuron-to-principal cell synapse. Application of 300 nM strychnine blocked 34.7 ± 14.9% of the initial amplitude (control, 154.2 ± 92.3 pA/2.2 ± 1.3 nS; strychnine 300 nM, 97.3 ± 59.6 pA/1.4 ± 0.9 nS, *n* = 13 cells; Fig. 7C,D), significantly more than at the PC synapse (Wilcoxon test, *p* = 0.0025). The percentage block by strychnine was highly variable between cells (minimum = 5.8%, maximum = 52.7%). At a concentration of 1 μM, strychnine produced a larger block of 51.1 ± 20.5% (73.8 ± 48.6 pA/1.1 ± 0.7 nS; *n* = 14 cells; Wilcoxon test paired, *n* = 10 cells paired, *p* = 0.0019; Fig. 7C,D), consistent with a nonspecific action on GABARs. Addition of 300 nM gabazine blocked virtually all the remaining current (94.2 ± 4.9% of the remaining value, 4.3 ± 3.6 pA/0.06 ± 0.05 nS, *n* = 7 cells; Fig. 7C,D). This is significantly different from the block of the isolated GABA component at the Purkinje cell synapses (84.5 ± 6.5%, *n* = 7 cells; Wilcoxon test, *p* = 0.0297), consistent with a difference in the molecular identity of GABAR present at the two synapses, as suggested by immunohistochemistry.

We applied the same two-step strategy as previously described at the Purkinje cell-to-principal neuron synapse, to provide a reliable estimate of the glycinergic and GABAergic components at the interneuronal synapse. Application of 300 nM gabazine blocked 76.7 ± 10.9% of the initial amplitude (control, 161.6 ± 169.6 pA/2.3 ± 2.4 nS; gabazine 300 nM, 29.6 ± 18.5 pA/0.42 ± 0.27 nS, *n* = 11 cells; Fig. 7E,F). Following application of strychnine 300 nM, the gabazine-resistant current was blocked by

56.3 ± 19.9% (14.5 ± 14.5 pA/0.21 ± 0.21 nS, *n* = 10 cells), significantly more than at the Purkinje cell synapse (Wilcoxon test *p* = 0.01099, Purkinje cells synapse, 27.2 ± 11.6%, *n* = 6 cells). This represented a fraction of the original current of 14.7 ± 8.2% (*n* = 11 cells), significantly higher than that at the Purkinje cell synapse (3.8 ± 1.2%, *n* = 6 cells, Wilcoxon test *p* = 0.02731; Fig. 7G). Correction for nonspecific block of the GABA component yielded an estimated glycinergic component of 13.6%.

These results provide the first evidence for functional inhibitory neurotransmission at interneuronal synapses onto principal cells of the CN. They establish the presence of a large glycinergic component, as a distinctive feature of interneuron IPSCs in principal cells.

Discussion

Inhibitory glycinergic neurons in the CN

We examined the function of CN glycinergic interneurons using the *GlyT2-eGFP* and *GlyT2-cre* transgenic models. Glycinergic CN neurons are specifically stained in adult *GlyT2-eGFP* animals, where GFP+ neurons form a population distinct from retrogradely labeled nucleo-olivary cells (Fig. 3) and morphologically different from principal cells. Only 40% of the glycinergic neurons express GFP in adult *GlyT2-eGFP* mice, as confirmed by the incomplete colocalization with GFP of GlyT2-immunoreactive profiles (Fig. 2) and of GABA-immunoreactive cell bodies (Fig. 3), and by the partial apposition of GFP with GlyR-enriched clusters (Fig. 5). Taking this mosaic expression into account, the total number of glycinergic neurons in the interposed and lateral CN can be estimated to 3200 bilaterally, similar to the 4000 neurons positive for GABA and glycine but lower than the 8600 glycine-only somata found by Bäumle and Grüsser-Cornehls (1997). Mild accumulation of glycine in glia through the GlyT1 transporter could explain the numerous glycine-only somata in that study. Finally, interneurons account for approximately half of the 10,000 small neurons found by Heckroth (1994) in the mouse CN, the other half being nucleo-olivary cells.

Although complete staining of the glycinergic population can be obtained in a *GlyT2-cre* model, when the cre recombinase is allowed to act on reporter constructs during the whole development (Fig. 2), aspecific expression of the marker extends to some vermal Purkinje cells and to a subpopulation of nucleo-olivary cells (Fig. 2). This pattern of expression might also be present in the young *GlyT2-eGFP* animals (which were generated using the same bacterial artificial chromosome), as indicated by the weak residual GFP staining in some nucleo-olivary cells at 2 months (data not shown). This lack of specificity in young *GlyT2-eGFP* mice might explain why two types of GFP+ cells were distinguished on electrophysiological criteria at P20–P27 (Uusisaari and Knöpfel, 2010). The first type fires spontaneously and is functionally similar to small GAD67-GFP-positive nucleo-olivary cells (Uusisaari et al., 2007; Uusisaari and Knöpfel, 2008). A second population of larger GFP+ neurons was spontaneously inactive, in agreement with the rare occurrence of spontaneous glycinergic events in principal cells (Chen and Hillman, 1993; Pedroarena and Kamphausen, 2008; this study). These neurons displayed a local axonal plexus, as described in this study, and may also project toward the cortex (Uusisaari and Knöpfel, 2010). Finally, these neurons fired at high frequency in response to large current injections (Uusisaari and Knöpfel, 2010), reminiscent of the bursts of high-frequency IPSCs we recorded in principal CN neurons in response to saturating optogenetic stimulations. We conclude that glycinergic CN neurons constitute a separate class of medium-sized spontaneously inac-

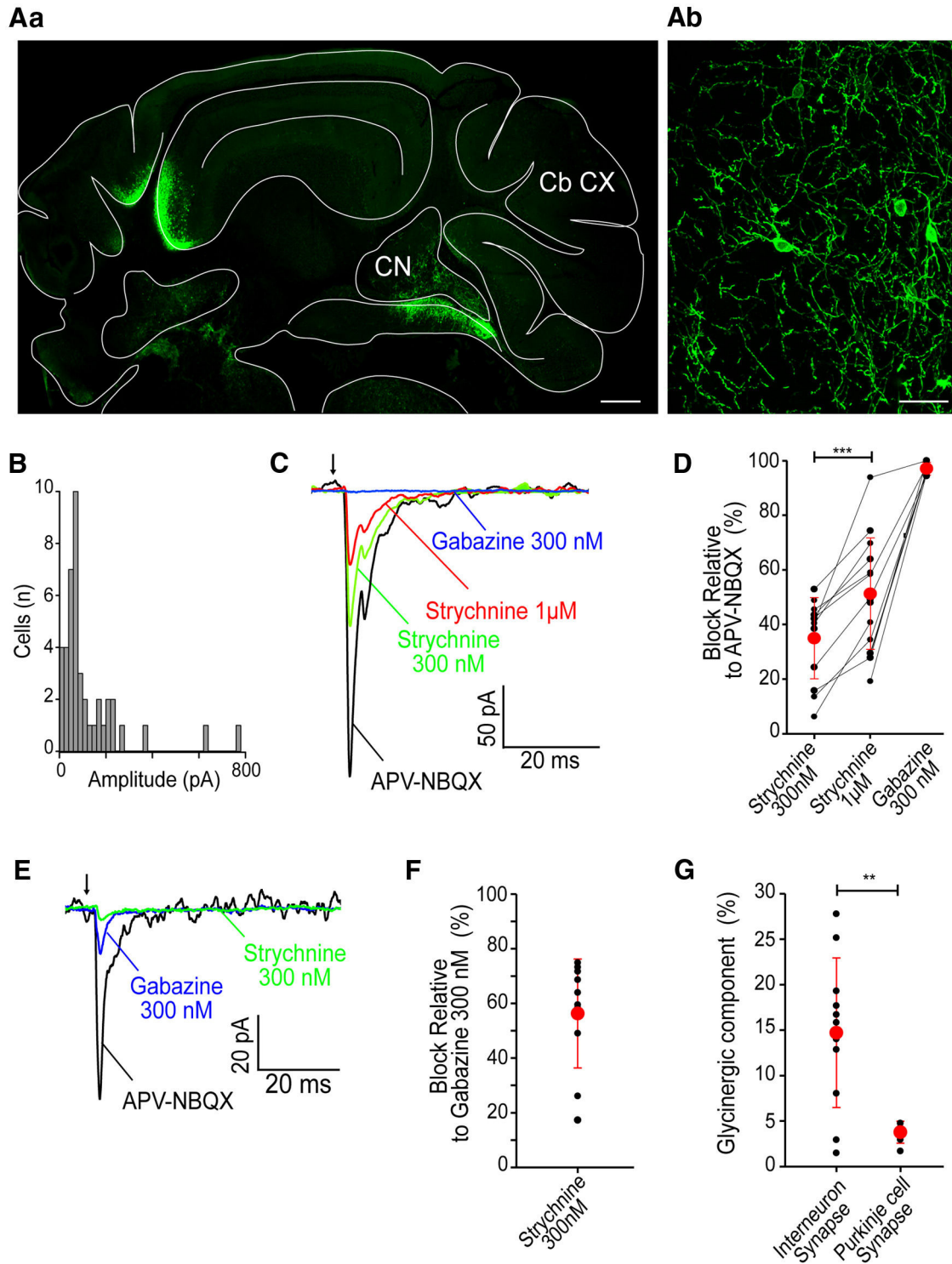


Figure 7. Mixed inhibition at CN interneuron synapses on principal cells. **Aa**, Coronal slice of cerebellum from a *GlyT2-Cre* mouse injected bilaterally into the CN with a flexed virus expressing ChR2-YFP. **Ab**, After 3 weeks of infection, GlyT2-expressing neurons exhibit ChR2-YFP staining at their membrane. **B**, Histogram of the peak amplitude of the synaptic currents evoked by 1 ms optogenetic stimulation of the CN glycinergic neurons and recorded in CN principal neurons ($n = 43$ cells). **C**, Example of averaged synaptic currents recorded in the presence of blockers of excitation ($50 \mu\text{M}$ D-APV and $10 \mu\text{M}$ NBQX) and of their block by successive application of strychnine and gabazine. **D**, Summary of the sensitivity of the synaptic currents to strychnine 300 nM and $1 \mu\text{M}$ ($n = 13$ and 14 cells, respectively; Wilcoxon test paired, $n = 10$ paired cells, $p = 0.0019$) and gabazine 300 nM ($97.0 \pm 2.3\%$ block relative to initial response amplitude, $n = 7$ cells). **E**, Example of average responses (in the presence of $50 \mu\text{M}$ D-APV and $10 \mu\text{M}$ NBQX) when reverse pharmacology was performed. Gabazine 300 nM was applied before 300 nM strychnine and blocked $76.7 \pm 10.9\%$ of the control amplitude ($n = 11$ cells). **F**, Percentage of block by strychnine 300 nM relative to the remaining current after application of 300 nM gabazine ($n = 11$ cells). **G**, Glycinergic component of the initial response was assessed by the following formula: [(Amplitude after 300 nM gabazine — Amplitude after 300 nM gabazine and 300 nM strychnine)/Amplitude of the initial response]. This glycinergic component is higher at the interneuronal synapse than at the Purkinje cell synapse ($n = 11$ and 6 cells, respectively; Wilcoxon test $p = 0.02731$). Scale bars: **Aa**, $500 \mu\text{m}$; **Ab**, $50 \mu\text{m}$. Cb Cx, Cerebellar cortex.

tive neurons, which may account for half of the non-principal neurons in the CN.

Some aspects of the microcircuit organization of glycinergic CN neurons appeared as incidental observations in previous studies (Chen and Hillman, 1993; De Zeeuw and Berrebi, 1995; Pedroarena and Kamphausen, 2008). We show here that glycinergic boutons face GlyR-enriched synapses (Figs. 3, 4) which account for ~4% of the number of inhibitory clusters on principal neurons. The existence of an equivalent population of GlyR-enriched clusters that is located neither on principal cells (Fig. 5) nor on the somata or primary dendrites of GlyT2-GFP interneurons confirms the early observation that glycinergic terminals contact GABA-containing neurons (De Zeeuw and Berrebi, 1995), most likely nucleo-olivary GABAergic cells.

Mixed GABA-glycine transmission in the CN

Mixed release of GABA and glycine is a common mode of inhibitory transmission in the cerebellar cortex (Dumoulin et al., 2001; Rousseau et al., 2012). In the CN, GlyT2-positive neurons express GAD67 (Tanaka and Ezure, 2004), as do nucleo-olivary cells (Fredette and Mugnaini, 1991; Tamamaki et al., 2003). Surprisingly, a single functional class of small GFP-positive neurons and a separate class of GFP-negative neurons was described in the CN of *GAD67-GFP* knock-in animals (Uusisaari et al., 2007; Uusisaari and Knöpfel, 2008), suggesting that glycinergic interneurons may not be stained in this transgenic line. We find here that most GlyT2-immunoreactive varicosities are positive for GAD, indicating that glycinergic CN neurons consistently corelease GABA and glycine.

We took advantage of the cell-type specificity of optogenetic stimulations to reveal and characterize the functional synapses between glycinergic interneurons and principal cells in the CN. Light-evoked IPSCs always contained both GABAR-mediated and GlyR-mediated components with an average GlyR contribution of 15% of the amplitude (Fig. 7). This large glycinergic component differentiates interneuron IPSCs from PC IPSCs (Fig. 6), for which <3% of the amplitude is mediated by GlyR, whereas IPSC decay kinetics are similar at both synapses. Paired stimulations gave similar PPRs at interneuronal (Fig. 7) and Purkinje synapses (Telgkamp et al., 2004), but longer stimulation trains should be tested. Spillover between release sites onto multiple receptor clusters (Telgkamp et al., 2004) accounts for sustained high-frequency transmission at large Purkinje cell boutons. The sensitivity of GlyR to glycine spillover and temporal summation (Beato et al., 2007; Balakrishnan et al., 2009) could favor GlyR currents during high-frequency activity at interneuronal synapses.

The presence of small aggregates of GlyR $\alpha 1$ subunits at PC synapses onto principal neurons and of a small glycinergic component of the IPSCs is surprising, as PCs are not known to release glycine (Tanaka and Ezure, 2004). GABA can activate GlyR with low efficacy (De Saint Jan et al., 2001; Legendre, 2001), evoking fast decaying GlyR-IPSCs (Lu et al., 2008) with kinetics similar to those of the PC IPSCs (Fig. 6; Person and Raman, 2012a). The functional role of this small glycinergic component is elusive, and the presence of GlyR at GABAergic synapses may result from structural entrapment during synapse formation (Dumoulin et al., 2000; Muller et al., 2004), as both GABAR (Sassoè-Pognetto et al., 2000) and GlyR (Meyer et al., 1995) bind to the same postsynaptic scaffolding protein, gephyrin.

At interneuronal synapses, GlyR-enriched clusters contain the $\alpha 1$ subunit of the glycine receptor (Fig. 4; Malosio et al., 1991), most likely associated with the β subunit, which is expressed in

the CN (Weltzien et al., 2012) and is responsible for the clustering of GlyR at synapses (Kneussel and Betz, 2000). GlyR-enriched clusters are virtually devoid of the $\alpha 1$ and $\gamma 2$ GABAR subunits, the most abundant subunits in the CN (Persohn et al., 1992; Gambarana et al., 1993), found at PC synapses onto principal cells (Fig. 4). However, pharmacological analysis of the interneuron IPSCs demonstrates the presence of functional GABAR (Fig. 7). Although $\alpha 3$ -GABAR subunits are expressed in the CN, they appear to mediate slow IPSCs at PC synapses onto GABAergic cells (Uusisaari and Knöpfel, 2008), different from the fast optically evoked IPSCs in principal cells. It is thus likely that other GABAR subunits, such as $\alpha 5$ or $\gamma 1$ (Pirker et al., 2000; Hörtnagl et al., 2013), are involved at interneuronal synapses onto principal cells.

Functional impact of interneuronal inhibition in the CN

The average IPSC conductance evoked by optogenetic stimulations (2 nS; Fig. 7) gives the strength of the interneuronal input to principal neurons. Because 40% of interneurons at best express ChR2 upon viral infection in *GlyT2-Cre* animals, the average interneuronal synaptic conductance should exceed 5 nS, ~4% of the average conductance evoked by maximal electrical stimulation of PC axons in the slice (Person and Raman, 2012a). Our optogenetic stimulations and the electrical stimulations of Person and Raman (2012b) represent a large underestimate of the total inputs, as many synapses will not be recruited due to failed stimulation or disrupted connectivity in slices. However, their ratio is in excellent agreement with previous electron microscopy estimates of glycine-containing synapses in the CN (2% of all contacts; De Zeeuw and Berrebi, 1995) and with our immunohistochemical staining (5% of contacts on principal cells).

Two types of spontaneous IPSCs/IPSPs have been recorded from CN principal neurons *in vivo* (Bengtsson et al., 2011; Witter et al., 2013): a barrage of low-amplitude and high-frequency synaptic events reflecting the spontaneous firing of presynaptic PCs (Person and Raman, 2012a), and giant low-frequency IPSC/PS. Giant IPSC/PS have been proposed to result from the synchronization of PCs by climbing fibers (Bengtsson et al., 2011; Person and Raman, 2012b; Witter et al., 2013). Indeed, large IPSCs are readily evoked during tactile stimulations of the cutaneous climbing fiber receptive field (Bengtsson and Jörntell, 2014) and by electrical stimulations of the inferior olive (Hoebeek et al., 2010; Bengtsson et al., 2011), driving powerful rebound firing of the CN cells which induces plasticity at CN synapses (Aizenman et al., 1998; Pugh and Raman, 2006). Surprisingly, direct synchronization of PCs by stimulation of the cerebellar cortex did not produce a robust rebound firing of CN cells (Hoebeek et al., 2010; Person and Raman, 2012a). The difference in the effects of olivary and cortical stimulations has been tentatively explained by assuming that inferior olive activity recruits functionally significant sparse patterns of PCs (Welsh et al., 1995; Ozden et al., 2009, 2012; Schultz et al., 2009). Alternatively, one should consider the possibility that giant IPSC/PS recorded from CN principal cells arise from the synchronous activity of several CN interneurons and not from PC synchronization.

References

- Aizenman CD, Manis PB, Linden DJ (1998) Polarity of long-term synaptic gain change is related to postsynaptic spike firing at a cerebellar inhibitory synapse. *Neuron* 21:827–835. [CrossRef Medline](#)
- Araki T, Sato M, Kiyama H, Manabe Y, Tohyama M (1992) Localization of GABAA-receptor gamma 2-subunit mRNA-containing neurons in the rat central nervous system. *Neuroscience* 47:45–61. [CrossRef Medline](#)
- Bagnall MW, Zingg B, Sakatos A, Moghadam SH, Zeilhofer HU, du Lac S

- (2009) Glycinergic projection neurons of the cerebellum. *J Neurosci* 29:10104–10110. [CrossRef Medline](#)
- Balakrishnan V, Kuo SP, Roberts PD, Trussell LO (2009) Slow glycinergic transmission mediated by transmitter pooling. *Nat Neurosci* 12:286–294. [CrossRef Medline](#)
- Bäurle J, Grüsser-Cornehls U (1997) Differential number of glycine- and GABA-immunopositive neurons and terminals in the deep cerebellar nuclei of normal and Purkinje cell degeneration mutant mice. *J Comp Neurol* 382:443–458. [CrossRef Medline](#)
- Beato M, Burzomato V, Sivilotti LG (2007) The kinetics of inhibition of rat recombinant heteromeric alpha1beta glycine receptors by the low-affinity antagonist SR-95531. *J Physiol* 580:171–179. [CrossRef Medline](#)
- Bengtsson F, Jörntell H (2014) Specific relationship between excitatory inputs and climbing fiber receptive fields in deep cerebellar nuclear neurons. *PLoS One* 9:e84616. [CrossRef Medline](#)
- Bengtsson F, Ekerot CF, Jörntell H (2011) In vivo analysis of inhibitory synaptic inputs and rebounds in deep cerebellar nuclear neurons. *PLoS One* 6:e18822. [CrossRef Medline](#)
- Best AR, Regehr WG (2009) Inhibitory regulation of electrically coupled neurons in the inferior olive is mediated by asynchronous release of GABA. *Neuron* 62:555–565. [CrossRef Medline](#)
- Bolte S, Cordelières FP (2006) A guided tour into subcellular colocalization analysis in light microscopy. *J Microsc* 224:213–232. [CrossRef Medline](#)
- Chaumont J, Guyon N, Valera AM, Dugué GP, Popa D, Marcaggi P, Gautheron V, Reibel-Foisset S, Dieudonné S, Stephan A, Barrot M, Cassel JC, Dupont JL, Doussau F, Poulain B, Selimi F, Léna C, Isope P (2013) Clusters of cerebellar Purkinje cells control their afferent climbing fiber discharge. *Proc Natl Acad Sci U S A* 110:16223–16228. [CrossRef Medline](#)
- Chen S, Hillman DE (1993) Colocalization of neurotransmitters in the deep cerebellar nuclei. *J Neurocytol* 22:81–91. [CrossRef Medline](#)
- Chen X, Kovalchuk Y, Adelsberger H, Henning HA, Sausbier M, Wietzorrek G, Ruth P, Yarom Y, Konnerth A (2010) Disruption of the olivocerebellar circuit by Purkinje neuron-specific ablation of BK channels. *Proc Natl Acad Sci U S A* 107:12323–12328. [CrossRef Medline](#)
- Curtis DR, Duggan AW, Felix D (1970) GABA and inhibition of Deiters' neurones. *Brain Res* 23:117–120. [CrossRef Medline](#)
- De Saint Jan D, David-Watine B, Korn H, Bregestovski P (2001) Activation of human alpha1 and alpha2 homomeric glycine receptors by taurine and GABA. *J Physiol* 535:741–755. [CrossRef Medline](#)
- De Zeeuw CI, Berrebi AS (1995) Postsynaptic targets of Purkinje cell terminals in the cerebellar and vestibular nuclei of the rat. *Eur J Neurosci* 7:2322–2333. [CrossRef Medline](#)
- De Zeeuw CI, Van Alphen AM, Hawkins RK, Ruigrok TJ (1997) Climbing fibre collaterals contact neurons in the cerebellar nuclei that provide a GABAergic feedback to the inferior olive. *Neuroscience* 80:981–986. [CrossRef Medline](#)
- Dougherty R (2005) Extensions of DAMAS and benefits and limitations of deconvolution in beamforming. Presented at the 11th AIAA/CEAS Aeroacoustics Conference, May 23–25, Monterey, CA.
- Dumoulin A, Lévi S, Riveau B, Gasnier B, Triller A (2000) Formation of mixed glycine and GABAergic synapses in cultured spinal cord neurons. *Eur J Neurosci* 12:3883–3892. [CrossRef Medline](#)
- Dumoulin A, Triller A, Dieudonné S (2001) IPSC kinetics at identified GABAergic and mixed GABAergic and glycinergic synapses onto cerebellar Golgi cells. *J Neurosci* 21:6045–6057. [Medline](#)
- Feng G, Mellor RH, Bernstein M, Keller-Peck C, Nguyen QT, Wallace M, Nerbonne JM, Lichtman JW, Sanes JR (2000) Imaging neuronal subsets in transgenic mice expressing multiple spectral variants of GFP. *Neuron* 28:41–51. [CrossRef Medline](#)
- Fredette BJ, Mugnaini E (1991) The GABAergic cerebello-olivary projection in the rat. *Anat Embryol (Berl)* 184:225–243. [CrossRef Medline](#)
- Gambarana C, Loria CJ, Siegel RE (1993) GABAA receptor messenger RNA expression in the deep cerebellar nuclei of Purkinje cell degeneration mutants is maintained following the loss of innervating Purkinje neurons. *Neuroscience* 52:63–71. [CrossRef Medline](#)
- Hamann M, Desarmenien M, Desaulles E, Bader MF, Feltz P (1988) Quantitative evaluation of the properties of a pyridazinyl GABA derivative (SR 95531) as a GABAA competitive antagonist. An electrophysiological approach. *Brain Res* 442:287–296. [CrossRef Medline](#)
- Hanus C, Vannier C, Triller A (2004) Intracellular association of glycine receptor with gephyrin increases its plasma membrane accumulation rate. *J Neurosci* 24:1119–1128. [CrossRef Medline](#)
- Heckroth JA (1994) Quantitative morphological analysis of the cerebellar nuclei in normal and lurcher mutant mice. I. Morphology and cell number. *J Comp Neurol* 343:173–182. [CrossRef Medline](#)
- Hoebeek FE, Witter L, Ruigrok TJ, De Zeeuw CI (2010) Differential olivocerebellar cortical control of rebound activity in the cerebellar nuclei. *Proc Natl Acad Sci U S A* 107:8410–8415. [CrossRef Medline](#)
- Hörtnagl H, Tasan RO, Wieselthaler A, Kirchmair E, Sieghart W, Sperk G (2013) Patterns of mRNA and protein expression for 12 GABAA receptor subunits in the mouse brain. *Neuroscience* 236:345–372. [CrossRef Medline](#)
- Houck BD, Person AL (2014) Cerebellar loops: a review of the nucleocortical pathway. *Cerebellum* 13:378–385. [CrossRef Medline](#)
- Isope P, Barbour B (2002) Properties of unitary granule cell->Purkinje cell synapses in adult rat cerebellar slices. *J Neurosci* 22:9668–9678. [Medline](#)
- Ito M, Yoshida M, Obata K, Kawai N, Udo M (1970) Inhibitory control of intracerebellar nuclei by the purkinje cell axons. *Exp Brain Res* 10:64–80. [CrossRef Medline](#)
- Jonas P, Bischofberger J, Sandkühler J (1998) Corelease of two fast neurotransmitters at a central synapse. *Science* 281:419–424. [CrossRef Medline](#)
- Kawa K (2003) Glycine receptors and glycinergic synaptic transmission in the deep cerebellar nuclei of the rat: a patch-clamp study. *J Neurophysiol* 90:3490–3500. [CrossRef Medline](#)
- Kneussel M, Betz H (2000) Clustering of inhibitory neurotransmitter receptors at developing postsynaptic sites: the membrane activation model. *Trends Neurosci* 23:429–435. [CrossRef Medline](#)
- Kravitz AV, Freeze BS, Parker PR, Kay K, Thwin MT, Deisseroth K, Kreitzer AC (2010) Regulation of parkinsonian motor behaviours by optogenetic control of basal ganglia circuitry. *Nature* 466:622–626. [CrossRef Medline](#)
- Legendre P (2001) The glycinergic inhibitory synapse. *Cell Mol Life Sci* 58:760–793. [CrossRef Medline](#)
- Lu T, Rubio ME, Trussell LO (2008) Glycinergic transmission shaped by the corelease of GABA in a mammalian auditory synapse. *Neuron* 57:524–535. [CrossRef Medline](#)
- Machado P, Rostaing P, Guignon JM, Renner M, Dumoulin A, Samson M, Vannier C, Triller A (2011) Heat shock cognate protein 70 regulates gephyrin clustering. *J Neurosci* 31:3–14. [CrossRef Medline](#)
- Malosio ML, Marqueze-Pouey B, Kuhse J, Betz H (1991) Widespread expression of glycine receptor subunit mRNAs in the adult and developing rat brain. *EMBO J* 10:2401–2409. [Medline](#)
- Matsushita M, Iwahori N (1971) Structural organization of the interpositus and the dentate nuclei. *Brain Res* 35:17–36. [CrossRef Medline](#)
- McCrea RA, Bishop GA, Kitai ST (1978) Morphological and electrophysiological characteristics of projection neurons in the nucleus interpositus of the cat cerebellum. *J Comp Neurol* 181:397–419. [CrossRef Medline](#)
- Medina JF, Nores WL, Ohyama T, Mauk MD (2000) Mechanisms of cerebellar learning suggested by eyelid conditioning. *Curr Opin Neurobiol* 10:717–724. [CrossRef Medline](#)
- Meyer G, Kirsch J, Betz H, Langosch D (1995) Identification of a gephyrin binding motif on the glycine receptor beta subunit. *Neuron* 15:563–572. [CrossRef Medline](#)
- Miles FA, Lisberger SG (1981) Plasticity in the vestibulo-ocular reflex: a new hypothesis. *Annu Rev Neurosci* 4:273–299. [CrossRef Medline](#)
- Muller E, Triller A, Legendre P (2004) Glycine receptors and GABA receptor alpha 1 and gamma 2 subunits during the development of mouse hypoglossal nucleus. *Eur J Neurosci* 20:3286–3300. [CrossRef Medline](#)
- Muzumdar MD, Tasic B, Miyamichi K, Li L, Luo L (2007) A global double-fluorescent Cre reporter mouse. *Genesis* 45:593–605. [CrossRef Medline](#)
- Obata K (1969) Gamma-aminobutyric acid in Purkinje cells and motoneurons. *Experientia* 25:1283. [CrossRef Medline](#)
- Ozden I, Sullivan MR, Lee HM, Wang SS (2009) Reliable coding emerges from coactivation of climbing fibers in microbands of cerebellar Purkinje neurons. *J Neurosci* 29:10463–10473. [CrossRef Medline](#)
- Ozden I, Dombeck DA, Hoogland TM, Tank DW, Wang SS (2012) Widespread state-dependent shifts in cerebellar activity in locomoting mice. *PLoS One* 7:e42650. [CrossRef Medline](#)
- Pedroarena CM, Kamphausen S (2008) Glycinergic synaptic currents in the deep cerebellar nuclei. *Neuropharmacology* 54:784–795. [CrossRef Medline](#)
- Persohn E, Malherbe P, Richards JG (1992) Comparative molecular neuro-

- anatomy of cloned GABAA receptor subunits in the rat CNS. *J Comp Neurol* 326:193–216. [CrossRef Medline](#)
- Person AL, Raman IM (2012a) Purkinje neuron synchrony elicits time-locked spiking in the cerebellar nuclei. *Nature* 481:502–505. [CrossRef Medline](#)
- Person AL, Raman IM (2012b) Synchrony and neural coding in cerebellar circuits. *Front Neural Circuits* 6:97. [CrossRef Medline](#)
- Pirker S, Schwarzer C, Wieselthaler A, Sieghart W, Sperk G (2000) GABA(A) receptors: immunocytochemical distribution of 13 subunits in the adult rat brain. *Neuroscience* 101:815–850. [CrossRef Medline](#)
- Pugh JR, Raman IM (2005) GABAA receptor kinetics in the cerebellar nuclei: evidence for detection of transmitter from distant release sites. *Biophys J* 88:1740–1754. [CrossRef Medline](#)
- Pugh JR, Raman IM (2006) Potentiation of mossy fiber EPSCs in the cerebellar nuclei by NMDA receptor activation followed by postinhibitory rebound current. *Neuron* 51:113–123. [CrossRef Medline](#)
- Rampon C, Luppi PH, Fort P, Peyron C, Jouvet M (1996) Distribution of glycine-immunoreactive cell bodies and fibers in the rat brain. *Neuroscience* 75:737–755. [CrossRef Medline](#)
- Rousseau CV, Dugué GP, Dumoulin A, Mugnaini E, Dieudonné S, Diana MA (2012) Mixed inhibitory synaptic balance correlates with glutamatergic synaptic phenotype in cerebellar unipolar brush cells. *J Neurosci* 32:4632–4644. [CrossRef Medline](#)
- Sassoè-Pognetto M, Panzanelli P, Sieghart W, Fritschy JM (2000) Colocalization of multiple GABA(A) receptor subtypes with gephyrin at postsynaptic sites. *J Comp Neurol* 420:481–498. [CrossRef Medline](#)
- Schindelin J, Arganda-Carreras I, Frise E, Kaynig V, Longair M, Pietzsch T, Preibisch S, Rueden C, Saalfeld S, Schmid B, Tinevez JY, White DJ, Hartenstein V, Eliceiri K, Tomancak P, Cardona A (2012) Fiji: an open-source platform for biological-image analysis. *Nat Methods* 9:676–682. [CrossRef Medline](#)
- Schultz SR, Kitamura K, Post-Uiterweer A, Krupic J, Häusser M (2009) Spatial pattern coding of sensory information by climbing fiber-evoked calcium signals in networks of neighboring cerebellar Purkinje cells. *J Neurosci* 29:8005–8015. [CrossRef Medline](#)
- Tamamaki N, Yanagawa Y, Tomioka R, Miyazaki J, Obata K, Kaneko T (2003) Green fluorescent protein expression and colocalization with calretinin, parvalbumin, and somatostatin in the GAD67-GFP knock-in mouse. *J Comp Neurol* 467:60–79. [CrossRef Medline](#)
- Tanaka I, Ezure K (2004) Overall distribution of GLYT2 mRNA-containing versus GAD67 mRNA-containing neurons and colocalization of both mRNAs in midbrain, pons, and cerebellum in rats. *Neurosci Res* 49:165–178. [CrossRef Medline](#)
- Telgkamp P, Padgett DE, Ledoux VA, Woolley CS, Raman IM (2004) Maintenance of high-frequency transmission at purkinje to cerebellar nuclear synapses by spillover from boutons with multiple release sites. *Neuron* 41:113–126. [CrossRef Medline](#)
- Teune TM, van der Burg J, de Zeeuw CI, Voogd J, Ruigrok TJ (1998) Single Purkinje cell can innervate multiple classes of projection neurons in the cerebellar nuclei of the rat: a light microscopic and ultrastructural triple-tracer study in the rat. *J Comp Neurol* 392:164–178. [CrossRef Medline](#)
- Uusisaari M, Knöpfel T (2008) GABAergic synaptic communication in the GABAergic and non-GABAergic cells in the deep cerebellar nuclei. *Neuroscience* 156:537–549. [CrossRef Medline](#)
- Uusisaari M, Knöpfel T (2010) GlyT2+ neurons in the lateral cerebellar nucleus. *Cerebellum* 9:42–55. [CrossRef Medline](#)
- Uusisaari MY, Knöpfel T (2012) Diversity of neuronal elements and circuitry in the cerebellar nuclei. *Cerebellum* 11:420–421. [CrossRef Medline](#)
- Uusisaari M, Obata K, Knöpfel T (2007) Morphological and electrophysiological properties of GABAergic and non-GABAergic cells in the deep cerebellar nuclei. *J Neurophysiol* 97:901–911. [CrossRef Medline](#)
- Wang H, Peca J, Matsuzaki M, Matsuzaki K, Noguchi J, Qiu L, Wang D, Zhang F, Boyden E, Deisseroth K, Kasai H, Hall WC, Feng G, Augustine GJ (2007) High-speed mapping of synaptic connectivity using photostimulation in Channelrhodopsin-2 transgenic mice. *Proc Natl Acad Sci U S A* 104:8143–8148. [CrossRef Medline](#)
- Wassef M, Simons J, Tappaz ML, Sotelo C (1986) Non-Purkinje cell GABAergic innervation of the deep cerebellar nuclei: a quantitative immunocytochemical study in C57BL and in Purkinje cell degeneration mutant mice. *Brain Res* 399:125–135. [CrossRef Medline](#)
- Welsh JP, Lang EJ, Sugghara I, Llinás R (1995) Dynamic organization of motor control within the olivocerebellar system. *Nature* 374:453–457. [CrossRef Medline](#)
- Weltzien F, Puller C, O'Sullivan GA, Paarmann I, Betz H (2012) Distribution of the glycine receptor beta-subunit in the mouse CNS as revealed by a novel monoclonal antibody. *J Comp Neurol* 520:3962–3981. [CrossRef Medline](#)
- Witter L, Canto CB, Hoogland TM, de Ruijl JR, De Zeeuw CI (2013) Strength and timing of motor responses mediated by rebound firing in the cerebellar nuclei after Purkinje cell activation. *Front Neural Circuits* 7:133. [CrossRef Medline](#)
- Yakushiji T, Tokutomi N, Akaike N, Carpenter DO (1987) Antagonists of GABA responses, studied using internally perfused frog dorsal root ganglion neurons. *Neuroscience* 22:1123–1133. [CrossRef Medline](#)
- Zafra F, Aragón C, Olivares L, Danbolt NC, Giménez C, Storm-Mathisen J (1995) Glycine transporters are differentially expressed among CNS cells. *J Neurosci* 15:3952–3969. [Medline](#)
- Zeilhofer HU, Studler B, Arabadzisz D, Schweizer C, Ahmadi S, Layh B, Bösl MR, Fritschy JM (2005) Glycinergic neurons expressing enhanced green fluorescent protein in bacterial artificial chromosome transgenic mice. *J Comp Neurol* 482:123–141. [CrossRef Medline](#)
- Zheng N, Raman IM (2010) Synaptic inhibition, excitation, and plasticity in neurons of the cerebellar nuclei. *Cerebellum* 9:56–66. [CrossRef Medline](#)

4.2. *Supplementary data*

4.2.1. *Transient expression of GlyT2 in nucleo-olivary neurons*

The use of transgenic lines where the GlyT2 promoter was used to express GFP or Cre-recombinase led to the conclusion that there was a transient expression of GFP in the nucleo-olivary cells during the development.

A mismatch exists in the calculated numbers of GlyT2-positive neurons in the cerebellar nuclei of the GlyT2-eGFP and the GlyT2-Cre x Rosa-mTmT adult mouse, suggesting that the expression of Cre-recombinase was not restricted to glycinergic neurons in the GlyT2-Cre mouse, putatively due to developmental leakage of Cre-recombinase expression.

In support of this hypothesis, we found evidence for the early expression of GFP in the nucleo-olivary neurons during the development of the GlyT2-eGFP mouse. We retrolabeled nucleo-olivary neurons by injecting retrobeads in the inferior olive of adult GlyT2-eGFP mice. These neurons displayed a level of GFP expression above the background. Expression was quantified by increasing the sensitivity of the fluorescence acquisition, leading to saturation over the somata of the GFP+ glycinergic neurons. We found that all the retrolabeled cells exhibit lower somatal GFP intensity than the GFP+ glycinergic neurons (see *figure 4.1.*).

We conclude that the nucleo-olivary neurons may express transiently during early developmental stages under the BAC fragment of the GlyT2-promoter used to produce the transgenic mice. An extensive developmental survey would be necessary to confirm and quantify this point.

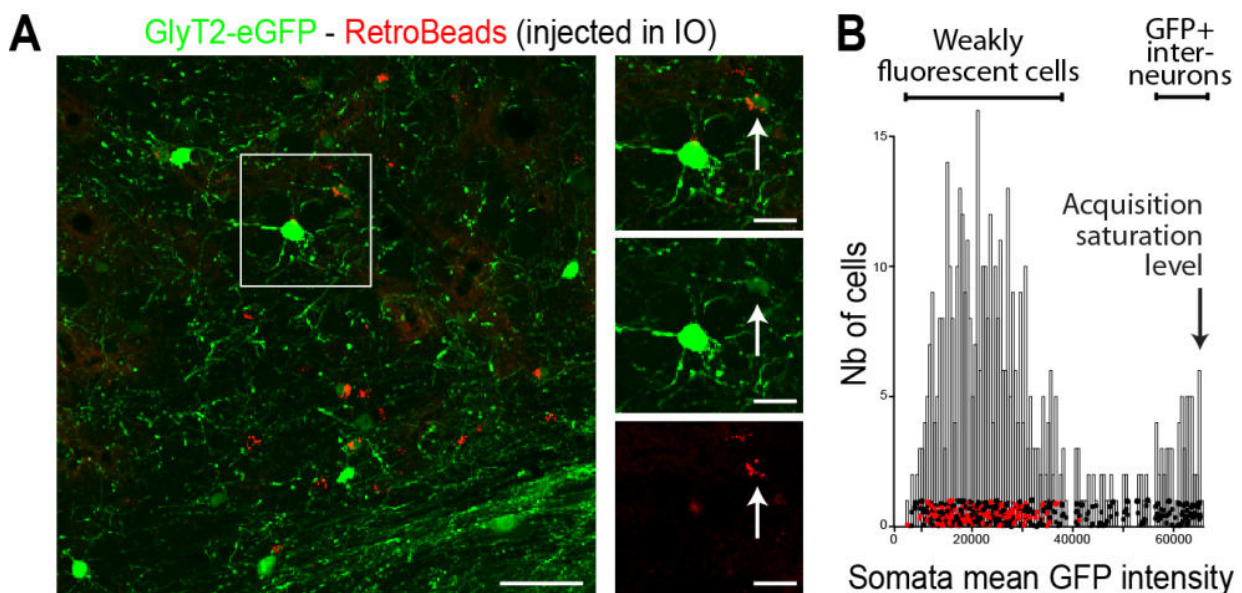


Figure 4.1. Weak expression of GFP in the nucleo-olivary neurons in the GlyT2-eGFP adult mouse. A- Interposed nucleus in a GlyT2-eGFP mouse, injected in the inferior olive with red Retrobeads. Some retrolabeled cells are faintly stained for GFP (arrows in the close up) (Z-thickness of projection: 8 μ m). B- GFP intensity of the GlyT2+ cell body was retrieved and demonstrated the existence of two populations of cells, the strongly-expressing population displaying saturated levels of fluorescence in these stacks. The strongly GFP+ cells were not retrolabeled from the IO (black dots, n = 182 cells) while faintly stained cells were retrolabeled nucleo-olivary neurons (red dots, n = 306 cells). Scale bars: A. 50 μ m. A close up. 20 μ m.

4.2.2. Extracellular recordings of the GlyT2-expressing interneurons

The firing behavior of the GlyT2-positive neurons in the cerebellar nuclei of GlyT2-Cre mice infected with flexed AAV coding for ChR2-YFP was investigated by extracellular recordings in acute slices. Light pulses of one millisecond and increasing power were used (as during the whole-cell recordings of the principal neurons).

The first interesting observation is the fact that GlyT2-expressing neurons did not seem to fire spontaneously, as no spikes could be seen before the onset of the light illumination. Only one cell out of the 11 recorded neurons exhibit a spontaneous firing rate around 20 Hz. All the recorded neurons ($n = 11$) responded to the illumination by firing high-frequency bursts of spikes (mean frequency during the burst: 467.5 ± 82.3 Hz, $n = 5$ cells). Increased illumination power elicited bursts with an increasing number of spikes (see *figure 4.2.A*).

Sequential bath applications of $1 \mu\text{M}$ gabazine, $50 \mu\text{M}$ APV- $10 \mu\text{M}$ NBQX did not block the burst firing or reduce the amplitude of the spike, suggesting that this firing pattern is only due to the intrinsic electrophysiological properties of the GlyT2-Cre positive neurons (see *figure 4.2.B*). Spikes were abolished by 200 nM tetrodotoxine (TTX), indicating that they depend on sodium channels.

These high frequency bursts of spikes are similar to the bursts of IPSCs recorded in principal neurons in response to high-intensity optogenetic stimulation (see *figure 4.2.C*).

4.3. Concluding remarks

For many years, authors have described populations of putative inhibitory interneurons in the cerebellar nuclei and proposed that they project onto principal neurons to control their activity without precisely demonstrating it. Additionally, little evidence for glycinergic transmission in the principal neurons came from heavy pharmacological manipulations of the presynaptic terminals. However, the gap which links both presynaptic activity of the putative glycinergic interneurons and the postsynaptic currents in the principal neurons was never filled.

Here, we demonstrated the functional inhibitory transmission between inhibitory neurons and principal neurons in the cerebellar nuclei. A population of local inhibitory neurons, which co-release GABA and glycine, make synapses on the somatic compartment of the principal neurons. The post-synaptic clusters at this synapse are mainly composed of $\alpha 1$ and β subunits of the glycine receptor and virtually devoid of the $\gamma 2$ and $\alpha 1$ subunits of GABA_A receptors. The IPSCs recorded are inhibited by both GABA_A and glycine receptors antagonists, gabazine and strychnine respectively, providing the first demonstration of mixed functional transmission in the cerebellar nuclei.

Additionally, we showed that post-synaptic clusters located at the Purkinje cell synapses are immunoreactive for glycine receptors. However, the percentage of glycine receptor – mediated currents is very low (less than 3 %) and did not interfere with the kinetics of the inhibitory currents.

Therefore, mixed inhibitory inputs arising from the interneuronal population are physiologically different from the GABAergic inputs from the Purkinje cells. Functional impact of the interneurons activity onto the principal neurons is not clear for now, mainly due to acute slices experiments limitations. *In vivo* studies, where inputs to cerebellar nuclei are preserved, may improve the comprehension of the interneuronal population activity and therefore their impact on cerebellar output.

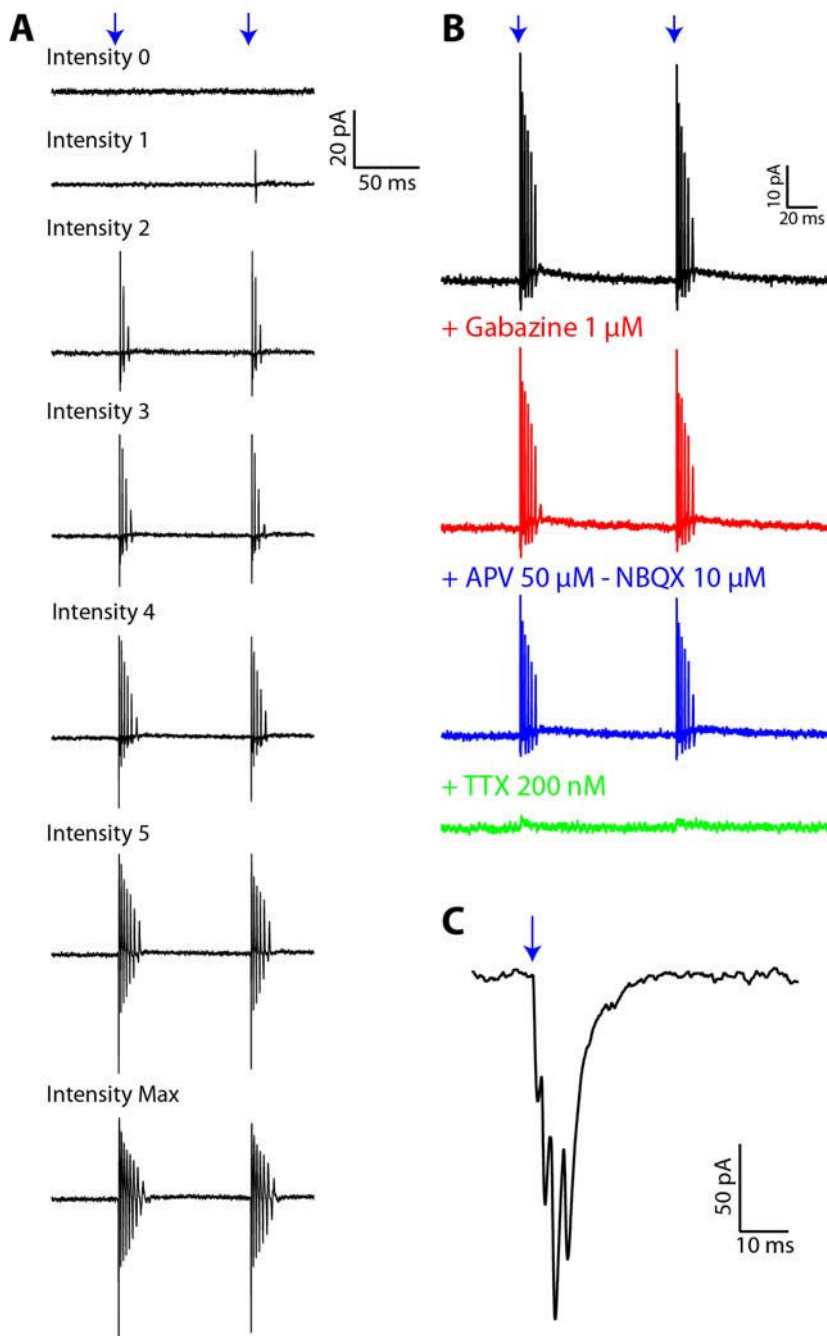


Figure 4.2.: Extracellular recordings of GlyT2-Cre positive ChR2-infected neurons during one millisecond whole field illumination. A- Recruitment curve of different illumination intensities (arbitrary units, A.U.). Onsets of the stimulations are indicated by the blue arrows. At low powers, neurons were not responding and do not exhibit spontaneous firing during baseline recordings. With increasing intensities, neurons respond in bursts with increasing number of spikes. B- Burst spiking phenotype was not affected by successive application of 1 μ M gabazine, 50 μ M APV/10 μ M NBQX, but was abolished by 200 nM TTX. Onsets of the stimulations are indicated by the blue arrows (1 ms illumination with maximum power intensity). C- High-frequency bursts of spikes of the GlyT2-expressing neurons elicited similar bursts of IPSCs in the principal neurons. Onset of the stimulation is indicated by the blue arrow (1 ms illumination with power 2 A.U. intensity)

CHAPTER 5: Beyond principal cells: the extended connectivity of the inhibitory glycinergic neurons of the cerebellar nuclei

The connectivity of the cerebellar nuclei remains still unclear, especially the nature of the neuronal networks involving the cell types other than the principal neurons.

In this chapter, we will describe another output of the cerebellar nuclei, the nucleo-cortical projection. Recently, a population of glycinergic neurons has been shown to be implied in the nucleo-cortical feedback loop. We investigated the hypothesis that the glycinergic nucleo-cortical neurons represent the same neuronal population as the population giving rise to the local mixed neurons we previously described. We find it is the case and describe the target of the inhibitory nucleo-cortical fibers in the cerebellar cortex and the synaptic properties of those inhibitory nuclear projections.

In addition, synaptic inputs onto this inhibitory neuronal population of the cerebellar nuclei have not been described. In this chapter, we investigated the Purkinje cell inputs onto inhibitory neurons, as well as the putative excitatory inputs arising from the mossy fiber or climbing fiber systems.

5.1. Intra-cerebellar output of the cerebellar nuclei: the inhibitory nucleo-cortical pathway

A population of glycinergic neurons has been shown to project to the granular layer of the cerebellar cortex (Uusisaari and Knopfel, 2010), consistent with the previous description of an inhibitory nucleo-cortical pathway (see Introduction, Chapter 3, *section 3.3.2.*). We therefore investigated whether the neurons identified genetically in our first study also projected to the cortex. The cerebellar nuclei of the adult GlyT2-Cre mouse were injected with a floxed AAV coding for YFP. After three weeks of expression we observed nucleo-cortical fibers leaving the cerebellar nuclei to reach the granular layer of the cortex (see *figure 5.1.A*). We therefore initiated a collaboration with M. Uusisaari and colleagues who had found similar nucleo-cortical projections in GAD65-Cre mice injected with a floxed AAVs (Uusisaari's data, not shown).

A low density axonal plexus restricted to the granular layer of the cerebellar cortex (see *figure 5.1.A*) was observed. Numerous large varicosities (about 2 μm of diameter) were distributed along thin and tortuous axons and were co-labelled for GAD65-67 (see *figure 5.1.B* and *figure 5.1.C. solid arrows*), indicating that they can co-release GABA and glycine.

One of the favorite target cells for those glycinergic nucleo-cortical fibers in the granular layer would be the Golgi cells, as they are known to express glycine receptors (Dumoulin et al., 2001). Golgi cells constitute a heterogeneous neuronal population (Pietrajtis and Dieudonné, 2012). Three

main types of Golgi neurons could be distinguished: glycinergic-only, GABAergic-only and mixed GABA/glycine Golgi cells. The GABAergic and mixed Golgi cells are also expressing neurogranin, a calcium binding protein.

GlyT2-eGFP mouse was used as a first approach to see Golgi cells in the granular layer. Constitutive AAVs coding for mCherry were injected in the cerebellar nuclei of GlyT2-eGFP mice. As the virus was not specific of the glycinergic neurons, we also labelled the glutamatergic nucleo-cortical neurons. However, those neurons won't be co-labeled for GFP. Moreover, it appeared that glutamatergic (GAD65-67 – negative) nucleo-cortical fibers are ending in glomeruli, in a rosette-like shape (see *figure 5.1.C.a. dashed arrow*) whereas inhibitory nucleo-cortical fibers make *en passant* varicosities, usually around 2 μm of diameter (see *figure 5.1.B, C, D, E*). mCherry+ inhibitory nucleo-cortical fibers could thus also distinguished based on their morphological characteristics. This was particularly useful, as we showed previously that about 40% only of the glycinergic neurons express GFP in the cerebellar nuclei of the GlyT2-eGFP mouse (see Results, Chapter 1, *section 1.1.*). Some examples of GFP- / mCherry + nucleo-cortical fibers are shown in *figure 5.1.D-E*.

Inhibitory nucleo-cortical fibers were found in apposition to dendrites of GlyT2-eGFP + Golgi cells (see *figure 5.1.C.a. solid arrows* and *figure 5.1.E. dashed arrows*). In some cases, the presynaptic terminals were not facing any GlyT2-eGFP+ elements, suggesting that the inhibitory nucleo-cortical fibers may contact others Golgi cell types. Neurogranin stainings revealed that inhibitory nucleo-cortical fibers often contact the neurogranin+ Golgi cell dendrites (see *figure 5.1.D-E. solid arrows*). To date, we found no apposition between nucleo-cortical inhibitory fibers and GlyT2-eGFP+/neurogranin+ neurites, suggesting that mixed Golgi cells may not be contacted by the inhibitory nucleo-cortical neurons. Further analysis need to be completed to confirm this hypothesis. Those findings are in agreement with the data provided by Uusisaari and colleagues, who demonstrated that inhibitory nucleo-cortical fibers contact GAD- positive Golgi neurons.

Therefore, inhibitory nucleo-cortical neurons, co-releasing GABA and glycine, project to the granular layer of the cortex where they contact Golgi cells. It seemed that the terminals preferentially end on glycinergic-only and GABAergic-only Golgi-cells, however further investigations are necessary to detail the connectivity of the nucleo-cortical fibers onto the different Golgi cell types.

To confirm that the nucleo-cortical projections onto Golgi cells were functional, we injected floxed AAV-ChR2-YFP in the cerebellar nuclei of GlyT2-Cre mice. After three weeks of incubations, Golgi cells were recorded in acute slices of cerebellar cortex²⁴ (see *Materials and Methods*). Inhibitory currents were elicited in Golgi cells (n = 6) by one-photon illumination of the GlyT2-Cre x AAV-ChR2-YFP nucleo-cortical fibers (see *Materials and Methods*) (see *figure 5.2.A.*). Application of 300 nM strychnine inhibited $27.2 \pm 19.6\%$ of the initial peak amplitude, while subsequent application of 2 μM gabazine fully blocked the response (see *figure 5.2.B.*). The decays of the IPSCs were fitted by a bi-exponential function. The fast component was found to be slower after the application of 300 nM strychnine (baseline: 10.95 ± 2.92 ms; after strychnine: 14.06 ± 4.94 ms, Wilcoxon paired test, p = 0.016), while the slow component was found unchanged (baseline: 90.48 ± 68.54 ms; after strychnine: 91.80 ± 48.80 ms, Wilcoxon paired test, p = 0.6875). Those results are consistent with the specific block by strychnine of a fast glycinergic component of the light-evoked nucleo-cortical IPSCs (see Introduction, Chapter 3, *section 3.2.2.*).

²⁴ All the Golgi cells recordings were performed by Kasia Pietrajtis.

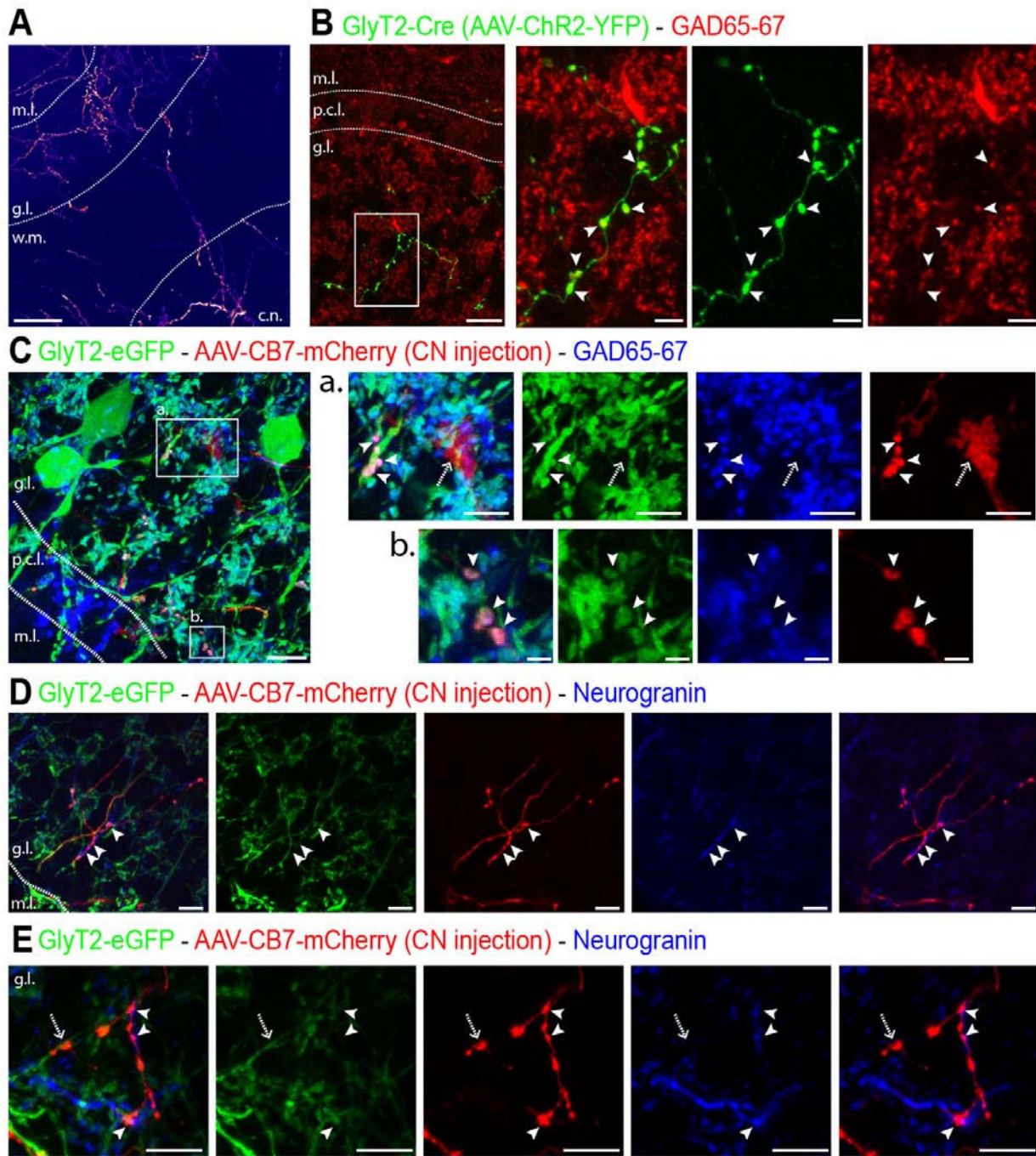


Figure 5.1: Mixed GABAergic/glycinergic nucleo-cortical neurons project to GlyT2 – positive and Neurogranin – positive Golgi cells in the granular layer of the cortex. A- Cortical projections of GlyT2-expressing neurons in the cerebellar nuclei of a GlyT2-Cre mouse injected with AAV-ChR2-YFP (Z-projection thickness: 84.6 μm). B- GlyT2-Cre x AAV-ChR2-YFP nucleo-cortical fibers (*in green*) are co-stained for GAD65-67 (*in red*) (Z-projection thickness: 12.2 μm). C- Nucleo-cortical fibers arising from glycinergic neurons were co-labeled for GFP (*in green*) and mCherry (*in red*) in GlyT2-eGFP mice injected in the cerebellar nuclei with AAV-CB7-mCherry. C. a-b- Those GlyT2-eGFP – positive nucleo-cortical fibers are co-stained for GAD65-67 (*in blue*, indicated by solid arrows), while GAD65-67 – negative glutamatergic nucleo-cortical fibers end in glomeruli in a rosette-like shape (indicated by dashed arrow). The GFP+/GAD65-67+ nucleo-cortical fibers are found in apposition to dendrites of GlyT2-eGFP – positive Golgi cells

(solid arrows). (Z-projection thickness: 9.5 μm). D-E- Glycinergic nucleo-cortical fibers (mCherry – positive *in red*) are not always stained for GFP (*in green*), as it was previously shown that only 40% of the glycinergic neurons are labeled for GFP in the cerebellar nuclei of the GlyT2-eGFP mouse. However, they are distinguished by their morphology: en passant varicosities are found in apposition to GlyT2-eGFP-/Neurogranin+ (*in blue*, indicated with solid arrows) and GlyT2-eGFP+/Neurogranin- elements (indicated by dashed arrow) (Z-projection thickness: D. 5.4 μm ; E. 10.8 μm). Abbreviations: m.l. molecular layer; g.l. granular layer; p.c.l. Purkinje cell layer; w.m. white matter; c.n. cerebellar nuclei. Scale bars: A. 50 μm . B. 20 μm . B. close up. 5 μm . C. 10 μm . C. close up a. 5 μm . b. 2 μm . D. 5 μm . E. 5 μm .

Overall, those data confirmed the projection of inhibitory nucleo-cortical neurons onto Golgi cells of the granular layer, and their mixed GABA/glycine phenotype. This provides the first evidence of functional inhibition from the nucleo-cortical projection in the granular layer.

The mixed GABA/glycine phenotype of those neurons, together with their presence in the GlyT2-eGFP and GlyT2-Cre mice in which we characterized a population of glycinergic neurons involved in intra-nuclear inhibition, lead us to conclude that both populations may actually constitute a single third cell type in the cerebellar nuclei (see *Discussion*). Those inhibitory neurons have local axonal collaterals which provide mixed inhibition within the cerebellar nuclei and an axonal projection to the granular layer of the cortex where they contact Golgi cells and may be involved in intra-cerebellar feedback loops.

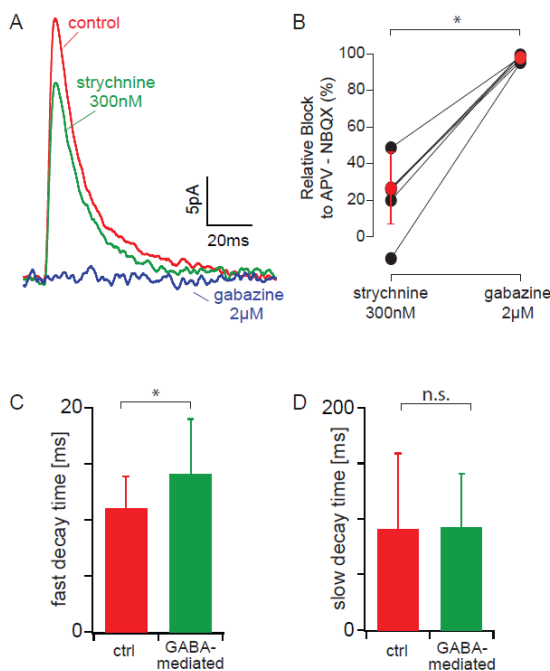


Figure 5.2: Mixed transmission at the nucleo-cortical neuron to Golgi cell synapses. A- Example of averaged (n=30) IPSCs recorded in Golgi cell elicited by optogenetic stimulation of inhibitory nucleo - cortical cell axons in the granular layer, in presence of blockers of excitation (50 μM D-APV and 2 μM NBQX). Strychnine 300nM and gabazine 2 μM were bath applied, resulting in the reduction of the amplitude. B- Summary plot of the percentage of block by strychnine (300nM) and gabazine (2 μM) (Wilcoxon paired test, n = 6 cells, p = 0.03). C- Fast decay time constant was significantly increased (Wilcoxon paired test, p = 0.016) while slow component of the decay was not significantly affected (D) (Wilcoxon paired test, p = 0.6875). Electrophysiological data provided by Katarzyna Pietrajtis.

5.2. Inputs to inhibitory neurons of the cerebellar nuclei

5.2.1. Purkinje cells inputs onto inhibitory neurons

Some anatomical (De Zeeuw and Berrebi, 1995a) and electrophysiological (Uusisaari and Knopfel, 2008) findings suggested that the Purkinje cells contact the mixed inhibitory neurons of the cerebellar nuclei. These inputs were first investigated by immunohistochemistry. Stainings for VIAAT in the GlyT2-eGFP mouse revealed sparse appositions between VIAAT – positive varicosities and the somata and proximal dendrites of the eGFP+ neurons (see *figure 5.3.A*). Their density appeared much lower than on principal neurons. Clusters of receptors containing the $\gamma 2$ or $\alpha 1$ subunits of the GABA_A receptors are found at the surface of eGFP+ neurons (see *figure 5.3.B-C*), facing either VIAAT – positive (see *figure 5.3.B*) or Calbindin²⁵ – positive terminals (see *figure 5.3.C*). No glycine receptor immunoreactivity was observed on the membrane of eGFP+ neurons (data not shown).

To confirm that the GABAergic synapses were functional, we took advantage of the two mouse lines available in our laboratory. We bred together the L7-ChR2-YFP mouse, which provides a great tool to specifically activate the Purkinje cells terminals, and the GlyT2-eGFP mouse, in which the mixed inhibitory nuclear neurons can be targeted easily using epifluorescence microscopy. During whole-cell patch clamp recordings of the eGFP+ neurons in the cerebellar nuclei, brief pulses of light (one millisecond) were delivered onto the cerebellar nuclei. Large inhibitory responses were elicited in the mixed inhibitory nuclear neurons (see *figure 5.3.D*) with a mean amplitude of 416.5 ± 332.1 pA ($n = 10$ cells). Those IPSCs were blocked by gabazine (87.1 ± 5.9 % by 300 nM gabazine, $n = 5$ cells; 98.1 ± 1.4 % by 1 μ M gabazine, $n = 9$ cells), indicating that they are mediated by GABA_A receptors (see *figure 5.3.E*). The decay times of the events were not significantly different before and after application of a sub-saturating concentration of gabazine (control: 3.28 ± 0.72 ms, $n = 10$ cells; gabazine 300 nM: 4.76 ± 3.53 ms, $n = 5$ cells, Wilcoxon test $p = 0.8591$).

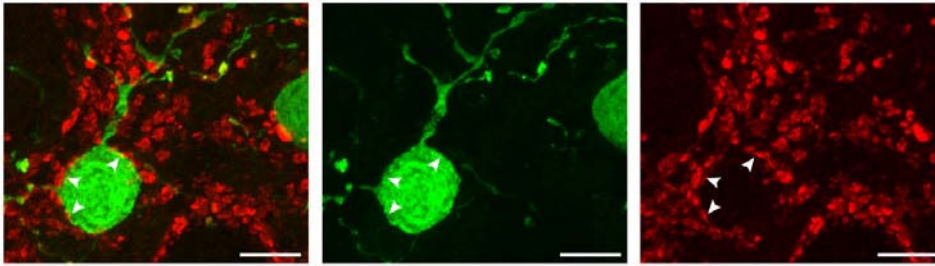
Those results represent the first functional demonstration of the Purkinje cells input, mediated by $\gamma 2$ - and $\alpha 1$ - containing GABA_A receptors, on mixed inhibitory neurons. These findings may have great impact on the current view of the inhibitory nucleo-cortical pathway, as it may provide a rapid feedback pathway for the regulation of Purkinje cells activity.

5.2.2. Excitatory inputs onto glycinergic neurons

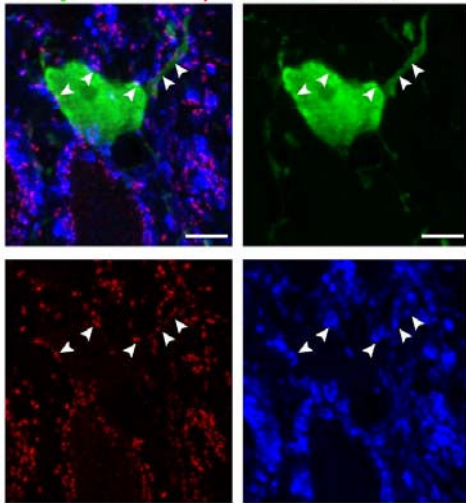
Collaterals of mossy fibers or climbing fibers may also control the inhibitory interneurons in the cerebellar nuclei. To investigate the presence of excitatory inputs on the mixed inhibitory neurons, we used the GlyT2-eGFP mouse in which we co-labelled the two vesicular transporters of glutamate VGLUT1 and VGLUT2. Co-stainings revealed that terminals labelled for VGLUT2 were in apposition with the dendrites of GlyT2-eGFP – -positive neurons (see *figure 5.4*). More rarely, varicosities stained for both VGLUT2 and VGLUT1 were contacting inhibitory neurons (see *figure 5.4.A(a)*).

²⁵ Calbindin is a calcium binding protein, found specifically in the Purkinje cells in the cerebellum. It was used as a marker for the Purkinje cells terminals in the cerebellar nuclei, as VIAAT labelling also includes the inhibitory terminals of local neurons.

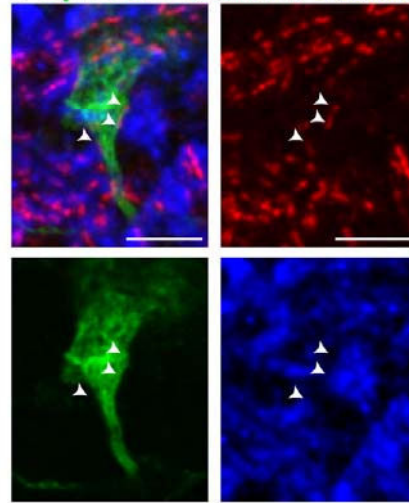
A GlyT2-eGFP - VIAAT



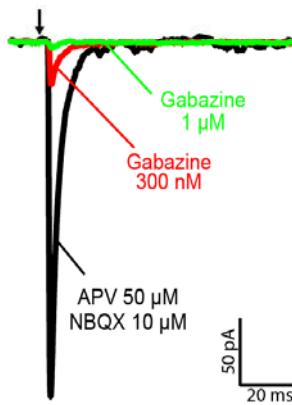
B GlyT2-eGFP - γ 2GABAR - VIAAT



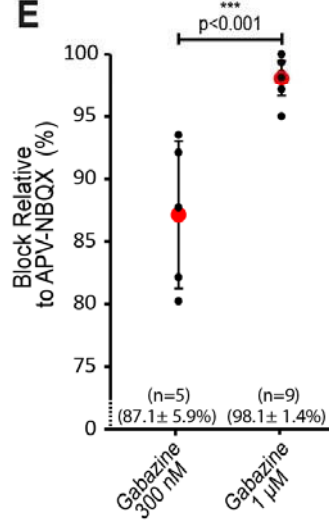
C GlyT2-eGFP - α 1GABAR - Calbindin



D



E



F

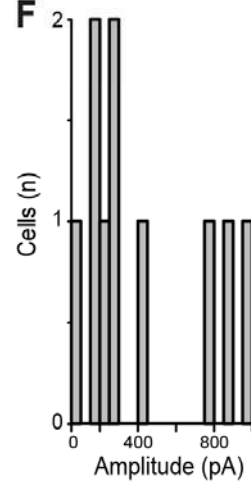
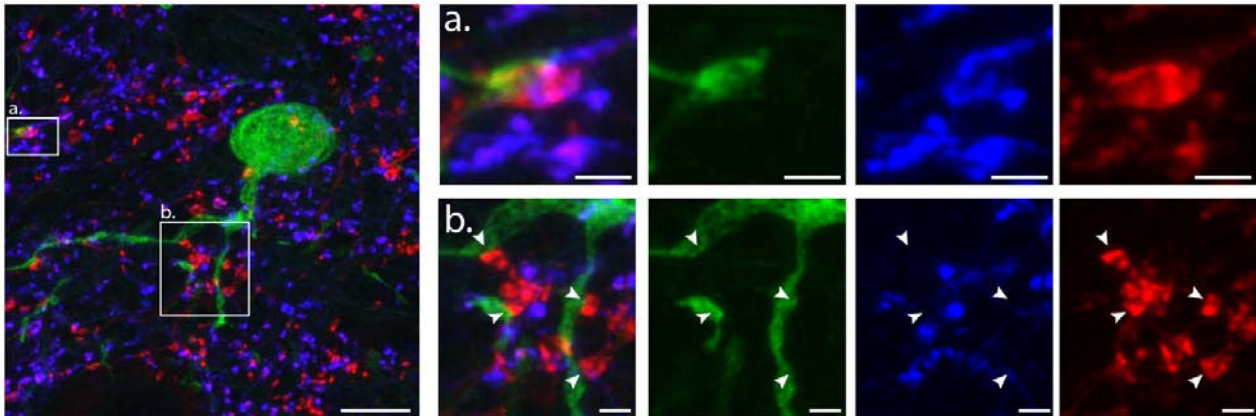


Figure 5.3: Purkinje cells GABAergic inputs onto GlyT2-positive neurons of the cerebellar nuclei in L7-ChR2-YFP x GlyT2-eGFP mice. (A) In the GlyT2-eGFP mouse, eGFP-positive neurons (*in green*) are contacted by VIAAT-positive varicosities (*in red*). Points of contacts are indicated by arrows. (Z-projection thickness: 4.6 μ m). (B) VIAAT-positive varicosities (*in blue*) are facing γ 2-containing GABA_A receptors (*in red*), on the proximal compartment of the GlyT2-eGFP-positive neurons (*in green*). (Z-projection thickness: 3.1 μ m). (C) Calbindin-positive terminals (*in blue*) face α 1-containing GABA_A receptors located at the membrane of GlyT2-eGFP-positive neurons (*in green*) (Z-projection thickness: 1.5 μ m). (D) One millisecond illumination with a 470 nm LED (indicated by the arrow) in the cerebellar nuclei elicited large inhibitory responses in the GlyT2-positive neurons. (E) The responses were inhibited by 300 nM gabazine and fully blocked by 1 μ M gabazine. (F) The amplitude of recorded responses varied among the cells. Scale bars: D. 10 μ m. E-F. 5 μ m.

Those findings indicate that the inhibitory neurons might receive excitatory inputs; however if they receive from mossy fibers, climbing fibers or both could not be assessed in these experiments. Because the mixed inhibitory neurons do not fire spontaneous action potentials, excitatory synaptic inputs are absolutely required to bring them to threshold. Further investigation of these inputs using optogenetic methods is therefore a priority.

A GlyT2-eGFP - VGLUT2 - VGLUT1



B GlyT2-eGFP - VGLUT2 - VGLUT1

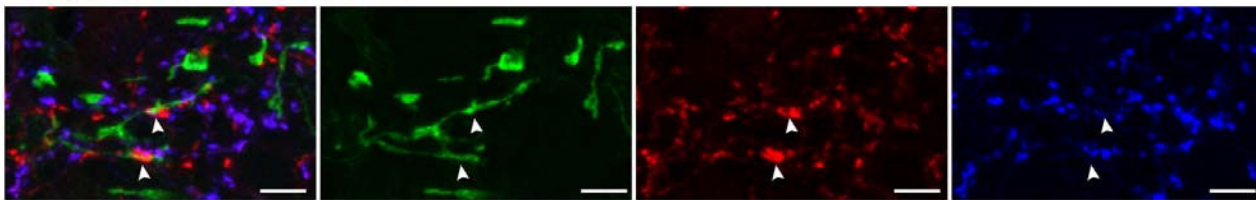


Figure 5.4: Excitatory inputs onto GlyT2-eGFP - positive neurons of the cerebellar nuclei. (A-B) VGLUT2 - positives varicosities (in red) were found in apposition to eGFP - positive neurons (in green) in co-stainings for VGLUT2 and VGLUT1 (in blue) in GlyT2-eGFP mouse. More rarely, mixed VGLUT2-VGLUT1 - positives varicosities were contacting dendrites of GlyT2-eGFP neurons (A-a). (Z-projection thickness: A: 5.1 μm ; B: 2.7 μm). Scale bars: A. 10 μm . close up A.a-b. 2 μm . B. 5 μm .

5.2.3. Excitatory inputs onto the principal neurons: mossy fiber versus climbing fiber inputs

The principal neurons of the cerebellar nuclei receive inhibitory inputs from local mixed neurons and from both climbing fiber and mossy fiber inputs. To assess if inhibitory neurons of the cerebellar nuclei receive from one or the two excitatory inputs, our goal was to record di-synaptic inhibitory inputs in the principal neurons following specific stimulations of either mossy or climbing fibers.

To dissociate the climbing fiber and the mossy fiber inputs, one possibility is to specifically inject AAVs expressing ChR2 in the inferior olive nuclei with minimal infection of the surrounding brainstem nuclei which are known to give rise to mossy fiber projections. In adult mice and with a dorsal approach, it was usually hard to target the inferior olive due to the depth of the target from the brain surface and to the spread of virus along the pipette tract. Therefore, we tried to aim at the inferior olive by a ventral approach in Po-P1 pups, as the olivary complex is lying on the ventral part of the medulla oblongata. The advantage of using neonatal animals was of two kinds: first, because AAVs requires three weeks of infection to be fully expressed in the targeted neurons, the animals are still young enough for acute slices experiments in the cerebellar nuclei at the time of highest expression; and secondly at neonatal stages the *foramen magnum* through which we are injecting (see *Materials and Methods*) is relatively accessible compared to the adult.

We injected AAVs expressing ChR2 under the control of the synapsin promoter in wild-type OF1 pups (see *Materials and Methods*). At the time of animal sacrifice for acute slices experiment, the medulla was fixed in PAF and sliced to check the injection site. The infection size varied between animals and was usually large, covering a large area of the medulla (see *figure 5.5.A*). In most of the case, the inferior olive was infected, but the surrounding precerebellar nuclei, notably the lateral reticular nuclei, were also labelled. Therefore, inferior olive injection by the ventral approach did not appear to be a better way to specifically target the olivary complex. The small size of the olivary nuclei in the mouse make them hard to target without affecting the surrounding areas and the absence of specificity of the promoter used in AAVs did not allow ChR2 expression in climbing fibers only.

However, these experiments were useful. Even though it was not possible to distinguish between climbing fiber projections and mossy fiber projections, we were able to record excitatory synaptic currents in response to flashes of light during whole-cell patch clamp recordings of the principal neurons of the cerebellar nuclei (see *figure 5.5.B*). Out of 32 recorded cells, 17 received a response to one millisecond illumination. Using high-chloride internal solution and holding the neurons at -70 mV, the mean amplitude of the responses was 319.1 ± 252.7 pA ($n = 11$ cells). The responses were not affected by the application of $1 \mu\text{M}$ gabazine, indicating that they were not mediated by GABA_A receptors, or did not involve di-synaptic inhibition. $50 \mu\text{M}$ APV, a selective blocker for NMDA receptors, inhibited about 25 % of the responses (24.8 ± 2.72 % of the initial amplitude, $n = 3$ cells), while $10 \mu\text{M}$ NBQX, an antagonist of AMPA receptors, blocked the remaining response ($n = 5$ cells) (see *figure 5.5.B*). Those results indicate that excitatory inputs onto principal neurons are mainly mediated by AMPA rather than NMDA receptors at hyperpolarized potentials. Whether those inputs correspond to climbing fibers or mossy fibers could not be said in this experimental protocol, as discussed previously.

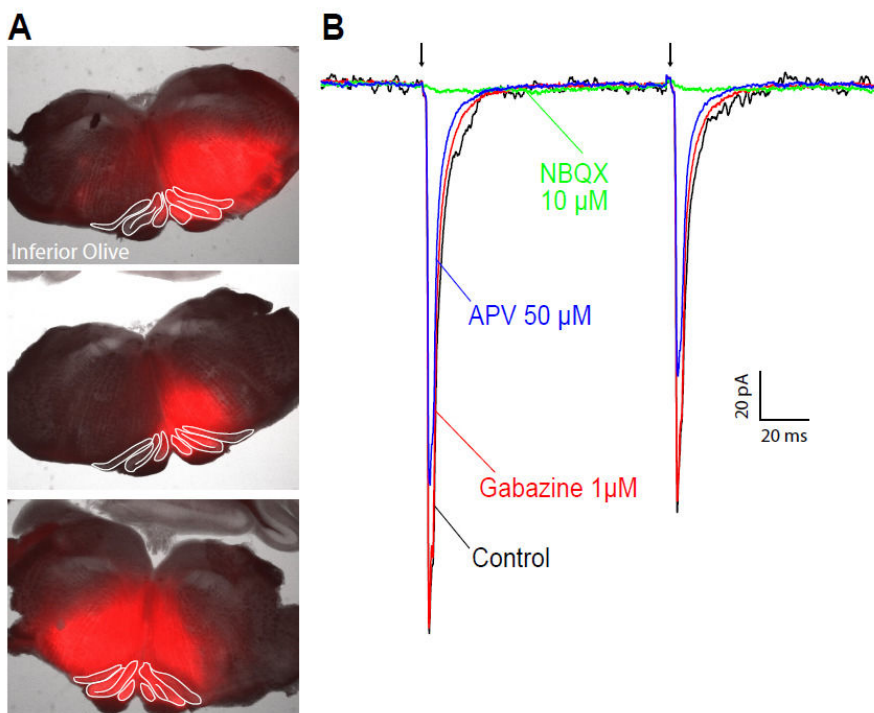


Figure 5.5: AAVs-ChR2 infection of inferior olive by ventral approach in OF1 neonatal pups and elicited responses in the principal neurons of the cerebellar nuclei. (A) Examples of injection sites three weeks after AAV-ChR2 injection into medulla of OF1 neonatal pups by ventral approach. Inferior olive nuclei delimitations are drawn in white. (B) One millisecond illumination with a 470 nm LED (indicated by the arrow) in the cerebellar nuclei elicited responses in the principal neurons. The responses were not influenced by the application of $1 \mu\text{M}$ gabazine and are partially blocked by $50 \mu\text{M}$ APV. The remaining amplitude is blocked by $10 \mu\text{M}$ NBQX.

At -70 mV, NMDA receptors are blocked by magnesium ions and NMDA-mediated currents are very small. To differentiate an outward inhibitory component from inward excitatory inputs, we also recorded the principal neurons at -20 mV using an internal solution with physiological chloride concentration (see *Materials and Methods*). As for the previous series of experiments, 17 cells out of 34 were responsive to one millisecond illuminations. Similarly, the peak amplitudes of the elicited responses were not affected by the application of 1 μ M gabazine and only partially inhibited by 50 μ M APV, while 10 μ M NBQX blocked all the remaining responses ($n = 5$ cells).

However, in three cells, blockade of inhibition by application of 1 μ M gabazine and 1 μ M strychnine led to an increase of the decay time of the responses (control: 5.39 ± 1.6 ms; gabazine/strychnine: 10.1 ± 1.8 ms, APV: 1.89 ± 0.72 ms, $n = 3$ cells for each condition) without affecting the peak amplitude (mean amplitude in control: 140.6 ± 53.2 pA; mean amplitude in gabazine/strychnine: 138.7 ± 53.4 pA, Wilcoxon test $p =$ (see *figure 5.6.A-B*). As the late component of the inward synaptic current is increased, this suggested that the cocktail of glycine and GABA_A receptors antagonists blocked an outward component. The slow component of the response was blocked by application of 50 μ M APV (see *figure 5.6.A*), with a peak amplitude reduction of about 50% (54.3 ± 28.2 % of the initial peak amplitude, Wilcoxon test $p = 0.2$). However, this slowing down of the decay time was not significantly different between each condition (Wilcoxon paired test, $p = 0.25$ between control and gabazine/strychnine application, and $p = 0.25$ between gabazine/strychnine application and APV application), surely due to the low number of cells analyzed.

Those results indicate that both NMDA and AMPA receptors mediate excitatory inputs onto the principal neurons. If one type of receptors is more specifically activated by mossy fibers or climbing fibers cannot be said, and the use of specific genetics tools to target the two systems separately will be necessary to investigate this issue. In some cases, di-synaptic inhibitory inputs are found, suggesting that they may have an important functional role in shaping the response to excitatory inputs but further experiments need to be done to confirm these findings.

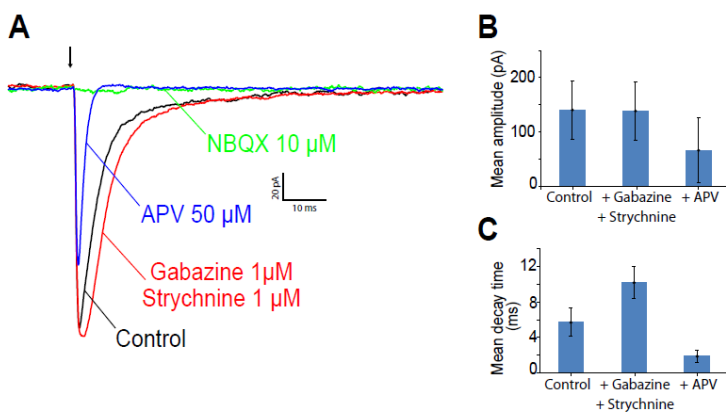


Figure 5.6. Excitatory responses in principal neurons recorded at -20 mV with physiological internal solution, in animals injected in the brainstem with AAVs expressing ChR2. (A) Example of averaged responses elicited by 1 ms illumination (indicated by the arrow) in principal neurons. Application of 1 μ M gabazine / 1 μ M strychnine did not reduce the peak amplitude (B) but slowed the decay time of the responses (C). Subsequent application of 50 μ M APV blocked about half of the peak amplitude and inhibited the slow component revealed by the gabazine/strychnine application.

5.3. Concluding remarks

We demonstrated here that the mixed inhibitory neurons of the nuclei are at the origin of the non-mossy inhibitory nucleo-cortical feedback pathway. The inhibitory nucleo-cortical fibers end in the granular layer of the cerebellar cortex, where they contact the Golgi cells dendrites. The mixed nature of these nucleo-cortical neurons at their cortical synapses onto Golgi cells was confirmed by

immunohistochemical and electrophysiological data. Therefore, we propose that the mixed inhibitory neurons of the cerebellar nuclei represent a distinct cell type, which provide mixed GABA/glycine inhibition through collateral arborization within the nuclei and through axonal projection to the cerebellar cortex. Functional implications of such findings will be discussed later.

Overall, we provide the first evidence for functional inhibitory nucleo-cortical transmission to the granular layer of the cerebellar cortex.

A growing body of evidence indicates that, in addition to the principal neurons, the two inhibitory cell types of the cerebellar nuclei are key elements of the cerebellar nuclei network. The description of their synaptic inputs needs to be continued to complete the knowledge of the cerebellar circuitry. Here, we demonstrated that the inhibitory neurons of the cerebellar nuclei receive GABAergic inhibitory inputs from the Purkinje cell terminals, which are found in apposition with $\gamma 2$ - and $\alpha 1$ -containing GABA_A receptors clusters. Those findings suggest that the glycinergic neuronal population may be an intrinsic part of the olivo-cortico-nuclear modular organization. Our immunohistochemical data suggest in addition that inhibitory neurons also receive excitatory inputs from varicosities expressing VGLUT2 or VGLUT1, although it was not possible to determine the origin of these inputs.

DISCUSSION

DISCUSSION

For a long time, the glutamatergic principal neurons have been thought to be the main cell type of the cerebellar nuclei, in number and in the key functional role they bear in the synaptic processing of the cerebellar nuclei. However, a growing body of evidence indicates that other neuronal population may also play an important role in the nuclear circuitry. For example, it is now well-accepted that the nucleo-olivary neurons are an integral part of the olivo-cerebellar modules and that they are involved in the fine retro-control of the Purkinje cell activity (Chen et al., 2010; Chaumont et al., 2013; Witter et al., 2013) and in supervised learning during plasticity processes (Rasmussen and Hesslow, 2014). In addition to the principal cells and the nucleo-olivary neurons, the cerebellar nuclei include a population of inhibitory glycinergic neurons whose properties were poorly understood.

Presence of functional glycinergic transmission in the cerebellar nuclei

Although the presence of glycinergic neurons and the expression of glycine receptors in the cerebellar nuclei were already reported, two studies only were able to show presence of glycinergic strychnine-sensitive currents in the principal neurons, using pharmacological and ionic stimulations of the presynaptic terminals.

In this thesis, we confirmed the presence of functional glycinergic transmission in the principal neurons of the cerebellar nuclei. A population of inhibitory neurons, co-releasing GABA and glycine, provide synaptic inputs to the glutamatergic neurons of the cerebellar nuclei and specific optogenetic stimulations of this population elicited inhibitory currents in the principal neurons. Those IPSCs were inhibited by both glycine receptors and GABA_A receptors antagonists, confirming the presence of mixed transmission in the cerebellar nuclei.

In previous studies, even with heavy non-selective stimulations, the detection rate of glycinergic synaptic currents was very low. Several experimental biases could explain why previous studies failed to demonstrate the existence of glycinergic currents. First, the low rate of detection may reflect the large predominance of GABAergic synapses over the glycinergic inputs. The GABAergic Purkinje cells are providing the large majority of principal neuron inputs (De Zeeuw and Berrebi, 1995a). We estimated that the glycinergic synapses represent about 4% of the total number of the inhibitory receptors clusters found on principal neurons. Moreover, we showed that inhibitory neurons are actually responsible for mixed GABA/glycine transmission rather than pure glycinergic currents. Therefore, the proportion of glycinergic component of the intra-nuclear inhibition is even lower than expected according to the initial idea that glycinergic interneurons provide pure glycinergic transmission. Secondly, GABA_A receptors antagonists, such as bicuculline (Yakushiji et al., 1987) or gabazine (Hamann et al., 1988), were used to isolate the glycinergic currents and were found to block virtually all the inhibitory responses (Mouginot and Gahwiler, 1995; Anchisi et al., 2001; Telgkamp and Raman, 2002; Pedroarena and Schwarz, 2003; Uusisaari and Knopfel, 2008), leading the authors to consider glycinergic transmission as non-existing in the cerebellar nuclei. However, glycine receptors are also inhibited by GABA_A receptors antagonists at high concentrations (Wang and Slaughter, 2005; Beato et al., 2007) and therefore glycinergic transmission could have been masked by non-specific inhibition from the GABA_A receptors antagonists. On

the other hand, glycine receptors antagonists such as strychnine or picrotoxin are also known to inhibit GABA_A receptors (Yakushiji et al., 1987; Jonas et al., 1998), possibly leading to an overestimation of the glycinergic component of the response. Here, we used lower concentrations of antagonists to reduce the cross-talk with GABA_A and glycine receptors. To assess the exact percentage of glycinergic and GABAergic component of the inhibitory responses, we used a two-step strategy by applying successively gabazine and strychnine, or inversely. The attention paid to the cross-inhibition with GABA_A and glycine receptors antagonists led us to estimate that about 14% of the inhibitory responses recorded at the inhibitory neurons to principal cells synapses were due to glycine receptors activation. This low percentage of glycine receptor involvement in inhibitory transmission may be indeed easily blocked by saturating concentration of GABA_A antagonists (for example: 10 μ M bicuculline blocked 20% of glycinergic currents (Protti et al., 1997) and 20 μ M of gabazine reduced 30% of glycinergic currents (Wang and Slaughter, 2005; Beato et al., 2007)). Use of more selective blockers for each inhibitory receptor may provide a better quantification of the two components (for example, ginkgolide B was shown to inhibit glycine receptors but not GABA_A receptors (Kondratskaya et al., 2005; Betz and Laube, 2006)). Finally, the delayed developmental maturation of glycinergic transmission in the cerebellar nuclei may have precluded earlier identification, as most of the experiments on the cerebellar nuclei physiology were done on animals younger than one month (Morishita and Sastry, 1995; Mougnot and Gahwiler, 1995; Telgkamp and Raman, 2002; Gauck and Jaeger, 2003; Pedroarena and Schwarz, 2003; Zhang et al., 2004; Uusisaari et al., 2007; Alvina and Khodakhah, 2008; Uusisaari and Knopfel, 2008; Pedroarena, 2010; Uusisaari and Knopfel, 2010; Person and Raman, 2012a) and therefore may have described immature networks in which glycinergic transmission may not have the same prevalence. In our experiments, we used young adult animals (P30 to P60 for electrophysiology and more than 2-3 months for immunostainings) and show that glycinergic transmission indeed occurs in the mature cerebellar nuclei microcircuit.

As discussed below, the last explanation for the difficulties to characterize glycinergic inputs onto principal neurons in the cerebellar nuclei could be the fact that mixed neurons fire at very low frequency (< 0.1 Hz). Consequently, it is not surprising that the occurrence of spontaneous glycinergic currents was very rare and necessitates the specific stimulation of the presynaptic neurons to depolarize them and allow them to fire.

Mixed GABA/glycine transmission in the cerebellar nuclei

Most of the glycinergic neurons of the cerebellar nuclei were found to co-localize GABA and glycine (Chen and Hillman, 1993; Baurle and Grusser-Cornehls, 1997; Baurle et al., 1997; Sultan et al., 2002; Tanaka and Ezure, 2004). It is actually not surprising that numerous neurons in the cerebellar nuclei were found mixed as they share a common ontogeny with the granular layer interneurons (Golgi cells and Lugaro cells), which are known to colocalize GABA and Glycine (Ottersen et al., 1988; Crook et al., 2006; Simat et al., 2007a). The GABAergic nucleo-olivary neurons are generated before the cerebellar interneurons and are closer to the Purkinje cell lineage (for review, (Elsen et al., 2013)). Indeed, we demonstrated that the inhibitory mixed neurons of the cerebellar nuclei constitute a distinct population from the nucleo-olivary neurons.

To characterize the inhibitory neurons of the cerebellar nuclei, we used transgenic mouse lines under the control of the glycine transporter GlyT2 promoter. GlyT2 is specifically expressed in

neuronal presynaptic terminals and involved in up-taking glycine from the extracellular medium (Zafra et al., 1997) and thus constitute a specific marker for glycinergic varicosities. Co-expression in presynaptic terminals of both GlyT2 and GAD enzymes, responsible for the synthesis of GABA from glutamate molecules (Erlander and Tobin, 1991), confer to the varicosities the ability to accumulate and release both GABA and glycine (Apostolides and Trussell, 2013). Indeed, axonal varicosities of the inhibitory neurons in the cerebellar nuclei were co-labelled for GlyT2 and GAD65-67, confirming their mixed GABAergic/glycinergic phenotype.

To specifically stimulate the mixed inhibitory neurons, we used the GlyT2-Cre transgenic mouse, in which GlyT2-expressing neurons also express the Cre-recombinase protein. Infection of the cerebellar nuclei with AAV-ChR2-YFP followed by GlyT2 immunostainings revealed that about 40 % of GlyT2-positive elements at best are co-labelled for YFP, indicating that only a part of the inhibitory neurons are actually stimulated during our optogenetical stimulations. The same rate of mis-labelling was found in the GlyT2-eGFP mouse.

In molecular layer interneurons, the GlyT2 promoter is expressed during cellular migration and its expression gradually decreases when interneurons stop their migration, while GAD67 expression is increasing (Simat et al., 2007b). Those results indicate that development of a GABAergic phenotype may lead to the disappearance of the GlyT2-eGFP expression at adult stages. This raises the possibility that the population of inhibitory neurons is actually composed of a gradient of mixed phenotypes, ranging from purely glycinergic neurons strongly labelled for GFP in GlyT2-eGFP mouse to purely GABAergic neurons not stained in the GlyT2-eGFP mouse.

This is in agreement with the fact that pure glycinergic and pure GABAergic cells were found in the cerebellar nuclei, in addition to mixed inhibitory neurons (Chen and Hillman, 1993). However, among all the evoked IPSCs recorded after specific stimulation of inhibitory neurons, we were not able to detect any gradient in the respective percentages of glycinergic and GABAergic components. Moreover, in Chen and Hillman's study, pure GABAergic neurons are most likely to represent nucleo-olivary neuron, while pure glycinergic cells may be glial cells which are known to accumulate glycine in their somata through the glycine transporter 1 (GlyT1, (Eulenburg et al., 2005)).

Similar viral infections and optogenetical stimulations in GAD-Cre mouse may provide clues for the identification of the heterogeneity of inhibitory neurons of the cerebellar nuclei. Further investigations of the inhibitory neuronal population diversity are necessary to conclude on this important question.

The axonal varicosities of the inhibitory neurons are in apposition to inhibitory receptors clusters containing functional glycine and GABA_A receptors. Immunohistochemical experiments demonstrated that those clusters were enriched in glycine receptors, notably the $\alpha 1$ subunit (see Results) (Malosio et al., 1991) most likely associated with the β subunit which is expressed in the CN (Weltzien et al., 2012) and is responsible for the clustering of glycine receptors at synapses (Kneussel and Betz, 2000). Those clusters were virtually devoid of the $\alpha 1$ and $\gamma 2$ GABA_A receptors subunits, which are the most abundant subunits in the cerebellar nuclei (Persohn et al., 1992; Gambarana et al., 1993). As the presence of functional GABA_A receptors was demonstrated by electrophysiological experiments, it is likely that other GABA_A receptors subunits, such as $\alpha 5$ or $\gamma 1$, (Pirker et al., 2000; Hortnagl et al., 2013) are involved at inhibitory neurons synapses onto principal cells.

Surprisingly, immunoreactivity for glycine receptors was found in GABA_A receptors clusters at the synapse with Purkinje cells onto principal neurons. However, Purkinje cells are not known to co-release glycine (Tanaka and Ezure, 2004) and the percentage of IPSC amplitude due to glycine receptor activation is low (less than 3%). We proposed that glycine receptors do not play a predominant role in the cortico-nuclear inhibition, but rather play a more ancillary role if they are entrapped during development of the synaptic clusters (Dumoulin et al., 2000; Garin and Escher, 2001). Indeed, glycine and GABA_A receptors are both expressed by the principal neurons and can bind to the same post-synaptic protein, gephyrin (Meyer et al., 1995; Sassoe-Pognetto and Fritschy, 2000).

It is interesting to note that in Gly2-Cre x R26-mTmT mice breeding, we noticed the presence of some Purkinje cells stained for the Tomato protein. Transient expression of GlyT2 promoter was shown in the nucleo-olivary neurons (see Results, *Chapter 1*) and in molecular layer interneurons (Simat et al., 2007b), suggesting that it may also occur in others cerebellar cell types such as subpopulation of Purkinje cell during the development. Glycine receptors may have an important role during the development of the cerebellar nuclei, as they were shown to participate to neuronal network maturation in other structures (Avila et al., 2013). Following this idea, glycine receptors would have been clustered at the Purkinje cell synapses releasing transiently glycine during the development, and remains entrapped in the GABAergic clusters at adult stages, without functional involvement. Detailed time-course of the development of inhibitory and mixed transmission in the cerebellar nuclei may provide great insights on this question.

In all the known case of mixed transmission, it was reported different kinetics of GABAergic and glycinergic components where the glycine receptor-mediated currents were usually faster than the GABAergic component. At the inhibitory neurons to principal cells synapses, the isolated glycinergic component of the IPSCs did not decay with a time constant significantly different from that of the original IPSC. Moreover, the decay of the IPSCs at GABAergic Purkinje cell synapses and at mixed inhibitory neuron synapses were similar. This indicates that despite the use of different neurotransmitters, the kinetic properties of the two synaptic currents are not different. This is a puzzling observation with respect to the large body of literature on mixed transmission and which will require further molecular investigation.

As a consequence, the principal neurons which were always thought to receive inhibition only from Purkinje cells, are in fact integrating two types of inhibitory inputs which have distinct molecular composition. A differential distribution of receptor subtypes or subunits at distinct junctions within the same cell has been reported previously for glutamate receptors (Dodt et al., 1998; Toth and McBain, 1998). In the cerebellar cortex, Golgi cell interneurons also present two types of inhibitory receptor clusters, both pure-GABAergic and mixed GABAergic/glycinergic, whose presynaptic inputs is coming from two different cell types (Dumoulin et al., 2001). In all cases, kinetic properties of the two inputs are significantly different and therefore modulate differentially the net activity of the post-synaptic neuron. At the principal neurons synapses, the two types of events recorded at the two synaptic junctions were not different regarding their kinetics properties, therefore it would be interesting to look for other synaptic properties which could differentiate those two inputs. Notably, the firing pattern of the two presynaptic neurons may play a role in the net inhibition perceived by the principal neurons. Physiology of inhibitory neurons needs to be further investigated to lead to a detailed representation of the intra-nuclear inhibitory networks.

Nucleo-cortical glycinergic projecting neurons: a third cell type?

A glycinergic nucleo-cortical pathway was previously described in the GlyT2-eGFP mouse (Uusisaari and Knopfel, 2010). Two populations of GFP-expressing neurons were described: a population of neurons spontaneously spiking around 10 Hz which were classified as interneurons by the authors, and a population of projecting neurons with local collaterals seen inactive in acute slices but able to generate high-frequency burst of spike after depolarizing steps.

In our experiments, the mixed inhibitory neurons of the cerebellar nuclei were characterized both in the GlyT2-eGFP and GlyT2-Cre mice, predicting that we would find the same dichotomy the glycinergic neuronal population. However, we never found any GlyT2-eGFP + or GlyT2-Cre x AAV-Chr2-YFP neurons spontaneously firing in acute slices (data not shown, and see Results, Chapter 4). All recorded neurons were silent in slices but can nevertheless burst at high-frequency when they are depolarized (by optogenetic stimulations). The fact that mixed inhibitory neurons are not spontaneously firing is a peculiar feature of this nuclear cell type and strongly suggest that both populations of mixed inhibitory neurons and glycinergic nucleo-cortical neurons described by Uusisaari and Knopfel may actually constitute a single third cell type in the cerebellar nuclei. Those inhibitory neurons would have local axonal collaterals (as shown by our data and by Uusisaari and Knopfel, 2010) which provide mixed inhibition within the cerebellar nuclei and an axonal to the granular layer of the cortex which may be involved in intra-cerebellar feedback loops.

The second population of active GlyT2-eGFP neurons described by Uusisaari and colleagues were characterized in young mice (P20-28). We have seen that the population of nucleo-olivary neurons were expressing GFP during the development, by numbering the GFP+ cells in the GlyT2-Cre x Rosa-mTmT mice, and that this faint GFP expression were found in the neurons even at adult stages in the GlyT2-eGFP mouse (see Results, Chapter 4). This raises the possibility that in young animals, some of GFP-expressing neurons recorded by Uusisaari and colleagues were actually not belonging to the population of mixed inhibitory neurons but rather to the nucleo-olivary neurons. Once again, the precise time course of GlyT2-eGFP expression in the inhibitory neurons of the cerebellar nuclei may provide important highlights on the heterogeneity of inhibitory neurons subpopulations described in early studies.

Taking into account those considerations, we described the cortical projections of GFP-expressing neurons both in the GlyT2-eGFP mouse and the GlyT2-Cre mouse injected in the cerebellar nuclei with AAV-CHR2-YFP. Those nucleo-cortical fibers terminate in the granular layer of the cerebellar cortex, where they contact specifically Golgi cells.

The Golgi cells represent a neuronal population with a large heterogeneity of molecular expression. Three populations can be distinguished with respect to their neurotransmitter contents: glycinergic-only, GABAergic-only and mixed GABA/glycine Golgi cells. Moreover, glycinergic Golgi cells express the metabotropic glutamate receptors mGluR2 while the Golgi neurons which express GABA (pure GABAergic and mixed GABA/glycine) are all labeled for neurogranin (see *Figure 6.1.*). This heterogeneity may reflect the diversity of function of various Golgi cell subtypes. We showed that nucleo-cortical GlyT2-expressing fibers seem to preferentially target the pure GABAergic and pure glycinergic Golgi cells rather than mixed GABA/glycine phenotypes. Further immunohistochemical explorations need to be done to confirm the preferential innervation of glycinergic nucleo-cortical fibers onto different subtypes of Golgi cells.

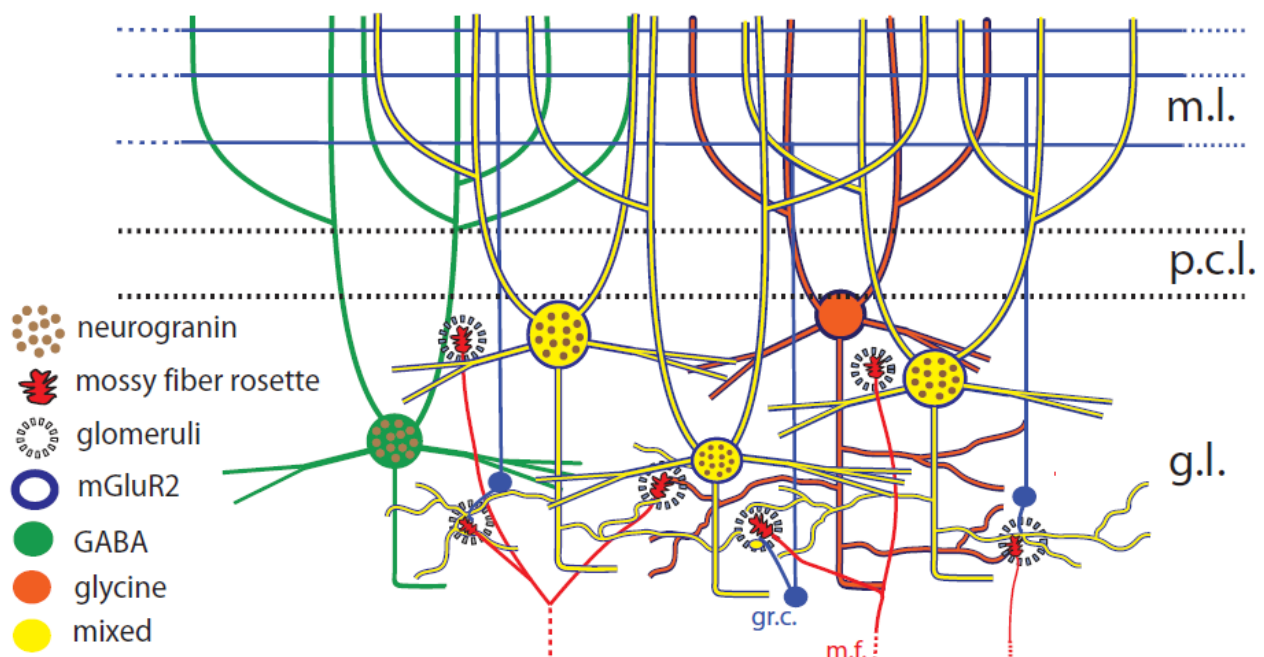


Figure 6.1.: Golgi cells heterogeneity. Different subtypes of Golgi cell found in the cerebellar cortex are depicted here with several molecular markers. Abbreviations: m.l. molecular layer, p.c.l. purkinje cell layer, g.l. granular layer, gr.c. granule cells, m.f. mossy fiber. (Adapted from Pietrajtis and Dieudonné, 2012.)

Electrophysiological and immunohistochemical experiments demonstrated that nucleo-cortical neurons are co-releasing GABA and glycine. This mixed GABA/glycine phenotype is in agreement with the hypothesis that the mixed inhibitory neurons in the cerebellar nuclei involved in local mixed inhibition also send an axonal projection to the cortex. Golgi neurons are expressing glycine receptors and mixed IPSCs were recorded in whole-cell configuration (Dumoulin et al., 2001). It was shown in the same studies that this mixed transmission is provided by Lugaro cells of the cerebellar cortex. Together with our recent findings, one should consider that it exist a second type of mixed inputs in the granular layer in addition to the Lugaro cells synapses. The important question which remains to be solved is whether these two mixed inputs contact the same type of Golgi cells.

Role and connectivity of the mixed inhibitory neurons of the cerebellar nuclei within the olivo-cerebellar modules

Cortico-nuclear projections are topographically organized in longitudinal modules and circumscribed clusters of Purkinje cells inhibited a small area of the cerebellar nuclei. The spatial organization of the Purkinje cell inputs onto mixed inhibitory neurons of the cerebellar nuclei is not known but would constitute critical information to understand the functional role of the mixed inhibitory neurons within the olivo-cerebellar modules.

Several studies suggest that the nucleo-cortical loops are closed and could be involved in the modular organization of the olivo-cerebellar system (Buisseret-Delmas and Angaut, 1989; Trott et al., 1998a, b). In reciprocal loops, Purkinje cells overlying the area of granular layer innervated by

the nucleo-cortical fibers will project back to the same circumscribed region of the cerebellar nuclei. While morphological evidence (De Zeeuw and Berrebi, 1995a; Uusisaari and Knopfel, 2008) suggested that Purkinje cells contact mixed inhibitory neurons of the cerebellar nuclei, no functional demonstration was provided to date. Combining immunohistochemical and electrophysiological experiments, we showed that inhibitory neurons receive GABAergic inhibitory inputs from Purkinje cells terminals, which are found in apposition with $\gamma 2$ - and $\alpha 1$ - containing GABA_A receptors clusters. The subunits composition of the clusters found at the Purkinje cell synapse onto the principal neurons is the same as that onto the mixed inhibitory neurons, as well as the kinetics properties of the events. This suggests that both principal and mixed inhibitory neurons of the cerebellar nuclei receive similar inputs from Purkinje cells. It is possible that a single Purkinje cell axon can innervate both principal and inhibitory neurons, as it was shown for nucleo-olivary neurons (Teune et al., 1998).

Several configurations of intra- and inter-modules connectivity of the mixed inhibitory neurons are possible, but none of them have been investigated for now. First, the mixed inhibitory neurons may contact principal neurons belonging to their olivo-cerebellar modules (see *Figure 6.2., (1)*) or to the neighboring modules (see *Figure 6.2., (2)*). Preliminary morphological data suggest however that the nuclear axonal projection is quite local, and may contact principal neurons located at a close distance from the mixed inhibitory neuron cell body. In the same manner, they can innervate Golgi cells in the granular layer located in the same or in a different cerebellar module (see *Figure 6.2., (3) – (4)* respectively). Secondly, it is possible that inhibitory neurons receive preferentially projections from the Purkinje cells innervating the principal neurons of the same area of the cerebellar nuclei (see *Figure 6.2., (5)*) or receive cortico-nuclear projection from neighboring longitudinal bands (see *Figure 6.2., (6)*).

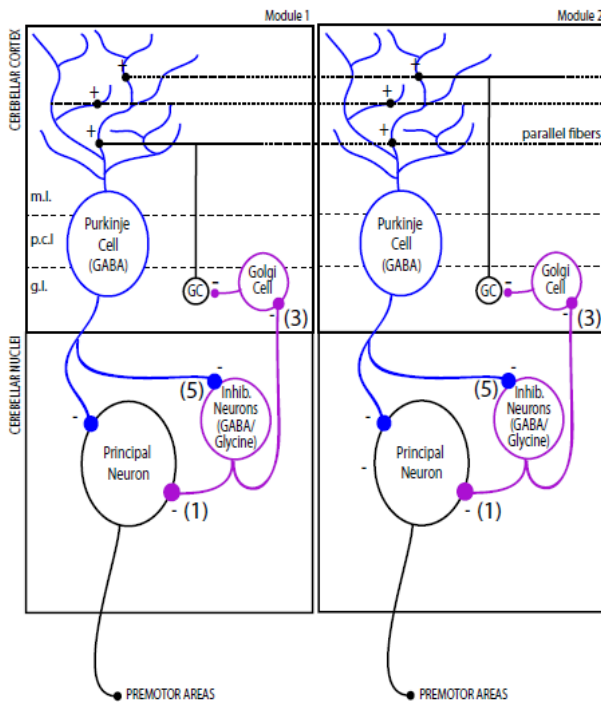
The closed inhibitory nucleo-cortical loop may be directly involved in the feedback control of the Purkinje cell activity, in the same manner as Purkinje cell inputs onto the nucleo-olivary neurons elicit feedback control loops to directly modulate their own excitability (Chaumont et al., 2013). On the other hand, the non-reciprocal connections between modules may be particularly important to link different cerebellar areas which receive different sensory-motor information. Such cellular organization to associate the olivo-cerebellar modules only exist at the level of parallel fibers inputs in the molecular layer of the cortex, thereby interactions at the nuclear level may provide an additional degree of modulation of the neuronal activity and timing across modules.

The connectivity of the inhibitory neurons within and across the modular organization of the cerebellum remains to be demonstrated to elucidate the putative functional role of those inhibitory neurons.

Excitatory inputs onto mixed inhibitory neurons of the cerebellar nuclei and their putative role in the cerebellar physiology

As previously mentioned, the mixed inhibitory neurons of the cerebellar nuclei are not spontaneously firing in acute slices. Therefore, characterization of their excitatory inputs, coming from mossy fibers, climbing fibers or both, is crucial to understand the driving force of their spiking activity and their putative role in the cerebellar physiology. Some authors suggested that, as they receive

A Intra-module connectivity



B Inter-module connectivity

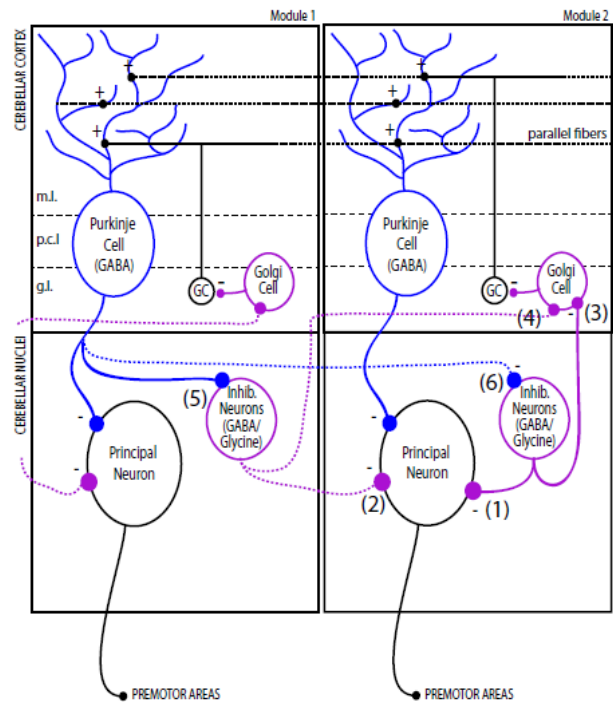


Figure 6.2.: Intra- and inter-modules connectivity of the inhibitory neurons of the cerebellar nuclei. (A) Within a given olivo-cerebellar modules, inhibitory neurons can contact principal neurons (1) and Golgi cells (3) and receive inhibitory inputs from Purkinje cells (5), all belonging to the same module as the inhibitory neuron. (B) Inhibitory neurons connectivity can also span across the modules: inhibitory neurons could contact preferentially principal neurons (2) and/or Golgi cells (4) located in the neighboring modules, while they could be inhibited by Purkinje cells located in a different olivo-cerebellar module (6). Abbreviations: m.l. molecular layer, p.c.l. purkinje cell layer, g.l. granular layer, GC granule cells.

less inhibitory inputs (Angaut and Sotelo, 1973; Chan-Palay, 1973a; De Zeeuw and Berrebi, 1995a; Sultan et al., 2002; Uusisaari and Knopfel, 2008), small neurons may rely to a greater extent on excitatory afferents.

The mixed inhibitory neurons are found contacted by VGLUT2 – positive or VGLUT1/VGLUT2 – positive presynaptic elements, indicating that they also receive excitatory inputs in addition to inhibitory inputs from Purkinje cells. In the cerebellar cortex, climbing fibers are expressing VGLUT2 only, while mossy fibers use VGLUT1, VGLUT2 or a mix of VGLUT1 and VGLUT2 depending on their precerebellar origin (Hioki et al., 2003). Therefore, VGLUT2 - positive varicosities of the cerebellar nuclei could be arising from either climbing fiber or mossy fiber inputs and it could not be told if the mixed inhibitory neurons were preferentially contacted by one or the other afferent systems.

In order to distinguish between the two types of excitatory inputs, climbing and mossy fibers, received by the cerebellar nuclei, we tried to target specifically the climbing fiber system by injecting locally in the inferior olive, using a ventral approach in neonatal pups. Unfortunately, the injection did not allow specific expression in the inferior olive without infecting the neighboring precerebellar

nuclei. Even if climbing fiber inputs could not be discriminated from mossy fiber inputs, we still recorded excitatory inputs in the principal neurons.

EPSPs were elicited by light stimulation of the presynaptic terminals in the cerebellar nuclei and were found mediated by both AMPA and NMDA receptors. Interestingly, it appeared that AMPA receptors are responsible for a major part of the EPSCs we recorded. Even though NMDA receptors may be only partially involved in excitatory transmission, the NMDA currents may be potentiated in some conditions by the glycine (Johnson and Ascher, 1987) released by the mixed inhibitory neurons. Mixed inhibitory neurons of the cerebellar nuclei may be a prominent source of glycine in the synaptic cleft, if excitatory and inhibitory synapses are located at proximity, and may be involved in modulating the long-term plasticity properties of the synapses onto principal neurons (Henneberger et al., 2013). Interactions between excitatory and inhibitory inputs upon the principal neurons remain to be clarified.

Little is known about the functional role of mixed inhibitory nucleo-cortical neurons in the cerebellar physiology. As inhibitory neurons have been shown to evoke hyperpolarizing currents in the principal neurons, they may have a role in the generation of a rebound firing of principal neurons. Indeed, two types of inhibitory inputs have been shown in the principal neurons *in vivo* (Bengtsson et al., 2011; Witter et al., 2013): a barrage of low-amplitude and high frequency synaptic events reflecting the spontaneous firing of presynaptic Purkinje cells (Bengtsson et al., 2011; Person and Raman, 2012a), and giant low-frequency IPSPs. Those giant IPSPs have been proposed to result from the massive inhibitory inputs following the synchronization of Purkinje cells by climbing fibers inputs (Hoebeek et al., 2010; Bengtsson et al., 2011; Person and Raman, 2012a; Witter et al., 2013; Bengtsson and Jorntell, 2014). However, direct synchronization of Purkinje cells by stimulation of the cerebellar cortex did not always produce a robust rebound firing of principal neurons (Hoebeek et al., 2010; Person and Raman, 2012a). This suggests that inhibition provided by the synchronous activity of several inhibitory neurons in the cerebellar nuclei may also be responsible for efficient hyperpolarization to evoke rebound firing in the principal neurons. Characterization of the inputs and understanding of the driving force of these inhibitory neurons will provide important source of knowledge for their putative role in the cerebellar nuclei physiology.

We used to have a vision of the cerebellar nuclei as composed mainly by the principal neurons, which are integrating information from two non-equivalent excitatory inputs (climbing fibers and mossy fibers) and a massive inhibitory input from the Purkinje cells. During the last decades, several feedback loops implying other cell types of the cerebellar nuclei have been described to modulate the principal neuron activity: closed loop with the inferior olive via the nucleo-olivary neurons, local intra-nuclear inhibition from the mixed inhibitory neurons and feedback control of the Purkinje cell discharge by the nucleo-cortical projections.

From now on, we should consider the cerebellar nuclei as composed of three types of different cells (glutamatergic principal neurons, nucleo-cortical mixed neurons with local collaterals and nucleo-olivary cells), numerically and functionally equivalents and receiving all inhibitory inputs from the Purkinje cells.

Therefore, the real *modus operandi* of the cerebello-olivary complex may be provided by the simultaneous control of the different cerebellar loops by the Purkinje cells, by which it achieves smooth control of movement.

BIBLIOGRAPHY and ANNEXES

BIBLIOGRAPHY

- Aizenman CD, Linden DJ (1999) Regulation of the rebound depolarization and spontaneous firing patterns of deep nuclear neurons in slices of rat cerebellum. *Journal of Neurophysiology* 82:1697-1709.
- Aizenman CD, Manis PB, Linden DJ (1998) Polarity of long-term synaptic gain change is related to postsynaptic spike firing at a cerebellar inhibitory synapse. *Neuron* 21:827-835.
- Aizenman CD, Huang EJ, Linden DJ (2003) Morphological correlates of intrinsic electrical excitability in neurons of the deep cerebellar nuclei. *Journal of Neurophysiology* 89:1738-1747.
- Akazawa C, Shigemoto R, Bessho Y, Nakanishi S, Mizuno N (1994) Differential Expression of 5 N-Methyl-D-Aspartate Receptor Subunit Messenger-Rnas in the Cerebellum of Developing-Rats and Adult-Rats. *Journal of Comparative Neurology* 347:150-160.
- Aksenov DP, Serdyukova NA, Bloedel JR, Bracha V (2005) Glutamate neurotransmission in the cerebellar interposed nuclei: involvement in classically conditioned eyeblinks and neuronal activity. *J Neurophysiol* 93:44-52.
- Albus JA (1971) A theory of Cerebellar Function. *Mathematical Biosciences*, American Elsevier Publishing Company, Inc 10:25-61.
- Allen GI, Gilbert PFC, Yin TCT (1978) Convergence of Cerebral Inputs onto Dentate Neurons in Monkey. *Experimental Brain Research* 32:151-170.
- Allen GI, Gilbert PFC, Marini R, Schultz W, Yin TCT (1977) Integration of Cerebral and Peripheral Inputs by Interpositus Neurons in Monkey. *Experimental Brain Research* 27:81-99.
- Alvina K, Khodakhah K (2008) Selective regulation of spontaneous activity of neurons of the deep cerebellar nuclei by N-type calcium channels in juvenile rats. *J Physiol-London* 586:2523-2538.
- Alvina K, Ellis-Davies G, Khodakhah K (2009) T-Type Calcium Channels Mediate Rebound Firing in Intact Deep Cerebellar Neurons. *Neuroscience* 158:635-641.
- Alvina K, Walter JT, Kohn A, Ellis-Davies G, Khodakhah K (2008) Questioning the role of rebound firing in the cerebellum. *Nature Neuroscience* 11:1256-1258.
- Amatuni A, Tarnecki R, Wrobel A, Rajkowski J (1981) Interaction of Extracerebellar and Cerebellar Cortical Inputs in Dentate Neurons of the Cat. *Acta Neurobiol Exp* 41:373-390.
- Anchisi D, Scelfo B, Tempia F (2001) Postsynaptic currents in deep cerebellar nuclei. *Journal of Neurophysiology* 85:323-331.
- Andersson G, Hesslow G (1987) Activity of Purkinje cells and interpositus neurones during and after periods of high frequency climbing fibre activation in the cat. *Exp Brain Res* 67:533-542.
- Andersson G, Garwicz M, Hesslow G (1988) Evidence for a GABA-mediated cerebellar inhibition of the inferior olive in the cat. *Exp Brain Res* 72:450-456.
- Angaut P, Sotelo C (1973) Fine-Structure of Cerebellar Central Nuclei in Cat .2. Synaptic Organization. *Experimental Brain Research* 16:431-454.
- Angaut P, Sotelo C (1987) The dentato-olivary projection in the rat as a presumptive GABAergic link in the olivocerebello-olivary loop. An ultrastructural study. *Neurosci Lett* 83:227-231.
- Angaut P, Sotelo C (1989) Synaptology of the cerebello-olivary pathway. Double labelling with anterograde axonal tracing and GABA immunocytochemistry in the rat. *Brain Res* 479:361-365.
- Angaut P, Cicirata F, Serapide F (1985) Topographic Organization of the Cerebello-Thalamic Projections in the Rat - an Autoradiographic Study. *Neuroscience* 15:389-401.
- Angaut P, Compoint C, BuisseretDelmas C, Batini C (1996) Synaptic connections of Purkinje cell axons with nucleocortical neurones in the cerebellar medial nucleus of the rat. *Neuroscience Research* 26:345-348.
- Apostolides PF, Trussell LO (2013) Rapid, activity-independent turnover of vesicular transmitter content at a mixed glycine/GABA synapse. *J Neurosci* 33:4768-4781.
- Apps R, Garwicz M (2005) Anatomical and physiological foundations of cerebellar information processing. *Nature Reviews Neuroscience* 6:297-311.
- Apps R, Hawkes R (2009) Cerebellar cortical organization: a one-map hypothesis. *Nat Rev Neurosci* 10:670-681.
- Arenz A, Bracey EF, Margrie TW (2009) Sensory representations in cerebellar granule cells. *Curr Opin Neurobiol* 19:445-451.
- Arenz A, Silver RA, Schaefer AT, Margrie TW (2008) The contribution of single synapses to sensory representation in vivo. *Science* 321:977-980.

- Armstrong DM, Rawson JA (1979a) Activity patterns of cerebellar cortical neurones and climbing fibre afferents in the awake cat. *J Physiol* 289:425-448.
- Armstrong DM, Rawson JA (1979b) Responses of Neurons in Nucleus Interpositus of the Cerebellum to Cutaneous Nerve Volleys in the Awake Cat. *J Physiol-London* 289:403-423.
- Armstrong DM, Edgley SA (1984) Discharges of Nucleus Interpositus Neurons during Locomotion in the Cat. *J Physiol-London* 351:411-432.
- Armstrong DM, Harvey RJ, Schild RF (1973a) Cerebello-cerebellar responses mediated via climbing fibres. *Exp Brain Res* 18:19-39.
- Armstrong DM, Harvey RJ, Schild RF (1973b) The spatial organisation of climbing fibre branching in the cat cerebellum. *Exp Brain Res* 18:40-58.
- Armstrong DM, Cogdell B, Harvey R (1975) Effects of afferent volleys from the limbs on the discharge patterns of interpositus neurones in cats anaesthetized with alpha-chloralose. *J Physiol* 248:489-517.
- Asanuma C, Thach WT, Jones EG (1980) Nucleus Interpositus Projection to Spinal Interneurons in Monkeys. *Brain Research* 191:245-248.
- Asanuma C, Thach WT, Jones EG (1983) Anatomical Evidence for Segregated Focal Groupings of Efferent Cells and Their Terminal Ramifications in the Cerebello-Thalamic Pathway of the Monkey. *Brain Res Rev* 5:267-269.
- Audinat E, Knopfel T, Gahwiler BH (1990) Responses to Excitatory Amino-Acids of Purkinje-Cells and Neurons of the Deep Nuclei in Cerebellar Slice Cultures. *J Physiol-London* 430:297-313.
- Audinat E, Gahwiler BH, Knopfel T (1992) Excitatory synaptic potentials in neurons of the deep nuclei in olivo-cerebellar slice cultures. *Neuroscience* 49:903-911.
- Avila A, Nguyen L, Rigo JM (2013) Glycine receptors and brain development. *Front Cell Neurosci* 7:184.
- Bagnall MW, Zingg B, Sakatos A, Moghadam SH, Zeilhofer HU, du Lac S (2009) Glycinergic Projection Neurons of the Cerebellum. *Journal of Neuroscience* 29:10104-10110.
- Balakrishnan V, Trussell LO (2008) Synaptic inputs to granule cells of the dorsal cochlear nucleus. *Journal of Neurophysiology* 99:208-219.
- Banke TG, McBain CJ (2006) GABAergic input onto CA3 hippocampal interneurons remains shunting throughout development. *Journal of Neuroscience* 26:11720-11725.
- Barbour B (1993) Synaptic currents evoked in Purkinje cells by stimulating individual granule cells. *Neuron* 11:759-769.
- Bardin JM, Batini C, Buisseret-Delmas C, Serviere J (1983a) Decrease of [¹⁴C]2-deoxyglucose uptake at the intracerebellar nuclei during cerebellar cortex stimulation. *Brain Res* 272:171-174.
- Bardin JM, Batini C, Billard JM, Buisseret-Delmas C, Conrath-Verrier M, Corvaja N (1983b) Cerebellar output regulation by the climbing and mossy fibers with and without the inferior olive. *J Comp Neurol* 213:464-477.
- Bartos M, Vida I, Frotscher M, Geiger JRP, Jonas P (2001) Rapid signaling at inhibitory synapses in a dentate gyrus interneuron network. *Journal of Neuroscience* 21:2687-2698.
- Batini C, Buisseret-Delmas C, Compoin C, Daniel H (1989) The GABAergic neurones of the cerebellar nuclei in the rat: projections to the cerebellar cortex. *Neurosci Lett* 99:251-256.
- Batini C, Benedetti F, Buisseret-Delmas C, Montarolo PG, Strata P (1984) Metabolic activity of intracerebellar nuclei in the rat: effects of inferior olive inactivation. *Exp Brain Res* 54:259-265.
- Batini C, Compoin C, Buisseretdelmas C, Daniel H, Guegan M (1992) Cerebellar Nuclei and the Nucleocortical Projections in the Rat - Retrograde Tracing Coupled to Gaba and Glutamate Immunohistochemistry. *Journal of Comparative Neurology* 315:74-84.
- Baurle J, GrusserCornehl U (1997) Differential number of glycine- and GABA-immunopositive neurons and terminals in the deep cerebellar nuclei of normal and Purkinje cell degeneration mutant mice. *Journal of Comparative Neurology* 382:443-458.
- Baurle J, Helmchen C, GrusserCornehl U (1997) Diverse effects of Purkinje cell loss on deep cerebellar and vestibular nuclei neurons in Purkinje cell degeneration mutant mice: A possible compensatory mechanism. *Journal of Comparative Neurology* 384:580-596.
- Baurle J, Hoshi M, Grusser-Cornehl U (1998) Dependence of parvalbumin expression on Purkinje cell input in the deep cerebellar nuclei. *Journal of Comparative Neurology* 392:499-514.
- Bazzigaluppi P, Ruigrok T, Saisan P, De Zeeuw CI, de Jeu M (2012) Properties of the nucleo-olivary pathway: an in vivo whole-cell patch clamp study. *PLoS One* 7:e46360.
- Beato M, Burzomato V, Sivilotti LG (2007) The kinetics of inhibition of rat recombinant heteromeric alpha 1 beta glycine receptors by the low-affinity antagonist SR-95531. *J Physiol-London* 580:171-179.

- Becker CM, Hoch W, Betz H (1988) Glycine receptor heterogeneity in rat spinal cord during postnatal development. *Embo J* 7:3717-3726.
- Beitz AJ (1976) The topographical organization of the olivo-dentate and dentato-olivary pathways in the cat. *Brain Res* 115:311-317.
- Beitz AJ, Chan-Palay V (1979a) Golgi Analysis of Neuronal Organization in the Medial Cerebellar Nucleus of the Rat. *Neuroscience* 4:47-63.
- Beitz AJ, Chan-Palay V (1979b) Medial Cerebellar Nucleus in the Rat - Nuclear Volume, Cell Number, Density and Orientation. *Neuroscience* 4:31-45.
- Benedetti F, Montarolo PG, Rabacchi S (1984) Inferior olive lesion induces long-lasting functional modification in the Purkinje cells. *Exp Brain Res* 55:368-371.
- Benedetti F, Montarolo PG, Strata P, Tempia F (1983) Inferior olive inactivation decreases the excitability of the intracerebellar and lateral vestibular nuclei in the rat. *J Physiol* 340:195-208.
- Beneyto M, Meador-Woodruff JH (2004) Expression of transcripts encoding AMPA receptor subunits and associated postsynaptic proteins in the macaque brain. *Journal of Comparative Neurology* 468:530-554.
- Bengtsson F, Jorntell H (2014) Specific Relationship between Excitatory Inputs and Climbing Fiber Receptive Fields in Deep Cerebellar Nuclear Neurons. *PLoS One* 9.
- Bengtsson F, Svensson P, Hesslow G (2004) Feedback control of Purkinje cell activity by the cerebello-olivary pathway. *Eur J Neurosci* 20:2999-3005.
- Bengtsson F, Ekerot CF, Jorntell H (2011) In vivo analysis of inhibitory synaptic inputs and rebounds in deep cerebellar nuclear neurons. *PLoS One* 6:e18822.
- Best AR, Regehr WG (2009) Inhibitory regulation of electrically coupled neurons in the inferior olive is mediated by asynchronous release of GABA. *Neuron* 62:555-565.
- Betz H, Laube B (2006) Glycine receptors: recent insights into their structural organization and functional diversity. *Journal of Neurochemistry* 97:1600-1610.
- Bidoret C, Ayon A, Barbour B, Casado M (2009) Presynaptic NR2A-containing NMDA receptors implement a high-pass filter synaptic plasticity rule. *Proc Natl Acad Sci U S A* 106:14126-14131.
- Blenkinsop TA, Lang EJ (2011) Synaptic action of the olivocerebellar system on cerebellar nuclear spike activity. *J Neurosci* 31:14708-14720.
- Boehme R, Uebele VN, Renger JJ, Pedroarena C (2011) Rebound excitation triggered by synaptic inhibition in cerebellar nuclear neurons is suppressed by selective T-type calcium channel block. *Journal of Neurophysiology* 106:2653-2661.
- Bolte S, Cordelieres FP (2006) A guided tour into subcellular colocalization analysis in light microscopy. *J Microsc-Oxford* 224:213-232.
- Bosman LW, Konnerth A (2009) Activity-dependent plasticity of developing climbing fiber-Purkinje cell synapses. *Neuroscience* 162:612-623.
- Brochu G, Maler L, Hawkes R (1990) Zebrin II: a polypeptide antigen expressed selectively by Purkinje cells reveals compartments in rat and fish cerebellum. *J Comp Neurol* 291:538-552.
- Brodal A (1976) The olivocerebellar projection in the cat as studied with the method of retrograde axonal transport of horseradish peroxidase. II. The projection to the uvula. *J Comp Neurol* 166:417-426.
- Brodal A, Courville J (1973) Cerebellar corticonuclear projection in the cat. Crus II. An experimental study with silver methods. *Brain Res* 50:1-23.
- Brodal A, Walberg F, Hoddevik GH (1975) The olivocerebellar projection in the cat studied with the method of retrograde axonal transport of horseradish peroxidase. *J Comp Neurol* 164:449-469.
- Brodal P, Dietrichs E, Walberg F (1986) Do pontocerebellar mossy fibres give off collaterals to the cerebellar nuclei? An experimental study in the cat with implantation of crystalline HRP-WGA. *Neurosci Res* 4:12-24.
- Brown IE, Bower JM (2001) Congruence of mossy fiber and climbing fiber tactile projections in the lateral hemispheres of the rat cerebellum. *J Comp Neurol* 429:59-70.
- Brown JT, Chan-Palay V, Palay SL (1977) A study of afferent input to the inferior olivary complex in the rat by retrograde axonal transport of horseradish peroxidase. *J Comp Neurol* 176:1-22.
- Brunner C (1919) Die zentralen Kleinhirnerkerne bei den Säugetieren. *Arb Neur H Inst Wien* 22:200-277.
- Buisseret-Delmas C (1988) Sagittal organization of the olivocerebellonuclear pathway in the rat. I. Connections with the nucleus fastigii and the nucleus vestibularis lateralis. *Neurosci Res* 5:475-493.
- Buisseret-Delmas C, Batini C (1978) Topology of the pathways to the inferior olive as ? study in cat. *Neurosci Lett*

10:207-214.

- Buisseret-Delmas C, Angaut P (1989) Anatomical mapping of the cerebellar nucleocortical projections in the rat: a retrograde labeling study. *J Comp Neurol* 288:297-310.
- Buisseret-Delmas C, Angaut P (1993) The cerebellar olivo-corticonuclear connections in the rat. *Prog Neurobiol* 40:63-87.
- Cain SM, Snutch TP (2010) Contributions of T-type calcium channel isoforms to neuronal firing. *Channels (Austin)* 4:475-482.
- Carpenter MB, Bard DS, Alling FA (1959) Anatomical Connections between the Fastigial Nuclei, the Labyrinth and the Vestibular Nuclei in the Cat. *Journal of Comparative Neurology* 111:1-25.
- Cerminara NL, Apps R (2011) Behavioural significance of cerebellar modules. *Cerebellum* 10:484-494.
- Cerminara NL, Aoki H, Loft M, Sugihara I, Apps R (2013) Structural basis of cerebellar microcircuits in the rat. *J Neurosci* 33:16427-16442.
- Chadderton P, Margrie TW, Hausser M (2004) Integration of quanta in cerebellar granule cells during sensory processing. *Nature* 428:856-860.
- Chambers WW, Sprague JM (1955) Functional localization in the cerebellum. I. Organization in longitudinal cortico-nuclear zones and their contribution to the control of posture, both extrapyramidal and pyramidal. *J Comp Neurol* 103:105-129.
- Chan-Palay V (1973a) Axon Terminals of Intrinsic Neurons in Nucleus Lateralis of Cerebellum - Electron-Microscope Study. *Z Anat Entwicklungs* 142:187-206.
- Chan-Palay V (1973b) Axon terminals of the intrinsic neurons in the nucleus lateralis of the cerebellum. An electron microscope study. *Z Anat Entwicklungsgesch* 142:187-206.
- Chan-Palay V (1973c) Neuronal circuitry in the nucleus lateralis of the cerebellum. *Z Anat Entwicklungsgesch* 142:259-265.
- Chan-Palay V (1973d) Light Microscope Study of Cytology and Organization of Neurons in Simple Mammalian Nucleus Lateralis - Columns and Swirls. *Z Anat Entwicklungs* 141:125-150.
- Chan-Palay V, Palay SL, Wu JY (1979) Gamma-Aminobutyric Acid Pathways in the Cerebellum Studied by Retrograde and Anterograde Transport of Glutamic-Acid Decarboxylase Antibody after In vivo Injections. *Anat Embryol* 157:1-14.
- Chan-Palay V, Palay SL, Brown JT, Van Itallie C (1977) Sagittal organization of olivocerebellar and reticulocerebellar projections: autoradiographic studies with ³⁵S-methionine. *Exp Brain Res* 30:561-576.
- Chaumont J, Guyon N, Valera AM, Dugue GP, Popa D, Marcaggi P, Gautheron V, Reibel-Foisset S, Dieudonne S, Stephan A, Barrot M, Cassel JC, Dupont JL, Doussau F, Poulain B, Selimi F, Lena C, Isope P (2013) Clusters of cerebellar Purkinje cells control their afferent climbing fiber discharge. *Proc Natl Acad Sci U S A* 110:16223-16228.
- Chen S, Hillman DE (1993) Colocalization of Neurotransmitters in the Deep Cerebellar Nuclei. *J Neurocytol* 22:81-91.
- Chen X, Kovalchuk Y, Adelsberger H, Henning HA, Sausbier M, Wietzorrek G, Ruth P, Yarom Y, Konnerth A (2010) Disruption of the olivo-cerebellar circuit by Purkinje neuron-specific ablation of BK channels. *Proc Natl Acad Sci U S A* 107:12323-12328.
- Chery N, De Koninck Y (1999) Junctional versus extrajunctional glycine and GABA(A) receptor-mediated IPSCs in identified lamina I neurons of the adult rat spinal cord. *Journal of Neuroscience* 19:7342-7355.
- Chung SH, Marzban H, Hawkes R (2009) Compartmentation of the cerebellar nuclei of the mouse. *Neuroscience* 161:123-138.
- Cicirata F, Angaut P, Serapide MF, Panto MR, Nicotra G (1992) Multiple Representation in the Nucleus Lateralis of the Cerebellum - an Electrophysiologic Study in the Rat. *Experimental Brain Research* 89:352-362.
- Cicirata F, Zappala A, Serapide MF, Parenti R, Panto MR, Paz C (2005) Different pontine projections to the two sides of the cerebellum. *Brain Res Rev* 49:280-294.
- Clarke PGH (1977) Some Visual and Other Connections to Cerebellum of Pigeon. *Journal of Comparative Neurology* 174:535-552.
- Cohen D, Yarom Y (1998) Patches of synchronized activity in the cerebellar cortex evoked by mossy-fiber stimulation: questioning the role of parallel fibers. *Proc Natl Acad Sci U S A* 95:15032-15036.
- Colin F, Manil J, Desclin JC (1980) The olivocerebellar system. I. Delayed and slow inhibitory effects: an overlooked salient feature of cerebellar climbing fibers. *Brain Res* 187:3-27.
- Compoint C, Buisseret-Delmas C, Diagne M, Buisseret P, Angaut P (1997) Connections between the cerebellar nucleus

- interpositus and the vestibular nuclei: an anatomical study in the rat. *Neuroscience Letters* 238:91-94.
- Courville J (1975) Distribution of olivocerebellar fibers demonstrated by a radioautographic tracing method. *Brain Res* 95:253-263.
- Courville J, Brodal A (1966) Rubro-Cerebellar Connections in Cat - an Experimental Study with Silver Impregnation Methods. *Journal of Comparative Neurology* 126:471-&.
- Courville J, Diakiw N, Brodal A (1973) Cerebellar corticonuclear projection in the cat. The paramedian lobule. An experimental study with silver methods. *Brain Res* 50:25-45.
- Crepel F, Mariani J, Delhayebouchaud N (1976) Evidence for a Multiple Innervation of Purkinje-Cells by Climbing Fibers in Immature Rat Cerebellum. *J Neurobiol* 7:567-578.
- Crook J, Hendrickson A, Robinson FR (2006) CO-LOCALIZATION of glycine and GABA immunoreactivity in interneurons in Macaca monkey cerebellar cortex. *Neuroscience* 141:1951-1959.
- Cull-Candy SG, Brickley SG, Misra C, Feldmeyer D, Momiyama A, Farrant M (1998) NMDA receptor diversity in the cerebellum: identification of subunits contributing to functional receptors. *Neuropharmacology* 37:1369-1380.
- Czubayko U, Sultan F, Thier P, Schwarz C (2001) Two types of neurons in the rat cerebellar nuclei as distinguished by membrane potentials and intracellular fillings. *Journal of Neurophysiology* 85:2017-2029.
- D'Hulst C, Atack JR, Kooy RF (2009) The complexity of the GABA(A) receptor shapes unique pharmacological profiles. *Drug Discov Today* 14:866-875.
- Danglot L, Rostaing P, Triller A, Bessis A (2004) Morphologically identified glycinergic synapses in the hippocampus. *Mol Cell Neurosci* 27:394-403.
- De Gruijl JR, Bosman LW, De Zeeuw CI, De Jeu MT (2013) Inferior Olive : All Ins and Outs. Handbook of the Cerebellum and Cerebellar Disorders, M Manto, DL Gruol, JD Schmahmann, N Koibuchi, F Rossi (eds), Springer Science+Business Media Dordrecht 2013.
- De Saint Jan D, David-Watine B, Korn H, Bregestovski P (2001) Activation of human alpha1 and alpha2 homomeric glycine receptors by taurine and GABA. *J Physiol* 535:741-755.
- De Schutter E, Steuber V (2009) Patterns and pauses in Purkinje cell simple spike trains: experiments, modeling and theory. *Neuroscience* 162:816-826.
- De Zeeuw CI, Berrebi AS (1995a) Postsynaptic targets of Purkinje cell terminals in the cerebellar and vestibular nuclei of the rat. *Eur J Neurosci* 7:2322-2333.
- De Zeeuw CI, Berrebi AS (1995b) Postsynaptic Targets of Purkinje-Cell Terminals in the Cerebellar and Vestibular Nuclei of the Rat. *European Journal of Neuroscience* 7:2322-2333.
- De Zeeuw CI, Holstege JC, Ruigrok TJ, Voogd J (1989) Ultrastructural study of the GABAergic, cerebellar, and mesodiencephalic innervation of the cat medial accessory olive: anterograde tracing combined with immunocytochemistry. *J Comp Neurol* 284:12-35.
- De Zeeuw CI, Holstege JC, Ruigrok TJ, Voogd J (1990a) Mesodiencephalic and cerebellar terminals terminate upon the same dendritic spines in the glomeruli of the cat and rat inferior olive: an ultrastructural study using a combination of [³H]leucine and wheat germ agglutinin coupled horseradish peroxidase anterograde tracing. *Neuroscience* 34:645-655.
- De Zeeuw CI, Wylie DR, Digiorgi PL, Simpson JI (1994) Projections of Individual Purkinje-Cells of Identified Zones in the Flocculus to the Vestibular and Cerebellar Nuclei in the Rabbit. *Journal of Comparative Neurology* 349:428-447.
- De Zeeuw CI, Van Alphen AM, Hawkins RK, Ruigrok TJ (1997) Climbing fibre collaterals contact neurons in the cerebellar nuclei that provide a GABAergic feedback to the inferior olive. *Neuroscience* 80:981-986.
- De Zeeuw CI, Holstege JC, Calkoen F, Ruigrok TJ, Voogd J (1988) A new combination of WGA-HRP anterograde tracing and GABA immunocytochemistry applied to afferents of the cat inferior olive at the ultrastructural level. *Brain Res* 447:369-375.
- De Zeeuw CI, Ruigrok TJ, Holstege JC, Jansen HG, Voogd J (1990b) Intracellular labeling of neurons in the medial accessory olive of the cat: II. Ultrastructure of dendritic spines and their GABAergic innervation. *J Comp Neurol* 300:478-494.
- De Zeeuw CI, Simpson JI, Hoogenraad CC, Galjart N, Koekkoek SK, Ruigrok TJ (1998) Microcircuitry and function of the inferior olive. *Trends Neurosci* 21:391-400.
- De Zeeuw CI, Hoebeek FE, Bosman LW, Schonewille M, Witter L, Koekkoek SK (2011) Spatiotemporal firing patterns in the cerebellum. *Nat Rev Neurosci* 12:327-344.
- De Zeeuw CI, Chorev E, Devor A, Manor Y, Van der Giessen RS, De Jeu MT, Hoogenraad CC, Bijman J, Ruigrok TJH,

- French P, Jaarsma D, Kistler WM, Meier C, Petrasch-Parwez E, Dermietzel R, Sohl G, Gueldenagel M, Willecke K, Yarom Y (2003) Deformation of network connectivity in the inferior olive of connexin 36-deficient mice is compensated by morphological and electrophysiological changes at the single neuron level. *Journal of Neuroscience* 23:4700-4711.
- Debanne D (2004) Information processing in the axon. *Nat Rev Neurosci* 5:304-316.
- Desclin JC (1974) Histological evidence supporting the inferior olive as the major source of cerebellar climbing fibers in the rat. *Brain Res* 77:365-384.
- Devor A, Yarom Y (2000) GABAergic modulation of olivary oscillations. *Prog Brain Res* 124:213-220.
- Devor A, Yarom Y (2002a) Electrotonic coupling in the inferior olivary nucleus revealed by simultaneous double patch recordings. *J Neurophysiol* 87:3048-3058.
- Devor A, Yarom Y (2002b) Generation and propagation of subthreshold waves in a network of inferior olivary neurons. *J Neurophysiol* 87:3059-3069.
- Devor A, Fritschy JM, Yarom Y (2001) Spatial distribution and subunit composition of GABA(A) receptors in the inferior olivary nucleus. *J Neurophysiol* 85:1686-1696.
- Dietrichs E (1981) The Cerebellar Corticonuclear and Nucleocortical Projections in the Cat as Studied with Anterograde and Retrograde Transport of Horseradish-Peroxidase .4. The Paraflocculus. *Experimental Brain Research* 44:235-242.
- Dietrichs E, Walberg F (1979) The cerebellar corticonuclear and nucleocortical projections in the cat as studied with anterograde and retrograde transport of horseradish peroxidase. I. The paramedian lobule. *Anat Embryol (Berl)* 158:13-39.
- Dietrichs E, Walberg F (1986) The cerebellar nucleo-olivary and olivocerebellar nuclear projections in the cat as studied with anterograde and retrograde transport in the same animal after implantation of crystalline WGA-HRP. III. The interposed nuclei. *Brain Res* 373:373-383.
- Dieudonné D, Diana M (2009) Postsynaptic determinants of inhibitory transmission at mixed GABAergic/glycinergic synapses. R;Gutierrez (ed) *Co-Existence and Co-release of Classical Neurotransmitters*, © Springer Science+Business Media, LLC
- Dieudonné S (1995) Glycinergic Synaptic Currents in Golgi Cells of the Rat Cerebellum. *P Natl Acad Sci USA* 92:1441-1445.
- Doty HU, Frick A, Kampe K, Zieglgansberger W (1998) NMDA and AMPA receptors on neocortical neurons are differentially distributed. *Eur J Neurosci* 10:3351-3357.
- Dufour A, Tell F, Kessler JP, Baude A (2010) Mixed GABA-glycine synapses delineate a specific topography in the nucleus tractus solitarii of adult rat. *J Physiol* 588:1097-1115.
- Dumoulin A, Triller A, Dieudonné S (2001) IPSC kinetics at identified GABAergic and mixed GABAergic and glycinergic synapses onto cerebellar Golgi cells. *Journal of Neuroscience* 21:6045-6057.
- Dumoulin A, Levi S, Riveau B, Gasnier B, Triller A (2000) Formation of mixed glycine and GABAergic synapses in cultured spinal cord neurons. *Eur J Neurosci* 12:3883-3892.
- Dumoulin A, Rostaing P, Bedet C, Levi S, Isambert MF, Henry JP, Triller A, Gasnier B (1999) Presence of the vesicular inhibitory amino acid transporter in GABAergic and glycinergic synaptic terminal boutons. *J Cell Sci* 112:811-823.
- Eager RP (1963) Cortical Association Pathways in the Cerebellum of the Cat. *J Comp Neurol* 121:381-393.
- Eccles JC, Llinas R, Sasaki K (1966) The excitatory synaptic action of climbing fibres on the Purkinje cells of the cerebellum. *J Physiol* 182:268-296.
- Eccles JC, Sabah NH, Taboriko.H (1974a) Excitatory and Inhibitory Responses of Neurons of Cerebellar Fastigial Nucleus. *Experimental Brain Research* 19:61-77.
- Eccles JC, Sabah NH, Taboriko.H (1974b) Pathways Responsible for Excitation and Inhibition of Fastigial Neurons. *Experimental Brain Research* 19:78-99.
- Eccles JC, Sabah NH, Taborikova H (1974c) The pathways responsible for excitation and inhibition of fastigial neurones. *Exp Brain Res* 19:78-99.
- Eccles JC, Sabah NH, Schmidt RF, Taborikova H (1972) Integration by Purkyne cells of mossy and climbing fiber inputs from cutaneous mechanoreceptors. *Exp Brain Res* 15:498-520.
- Eccles JC, Rantucci T, Sabah NH, Taborikova H (1974d) Somatotopic studies on cerebellar fastigial cells. *Exp Brain Res* 19:100-118.
- Eccles JC, Faber DS, Murphy JT, Sabah NH, Taborikova H (1971) Afferent volleys in limb nerves influencing impulse

- discharges in cerebellar cortex. I. In mossy fibers and granule cells. *Exp Brain Res* 13:15-35.
- Ekerot CF, Larson B (1973) Correlation between sagittal projection zones of climbing and mossy fibre paths in cat cerebellar anterior lobe. *Brain Res* 64:446-450.
- Ekerot CF, Larson B (1980) Termination in overlapping sagittal zones in cerebellar anterior lobe of mossy and climbing fiber paths activated from dorsal funiculus. *Exp Brain Res* 38:163-172.
- Ekerot CF, Kano M (1985) Long-term depression of parallel fibre synapses following stimulation of climbing fibres. *Brain Res* 342:357-360.
- Ekerot CF, Jorntell H (2001) Parallel fibre receptive fields of Purkinje cells and interneurons are climbing fibre-specific. *Eur J Neurosci* 13:1303-1310.
- Elsen GE, Juric-Sekhar G, Daza RAM, Hevner RF (2013) Development of Cerebellar Nuclei. *Handbook of the Cerebellum and Cerebellar Disorders*, M Manto, DL Gruol, JD Schmahmann, N Koibuchi, F Rossi (eds), Springer Science+Business Media Dordrecht 2013.
- Engbers JD, Anderson D, Tadayonnejad R, Mehaffey WH, Molineux ML, Turner RW (2011) Distinct roles for I(T) and I(H) in controlling the frequency and timing of rebound spike responses. *J Physiol* 589:5391-5413.
- Engbers JDT, Anderson D, Zamponi GW, Turner RW (2013) Signal processing by T-type calcium channel interactions in the cerebellum. *Front Cell Neurosci* 7.
- Engbers JDT, Anderson D, Asmara H, Rehak R, Mehaffey WH, Hameed S, McKay BE, Kruskic M, Zamponi GW, Turner RW (2012) Intermediate conductance calcium-activated potassium channels modulate summation of parallel fiber input in cerebellar Purkinje cells. *P Natl Acad Sci USA* 109:2601-2606.
- Epema AH, Guldmond JM, Voogd J (1985) Reciprocal Connections between the Caudal Vermis and the Vestibular Nuclei in the Rabbit. *Neuroscience Letters* 57:273-278.
- Erlander MG, Tobin AJ (1991) The structural and functional heterogeneity of glutamic acid decarboxylase: a review. *Neurochem Res* 16:215-226.
- Esclapez M, Tillakaratne NJK, Kaufman DL, Tobin AJ, Houser CR (1994) Comparative Localization of 2 Forms of Glutamic-Acid Decarboxylase and Their Messenger-Rnas in Rat-Brain Supports the Concept of Functional Differences between the Forms. *Journal of Neuroscience* 14:1834-1855.
- Essrich C, Lorez M, Benson JA, Fritschy JM, Luscher B (1998) Postsynaptic clustering of major GABA(A) receptor subtypes requires the gamma 2 subunit and gephyrin. *Nature Neuroscience* 1:563-571.
- Eulenburg V, Armsen W, Betz H, Gomez J (2005) Glycine transporters: essential regulators of neurotransmission. *Trends Biochem Sci* 30:325-333.
- Feirabend HK, Voogd J (1986) Myeloarchitecture of the cerebellum of the chicken (*Gallus domesticus*): an atlas of the compartmental subdivision of the cerebellar white matter. *J Comp Neurol* 251:44-66.
- Feng GP, Mellor RH, Bernstein M, Keller-Peck C, Nguyen QT, Wallace M, Nerbonne JM, Lichtman JW, Sanes JR (2000) Imaging neuronal subsets in transgenic mice expressing multiple spectral variants of GFP. *Neuron* 28:41-51.
- Flood S, Jansen J (1961) On the cerebellar nuclei in the cat. *Acta Anat (Basel)* 46:52-72.
- Fortin M, Marchand R, Parent A (1998) Calcium-binding proteins in primate cerebellum. *Neurosci Res* 30:155-168.
- Fredette BJ, Mugnaini E (1991) The GABAergic cerebello-olivary projection in the rat. *Anat Embryol (Berl)* 184:225-243.
- Friauf E, Hammerschmidt B, Kirsch J (1997) Development of adult-type inhibitory glycine receptors in the central auditory system of rats. *J Comp Neurol* 385:117-134.
- Gambarana C, Loria CJ, Siegel RE (1993) GABAA receptor messenger RNA expression in the deep cerebellar nuclei of Purkinje cell degeneration mutants is maintained following the loss of innervating Purkinje neurons. *Neuroscience* 52:63-71.
- Gao BX, Stricker C, Ziskind-Conhaim L (2001) Transition from GABAergic to glycinergic synaptic transmission in newly formed spinal networks. *Journal of Neurophysiology* 86:492-502.
- Garcia KS, Mauk MD (1998) Pharmacological analysis of cerebellar contributions to the timing and expression of conditioned eyelid responses. *Neuropharmacology* 37:471-480.
- Garcialadona FJ, Palacios JM, Debarry J, Gombos G (1990) Developmentally Regulated Changes of Glutamate Binding-Sites in Mouse Deep Cerebellar Nuclei. *Neuroscience Letters* 110:256-260.
- Gardette R, Crepel F (1986) Chemosensitiveness of Intracerebellar Nuclei Neurons to L-Aspartate, L-Glutamate and Related Derivatives in Rat Cerebellar Slices Maintained In Vitro. *Neuroscience* 18:93-103.
- Garifoli A, Scardilli G, Perciavalle V (2001) Effects of cerebellar dentate nucleus GABAergic cells on rat inferior olivary neurons. *Neuroreport* 12:3709-3713.

- Garin N, Escher G (2001) The development of inhibitory synaptic specializations in the mouse deep cerebellar nuclei. *Neuroscience* 105:431-441.
- Garwick M, Ekerot CF, Jörntell H (1998) Organizational Principles Of Cerebellar Neuronal Circuitry. *News Physiology Sciences - Int Union Physiol Sci/Am Physiol Soc* 13.
- Gauck V, Jaeger D (2000) The control of rate and timing of spikes in the deep cerebellar nuclei by inhibition. *Journal of Neuroscience* 20:3006-3016.
- Gauck V, Jaeger D (2003) The contribution of NMDA and AMPA conductances to the control of spiking in neurons of the deep cerebellar nuclei. *Journal of Neuroscience* 23:8109-8118.
- Gauck V, Thomann M, Jaeger D, Borst A (2001) Spatial distribution of low- and high-voltage-activated calcium currents in neurons of the deep cerebellar nuclei. *J Neurosci* 21:RC158.
- Gebre SA, Reeber SL, Sillitoe RV (2012) Parasagittal compartmentation of cerebellar mossy fibers as revealed by the patterned expression of vesicular glutamate transporters VGLUT1 and VGLUT2. *Brain Struct Funct* 217:165-180.
- Gerrits NM, Voogd J (1987) The Projection of the Nucleus Reticularis Tegmenti Pontis and Adjacent Regions of the Pontine Nuclei to the Central Cerebellar Nuclei in the Cat. *Journal of Comparative Neurology* 258:52-69.
- Gilbert PF, Thach WT (1977) Purkinje cell activity during motor learning. *Brain Res* 128:309-328.
- Gould BB (1979) Organization of Afferents to the Cerebellar Cortex in the Cat - Projections from the Deep Cerebellar Nuclei. *Journal of Comparative Neurology* 184:27-&.
- Gould BB, Graybiel AM (1976) Afferents to Cerebellar Cortex in Cat - Evidence for an Intrinsic Pathway Leading from Deep Nuclei to Cortex. *Brain Research* 110:601-611.
- Gould TJ, Adams CE, Bickford PC (1997) beta-adrenergic modulation of GABAergic inhibition in the deep cerebellar nuclei of F344 rats. *Neuropharmacology* 36:75-81.
- Gravel C, Hawkes R (1990) Parasagittal Organization of the Rat Cerebellar Cortex - Direct Comparison of Purkinje-Cell Compartments and the Organization of the Spinocerebellar Projection. *Journal of Comparative Neurology* 291:79-102.
- Graybiel AM, Nauta HJ, Lasek RJ, Nauta WJ (1973) A cerebello-olivary pathway in the cat: an experimental study using autoradiographic tracing technics. *Brain Res* 58:205-211.
- Groenewegen HJ, Voogd J (1977) The parasagittal zonation within the olivocerebellar projection. I. Climbing fiber distribution in the vermis of cat cerebellum. *J Comp Neurol* 174:417-488.
- Grudt TJ, Henderson G (1998) Glycine and GABAA receptor-mediated synaptic transmission in rat substantia gelatinosa: inhibition by mu-opioid and GABAB agonists. *J Physiol* 507 (Pt 2):473-483.
- Haines DE (1988) Evidence of intracerebellar collateralization of nucleocortical cell processes in a prosimian primate (Galago): a fluorescence retrograde study. *J Comp Neurol* 275:441-451.
- Haines DE, Pearson JC (1979) Cerebellar corticonuclear - nucleocortical topography: a study of the tree shrew (Tupaia) paraflocculus. *J Comp Neurol* 187:745-758.
- Haines DE, Manto MU (2009) The Discovery and Definitive Proof of Cerebellar Nucleocortical Projections. *Cerebellum* 8:1-2.
- Hamann M, Desarmenien M, Desaulles E, Bader MF, Feltz P (1988) Quantitative-Evaluation of the Properties of a Pyridazinyl Gaba Derivative (Sr-95531) as a Gabaa Competitive Antagonist - an Electrophysiological Approach. *Brain Research* 442:287-296.
- Hamori J, Takacs J (1989) 2 Types of Gaba-Containing Axon Terminals in Cerebellar Glomeruli of Cat - an Immunogold-Em Study. *Experimental Brain Research* 74:471-479.
- Hamori J, Mezey E, Szentagothai J (1981) Electron microscopic identification of cerebellar nucleo-cortical mossy terminals in the rat. *Exp Brain Res* 44:97-100.
- Hansel C, Linden DJ, D'Angelo E (2001) Beyond parallel fiber LTD: the diversity of synaptic and non-synaptic plasticity in the cerebellum. *Nat Neurosci* 4:467-475.
- Hanson CL, Chen G, Ebner TJ (2000) Role of climbing fibers in determining the spatial patterns of activation in the cerebellar cortex to peripheral stimulation: an optical imaging study. *Neuroscience* 96:317-331.
- Hashimoto K, Ichikawa R, Kitamura K, Watanabe M, Kano M (2009) Translocation of a "winner" climbing fiber to the Purkinje cell dendrite and subsequent elimination of "losers" from the soma in developing cerebellum. *Neuron* 63:106-118.
- Hausser M, Clark BA (1997) Tonic synaptic inhibition modulates neuronal output pattern and spatiotemporal synaptic integration. *Neuron* 19:665-678.

- Hawkes R, Leclerc N (1987) Antigenic map of the rat cerebellar cortex: the distribution of parasagittal bands as revealed by monoclonal anti-Purkinje cell antibody mabQ113. *J Comp Neurol* 256:29-41.
- Heckroth JA, Eisenman LM (1988) Parasagittal organization of mossy fiber collaterals in the cerebellum of the mouse. *J Comp Neurol* 270:385-394.
- Henneberger C, Bard L, King C, Jennings A, Rusakov DA (2013) NMDA Receptor Activation: Two Targets for Two Co-Agonists. *Neurochemical Research* 38:1156-1162.
- Hess DT, Voogd J (1986) Chemoarchitectonic zonation of the monkey cerebellum. *Brain Res* 369:383-387.
- Hioki H, Fujiyama F, Taki K, Tomioka R, Furuta T, Tamamaki N, Kaneko T (2003) Differential distribution of vesicular glutamate transporters in the rat cerebellar cortex. *Neuroscience* 117:1-6.
- Hoebeek FE, Witter L, Ruigrok TJ, De Zeeuw CI (2010) Differential olivo-cerebellar cortical control of rebound activity in the cerebellar nuclei. *Proc Natl Acad Sci U S A* 107:8410-8415.
- Hoge GJ, Davidson KG, Yasumura T, Castillo PE, Rash JE, Pereda AE (2011) The extent and strength of electrical coupling between inferior olivary neurons is heterogeneous. *J Neurophysiol* 105:1089-1101.
- Hortnagl H, Tasan RO, Wieselthaler A, Kirchmair E, Sieghart W, Sperk G (2013) Patterns of mRNA and protein expression for 12 GABAA receptor subunits in the mouse brain. *Neuroscience* 236:345-372.
- Houck BD, Person AL (2014) Cerebellar Loops: A Review of the Nucleocortical Pathway. *Cerebellum* 13:378-385.
- Isope P, Barbour B (2002) Properties of unitary granule cell->Purkinje cell synapses in adult rat cerebellar slices. *J Neurosci* 22:9668-9678.
- Ito M, Kano M (1982) Long-lasting depression of parallel fiber-Purkinje cell transmission induced by conjunctive stimulation of parallel fibers and climbing fibers in the cerebellar cortex. *Neurosci Lett* 33:253-258.
- Ito M, Yoshida M, Obata K, Kawai N, Udo M (1970) Inhibitory control of intracerebellar nuclei by the purkinje cell axons. *Exp Brain Res* 10:64-80.
- Jacobson GA, Rokni D, Yarom Y (2008) A model of the olivo-cerebellar system as a temporal pattern generator. *Trends Neurosci* 31:617-625.
- Jahnsen H (1986a) Electrophysiological Characteristics of Neurons in the Guinea-Pig Deep Cerebellar Nuclei *In Vitro*. *J Physiol-London* 372:129-&.
- Jahnsen H (1986b) Extracellular Activation and Membrane Conductances of Neurons in the Guinea-Pig Deep Cerebellar Nuclei *In Vitro*. *J Physiol-London* 372:149-168.
- Jansen J, Brodal A (1940) Experimental studies on the intrinsic fibers of the cerebellum. *Journal of Comparative Neurology* 73:267-321.
- Jansen J, Jansen J (1955) On the Efferent Fibers of the Cerebellar Nuclei in the Cat. *Journal of Comparative Neurology* 102:607-632.
- Jasmin L, Courville J (1987) Distribution of external cuneate nucleus afferents to the cerebellum: II. Topographical distribution and zonal pattern--an experimental study with radioactive tracers in the cat. *J Comp Neurol* 261:497-514.
- Ji Z, Hawkes R (1994) Topography of Purkinje cell compartments and mossy fiber terminal fields in lobules II and III of the rat cerebellar cortex: spinocerebellar and cuneocerebellar projections. *Neuroscience* 61:935-954.
- Johnson JW, Ascher P (1987) Glycine Potentiates the Nmda Response in Cultured Mouse-Brain Neurons. *Nature* 325:529-531.
- Jonas P, Bischofberger J, Sandkuhler J (1998) Corelease of two fast neurotransmitters at a central synapse. *Science* 281:419-424.
- Kalil K (1979) Projections of the cerebellar and dorsal column nuclei upon the inferior olive in the rhesus monkey: an autoradiographic study. *J Comp Neurol* 188:43-62.
- Kandel ER, Schwartz J, Jessell T (2000) *Principles of Neural Sciences, Fourth Edition*. McGraw-Hill Companies, Incorporated.
- Kawa K (2003) Glycine receptors and glycinergic synaptic transmission in the deep cerebellar nuclei of the rat: A patch-clamp study. *Journal of Neurophysiology* 90:3490-3500.
- Keller AF, Coull JA, Chery N, Poisbeau P, De Koninck Y (2001) Region-specific developmental specialization of GABA-glycine cosynapses in laminae I-II of the rat spinal dorsal horn. *J Neurosci* 21:7871-7880.
- Khaliq ZM, Raman IM (2005) Axonal propagation of simple and complex spikes in cerebellar Purkinje neurons. *J Neurosci* 25:454-463.
- Khosrovani S, Van Der Giessen RS, De Zeeuw CI, De Jeu MT (2007) In vivo mouse inferior olive neurons exhibit heterogeneous subthreshold oscillations and spiking patterns. *Proc Natl Acad Sci U S A* 104:15911-15916.

- Kim JJ, Krupa DJ, Thompson RF (1998) Inhibitory cerebello-olivary projections and blocking effect in classical conditioning. *Science* 279:570-573.
- King JS (1976) The synaptic cluster (glomerulus) in the inferior olivary nucleus. *J Comp Neurol* 165:387-400.
- Kirsch J, Wolters I, Triller A, Betz H (1993) Gephyrin Antisense Oligonucleotides Prevent Glycine Receptor Clustering in Spinal Neurons. *Nature* 366:745-748.
- Kistler WM, De Zeeuw CI (2003) Time windows and reverberating loops: a reverse-engineering approach to cerebellar function. *Cerebellum* 2:44-54.
- Kitai ST, McCrea RA, Preston RJ, Bishop GA (1977) Electrophysiological and horseradish peroxidase studies of precerebellar afferents to the nucleus interpositus anterior. I. Climbing fiber system. *Brain Res* 122:197-214.
- Kitazawa S, Kimura T, Yin PB (1998) Cerebellar complex spikes encode both destinations and errors in arm movements. *Nature* 392:494-497.
- Kneussel M, Betz H (2000) Receptors, gephyrin and gephyrin-associated proteins: novel insights into the assembly of inhibitory postsynaptic membrane specializations. *J Physiol* 525 Pt 1:1-9.
- Kolston J, Apps R, Trott JR (1995) A Combined Retrograde Tracer and Gaba-Immunocytochemical Study of the Projection from Nucleus Interpositus Posterior to the Posterior Lobe C(2) Zone of the Cat Cerebellum. *European Journal of Neuroscience* 7:926-933.
- Kondratskaya EL, Betz H, Krishtal OA, Laube B (2005) The beta subunit increases the ginkgolide B sensitivity of inhibitory glycine receptors. *Neuropharmacology* 49:945-951.
- Konnerth A, Llano I, Armstrong CM (1990) Synaptic currents in cerebellar Purkinje cells. *Proc Natl Acad Sci U S A* 87:2662-2665.
- Kotak VC, Korada S, Schwartz IR, Sanes DH (1998) A developmental shift from GABAergic to glycinergic transmission in the central auditory system. *J Neurosci* 18:4646-4655.
- Kuo SP, Bradley LA, Trussell LO (2009) Heterogeneous kinetics and pharmacology of synaptic inhibition in the chick auditory brainstem. *J Neurosci* 29:9625-9634.
- Lang EJ (2002) GABAergic and glutamatergic modulation of spontaneous and motor-cortex-evoked complex spike activity. *J Neurophysiol* 87:1993-2008.
- Lang EJ, Sugihara I, Llinas R (1996) GABAergic modulation of complex spike activity by the cerebellar nucleoolivary pathway in rat. *J Neurophysiol* 76:255-275.
- Lang EJ, Sugihara I, Welsh JP, Llinas R (1999) Patterns of spontaneous purkinje cell complex spike activity in the awake rat. *J Neurosci* 19:2728-2739.
- Larsell O (1952) The morphogenesis and adult pattern of the lobules and fissures of the cerebellum of the white rat. *J Comp Neurol* 97:281-356.
- Leclerc N, Dore L, Parent A, Hawkes R (1990) The compartmentalization of the monkey and rat cerebellar cortex: zebrin I and cytochrome oxidase. *Brain Res* 506:70-78.
- Lefler Y, Yarom Y, Uusisaari MY (2014) Cerebellar inhibitory input to the inferior olive decreases electrical coupling and blocks subthreshold oscillations. *Neuron* 81:1389-1400.
- Legendre A, Courville J (1986) Cerebellar nucleocortical projection with a survey of factors affecting the transport of radioactive tracers. *J Comp Neurol* 252:392-403.
- Legendre A, Courville J (1987) Origin and trajectory of the cerebello-olivary projection: an experimental study with radioactive and fluorescent tracers in the cat. *Neuroscience* 21:877-891.
- Legendre P (2001) The glycinergic inhibitory synapse. *Cellular and Molecular Life Sciences* 58:760-793.
- Leznik E, Makarenko V, Llinas R (2002) Electrotonically mediated oscillatory patterns in neuronal ensembles: an in vitro voltage-dependent dye-imaging study in the inferior olive. *J Neurosci* 22:2804-2815.
- Li Y, Wu LJ, Legendre P, Xu TL (2003) Asymmetric cross-inhibition between GABAA and glycine receptors in rat spinal dorsal horn neurons. *J Biol Chem* 278:38637-38645.
- Lim R, Alvarez FJ, Walmsley B (2000) GABA mediates presynaptic inhibition at glycinergic synapses in a rat auditory brainstem nucleus. *J Physiol* 525 Pt 2:447-459.
- Lisberger SG, Fuchs AF (1978) Role of Primate Flocculus during Rapid Behavioral Modification of Vestibuloocular Reflex .2. Mossy Fiber Firing Patterns during Horizontal Head Rotation and Eye-Movement. *Journal of Neurophysiology* 41:764-777.
- Llinas R, Volkind RA (1973) The olivo-cerebellar system: functional properties as revealed by harmaline-induced tremor. *Exp Brain Res* 18:69-87.
- Llinas R, Yarom Y (1986) Oscillatory properties of guinea-pig inferior olivary neurones and their pharmacological

- modulation: an in vitro study. *J Physiol* 376:163-182.
- Llinas R, Muhlethaler M (1988) Electrophysiology of guinea-pig cerebellar nuclear cells in the in vitro brain stem-cerebellar preparation. *J Physiol* 404:241-258.
- Llinas R, Baker R, Sotelo C (1974) Electrotonic coupling between neurons in cat inferior olive. *J Neurophysiol* 37:560-571.
- Loewenstein Y, Mahon S, Chadderton P, Kitamura K, Sompolinsky H, Yarom Y, Hausser M (2005) Bistability of cerebellar Purkinje cells modulated by sensory stimulation. *Nat Neurosci* 8:202-211.
- Lu T, Rubio ME, Trussell LO (2008) Glycinergic transmission shaped by the corelease of GABA in a mammalian auditory synapse. *Neuron* 57:524-535.
- Lynch JW (2004) Molecular structure and function of the glycine receptor chloride channel. *Physiol Rev* 84:1051-1095.
- Lynch JW (2009) Native glycine receptor subtypes and their physiological roles. *Neuropharmacology* 56:303-309.
- Macdonald RL, Olsen RW (1994) Gaba(a) Receptor Channels. *Annu Rev Neurosci* 17:569-602.
- Machado P, Rostaing P, Guigonis JM, Renner M, Dumoulin A, Samson M, Vannier C, Triller A (2011) Heat Shock Cognate Protein 70 Regulates Gephyrin Clustering. *Journal of Neuroscience* 31:3-14.
- Malosio ML, Marquezepouey B, Kuhse J, Betz H (1991) Widespread Expression of Glycine Receptor Subunit Messenger-Rnas in the Adult and Developing Rat-Brain. *Embo J* 10:2401-2409.
- Marr D (1969) A theory of cerebellar cortex. *J Physiol* 202:437-470.
- Marshall SP, van der Giessen RS, de Zeeuw CI, Lang EJ (2007) Altered olivocerebellar activity patterns in the connexin36 knockout mouse. *Cerebellum* 6:287-299.
- Martin GF, Henkel CK, King JS (1976) Cerebello-olivary fibers: their origin, course and distribution in the North American opossum. *Exp Brain Res* 24:219-236.
- Maruta J, Hensbroek RA, Simpson JI (2007) Intraburst and interburst signaling by climbing fibers. *Journal of Neuroscience* 27:11263-11270.
- Mathy A, Clark BA (2013) Dynamics of the Inferior Olive Oscillator and Cerebellar Function. *Handbook of the Cerebellum and Cerebellar Disorders*, M Manto, DL Gruol, JD Schmammann, N Koibuchi, F Rossi (eds), Springer Science+Business Media Dordrecht 2013.
- Mathy A, Clark BA, Hausser M (2014) Synaptically induced long-term modulation of electrical coupling in the inferior olive. *Neuron* 81:1290-1296.
- Mathy A, Ho SS, Davie JT, Duguid IC, Clark BA, Hausser M (2009) Encoding of oscillations by axonal bursts in inferior olive neurons. *Neuron* 62:388-399.
- Matsushita M, Ikeda M (1970) Spinal Projections to Cerebellar Nuclei in Cat. *Experimental Brain Research* 10:501-&.
- Matsushita M, Iwahori N (1971a) Structural Organization of Interpositus and Dentate Nuclei. *Brain Research* 35:17-&.
- Matsushita M, Iwahori N (1971b) Structural Organization of Fastigial Nucleus .1. Dendrites and Axonal Pathways. *Brain Research* 25:597-&.
- Matsushita M, Iwahori N (1971c) Structural Organization of Fastigial Nucleus .2. Afferent Fiber Systems. *Brain Research* 25:611-&.
- Matsushita M, Iwahori N (1971d) Structural organization of the interpositus and the dentate nuclei. *Brain Res* 35:17-36.
- Matsushita M, Ikeda M (1976) Projections from Lateral Reticular Nucleus to Cerebellar Cortex and Nuclei in Cat. *Experimental Brain Research* 24:403-421.
- McCormick DA, Thompson RF (1984) Cerebellum: essential involvement in the classically conditioned eyelid response. *Science* 223:296-299.
- Mccrea RA, Bishop GA, Kitai ST (1978) Morphological and Electrophysiological Characteristics of Projection Neurons in Nucleus Interpositus of Cat Cerebellum. *Journal of Comparative Neurology* 181:397-419.
- Mcdevitt CJ, Ebner TJ, Bloedel JR (1987) Relationships between Simultaneously Recorded Purkinje-Cells and Nuclear Neurons. *Brain Research* 425:1-13.
- McKay BE, McRory JE, Molineux ML, Hamid J, Snutch TP, Zamponi GW, Turner RW (2006) Ca(V)₃ T-type calcium channel isoforms differentially distribute to somatic and dendritic compartments in rat central neurons. *Eur J Neurosci* 24:2581-2594.
- McKernan RM, Whiting PJ (1996) Which GABA(A)-receptor subtypes really occur in the brain? *Trends in Neurosciences* 19:139-143.
- Medina JF, Mauk MD (1999) Simulations of cerebellar motor learning: computational analysis of plasticity at the mossy fiber to deep nucleus synapse. *J Neurosci* 19:7140-7151.
- Medina JF, Lisberger SG (2008) Links from complex spikes to local plasticity and motor learning in the cerebellum of

- awake-behaving monkeys. *Nat Neurosci* 11:1185-1192.
- Meyer G, Kirsch J, Betz H, Langosch D (1995) Identification of a Gephyrin Binding Motif on the Glycine Receptor-Beta Subunit. *Neuron* 15:563-572.
- Molineux ML, Mehaffey WH, Tadayonnejad R, Anderson D, Tennent AF, Turner RW (2008) Ionic factors governing rebound burst phenotype in rat deep cerebellar neurons. *Journal of Neurophysiology* 100:2684-2701.
- Molineux ML, McRory JE, McKay BE, Hamid J, Mehaffey WH, Rehak R, Snutch TP, Zamponi GW, Turner RW (2006) Specific T-type calcium channel isoforms are associated with distinct burst phenotypes in deep cerebellar nuclear neurons. *Proc Natl Acad Sci U S A* 103:5555-5560.
- Monsivais P, Clark BA, Roth A, Hausser M (2005) Determinants of action potential propagation in cerebellar Purkinje cell axons. *J Neurosci* 25:464-472.
- Morishita W, Sastry BR (1995) Pharmacological Characterization of Pre-and Postsynaptic Gaba(B) Receptors in the Deep Nuclei of Rat Cerebellar Slices. *Neuroscience* 68:1127-1137.
- Morishita W, Sastry BR (1996) Postsynaptic mechanisms underlying long-term depression of GABAergic transmission in neurons of the deep cerebellar nuclei. *J Neurophysiol* 76:59-68.
- Mouginot D, Gahwiler BH (1995) Characterization of Synaptic Connections between Cortex and Deep Nuclei of the Rat Cerebellum in-Vitro. *Neuroscience* 64:699-712.
- Muller E, Triller A, Legendre P (2004) Glycine receptors and GABA receptor alpha 1 and gamma 2 subunits during the development of mouse hypoglossal nucleus. *Eur J Neurosci* 20:3286-3300.
- Murano M, Saitow F, Suzuki H (2011) Modulatory Effects of Serotonin on Glutamatergic Synaptic Transmission and Long-Term Depression in the Deep Cerebellar Nuclei. *Neuroscience* 172:118-128.
- Muri R, Knopfel T (1994) Activity induced elevations of intracellular calcium concentration in neurons of the deep cerebellar nuclei. *Journal of Neurophysiology* 71:420-428.
- Muzumdar MD, Tasic B, Miyamichi K, Li L, Luo LQ (2007) A global double-fluorescent cre reporter mouse. *Genesis* 45:593-605.
- Noda H (1981) Visual mossy fiber inputs to the flocculus of the monkey. *Ann N Y Acad Sci* 374:465-475.
- O'Brien JA, Berger AJ (1999) Cotransmission of GABA and glycine to brain stem motoneurons. *Journal of Neurophysiology* 82:1638-1641.
- Ohyama T, Mauk M (2001) Latent acquisition of timed responses in cerebellar cortex. *J Neurosci* 21:682-690.
- Ohyama T, Nores WL, Medina JF, Riusech FA, Mauk MD (2006) Learning-induced plasticity in deep cerebellar nucleus. *J Neurosci* 26:12656-12663.
- Ojakangas CL, Ebner TJ (1992) Purkinje cell complex and simple spike changes during a voluntary arm movement learning task in the monkey. *J Neurophysiol* 68:2222-2236.
- Ojakangas CL, Ebner TJ (1994) Purkinje cell complex spike activity during voluntary motor learning: relationship to kinematics. *J Neurophysiol* 72:2617-2630.
- Olsen RW, Sieghart W (2008) International union of pharmacology. LXX. Subtypes of gamma-aminobutyric Acid(A) receptors: Classification on the basis of subunit composition, pharmacology, and function. Update. *Pharmacol Rev* 60:243-260.
- Oltmans GA, Lorden JF, Beales M (1985) Lesions of the inferior olive increase glutamic acid decarboxylase activity in the deep cerebellar nuclei of the rat. *Brain Res* 347:154-158.
- Oscarsson O (1968) Termination and functional organization of the ventral spino-olivocerebellar path. *J Physiol* 196:453-478.
- Oscarsson O (1979) Functional units of the cerebellum - sagittal zones and microzones. *TINS* June 1979 Elsevier/North-Holland Biomedical Press 1979.
- Ottersen OP, Stormmathisen J, Somogyi P (1988) Colocalization of Glycine-Like and Gaba-Like Immunoreactivities in Golgi Cell Terminals in the Rat Cerebellum - a Postembedding Light and Electron-Microscopic Study. *Brain Research* 450:342-353.
- Ouardouz M, Sastry BR (2000) Mechanisms underlying LTP of inhibitory synaptic transmission in the deep cerebellar nuclei. *J Neurophysiol* 84:1414-1421.
- Ovsepian SV, Steuber V, Le Berre M, O'Hara L, O'Leary VB, Dolly JO (2013) A defined heteromeric K(V)₁ channel stabilizes the intrinsic pacemaking and regulates the output of deep cerebellar nuclear neurons to thalamic targets. *J Physiol-London* 591:1771-1791.
- Ozden I, Sullivan MR, Lee HM, Wang SS (2009) Reliable coding emerges from coactivation of climbing fibers in microbands of cerebellar Purkinje neurons. *J Neurosci* 29:10463-10473.

- Palkovits M, Mezey E, Hamori J, Szentagothai J (1977) Quantitative Histological Analysis of Cerebellar Nuclei in Cat .1. Numerical Data on Cells and on Synapses. *Experimental Brain Research* 28:189-209.
- Payne JN (1983) The Cerebellar Nucleo-Cortical Projection in the Rat Studied by the Retrograde Fluorescent Double- Labelling Method. *Brain Research* 271:141-144.
- Pedroarena CM (2010) Mechanisms Supporting Transfer of Inhibitory Signals into the Spike Output of Spontaneously Firing Cerebellar Nuclear Neurons In Vitro. *Cerebellum* 9:67-76.
- Pedroarena CM, Schwarz C (2003) Efficacy and short-term plasticity at GABAergic synapses between Purkinje and cerebellar nuclei neurons. *Journal of Neurophysiology* 89:704-715.
- Pedroarena CM, Kamphausen S (2008) Glycinergic synaptic currents in the deep cerebellar nuclei. *Neuropharmacology* 54:784-795.
- Persohn E, Malherbe P, Richards JG (1992) Comparative molecular neuroanatomy of cloned GABAA receptor subunits in the rat CNS. *J Comp Neurol* 326:193-216.
- Person AL, Raman IM (2012a) Purkinje neuron synchrony elicits time-locked spiking in the cerebellar nuclei. *Nature* 481:502-505.
- Person AL, Raman IM (2012b) Synchrony and neural coding in cerebellar circuits. *Front Neural Circuit* 6.
- Pham NQ, Fujita H, Sakamoto Y, Na J, Sugihara I (2011) Projection Patterns of Single Mossy Fiber Axons Originating from the Dorsal Column Nuclei Mapped on the Aldolase C Compartments in the Rat Cerebellar Cortex. *Journal of Comparative Neurology* 519:874-899.
- Pietrajtis K, Dieudonné S (2012) Golgi Neurons. M Manto, DL Gruol, JD Schmammann, N Koibuchi, F Rossi (eds), *Handbook of the Cerebellum and Cerebellar Disorders*, (c) Springer Science+Business Media, LLC 2012.
- Pijpers A, Ruigrok TJ (2006) Organization of pontocerebellar projections to identified climbing fiber zones in the rat. *J Comp Neurol* 496:513-528.
- Pijpers A, Voogd J, Ruigrok TJ (2005) Topography of olivo-cortico-nuclear modules in the intermediate cerebellum of the rat. *J Comp Neurol* 492:193-213.
- Pijpers A, Winkelman BH, Bronsing R, Ruigrok TJ (2008) Selective impairment of the cerebellar C1 module involved in rat hind limb control reduces step-dependent modulation of cutaneous reflexes. *J Neurosci* 28:2179-2189.
- Pijpers A, Apps R, Pardoe J, Voogd J, Ruigrok TJ (2006) Precise spatial relationships between mossy fibers and climbing fibers in rat cerebellar cortical zones. *J Neurosci* 26:12067-12080.
- Pirker S, Schwarzer C, Wieselthaler A, Sieghart W, Sperk G (2000) GABA(A) receptors: immunocytochemical distribution of 13 subunits in the adult rat brain. *Neuroscience* 101:815-850.
- Placantonakis D, Welsh J (2001) Two distinct oscillatory states determined by the NMDA receptor in rat inferior olive. *J Physiol* 534:123-140.
- Placantonakis DG, Schwarz C, Welsh JP (2000) Serotonin suppresses subthreshold and suprathreshold oscillatory activity of rat inferior olivary neurones in vitro. *J Physiol* 524 Pt 3:833-851.
- Placantonakis DG, Bukovsky AA, Aicher SA, Kiem HP, Welsh JP (2006) Continuous electrical oscillations emerge from a coupled network: A study of the inferior olive using lentiviral knockdown of Connexin36. *Journal of Neuroscience* 26:5008-5016.
- Porter NM, Angelotti TP, Twyman RE, Macdonald RL (1992) Kinetic-Properties of Alpha-1-Beta-1-Gamma-Aminobutyric Acid(a) Receptor Channels Expressed in Chinese-Hamster Ovary Cells - Regulation by Pentobarbital and Picrotoxin. *Mol Pharmacol* 42:872-881.
- Pribilla I, Takagi T, Langosch D, Bormann J, Betz H (1992) The Atypical M2-Segment of the Beta-Subunit Confers Picrotoxinin Resistance to Inhibitory Glycine Receptor Channels. *Embo J* 11:4305-4311.
- Protti DA, Gerschenfeld HM, Llano I (1997) GABAergic and glycinergic IPSCs in ganglion cells of rat retinal slices. *J Neurosci* 17:6075-6085.
- Provini L, Marcotti W, Morara S, Rosina A (1998) Somatotopic nucleocortical projections to the multiple somatosensory cerebellar maps. *Neuroscience* 83:1085-1104.
- Pugh JR, Raman IM (2005) GABAA receptor kinetics in the cerebellar nuclei: Evidence for detection of transmitter from distant release sites. *Biophysical Journal* 88:1740-1754.
- Pugh JR, Raman IM (2006) Potentiation of mossy fiber EPSCs in the cerebellar nuclei by NMDA receptor activation followed by postinhibitory rebound current. *Neuron* 51:113-123.
- Pugh JR, Raman IM (2008) Mechanisms of potentiation of mossy fiber EPSCs in the cerebellar nuclei by coincident synaptic excitation and inhibition. *J Neurosci* 28:10549-10560.
- Pugh JR, Raman IM (2009) Nothing can be coincidence: synaptic inhibition and plasticity in the cerebellar nuclei.

- Trends Neurosci 32:170-177.
- Qvist H (1989) Demonstration of Axonal Branching of Fibers from Certain Precerebellar Nuclei to the Cerebellar Cortex and Nuclei - a Retrograde Fluorescent Double-Labeling Study in the Cat. *Experimental Brain Research* 75:15-27.
- Raman IM, Bean BP (1997) Resurgent sodium current and action potential formation in dissociated cerebellar Purkinje neurons. *Journal of Neuroscience* 17:4517-4526.
- Raman IM, Gustafson AE, Padgett D (2000) Ionic currents and spontaneous firing in neurons isolated from the cerebellar nuclei. *Journal of Neuroscience* 20:9004-9016.
- Rampon C, Luppi PH, Fort P, Peyron C, Jouvet M (1996) Distribution of glycine-immunoreactive cell bodies and fibers in the rat brain. *Neuroscience* 75:737-755.
- Rancz EA, Ishikawa T, Duguid I, Chadderton P, Mahon S, Hausser M (2007) High-fidelity transmission of sensory information by single cerebellar mossy fibre boutons. *Nature* 450:1245-1248.
- Rasmussen A, Hesslow G (2014) Feedback control of learning by the cerebello-olivary pathway. *Prog Brain Res* 210:103-119.
- Rispaal-padel L, Cicirata F, Pons C (1982) Cerebellar Nuclear Topography of Simple and Synergistic Movements in the Alert Baboon (Papio-Papio). *Experimental Brain Research* 47:365-380.
- Ristanovic D, Milosevic NT, Stefanovic BD, Maric DL, Rajkovic K (2010) Morphology and classification of large neurons in the adult human dentate nucleus: A qualitative and quantitative analysis of 2D images. *Neuroscience Research* 67:1-7.
- Rivera C, Voipio J, Payne JA, Ruusuvuori E, Lahtinen H, Lamsa K, Pirvola U, Saarma M, Kaila K (1999) The K⁺/Cl⁻ co-transporter KCC2 renders GABA hyperpolarizing during neuronal maturation. *Nature* 397:251-255.
- Rofflertarlov S, Beart PM, Ogorman S, Sidman RL (1979) Neurochemical and Morphological Consequences of Axon Terminal Degeneration in Cerebellar Deep Nuclei of Mice with Inherited Purkinje-Cell Degeneration. *Brain Research* 168:75-95.
- Rogers JH (1989) Immunoreactivity for Calretinin and Other Calcium-Binding Proteins in Cerebellum. *Neuroscience* 31:711-721.
- Rosen I, Scheid P (1972) Cerebellar Surface Cooling Influencing Evoked Activity in Cortex and in Interpositus Nucleus. *Brain Research* 45:580-&.
- Rousseau CV, Dugue GP, Dumoulin A, Mugnaini E, Dieudonne S, Diana MA (2012) Mixed Inhibitory Synaptic Balance Correlates with Glutamatergic Synaptic Phenotype in Cerebellar Unipolar Brush Cells. *Journal of Neuroscience* 32:4632-4644.
- Rowland NC, Jaeger D (2005) Coding of tactile response properties in the rat deep cerebellar nuclei. *Journal of Neurophysiology* 94:1236-1251.
- Rowland NC, Jaeger D (2008) Responses to tactile stimulation in deep cerebellar nucleus neurons result from recurrent activation in multiple pathways. *J Neurophysiol* 99:704-717.
- Ruigrok TJ (2003) Collateralization of climbing and mossy fibers projecting to the nodulus and flocculus of the rat cerebellum. *J Comp Neurol* 466:278-298.
- Ruigrok TJ (2011) Ins and outs of cerebellar modules. *Cerebellum* 10:464-474.
- Ruigrok TJ, Voogd J (1990) Cerebellar nucleo-olivary projections in the rat: an anterograde tracing study with Phaseolus vulgaris-leucoagglutinin (PHA-L). *J Comp Neurol* 298:315-333.
- Ruigrok TJ, Voogd J (2000) Organization of projections from the inferior olive to the cerebellar nuclei in the rat. *J Comp Neurol* 426:209-228.
- Ruigrok TJ, Pijpers A, Goedknegt-Sabel E, Coulon P (2008) Multiple cerebellar zones are involved in the control of individual muscles: a retrograde transneuronal tracing study with rabies virus in the rat. *Eur J Neurosci* 28:181-200.
- Russier M, Kopysova IL, Ankri N, Ferrand N, Debanne D (2002) GABA and glycine co-release optimizes functional inhibition in rat brainstem motoneurons in vitro. *J Physiol* 541:123-137.
- Sagne C, ElMestikawy S, Isambert MF, Hamon M, Henry JP, Giros B, Gasnier B (1997) Cloning of a functional vesicular GABA and glycine transporter by screening of genome databases. *Febs Letters* 417:177-183.
- Saitow F, Murano M, Suzuki H (2009) Modulatory Effects of Serotonin on GABAergic Synaptic Transmission and Membrane Properties in the Deep Cerebellar Nuclei. *Journal of Neurophysiology* 101:1361-1374.
- Salin PA, Malenka RC, Nicoll RA (1996) Cyclic AMP mediates a presynaptic form of LTP at cerebellar parallel fiber synapses. *Neuron* 16:797-803.

- Sassoe-Pognetto M, Fritschy JM (2000) Gephyrin, a major postsynaptic protein of GABAergic synapses. *European Journal of Neuroscience* 12:2205-2210.
- Sastry BR, Morishita W, Yip S, Shew T (1997) Gaba-ergic transmission in deep cerebellar nuclei. *Progress in Neurobiology* 53:259-271.
- Sato K, Zhang JH, Saika T, Sato M, Tada K, Tohyama M (1991) Localization of Glycine Receptor Alpha-1 Subunit Messenger Rna-Containing Neurons in the Rat-Brain - an Analysis Using Insitu Hybridization Histochemistry. *Neuroscience* 43:381-395.
- Sato Y, Miura A, Fushiki H, Kawasaki T (1992) Short-term modulation of cerebellar Purkinje cell activity after spontaneous climbing fiber input. *J Neurophysiol* 68:2051-2062.
- Schindelin J, Arganda-Carreras I, Frise E, Kaynig V, Longair M, Pietzsch T, Preibisch S, Rueden C, Saalfeld S, Schmid B, Tinevez JY, White DJ, Hartenstein V, Eliceiri K, Tomancak P, Cardona A (2012) Fiji: an open-source platform for biological-image analysis. *Nat Methods* 9:676-682.
- Schneider ER, Civillico EF, Wang SS (2013) Calcium-based dendritic excitability and its regulation in the deep cerebellar nuclei. *Journal of Neurophysiology* 109:2282-2292.
- Schultz SR, Kitamura K, Post-Uiterweer A, Krupic J, Hausser M (2009) Spatial pattern coding of sensory information by climbing fiber-evoked calcium signals in networks of neighboring cerebellar Purkinje cells. *J Neurosci* 29:8005-8015.
- Schwartz EJ, Rothman JS, Dugue GP, Diana M, Rousseau C, Silver RA, Dieudonne S (2012) NMDA receptors with incomplete Mg(2)(+) block enable low-frequency transmission through the cerebellar cortex. *J Neurosci* 32:6878-6893.
- Schwarz C, Schmitz Y (1997) Projection from the cerebellar lateral nucleus to precerebellar nuclei in the mossy fiber pathway is glutamatergic: A study combining anterograde tracing with immunogold labeling in the rat. *Journal of Comparative Neurology* 381:320-334.
- Scott TG (1963) A Unique Pattern of Localization within the Cerebellum. *Nature* 200:793.
- Shambes GM, Gibson JM, Welker W (1978) Fractured Somatotopy in Granule Cell Tactile Areas of Rat Cerebellar Hemispheres Revealed by Micromapping. *Brain Behav Evolut* 15:94-140.
- Shi SR, Key ME, Kalra KL (1991) Antigen Retrieval in Formalin-Fixed, Paraffin-Embedded Tissues - an Enhancement Method for Immunohistochemical Staining Based on Microwave-Oven Heating of Tissue-Sections. *J Histochem Cytochem* 39:741-748.
- Shinoda Y (1999) Visualization of the entire trajectory of long axons of single mammalian CNS neurons. *Brain Research Bulletin* 50:387-388.
- Shinoda Y, Sugiuchi Y, Futami T (1987) Excitatory inputs to cerebellar dentate nucleus neurons from the cerebral cortex in the cat. *Exp Brain Res* 67:299-315.
- Sillitoe RV, Vogel MW, Joyner AL (2010) Engrailed Homeobox Genes Regulate Establishment of the Cerebellar Afferent Circuit Map. *Journal of Neuroscience* 30:10015-10024.
- Simat M, Parpan F, Fritschy JM (2007a) Heterogeneity of glycinergic and gabaergic interneurons in the granule cell layer of mouse cerebellum. *Journal of Comparative Neurology* 500:71-83.
- Simat M, Ambrosetti L, Lardi-Studler B, Fritschy JM (2007b) GABAergic synaptogenesis marks the onset of differentiation of basket and stellate cells in mouse cerebellum. *Eur J Neurosci* 26:2239-2256.
- Snider RS (1940) Morphology of the cerebellar nuclei in the rabbit and cat. *Journal of Comparative Neurology* 72:399-415.
- Sola M, Bavro VN, Timmins J, Franz T, Ricard-Blum S, Schoehn G, Ruigrok RWH, Paarmann I, Saiyed T, O'Sullivan GA, Schmitt B, Betz H, Weissenhorn W (2004) Structural basis of dynamic glycine receptor clustering by gephyrin. *Embo J* 23:2510-2519.
- Sotelo C, Angaut P (1973) Fine-Structure of Cerebellar Central Nuclei in Cat .1. Neurons and Neuroglial Cells. *Experimental Brain Research* 16:410-430.
- Steuber V, Jaeger D (2013) Modeling the generation of output by the cerebellar nuclei. *Neural Networks* 47:112-119.
- Steuber V, Schultheiss NW, Silver RA, De Schutter E, Jaeger D (2011) Determinants of synaptic integration and heterogeneity in rebound firing explored with data-driven models of deep cerebellar nucleus cells. *J Comput Neurosci* 30:633-658.
- Sugihara I (2006) Organization and remodeling of the olivocerebellar climbing fiber projection. *Cerebellum* 5:15-22.
- Sugihara I, Shinoda Y (2004) Molecular, topographic, and functional organization of the cerebellar cortex: a study with combined aldolase C and olivocerebellar labeling. *J Neurosci* 24:8771-8785.

- Sugihara I, Shinoda Y (2007) Molecular, topographic, and functional organization of the cerebellar nuclei: analysis by three-dimensional mapping of the olivonuclear projection and aldolase C labeling. *J Neurosci* 27:9696-9710.
- Sugihara I, Wu H, Shinoda Y (1996) Morphology of axon collaterals of single climbing fibers in the deep cerebellar nuclei of the rat. *Neurosci Lett* 217:33-36.
- Sugihara I, Wu H, Shinoda Y (1999) Morphology of single olivocerebellar axons labeled with biotinylated dextran amine in the rat. *J Comp Neurol* 414:131-148.
- Sugihara I, Wu HS, Shinoda Y (2001) The entire trajectories of single olivocerebellar axons in the cerebellar cortex and their contribution to Cerebellar compartmentalization. *J Neurosci* 21:7715-7723.
- Sugihara I, Fujita H, Na J, Quy PN, Li BY, Ikeda D (2009) Projection of Reconstructed Single Purkinje Cell Axons in Relation to the Cortical and Nuclear Aldolase C Compartments of the Rat Cerebellum. *Journal of Comparative Neurology* 512:282-304.
- Sultan F, Konig T, Mock M, Thier P (2002) Quantitative organization of neurotransmitters in the deep cerebellar nuclei of the Lurcher mutant. *Journal of Comparative Neurology* 452:311-323.
- Svensson P, Bengtsson F, Hesslow G (2006) Cerebellar inhibition of inferior olivary transmission in the decerebrate ferret. *Exp Brain Res* 168:241-253.
- Tadayonnejad R, Mehaffey WH, Anderson D, Turner RW (2009) Reliability of triggering postinhibitory rebound bursts in deep cerebellar neurons. *Channels (Austin)* 3:149-155.
- Tadayonnejad R, Anderson D, Molineux ML, Mehaffey WH, Jayasuriya K, Turner RW (2010) Rebound discharge in deep cerebellar nuclear neurons in vitro. *Cerebellum* 9:352-374.
- Takahashi T, Momiyama A, Hirai K, Hishinuma F, Akagi H (1992) Functional correlation of fetal and adult forms of glycine receptors with developmental changes in inhibitory synaptic receptor channels. *Neuron* 9:1155-1161.
- Tamamaki N, Yanagawa Y, Tomioka R, Miyazaki JL, Obata K, Kaneko T (2003) Green fluorescent protein expression and colocalization with calretinin, parvalbumin, and somatostatin in the GAD67-GFP knock-in mouse. *Journal of Comparative Neurology* 467:60-79.
- Tanaka I, Ezure K (2004) Overall distribution of GLYT2 mRNA-containing versus GAD67 mRNA-containing neurons and colocalization of both mRNAs in midbrain, pons, and cerebellum in rats. *Neuroscience Research* 49:165-178.
- Telgkamp P, Raman IM (2002) Depression of inhibitory synaptic transmission between Purkinje cells and neurons of the cerebellar nuclei. *Journal of Neuroscience* 22:8447-8457.
- Telgkamp P, Padgett DE, Ledoux VA, Woolley CS, Raman IM (2004) Maintenance of high-frequency transmission at Purkinje to cerebellar nuclear synapses by spillover from boutons with multiple release sites. *Neuron* 41:113-126.
- Teune TM, van der Burg J, de Zeeuw CI, Voogd J, Ruigrok TJ (1998) Single Purkinje cell can innervate multiple classes of projection neurons in the cerebellar nuclei of the rat: a light microscopic and ultrastructural triple-tracer study in the rat. *J Comp Neurol* 392:164-178.
- Teune TM, van der Burg J, van der Moer J, Voogd J, Ruigrok TJH (2000) Topography of cerebellar nuclear projections to the brain stem in the rat. *Cerebellar Modules: Molecules, Morphology, and Function* 124:141-172.
- Thach WT (1968) Discharge of Purkinje and Cerebellar Nuclear Neurons during Rapidly Alternating Arm Movements in Monkey. *Journal of Neurophysiology* 31:785-800.
- Tokuda IT, Hoang H, Schweighofer N, Kawato M (2013) Adaptive coupling of inferior olive neurons in cerebellar learning. *Neural Networks* 47:42-50.
- Tolbert D, Kultas-Ilinsky K, Ilinsky I (1980) EM-autoradiography of cerebellar nucleocortical terminals in the cat. *Anat Embryol (Berl)* 161:215-223.
- Tolbert DL, Bantli H (1979) Hrp and Autoradiographic Study of Cerebellar Corticonuclear-Nucleocortical Reciprocity in the Monkey. *Experimental Brain Research* 36:563-571.
- Tolbert DL, Bantli H, Bloedel JR (1976a) Anatomical and Physiological Evidence for a Cerebellar Nucleo-Cortical Projection in Cat. *Neuroscience* 1:208-220.
- Tolbert DL, Bantli H, Bloedel JR (1977) Intracerebellar Nucleocortical Projection in a-Primate. *Experimental Brain Research* 30:425-434.
- Tolbert DL, Bantli H, Bloedel JR (1978a) Organizational Features of Cat and Monkey Cerebellar Nucleocortical Projection. *Journal of Comparative Neurology* 182:39-56.
- Tolbert DL, Bantli H, Bloedel JR (1978b) Multiple Branching of Cerebellar Efferent Projections in Cats. *Experimental Brain Research* 31:305-316.

- Tolbert DL, Massopust LC, Murphy MG, Young PA (1976b) The anatomical organization of the cerebello-olivary projection in the cat. *J Comp Neurol* 170:525-544.
- Toth K, McBain CJ (1998) Afferent-specific innervation of two distinct AMPA receptor subtypes on single hippocampal interneurons. *Nat Neurosci* 1:572-578.
- Trombley PQ, Hill BJ, Horning MS (1999) Interactions between GABA and glycine at inhibitory amino acid receptors on rat olfactory bulb neurons. *Journal of Neurophysiology* 82:3417-3422.
- Trott JR, Apps R, Armstrong DM (1998a) Zonal organization of cortico-nuclear and nucleo-cortical projections of the paramedian lobule of the cat cerebellum. 1. The C-1 zone. *Experimental Brain Research* 118:298-315.
- Trott JR, Apps R, Armstrong DM (1998b) Zonal organization of cortico-nuclear and nucleo-cortical projections of the paramedian lobule of the cat cerebellum. 2. The C-2 zone. *Experimental Brain Research* 118:316-330.
- Tsukahara N, Bando T (1970) Red Nuclear and Interposate Nuclear Excitation of Pontine Nuclear Cells. *Brain Research* 19:295-8.
- Tsukahara N, Bando T, Murakami F, Oda Y (1983) Properties of Cerebello-Precerebellar Reverberating Circuits. *Brain Research* 274:249-259.
- Turecek R, Trussell LO (2001) Presynaptic glycine receptors enhance transmitter release at a mammalian central synapse. *Nature* 411:587-590.
- Uusisaari M, Knopfel T (2008) GABAergic synaptic communication in the GABAergic and non-GABAergic cells in the deep cerebellar nuclei. *Neuroscience* 156:537-549.
- Uusisaari M, Knopfel T (2010) GlyT2+Neurons in the Lateral Cerebellar Nucleus. *Cerebellum* 9:42-55.
- Uusisaari M, Knopfel T (2011) Functional Classification of Neurons in the Mouse Lateral Cerebellar Nuclei. *Cerebellum* 10:637-646.
- Uusisaari M, Obata K, Knopfel T (2007) Morphological and electrophysiological properties of GABAergic and non-GABAergic cells in the deep cerebellar nuclei. *Journal of Neurophysiology* 97:901-911.
- Uusisaari MY, Knopfel T (2013) Neurons of the Deep Cerebellar Nuclei. *Handbook of the Cerebellum and Cerebellar Disorders*, M Manto, DL Gruol, JD Schmahmann, N Koibuchi, F Rossi (eds), Springer Science+Business Media Dordrecht 2013.
- Van der Want JJ, Voogd J (1987) Ultrastructural identification and localization of climbing fiber terminals in the fastigial nucleus of the cat. *J Comp Neurol* 258:81-90.
- Van der Want JJ, Wiklund L, Guegan M, Ruigrok T, Voogd J (1989) Anterograde tracing of the rat olivocerebellar system with Phaseolus vulgaris leucoagglutinin (PHA-L). Demonstration of climbing fiber collateral innervation of the cerebellar nuclei. *J Comp Neurol* 288:1-18.
- Van der Want JJJ, Gerrits NM, Voogd J (1987) Autoradiography of Mossy Fiber Terminals in the Fastigial Nucleus of the Cat. *Journal of Comparative Neurology* 258:70-80.
- Verveer C, Hawkins RK, Ruigrok TJH, DeZeeuw CI (1997) Ultrastructural study of the GABAergic and cerebellar input to the nucleus reticularis tegmenti pontis. *Brain Research* 766:289-296.
- Voogd J, Glickstein M (1998) The anatomy of the cerebellum. *Trends Neurosci* 21:370-375.
- Voogd J, Pardoe J, Ruigrok TJ, Apps R (2003) The distribution of climbing and mossy fiber collateral branches from the copula pyramidis and the paramedian lobule: congruence of climbing fiber cortical zones and the pattern of zebrin banding within the rat cerebellum. *J Neurosci* 23:4645-4656.
- Walter JT, Khodakhah K (2009) The advantages of linear information processing for cerebellar computation. *P Natl Acad Sci USA* 106:4471-4476.
- Wang H, Peca J, Matsuzaki M, Matsuzaki K, Noguchi J, Qiu L, Wang D, Zhangn F, Boyden E, Deisserothl K, Kasai H, Hall WC, Feng G, Augustine GJ (2007) High-speed mapping of synaptic connectivity using photostimulation in Channel rhodopsin-2 transgenic mice. *P Natl Acad Sci USA* 104:8143-8148.
- Wang PY, Slaughter MM (2005) Effects of GABA receptor antagonists on retinal glycine receptors and on homomeric glycine receptor alpha subunits. *Journal of Neurophysiology* 93:3120-3126.
- Wassef M, Simons J, Tappaz ML, Sotelo C (1986) Non-Purkinje Cell Gabaergic Innervation of the Deep Cerebellar Nuclei - a Quantitative Immunocytochemical Study in C57bl and in Purkinje-Cell Degeneration Mutant Mice. *Brain Research* 399:125-135.
- Watanabe E, Akagi H (1995) Distribution patterns of mRNAs encoding glycine receptor channels in the developing rat spinal cord. *Neurosci Res* 23:377-382.
- Watanabe M, Kano M (2011) Climbing fiber synapse elimination in cerebellar Purkinje cells. *Eur J Neurosci* 34:1697-1710.

- Weidenreich F (1899) Zur Anatomie der centralen Kleinhirnerne der Säuger. *Z MorphAnthrop* 1:259-312.
- Welsh JP, Llinas R (1997) Some organizing principles for the control of movement based on olivocerebellar physiology. *Prog Brain Res* 114:449-461.
- Welsh JP, Lang EJ, Sugihara I, Llinas R (1995) Dynamic organization of motor control within the olivocerebellar system. *Nature* 374:453-457.
- Weltzien F, Puller C, O'Sullivan GA, Paarmann I, Betz H (2012) Distribution of the Glycine Receptor beta-Subunit in the Mouse CNS as Revealed by a Novel Monoclonal Antibody. *Journal of Comparative Neurology* 520:3962-3981.
- Werner M, von Wasielewski R, Komminoth P (1996) Antigen retrieval, signal amplification and intensification in immunohistochemistry. *Histochem Cell Biol* 105:253-260.
- Wetmore DZ, Mukamel EA, Schnitzer MJ (2008) Lock-and-key mechanisms of cerebellar memory recall based on rebound currents. *Journal of Neurophysiology* 100:2328-2347.
- Wiklund L, Toggenburger G, Cuenod M (1984) Selective retrograde labelling of the rat olivocerebellar climbing fiber system with D-[³H]aspartate. *Neuroscience* 13:441-468.
- Wise AK, Cerminara NL, Marple-Horvat DE, Apps R (2010) Mechanisms of synchronous activity in cerebellar Purkinje cells. *J Physiol* 588:2373-2390.
- Witter L, Canto CB, Hoogland TM, de Gruijl JR, De Zeeuw CI (2013) Strength and timing of motor responses mediated by rebound firing in the cerebellar nuclei after Purkinje cell activation. *Front Neural Circuit* 7.
- Woolston DC, Kassel J, Gibson JM (1981) Trigemino-cerebellar Mossy Fiber Branching to Granule Cell Layer Patches in the Rat Cerebellum. *Brain Research* 209:255-269.
- Wu HS, Sugihara I, Shinoda Y (1999) Projection patterns of single mossy fibers originating from the lateral reticular nucleus in the rat cerebellar cortex and nuclei. *Journal of Comparative Neurology* 411:97-118.
- Yaginuma H, Matsushita M (1987) Spinocerebellar Projections from the Thoracic Cord in the Cat, as Studied by Anterograde Transport of Wheat-Germ Agglutinin-Horseradish Peroxidase. *Journal of Comparative Neurology* 258:1-27.
- Yakushiji T, Tokutomi N, Akaike N, Carpenter DO (1987) Antagonists of Gaba Responses, Studied Using Internally Perfused Frog Dorsal-Root Ganglion Neurons. *Neuroscience* 22:1123-1133.
- Ye JH (2000) Physiology and pharmacology of native glycine receptors in developing rat ventral tegmental area neurons. *Brain Research* 862:74-82.
- Zafra F, Aragon C, Gimenez C (1997) Molecular biology of glycinergic neurotransmission. *Mol Neurobiol* 14:117-142.
- Zeilhofer HU, Studler B, Arabadzisz D, Schweizer C, Ahmadi S, Layh B, Bosl MR, Fritschy JM (2005) Glycinergic neurons expressing enhanced green fluorescent protein in bacterial artificial chromosome transgenic mice. *Journal of Comparative Neurology* 482:123-141.
- Zhang W, Linden DJ (2006) Long-term depression at the mossy fiber-deep cerebellar nucleus synapse. *J Neurosci* 26:6935-6944.
- Zhang W, Shin JH, Linden DJ (2004) Persistent changes in the intrinsic excitability of rat deep cerebellar nuclear neurones induced by EPSP or IPSP bursts. *J Physiol-London* 561:703-719.
- Zheng N, Raman IM (2009) Ca currents activated by spontaneous firing and synaptic disinhibition in neurons of the cerebellar nuclei. *J Neurosci* 29:9826-9838.
- Zheng N, Raman IM (2010) Synaptic inhibition, excitation, and plasticity in neurons of the cerebellar nuclei. *Cerebellum* 9:56-66.

LIST OF ABBREVIATIONS

AAV	Adeno-Associated Virus
AMPA	Alpha-amino-3- hydroxy-5-methyl-4-isoxazole propionate
APV	D-2-amino-5-phosphonopentaoate
ChR2	Channel Rhodopsine 2
CN	Cerebellar Nuclei
EPSC	Excitatory Post-Synaptic Current
EPSP	Excitatory Post-Synaptic Potential
GABA	Gamma-AminoButyric Acid
GABAR	GABA Receptor
GAD	Glutamic Acid Decarboxylase
GFP	Green Fluorescent Protein
GlyR	Glycine Receptor
GlyT2	Glycine Transporter 2
IO	Inferior olive
IPSC	Inhibitory Post-Synaptic Current
IPSP	Inhibitory Post-Synaptic Potential
NBQX	6-nitro-7-sulfamoylbenzo(f)-quinoxaline-2,3-dione
NMDA	Non-N-methyl-D-aspartate
PCD	Purkinje cell – degeneration
TTX	Tetrodotoxin
VGluT1	Vesicular Glutamate Transporter 1
VGluT2	Vesicular Glutamate Transporter 2
VIAAT	Vesicular Inhibitory Amino Acid Transporter
VIAAT	Vesicular Inhibitory Amino Acids Transporter
YFP	Yellow Fluorescent Protein

LIST OF FIGURES

Introduction

Chapter 1:

Figure 1.1: Anatomical and molecular segmentation of the cerebellar cortex and nuclei

Figure 1.2: Mossy fibers inputs to the cerebellar cortex

Figure 1.3: Principal neurons of the cerebellar nuclei convey the output information

Figure 1.4: Rebound discharge phenotypes in principal neurons of the cerebellar nuclei

Chapter 2:

Figure 2.1: Climbing fiber innervation in the cerebellar cortex

Figure 2.2: Oscillatory phenotypes in the inferior olive and its control by the nucleo-olivary pathway

Figure 2.3: Climbing fiber innervation in the cerebellar nuclei

Figure 2.4: Modular organization of the olivo-cortico-nuclear system

Figure 2.5: Synaptic plasticity in the cerebellum

Results

Chapter 4:

Figure 4.1: Weak expression of GFP in nucleo-olivary neurons in the GlyT2-eGFP adult mouse.

Figure 4.2: Extracellular recordings of GlyT2-cre positive ChR2-infected neurons during one millisecond whole field illumination.

Chapter 5:

Figure 5.1: Mixed GABAergic/glycinergic nucleo-cortical neurons project to GlyT2 – positive and Neurogranin – positive Golgi cells in the granular layer of the cortex.

Figure 5.2: Mixed transmission at the nucleo-cortical neuron to Golgi cell synapses.

Figure 5.3: Purkinje cells GABAergic inputs onto GlyT2-positive neurons of the cerebellar nuclei in L7-ChR2-YFP x GlyT2-eGFP mice

Figure 5.4: Excitatory inputs onto GlyT2-eGFP – positive neurons of the cerebellar nuclei

Figure 5.5: AAVs-ChR2 infection of inferior olive by ventral approach in OF1 neonatal pups and elicited responses in the principal neurons of the cerebellar nuclei.

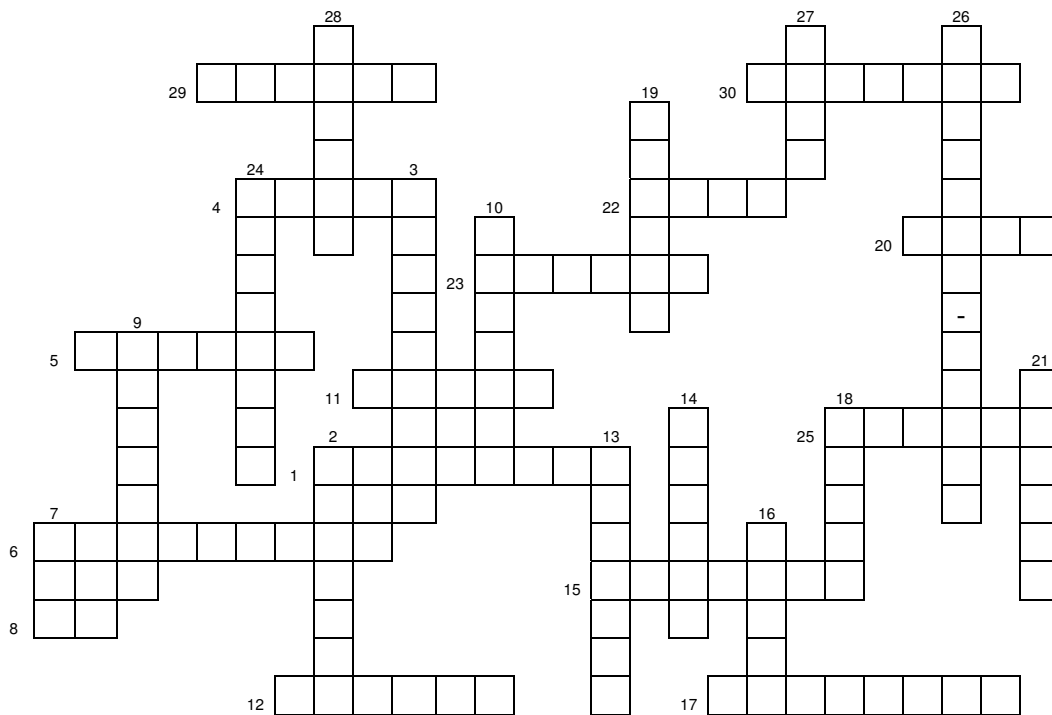
Figure 5.6: Excitatory responses in principal neurons recorded at -20 mV with physiological internal solution, in animals injected in the brainstem with AAVs expressing ChR2

Discussion

Figure 6.1: Golgi cells heterogeneity.

Figure 6.2: Intra- and inter-modules connectivity of the inhibitory neurons of the cerebellar nuclei.

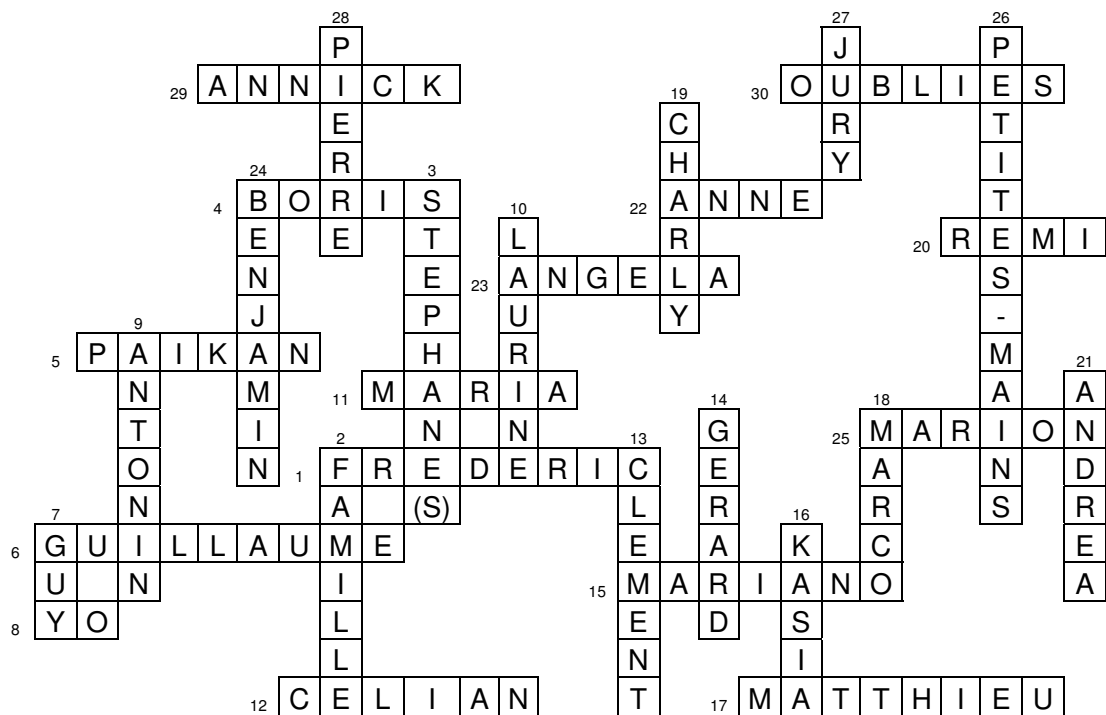
Acknowledgments



- 1- The number one.
- 2- From Agen to Paris, those who always count.
- 3- They make a pair, and their differences are their team's strength.
- 4- Apples and English grammar lover.
- 5- From Marseilles, with colorful pants.
- 6- Often masked, sometimes worried, always « full on »
- 7- Informed bibliographer.
- 8- Who do not talk much.
- 9- Eat two when I eat one.
- 10- "Culturiste" (= Bodybuilder) who transports me.
- 11- Eat raw fennel.
- 12- From « la Loire », disciple of You Tube links and wild camping.
- 13- Reputed orator.
- 14- The crazy welding.
- 15- "Young" dad.
- 16- Companion on the road (and of rout).
- 17- Future well-balanced doctor.
- 18- Italian with glasses.

- 19- Guide of the beginning
- 20- Some tear his shirt; others are just satisfied by his quality of climber and his good mood.
- 21- Owner of the fridges full of interesting antibodies on the 3rd floor.
- 22- The one who make coffee for the braves on the early mornings.
- 23- Mother of Pénélope who gave me her first « baby ».
- 24- Responsible of the imaging facility in good shape
- 25- Retired teacher for olivary injection in pups.
- 26- Administrators, secretaries, technicians, animal house technicians and others, too often forgotten from the acknowledgments.
- 27- Those who accepted the reading and the criticism.
- 28- Our master.
- 29- "Young" mother with precious immunohistochemical knowledge.
- 30- All of those whose names are not in the little boxes of the crossword but who will stay in the little boxes of my memories for a long time.

Remerciements / Acknowledgments (Solutions)



Merci à tous (même aux tricheurs...)
 Merci pour tout (même pour la triche...)

*Thanks to all (even to cheaters...)
 Thanks for everything (even for cheating...)*